

INFORMATION TO USERS

This manuscript has been reproduced from the microfilm master. UMI films the text directly from the original or copy submitted. Thus, some thesis and dissertation copies are in typewriter face, while others may be from any type of computer printer.

The quality of this reproduction is dependent upon the quality of the copy submitted. Broken or indistinct print, colored or poor quality illustrations and photographs, print bleedthrough, substandard margins, and improper alignment can adversely affect reproduction.

In the unlikely event that the author did not send UMI a complete manuscript and there are missing pages, these will be noted. Also, if unauthorized copyright material had to be removed, a note will indicate the deletion.

Oversize materials (e.g., maps, drawings, charts) are reproduced by sectioning the original, beginning at the upper left-hand corner and continuing from left to right in equal sections with small overlaps. Each original is also photographed in one exposure and is included in reduced form at the back of the book.

Photographs included in the original manuscript have been reproduced xerographically in this copy. Higher quality 6" x 9" black and white photographic prints are available for any photographs or illustrations appearing in this copy for an additional charge. Contact UMI directly to order.

UMI

A Bell & Howell Information Company
300 North Zeeb Road, Ann Arbor MI 48106-1346 USA
313/761-4700 800/521-0600

NOTE TO USERS

The original manuscript received by UMI contains pages with indistinct and/or slanted print. Pages were microfilmed as received.

This reproduction is the best copy available

UMI

UNIVERSITY OF OKLAHOMA
GRADUATE COLLEGE

NITROSYL AND NITROSO COMPLEXES OF GROUP 8
METALLOPORPHYRINS

A Dissertation
SUBMITTED TO THE GRADUATE FACULTY
in partial fulfillment of the requirements for the
degree of
Doctor of Philosophy

By
LI CHEN
Norman, Oklahoma
1998

UMI Number: 9839784

UMI Microform 9839784
Copyright 1998, by UMI Company. All rights reserved.

**This microform edition is protected against unauthorized
copying under Title 17, United States Code.**

UMI
300 North Zeeb Road
Ann Arbor, MI 48103

© Copyright by LI CHEN 1998
All Rights Reserved.

NITROSYL AND NITROSO COMPLEXES OF GROUP 8
METALLOPORPHYRINS

A Dissertation APPROVED FOR THE
DEPARTMENT OF CHEMISTRY AND BIOCHEMISTRY

BY

Gilchrist, Adels
K. M. Nicholas
Lance Lobban
Richard W. Tyle
John W. Tyle

Acknowledgments

First, I would like to express my deepest gratitude to my mentor, Dr. George B. Richter-Addo for his guidance, support, encouragement throughout my graduate studies. I would also like to thank Drs. G. Atkinson, L. L. Lobban, K. M. Nicholas, R. W. Taylor, and R. A. Wheeler for serving as my advisory committee members. Their guidance has helped me survive the graduate studies along the way. Special thanks to Drs. Masood Khan, Victor Young, Jr. (at the University of Minnesota), and Douglas Powell (at the University of Wisconsin, Madison) for X-ray studies.

I would like to give my thanks to all my coworkers present and past in Dr. Richter-Addo's group: Lin Cheng, Heesun Chung, Jesse and Shelia Fox, Shelly Hodge, Jonghyuk Lee, Aaron Nichols, Li-Sheng Wang, Geun-Bae Yi. I would also like to thank other fellow Inorganic Division graduate students: Susan Alguindigue, Sam Asirvatham, John Lilly, Danny McGuire, and Kris Wise.

I also deeply appreciate the teaching assistantship offered by the Department of Chemistry and Biochemistry at the University of Oklahoma, and the research assistantship funded by the National Institutes of Health (NIH) and National Science Foundation (NSF).

Finally, I wish to thank my parents, parents-in-law, sister, brother, brother-in-law, sister-in-law and my niece for their support, love, and for taking care of my daughter when I was away from her. I wish to dedicate this dissertation to my husband Hengguo Ma and my lovely daughter Chuchu for their love, support, understanding and sacrifice to help me through and make this work possible.

Table of Contents

	Page
List of Tables	vii
List of Figures	ix
Reproduction Permission	xii
Abstract	xiii
Chapter 1	
Nitrosylation of Osmium Porphyrins with Thionitrites and Alkyl Nitrites	
Introduction	1
Experimental Section	6
Results and Discussion	
* Addition of RSNO to (OEP)Os(CO).	15
* Addition of RONO to (por)Os(CO).	17
* Addition of RSNO and RONO to [(OEP)Os] ₂ .	28
* Further Investigation of the Reaction Pathway for RSNO Addition.	28
* Reaction of RSNO with an Os ^{III} Porphyrin	36
Conclusion	50
References and Notes	51
Chapter 2	
Nitrosamine and Nitrosoarene Complexes of Metalloporphyrins	
Introduction	58
Experimental Section	63
Results and Discussion	
* Synthesis and Characterization of Nitrosamine Complexes of Iron and Osmium Porphyrins.	76
* Extension of the η^1 -O Nitrosamine Binding Feature to the Preparation of the First Transition Metal η^1 -O Bound Nitrosoarene Complexes.	91
* The η^1 -N Binding of Nitrosoarenes to Os ^{II} Porphyrins.	105
Conclusion	133
References and Notes	134

Chapter 3	Synthesis and Characterization of Osmium Nitrosyl Porphyrins Containing Organo, Chloro and μ -Oxo Ligands, and Extension to the First Organoosmium Thionitrosyl Porphyrin	
	Introduction	141
	Experimental Section	144
	Results and Discussion	
	* Synthesis and Characterization of Organoosmium Nitrosyl Porphyrin Complexes.	149
	* Synthesis and Characterization of Osmium Nitrosyl Porphyrin Chloro and μ -Oxo Dimer Complexes.	153
	* Synthesis and Characterization of Osmium Thionitrosyl Porphyrin Chloro and Methyl Complexes.	158
	Conclusion	167
	References and Notes	168

List of Tables

		Page
Table 1.1	Bond Lengths (Å) for (OEP)Os(NO)(O- <i>n</i> -C ₄ H ₉)	23
Table 1.2	Bond Angles (°) for (OEP)Os(NO)(O- <i>n</i> -C ₄ H ₉)	24
Table 1.3	Structural Parameters (in Å and °) for Osmium Nitrosyl Complexes	26
Table 1.4	Structurally Characterized Monometallic Osmium Porphyrins with <i>O</i> - and <i>S</i> - Donor Ligands	27
Table 1.5	Bond Lengths (Å) for (OEP)Os(SPh) ₂	34
Table 1.6	Bond Angles (°) for (OEP)Os(SPh) ₂	34
Table 1.7	Bond Lengths (Å) for (OEP)Os(NO)(O ₂ PF ₂)	40
Table 1.8	Bond Angles (°) for (OEP)Os(NO)(O ₂ PF ₂)	41
Table 1.9	Metric Parameters (in Å and °) for Transition Metal η^1 -OP(=O)F ₂ Complexes	44
Table 1.10	Bond Lengths (Å) for (OEP)Os(NS)(O ₂ PF ₂)	47
Table 1.11	Bond Angles (°) for (OEP)Os(NS)(O ₂ PF ₂)	48
Table 2.1	Selected Bond Lengths (Å) for (TTP)Os(CO)(Et ₂ NNO)	84
Table 2.2	Selected Bond Angles (°) for (TTP)Os(CO)(Et ₂ NNO)	85
Table 2.3	Os-N(por) Bond Lengths (Å) for Os ^{II} Porphyrin Complexes	87
Table 2.4	Structural Parameters (in Å and °) for (por)Os ^{II} (CO)(L) complexes	88
Table 2.5	Spin States for (por)Fe ^{III} Complexes	93
Table 2.6	Selected Bond Lengths (Å) for [(TPP)Fe(ONC ₆ H ₄ NEt ₂) ₂] ⁺	100
Table 2.7	Selected Bond Angles (°) for [(TPP)Fe(ONC ₆ H ₄ NEt ₂) ₂] ⁻	101
Table 2.8	Selected Bond Lengths (Å) for [(TPP)Mn(ONC ₆ H ₄ NEt ₂) ₂] ⁻	102
Table 2.9	Selected Bond Angles (°) for [(TPP)Mn(ONC ₆ H ₄ NEt ₂) ₂] ⁺	103
Table 2.10	Selected Bond Lengths (Å) for (TTP)Os(PhNO) ₂	114
Table 2.11	Selected Bond Angles (°) for (TTP)Os(PhNO) ₂	115

Table 2.12	Selected Bond Lengths (Å) for (TTP)Os(CO)(PhNO)	116
Table 2.13	Selected Bond Angles (°) for (TTP)Os(CO)(PhNO)	117
Table 2.14	Selected Bond Lengths (Å) for (TPP)Os(PhNO) ₂	118
Table 2.15	Selected Bond Angles (°) for (TPP)Os(PhNO) ₂	119
Table 2.16	Selected Bond Lengths (Å) for (TMP)Os(PhNO) ₂	121
Table 2.17	Selected Bond Angles (°) for (TMP)Os(PhNO) ₂	122
Table 2.18	Selected Bond Lengths (Å) for (OEP)Os(<i>o</i> -tolNO) ₂	124
Table 2.19	Selected Bond Angles (°) for (OEP)Os(<i>o</i> -tolNO) ₂	125
Table 3.1	Selected Spectral Data for (OEP)Os(NE)X (E = O, S) and Related Compounds	152
Table 3.2	Selected Bond Lengths (Å) for [(OEP)Os(NO)] ₂ (μ-O)	156
Table 3.3	Selected Bond Angles (°) for [(OEP)Os(NO)] ₂ (μ-O)	156
Table 3.4	Structural Parameters (in Å and °) for Group 8 Oxo-Bridged Dimers	157
Table 3.5	Selected Bond Lengths (Å) for (OEP)Os(NS)Cl	160
Table 3.6	Selected Bond Angles (°) for (OEP)Os(NS)Cl	160
Table 3.7	Selected Structural Data for Osmium and Ruthenium Thionitrosyl Complexes	162
Table 3.8	Selected Bond Lengths (Å) for (OEP)Os(NS)(Me)	165
Table 3.9	Selected Bond Angles (°) for (OEP)Os(NS)(Me)	166

List of Figures

		Page
Figure 1.1	Molecular structure of (OEP)Ru(NO)(SR) (SR = <i>N</i> -acetyl-L-cysteine methyl ester).	3
Figure 1.2	Molecular structure of (TTP)Os(NO)(S- <i>i</i> -C ₅ H ₁₁).	4
Figure 1.3	IR spectrum of the reaction solution (CH ₂ Cl ₂) containing the starting (OEP)Os(CO) ($\nu_{\text{CO}} = 1883 \text{ cm}^{-1}$), intermediate (OEP)Os(CO)(SPh) ($\nu_{\text{CO}} = 1957 \text{ cm}^{-1}$), and the final (OEP)Os(NO)(SPh) product ($\nu_{\text{NO}} = 1766 \text{ cm}^{-1}$).	18
Figure 1.4	IR monitoring (in CH ₂ Cl ₂) of the reaction of (TTP)Os(CO) ($\nu_{\text{CO}} = 1898 \text{ cm}^{-1}$, spectrum a) with isoamyl nitrite to give (TTP)Os(NO)(O- <i>i</i> -C ₅ H ₁₁) ($\nu_{\text{NO}} = 1766 \text{ cm}^{-1}$, spectrum c), spectrum b: after addition of isoamyl nitrite, showing the intermediate (TTP)Os(CO)(O- <i>i</i> -C ₅ H ₁₁) ($\nu_{\text{CO}} = 1968 \text{ cm}^{-1}$) and the product (TTP)Os(NO)(O- <i>i</i> -C ₅ H ₁₁).	20
Figure 1.5	(a) Molecular structure of (OEP)Os(NO)(O- <i>n</i> -C ₄ H ₉). (b) View along the O(2)–Os(1) bond showing the orientation of the axial <i>n</i> -C ₄ H ₉ alkoxide ligand relative to the porphyrin core. (c) Ball and stick structure showing the labeling of the atoms.	22
Figure 1.6	(a) Molecular structure of (OEP)Os(SPh) ₂ . (b) View of the thiolate orientation relative to the porphyrin core, with the view along the S(1)–Os(1) bond.	33
Figure 1.7	IR spectrum of the reaction (10 min) of [(OEP)Os ^{III}] ₂ (PF ₆) ₂ with isoamyl thionitrite in CH ₂ Cl ₂ .	37
Figure 1.8	(a) Molecular structure of (OEP)Os(NO)(O ₂ PF ₂). (b) View of the O ₂ PF ₂ ligand relative to the porphyrin core, with the view along the O(2)–Os(1) bond.	39
Figure 1.9	(a) Molecular structure of (OEP)Os(NS)(O ₂ PF ₂). (b) View of the O ₂ PF ₂ ligand relative to the porphyrin core, with the view along the O(1)–Os(1) bond.	46
Figure 2.1	Proposed interactions of nitrosamines with the heme site of cytochrome P450.	59
Figure 2.2	Possible redox intermediates between amphetamine 1 and its corresponding nitro compound 5 .	61
Figure 2.3	Coordination modes of C–nitroso ligands to monometallic centers.	61
Figure 2.4	IR spectra of [(TTP)Fe(Et ₂ NNO) ₂](SbF ₆) (top) and [(TTP)Fe(Et ₂ N ¹⁵ NO) ₂](SbF ₆) (bottom).	77

Figure 2.5	IR spectra (KBr) of [(TTP)Fe(Et ₂ NNO) ₂](SbF ₆) (top) and proposed [(TTP)Fe(NO)(Et ₂ NNO)](SbF ₆) (bottom).	79
Figure 2.6	IR spectra (KBr) of (TTP)Os(CO) (top) and (TTP)Os(CO)(Et ₂ NNO) (bottom).	81
Figure 2.7	(a) Molecular structure of (TTP)Os(CO)(Et ₂ NNO). (b) View along the O(2)–Os(1) bond showing the nitrosamine orientation relative to the porphyrin core. (c) Ball and stick structure showing the atom labelings.	83
Figure 2.8	IR spectra (KBr) of (OEP)Os(CO) (top) and (OEP)Os(CO)(Et ₂ NNO) (bottom).	89
Figure 2.9	UV–vis spectra of the Fe ^{III} bis-nitrosoarene complexes in C ₆ H ₆ .	94
Figure 2.10	(a) Molecular structure of [(TPP)Fe(ONC ₆ H ₄ NEt ₂) ₂] ⁺ . (b) Disorder of the ligands.	98
Figure 2.11	(a) Molecular structure of [(TPP)Mn(ONC ₆ H ₄ NEt ₂) ₂] ⁺ . (b) View of ligand orientations relative to the porphyrin core, with the view along the O(1)–Mn(1) bond (two orientations due to the disorder of the ligands).	99
Figure 2.12	IR spectra (KBr) showing the ν_{CO} 's for (TTP)Os(CO) (top, 1916 cm ⁻¹) and (TTP)Os(CO)(PhNO) (bottom, 1972 cm ⁻¹).	108
Figure 2.13	Molecular structure of (TTP)Os(PhNO) ₂ .	109
Figure 2.14	Molecular structure of (TTP)Os(CO)(PhNO).	110
Figure 2.15	Molecular structure of (TPP)Os(PhNO) ₂ .	111
Figure 2.16	Molecular structure of (TMP)Os(PhNO) ₂ .	112
Figure 2.17	(a) Molecular structure (OEP)Os(<i>o</i> -tolNO) ₂ . (b) View along the N(3)–Os(1) bond showing the orientation of the axial <i>o</i> -tolNO ligand relative to the porphyrin core (two positions due to the disorder of the <i>o</i> -tolNO ligand).	113
Figure 2.18	Structural data for (TTP)Os(PhNO) ₂ : selected bond lengths and bond angles are shown on the left. Also shown are the O–N–Os–N(1) torsion angles on the right: the solid line represents the nitroso group of the PhNO ligand above the plane and the dashed line represents the equivalent nitroso group below the plane.	129
Figure 2.19	Structural data for (TTP)Os(CO)(PhNO): selected bond lengths and bond angles are shown on the left. Also shown is the O–N–Os–N(2A) torsion angle on the right.	130

Figure 2.20	Structural data for (TPP)Os(PhNO) ₂ : selected bond lengths and bond angles are shown on the left. Also shown are the O–N–Os–N(2) torsion angles on the right: the solid line represents the nitroso group of the PhNO ligand above the plane and the dashed line represents the equivalent nitroso group below the plane.	131
Figure 2.21	Structural data for (TMP)Os(PhNO) ₂ : selected bond lengths and bond angles are shown on the left. Also shown are the O–N–Os–N(3) torsion angles on the right: the solid line represents the nitroso group of the PhNO ligand above the plane and the dashed line represents the equivalent nitroso group below the plane.	132
Figure 3.1	(a) Molecular structure of [(OEP)Os(NO)] ₂ (μ-O). (b) View from the bottom of the molecule.	155
Figure 3.2	Molecular structure of (OEP)Os(NS)(Cl) (only one of the disordered NS/Cl orientations is shown).	159
Figure 3.3	Molecular structure of (OEP)Os(NS)(Me) (only one of the disordered NS/Me orientations is shown).	164

Reproduction Permission

Portions of this dissertation have been reported in the following published or submitted papers:

(1) "Nitrosylation of Octaethylporphyrin Osmium Complexes with Alkyl Nitrites and Thionitrites: Molecular Structures of Three Osmium Porphyrin Derivatives" Chen, L.; Khan, M. A.; Richter-Addo, G. B. *Inorg. Chem.* **1998**, *37*, 533-540.

Reprinted in part with permission from Inorganic Chemistry. Copyright 1998 American Chemical Society.

(2) "Activation of Thionitrites and Isoamyl Nitrite by Group 8 Metalloporphyrins and the Subsequent Generation of Nitrosyl Thiulates and Alkoxides of Ruthenium and Osmium Porphyrins" Yi, G.-B.; Chen, L.; Khan, M. A.; Richter-Addo, G. B. *Inorg. Chem.* **1997**, *36*, 3876-3885.

Reprinted in part with permission from Inorganic Chemistry. Copyright 1997 American Chemical Society.

(3) "Nitrosoarene Complexes of Manganese Porphyrins" Fox, S. J. (S.); Chen, L.; Khan, M. A.; Richter-Addo, G. B. *Inorg. Chem.* **1997**, *36*, 6465-6467.

Reprinted in part with permission from Inorganic Chemistry. Copyright 1997 American Chemical Society.

(4) "The first structural studies of nitrosoarene binding to iron-(II) and -(III) porphyrins" Wang, L.-S.; Chen, L.; Khan, M. A.; Richter-Addo, G. B. *Chem. Commun.* **1996**, 323-324.

Reproduced by Permission of The Royal Society of Chemistry.

(5) "Synthesis, Characterization, and Molecular Structures of Diethylnitrosamine Metalloporphyrin Complexes of Iron, Ruthenium and Osmium" Chen, L.; Yi, G.-B.; Wang, L.-S.; Dharmawardana, U. R.; Dart, A. C.; Khan, M. A.; Richter-Addo, G. B. Submitted to *Inorg. Chem.* February 9, 1998.

Reprinted in part with permission from Inorganic Chemistry, submitted for publication. Unpublished work copyright 1998 American Chemical Society.

(6) "Synthesis and Characterization of Osmium Nitrosyl Porphyrins Containing Organo, Halogeno and μ -Oxo Ligands, and Extensions to the first Organometallic Thionitrosyl Porphyrin" Cheng, L.; Chen, L.; Chung, H.-S.; Khan, M. A.; Richter-Addo, G. B. Submitted to *Organometallics* March 16, 1998.

Reprinted in part with permission from Organometallics, submitted for publication. Unpublished work copyright 1998 American Chemical Society.

Abstract

Chapter 1 of this dissertation describes the formal *trans* addition of thionitrites (RSNO) and alkyl nitrites (RONO) to Os^{II} porphyrins, and the investigation of the reaction pathway of the thionitrite additions to Os^{II} porphyrins. The extension of the thionitrite reaction chemistry with a (OEP)Os^{III} complex is also described (OEP = 2, 3, 7, 8, 12, 13, 17, 18-octaethylporphyrinato dianion). The reactions of (OEP)Os(CO) with isoamyl thionitrite and phenyl thionitrite give the *trans* addition products (OEP)Os(NO)(S-*i*-C₅H₁₁) and (OEP)Os(NO)(SPh), respectively. The related reactions of (por)Os(CO) (por = OEP, TTP; TTP = 5, 10, 15, 20-tetra-*p*-tolylporphyrinato dianion) with alkyl nitrites give the corresponding nitrosyl alkoxides (por)Os(NO)(OR). The reaction of isoamyl thionitrite and isoamyl nitrite with the non-carbonyl-containing [(OEP)Os]₂ also give the *trans* addition products. Interestingly, the reaction of O₂NC₆H₄N=NSPh with [(OEP)Os]₂ gives the (OEP)Os(SPh)₂ product with loss of the arylazo fragments. The reaction of the cationic [(OEP)Os]₂(PF₆)₂ reagent with isoamyl thionitrite gives the nitrosylated product, [(OEP)Os(NO)](PF₆), which undergoes anion hydrolysis to give the isolable difluorophosphate (OEP)Os(NO)(O₂PF₂) derivative. The analogous (OEP)Os(NS)(O₂PF₂) compound is prepared via the anion hydrolysis of [(OEP)Os(NS)](PF₆). The solid-state structures of (OEP)Os(NO)(O-*n*-C₄H₉), (OEP)Os(SPh)₂, (OEP)Os(NO)(O₂PF₂) and (OEP)Os(NS)(O₂PF₂) have been determined by X-ray crystallography.

Chapter 2 of this dissertation describes the adduct formation of nitrosamine and nitrosoarene compounds to Fe^{III} and Os^{II} porphyrins. The reaction of [(TTP)Fe(THF)₂](SbF₆) with Et₂NNO generates the [(TTP)Fe(Et₂NNO)₂](SbF₆) complex in 70% yield. Reaction of [(TTP)Fe(Et₂NNO)₂](SbF₆) with NO gas in CH₂Cl₂ results in the displacement of one of the Et₂NNO ligands to give the thermally unstable [(TTP)Fe(NO)(Et₂NNO)](SbF₆) complex. The (TTP)Os(CO)(Et₂NNO) and

(OEP)Os(CO)(Et₂NNO) complexes are prepared in 74% and 66% yields, respectively, by Et₂NNO addition to the precursor (por)Os(CO) compounds in CH₂Cl₂. The nitrosyl [(OEP)Os(NO)(Et₂NNO)](BF₄) derivative is obtained in quantitative yield by the reaction of (OEP)Os(CO)(Et₂NNO) with NOBF₄. The solid-state structure of (TTP)Os(CO)(Et₂NNO) has been determined by single-crystal X-ray diffraction. The Et₂NNO ligand displays an η¹-O binding mode in (TTP)Os(CO)(Et₂NNO). The η¹-O binding mode has been extended to the binding of nitrosoarene ligands to Fe^{III} as well as Mn^{III} porphyrins. The reactions of [(por)Fe(THF)₂](SbF₆) (por = TPP, TTP; TPP = 5, 10, 15, 20-tetraphenylporphyrinato dianion) with *para*-dialkylamino substituted nitrosoarenes R₂NC₆H₄NO (R = Me, Et) result in the formation of bis-adducts [(por)Fe(ONC₆H₄NR₂)₂](SbF₆) in 55–83% yields. The R₂NC₆H₄NO ligands are weakly coordinated to the Fe^{III} center, as indicated by the facile substitution of Me₂NC₆H₄NO by THF. The solid-state structures of [(TPP)Fe(ONC₆H₄NEt₂)₂](SbF₆) and [(TPP)Mn(ONC₆H₄NEt₂)₂](SbF₆) have been determined by X-ray crystallography. The Et₂NC₆H₄NO ligand displays an η¹-O binding mode in both complexes. The (por)Os^{II} bis-nitrosoarene complexes are prepared via the reaction of (por)Os(CO) (por = TTP, TPP, TMP, OEP; TMP = 5, 10, 15, 20-tetramesitylporphyrinato dianion) with excess PhNO or *o*-tolNO at high temperature. The room temperature reaction of (TTP)Os(CO) with less than two equivalents of PhNO gives a mixture of (TTP)Os(PhNO)₂ and (TTP)Os(CO)(PhNO) in a 3:1 ratio. The solid-state structures of (TTP)Os(PhNO)₂, (TTP)Os(CO)(PhNO), (TPP)Os(PhNO)₂, (TMP)Os(PhNO)₂ and (OEP)Os(*o*-tolNO)₂ have also been determined by single-crystal X-ray diffraction. The nitrosoarene ligands PhNO and *o*-tolNO display an η¹-N binding mode in all five (por)Os^{II} nitrosoarene complexes.

Chapter 3 of this dissertation describes the synthesis and characterization of osmium nitrosyl porphyrins containing organo, chloro and μ-oxo ligands and the extensions of the synthetic methodology to the preparation of the first organoosmium

thionitrosyl porphyrin. The reactions of [(por)Os(NO)](PF₆) (por = TTP, OEP) with Grignard reagents generate the (por)Os(NO)R (por = TTP, R = Me; por = OEP, R = Me, *i*-Pr) complexes in 30–44% yields. The related reaction of [(OEP)Os(NO)](PF₆) with excess EtMgCl generates a 2:1 mixture of (OEP)Os(NO)(Et) and (OEP)Os(Et)₂ in 39% yield. The (OEP)Os(NO)Cl and the μ -oxo [(OEP)Os(NO)]₂(μ -O) dimer are prepared by the reaction of (OEP)Os(CO) with ClNO. The solid-state structure of [(OEP)Os(NO)]₂(μ -O) has been determined by X-ray crystallography. The reaction of (OEP)Os(CO) with (NSCl)₃ in refluxing THF generates (OEP)Os(NS)Cl in 49% yield. A 3:2 mixture of (OEP)Os(NS)(Me) and (OEP)Os(Me)₂ is obtained from the reaction of (OEP)Os(NS)Cl with excess MeMgBr. The solid-state structures of (OEP)Os(NS)Cl and (OEP)Os(NS)(Me) have also been determined by X-ray crystallography.

Chapter 1. Nitrosylation of Osmium Porphyrins with Thionitrites and Alkyl Nitrites

Introduction

Nitric oxide (NO) chemistry and biochemistry received a surge of renewed interest about a decade ago when it was proposed that the radical species referred to as endothelium-derived relaxing factor (EDRF) was NO.¹ It is now known that NO activates the enzyme guanylyl cyclase (GC) by binding to its heme moiety.² Also, the biosynthesis of NO involves the heme-containing NO synthase.³ Thus, it has been established that the heme group is vital in NO biochemistry and pharmacology both in NO consumption (by GC) and production (by NO synthase).

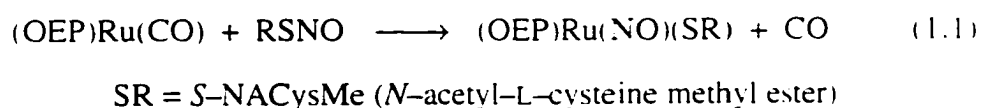
Thionitrites (RSNO) are a class of compounds containing the *S*-nitroso functional group, and their pharmacological properties are linked to the chemistry and biochemistry of NO.⁴⁻⁸ Important questions have been raised over the last few years on the true identity of EDRF. While it is generally accepted that EDRF is NO, there are a few published reports showing that some thionitrites possess EDRF-like properties in a manner independent of NO.⁹⁻¹³ Protein thiols may be nitrosated under physiological conditions to produce *S*-nitroso derivatives.¹⁴ The reported role of thionitrites (RSNO) as NO-storage and NO-carrier entities *in vivo* is also intriguing. Hemoglobin is also reported to be an NO-carrier by using its cysteine groups on the protein to form RSNO groups.¹⁵ Furthermore, the ability of nitrosomethane to bind directly to the heme of GC has also prompted the suggestion that RSNO may actually be able to bind directly to the heme site in GC.¹⁶ It has also been suggested that one of the possible pathways for the NO-activation of GC is by its binding to an as-yet unidentified non-heme site followed by transfer of the NO group to the heme iron.¹⁷

Recent investigations into RSNO stability revealed that the presence of trace Cu²⁺ (even in distilled water) plays an important role in RSNO decomposition catalysis

by Cu⁺.¹⁸ Thus, removal of trace metal ions (e.g., by EDTA addition) has been found to markedly enhance RSNO stability. This finding thus raises the question of the role of iron and copper metal ions in RSNO pharmacology.¹⁹

The possibility of a direct interaction of RSNO with heme led us to investigate the chemical reactions of RSNO with synthetic metalloporphyrins of the group 8 metals. Our laboratory has demonstrated that organic nitroso compounds such as nitrosamines (*N*-nitroso),²⁰ Cupferron (*N*-nitroso),²¹ nitrosoarenes (*C*-nitroso),²² thionitrites (*S*-nitroso), and alkyl nitrites (*O*-nitroso)²³ interact with heme models to result in either simple adduct formation or activation of the organic nitroso groups to give metal nitrosyls.

Of particular interest was a recent report from our laboratory that thionitrites and isoamyl nitrite add to the group 8 metalloporphyrins via a formal *trans* addition process to give nitrosyl thiolates and alkoxides, respectively.²³ For example, the reaction of (OEP)Ru(CO) (OEP = 2, 3, 7, 8, 12, 13, 17, 18-octaethylporphyrinato dianion) with 1 equiv of solid *S*-nitroso-*N*-acetyl-L-cysteine methyl ester produced the *trans* addition product (OEP)Ru(NO)(*S*-NACysMe) (eq 1.1).



The molecular structure of the product was determined by single-crystal X-ray diffraction and reveals that the NO and SR ligands are indeed located *trans* to each other (Figure 1.1).

Other *trans* addition products such as (OEP)Ru(NO)(SCH₂CF₃)^{23b} and (TTP)Ru(NO)(*O*-*i*-C₅H₁₁)^{23b} (TTP = 5, 10, 15, 20-tetra-*p*-tolylporphyrinato dianion) are obtained via the reaction of (por)Ru(CO) (por = OEP or TTP) with the corresponding CF₃CH₂SNO and isoamyl nitrite reagents, respectively.

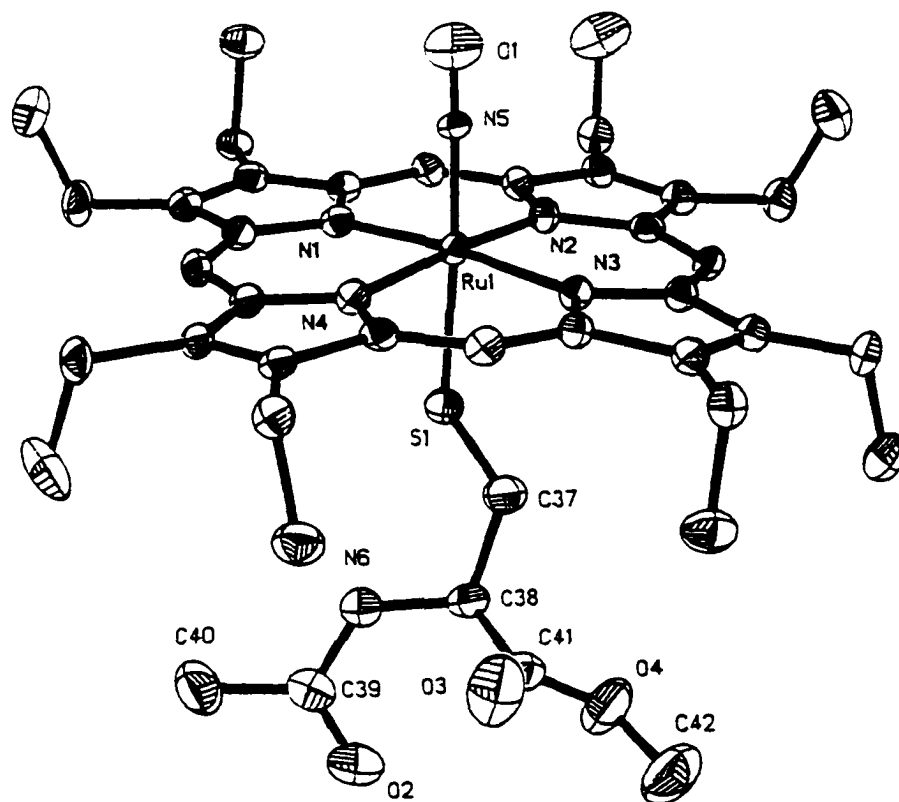
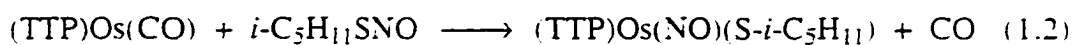


Figure 1.1. Molecular structure of (OEP)Ru(NO)(SR)
(SR = *N*-acetyl-L-cysteine methyl ester).²³

It has also been demonstrated that (TTP)Os(CO) reacts with isoamyl thionitrite to give the *trans* addition product (TTP)Os(NO)(S-*i*-C₅H₁₁) (eq 1.2).^{23b}



The identity of the product was also confirmed by single-crystal X-ray diffraction (Figure 1.2).

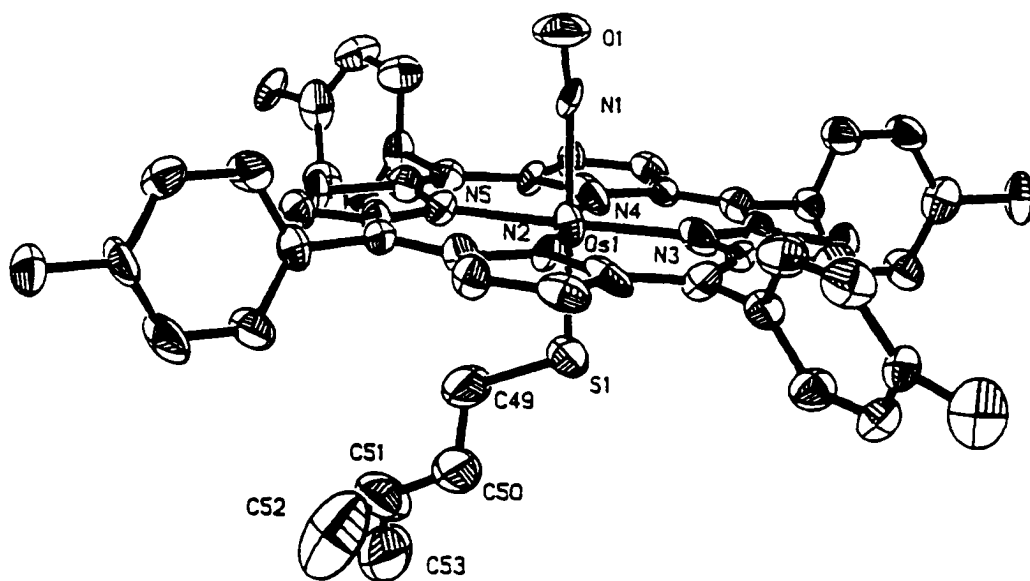
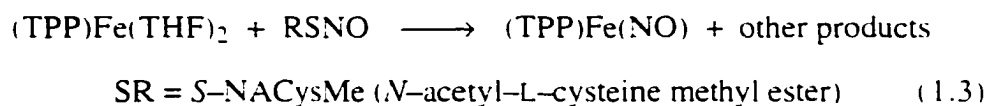


Figure 1.2. Molecular structure of (TTP)Os(NO)(S-*i*-C₅H₁₁).^{23b}

Unlike the reactions with Ru^{II} and Os^{II}, however, the reaction of (TPP)Fe^{II}(THF)₂ (TPP = 5, 10, 15, 20-tetraphenylporphyrinato dianion) with *S*-nitroso-*N*-acetyl-L-cysteine methyl ester generates the known five-coordinate (TPP)Fe(NO) complex (eq 1.3).



NO is known to form adducts with NO synthase and cytochrome P450 although some of these NO adducts are known to decompose to form the five-coordinate (por)Fe(NO) derivatives. Therefore, it is conceivable that, in this reaction, the *trans* addition product (TPP)Fe(NO)(SR) forms first, which then decomposes to give the (TPP)Fe(NO) complex.

Although a number of ruthenium porphyrin nitrosyls are now known,^{20b,23-26} only four osmium porphyrin nitrosyls were reported prior to our initial studies, namely (OEP)Os(NO)X (X = F, NO, OMe, OClO₃),²⁷ with X-ray structural data on osmium nitrosyl porphyrins being available only for (TTP)Os(NO)(*S*-*i*-C₅H₁₁).^{23b} This chapter focuses on the extension of the reaction chemistry involving osmium porphyrins with thionitrites and alkyl nitrites. This work also provides new chemical insight on the mode of interaction of RSNO and RONO ligands with osmium porphyrins.

Experimental Section

All reactions were performed under an atmosphere of prepurified nitrogen using standard Schlenk techniques and/or in an Innovative Technology Labmaster 100 Dry Box unless stated otherwise. Solvents were distilled from appropriate drying agents under nitrogen just prior to use: CH_2Cl_2 (CaH₂), benzene (Na), hexane (Na/benzophenone/tetraglyme), and THF (Na/benzophenone).

Chemicals. $(\text{TTP})\text{Os}(\text{CO})$,²⁸ $(\text{OEP})\text{Os}(\text{CO})$ ²⁸ and $[(\text{OEP})\text{Os}]_2$ ^{29a} were prepared by literature methods. The known $[(\text{OEP})\text{Os}]_2(\text{PF}_6)_2$ ^{29b} was prepared by AgPF_6 oxidation of $[(\text{OEP})\text{Os}]_2$. Isoamyl nitrite (*i*-C₅H₁₁ONO, 97%), isoamyl thiol (mercaptan, *i*-C₅H₁₁SH, 97%), *n*-butyl nitrite (95%), thiophenol (97%), AgPF_6 (98%), and NOPF_6 (96%) were purchased from Aldrich Chemical Co. Chloroform-*d* (99.8%) was obtained from Cambridge Isotope Laboratories, subjected to three freeze-pump-thaw cycles, and stored over Linde 4Å molecular sieves. Elemental analyses were performed by Atlantic Microlab, Norcross, GA. Nitric oxide (98%, Matheson Gas) was passed through KOH pellets and a cold trap (Dry Ice/acetone, -78 °C) to remove higher nitrogen oxides.

Instrumentation. Infrared spectra were recorded on a Bio-Rad FT-155 FTIR spectrometer. ¹H NMR spectra were obtained on a Varian XL-300 spectrometer and the signals were referenced to the residual signal of the solvent employed. All chemical shifts are in ppm. All coupling constants are in Hz. The ³¹P NMR spectrum was recorded on a Varian 400MHz spectrometer, and the signals were referenced to external H₃PO₄ (δ at 0 ppm). The ¹⁹F NMR spectrum was also recorded on the same 400MHz instrument, and the signals were referenced to external trifluoroacetic acid (δ at -79.45 ppm). FAB mass spectra were obtained on a VG-ZAB-E mass spectrometer. UV-vis spectra were recorded on a Hewlett-Packard HP8453 Diode Array instrument.

Preparation of Thionitrites. The preparations of thionitrites (*i*-C₅H₁₁SNO and PhSNO) follow established routes from their precursor thiols.³⁰ The following

example is representative: Isoamyl mercaptan (0.418g, 4.011 mmol) in acetic acid (2 mL) was treated with an aqueous solution (1 mL) of NaNO_2 (0.277g, 4.015mmol) at 0 °C. The solution turned deep red immediately. The red product was rapidly extracted with CH_2Cl_2 (20 mL) after 2 min of stirring. The organic layer was separated and washed with aqueous NaHCO_3 solution. The organic layer was separated again and dried over MgSO_4 to give CH_2Cl_2 solution of isoamyl thionitrite. The preparation of PhSNO was performed at low temperature (-8 °C), since this thionitrite decomposes at room temperature in solution.

Preparation of $(\text{OEP})\text{Os}(\text{NO})(\text{O}-n\text{-C}_4\text{H}_9)$. To a CH_2Cl_2 (20 mL) solution of $(\text{OEP})\text{Os}(\text{CO})$ (0.075 g, 0.100 mmol) was added excess *n*-butyl nitrite (0.4 mL, 3 mmol). The color of the solution changed from pink red to bright red immediately. The mixture was left to stir for 40 min. The mixture was taken to dryness and the residue was redissolved in CH_2Cl_2 . The solvent was allowed to evaporate under inert atmosphere to generate a crystalline solid residue. The resulting crystals were washed with hexane to remove a green-colored component, and the remaining solid was redissolved in CH_2Cl_2 /hexane (1:2) and filtered over a neutral alumina column in air. The column was washed with more of the solvent mixture, and then with CH_2Cl_2 until the washings were colorless. The filtrate was taken to dryness in vacuo, and the residue was dried in vacuo for 5 h to give $(\text{OEP})\text{Os}(\text{NO})(\text{O}-n\text{-C}_4\text{H}_9)\cdot 1.4\text{CH}_2\text{Cl}_2$ (0.055 g, 0.058 mmol, 58% yield). Anal. Calcd for $\text{C}_{40}\text{H}_{53}\text{O}_2\text{N}_5\text{Os}_1\cdot 1.4\text{CH}_2\text{Cl}_2$: C, 52.62; H, 5.95; N, 7.41; Cl, 10.50. Found: C, 52.32; H, 5.83; N, 7.56; Cl, 10.60. IR (CH_2Cl_2 , cm^{-1}): $\nu_{\text{NO}} = 1757$. IR (KBr, cm^{-1}): $\nu_{\text{NO}} = 1743$ s; also 2962 w, 2931 w, 2868 w, 1790 w, 1467 m, 1451 m, 1372 m, 1316 w, 1274 m, 1263 m, 1230 w, 1155 m, 1111 w, 1077 w, 1056 m, 1021 m, 993 m, 963 m, 860 w, 843 m, 764 w, 746 s, 718 w, 705 w, 596 m br. ^1H NMR (CDCl_3 , δ): 10.32 (s, 4H, *meso*-H of OEP), 5.27 (s, CH_2Cl_2), 4.16 (q, $J = 8$, 16H, CH_3CH_2 of OEP), 2.00 (t, $J = 8$, 24H, CH_3CH_2 of OEP), -0.55 (t, $J = 7$, 3H,

CH₃CH₂CH₂CH₂O). -1.53 (m (qt), *J* = 7/8, 2H, CH₃CH₂CH₂CH₂O). -2.73 (t, *J* = 7, 2H, CH₃CH₂CH₂CH₂O). -3.04 (m (tt), *J* = 8/7, 2H, CH₃CH₂CH₂CH₂O). Low-resolution mass spectrum (FAB): *m/z* 827 [(OEP)Os(NO)(OC₄H₉)]⁺ (17%), 754 [(OEP)Os(NO)]⁺ (100%), 724 [(OEP)Os]⁻ (19%). UV-vis spectrum (λ (ϵ , mM⁻¹ cm⁻¹), 1.31 x 10⁻⁵ M in CH₂Cl₂): 342 (40), 418 (91), 533 (17), 567 (26) nm.

A suitable crystal for structure determination was grown by slow evaporation of a CH₂Cl₂ solution of the compound.

Preparation of (TTP)Os(NO)(O-*i*-C₅H₁₁). A CH₂Cl₂ solution (10 mL) of (TTP)Os(CO) (0.065 g, 0.073 mmol) was reacted with *i*-C₅H₁₁ONO (0.20 mL, 1.4 mmol). The solution was gently heated and left to stir for 15 min. The color of the solution did not change very much (from red to purplish red). All the solvent was then removed in vacuo. The residue was redissolved in toluene (2 mL). Hexane (5 mL) was then added, and the resultant mixture was kept overnight at -20 °C. The supernatant solution was discarded, and the purple crystalline solid was washed with hexane (3 x 5 mL) and dried in vacuo for 3 h to give (TTP)Os(NO)(O-*i*-C₅H₁₁) (0.041 g, 0.042 mmol, 57% yield). Anal. Calcd for C₅₃H₄₇O₂N₅Os₁: C, 65.21; H, 4.85; N, 7.17. Found: C, 65.15; H, 4.93; N, 7.13. IR (CH₂Cl₂, cm⁻¹): ν_{NO} = 1766. IR (KBr, cm⁻¹): ν_{NO} = 1770 s; also 3024 w, 2947 w, 2918 w, 2865 w, 1806 w, 1528 w, 1512 w, 1494 w, 1455 w, 1365 w, 1351 m, 1306 w, 1214 m, 1183 m, 1110 w, 1075 m, 1018 s, 978 w, 848 w, 798 s, 719 m, 644 m, 599 w, 594 w, 523 m. ¹H NMR (CDCl₃, δ): 8.93 (s, 8H, *pyr*-H of TTP), 8.12 (app t (overlapping d's), 8H, *o*-H of TTP), 7.56 (m (overlapping d's), 8H, *m*-H of TTP), 2.70 (s, 12H, CH₃ of TTP), -0.61 (d, *J* = 7, 6H, (CH₃)₂CHCH₂CH₂O), -1.07 (m, 1H, (CH₃)₂CHCH₂CH₂O), -2.27 (t, *J* = 7, 2H, (CH₃)₂CHCH₂CH₂O), -2.82 (dt (app q), *J* = 7/7, 2H, (CH₃)₂CHCH₂CH₂O). Low-resolution mass spectrum (FAB): *m/z* 977 [(TTP)Os(NO)(O-*i*-C₅H₁₁)]⁺ (24%), 890 [(TTP)Os(NO)]⁺ (100%), 860 [(TTP)Os]⁺

(34%). UV-vis spectrum (λ (ϵ , mM⁻¹ cm⁻¹), 3.85 x 10⁻⁶ M in CH₂Cl₂): 317 (37), 437 (277), 551 (36), 588 (13) nm.

Preparation of (OEP)Os(NO)(O-*i*-C₅H₁₁). **Method I.** To a CH₂Cl₂ (20 mL) solution of (OEP)Os(CO) (0.080 g, 0.107 mmol) was added excess isoamyl nitrite (0.20 mL, 1.5 mmol). The color of the solution changed from pink red to bright red immediately. The solution was stirred for another 30 min. The mixture was taken to dryness in vacuo, and the product was redissolved in a CH₂Cl₂/hexane (1:2) mixture and filtered through a neutral alumina column in air. The column was washed with more of the solvent mixture until the washings were colorless. The filtrate was taken to dryness in vacuo, and the product obtained was dried in vacuo for 5 h to give (OEP)Os(NO)(O-*i*-C₅H₁₁)·0.85CH₂Cl₂ (0.050 g, 0.055 mmol, 51% yield). Anal. Calcd for C₄₁H₅₅O₂N₅Os₁·0.85CH₂Cl₂: C, 55.10; H, 6.26; N, 7.68; Cl, 6.61. Found: C, 54.86; H, 6.23; N, 7.74; Cl, 6.98. IR (CH₂Cl₂, cm⁻¹): ν_{NO} = 1756. IR (KBr, cm⁻¹): ν_{NO} = 1747 s; also 2962 w, 2928 w, 2864 w, 2020 w, 1954 w, 1794 w, 1685 w, 1560 w, 1508 w, 1465 s br, 1372 m, 1316 w, 1272 m, 1230 w, 1200 w, 1153 s, 1111 s, 1077 s, 1056 s, 1020 s, 993 m, 962 m, 856 w, 842 m, 744 s, 738 s, 717 m, 704 w, 642 w, 589 m. ¹H NMR (CDCl₃, δ): 10.31 (s, 4H, *meso*-H of OEP), 5.27 (s, CH₂Cl₂), 4.15 (q, J = 8, 16H, CH₃CH₂ of OEP), 1.99 (t, J = 8, 24H, CH₃CH₂ of OEP), -0.70 (d, J = 7, 6H, (CH₃)₂CHCH₂CH₂O), -1.19 (m, 1H, (CH₃)₂CHCH₂CH₂O), -2.72 (t, J = 8, 2H, (CH₃)₂CHCH₂CH₂O), -3.27 (dt (app q), J = 7/8, 2H, (CH₃)₂CHCH₂CH₂O). Low-resolution mass spectrum (FAB): m/z : 841 [(OEP)Os(NO)(O-*i*-C₅H₁₁)]⁺ (16%), 754 [(OEP)Os(NO)]⁺ (100%), 724 [(OEP)Os]⁺ (19%). UV-vis spectrum (λ (ϵ , mM⁻¹ cm⁻¹), 1.29 x 10⁻⁵ M in CH₂Cl₂): 341 (41), 418 (102), 533 (19), 567 (30) nm.

Method II. To a CH₂Cl₂ (15 mL) solution of [(OEP)Os]₂ (0.030 g, 0.021 mmol) was added excess isoamyl nitrite (0.10 mL, 0.75 mmol). The color of the solution changed from brown to bright red immediately. The mixture was left to stir

for another 3 h. The mixture was taken to dryness, and the residue was redissolved in CH₂Cl₂/hexane (1:2) and filtered over a neutral alumina column in air. The column was washed with more of the solvent mixture until the washings were colorless. The filtrate was taken to dryness in vacuo, and the residue was dried in vacuo for 3 h to give (OEP)Os(NO)(O-*i*-C₅H₁₁) in 29% isolated yield.

Preparation of (OEP)Os(NO)(S-*i*-C₅H₁₁). Method I. To a CH₂Cl₂ (20 mL) solution of (OEP)Os(CO) (0.080 g, 0.107 mmol) was added excess isoamyl thionitrite (ca. 1 mmol). The color of the solution changed gradually from pink red to bright red over a period of 1 h. The mixture was left to stir for another 4 h. The mixture was taken to dryness, and the residue was redissolved in CH₂Cl₂/hexane (1:2) and filtered over a neutral alumina column in air. The column was washed with more of the solvent mixture until the washings were colorless. The filtrate was taken to dryness in vacuo, and the residue was dried in vacuo for 5 h to give (OEP)Os(NO)(S-*i*-C₅H₁₁)·0.3CH₂Cl₂ (0.031 g, 0.035 mmol, 33% yield). Anal. Calcd for C₄₁H₅₅O₁S₁N₅O₈·0.3 CH₂Cl₂: C, 56.26; H, 6.36; N, 7.94; Cl, 2.41; S, 3.64. Found: C, 56.12; H, 6.39; N, 7.80; Cl, 2.58; S, 3.55. IR (CH₂Cl₂, cm⁻¹): ν_{NO} = 1757. IR (KBr, cm⁻¹): ν_{NO} = 1751 s; also 2964 w, 2932 w, 2870 w, 1467 m, 1450 m, 1373 w, 1316 w, 1271 m, 1229 w, 1154 m, 1110 w, 1057 m, 1020 m, 993 m, 962 m, 843 m, 746 m, 729 m, 717 w. ¹H NMR (CDCl₃, δ): 10.29 (s, 4H, *meso*-H of OEP), 5.28 (s, CH₂Cl₂), 4.14 (q br, 16H, CH₃CH₂ of OEP), 1.99 (t, *J* = 8, 24H, CH₃CH₂ of OEP), -0.35 (d, *J* = 6, 6H, (CH₃)₂CHCH₂CH₂S), -0.43 (m, 1H, (CH₃)₂CHCH₂CH₂S), -1.92 (dt (app q), *J* = 6/8, 2H, (CH₃)₂CHCH₂CH₂S), -3.26 (t, *J* = 8, 2H, (CH₃)₂CHCH₂CH₂S). Low-resolution mass spectrum (FAB): *m/z* 827 [(OEP)Os(S-*i*-C₅H₁₁)]⁺ (7%), 754 [(OEP)Os(NO)]⁺ (96%), 724 [(OEP)Os]⁺ (28%). UV-vis spectrum (λ (ε, mM⁻¹ cm⁻¹), 1.18 x 10⁻⁵ M in CH₂Cl₂): 354 (69), 441 (38), 551 (15), 584 (11) nm.

Method II. To a CH_2Cl_2 (15 mL) solution of $[(\text{OEP})\text{Os}]_2$ (0.030 g, 0.021 mmol) was added excess isoamyl thionitrite (ca. 0.7 mmol). The color of the solution changed from brown to bright red immediately. The mixture was left to stir for another 5 h. The mixture was taken to dryness, and the residue was redissolved in CH_2Cl_2 /hexane (1:2) and filtered over a neutral alumina column in air. The column was washed with more of the solvent mixture until the washings were colorless. The filtrate was taken to dryness in vacuo, and the residue was dried in vacuo for 3 h to give $(\text{OEP})\text{Os}(\text{NO})(\text{S-}i\text{-C}_5\text{H}_{11})$ in 33% isolated yield.

Preparation of $(\text{OEP})\text{Os}(\text{NO})(\text{SPh})$. To a CH_2Cl_2 solution of $(\text{OEP})\text{Os}(\text{CO})$ (0.064 g, 0.085 mmol) was added excess freshly prepared PhSNO (ca. 3 mmol), and the reaction was left to stir for 90 min. The color of the solution changed from pink red to bright red immediately. The mixture was taken to dryness in vacuo. The residue was redissolved in benzene and purified by chromatography using a neutral alumina column under nitrogen with benzene as first eluent. The green elute was discarded. A red fraction was then eluted with CH_2Cl_2 . All the solvent was removed from this elute, and the resulting solid was dried in vacuo for 5 h to give $(\text{OEP})\text{Os}(\text{NO})(\text{SPh})\cdot 0.65\text{CH}_2\text{Cl}_2$ (0.035 g, 0.038 mmol, 45% yield). Anal. Calcd for $\text{C}_{42}\text{H}_{49}\text{N}_5\text{O}_1\text{S}_1\text{Os}_1\cdot 0.65\text{CH}_2\text{Cl}_2$: C, 55.84; H, 5.53; N, 7.63; Cl, 5.02; S, 3.49. Found: C, 56.49; H, 5.69; N, 7.64; Cl, 5.39; S, 3.47. IR (CH_2Cl_2 , cm^{-1}): $\nu_{\text{NO}} = 1766$. IR (KBr, cm^{-1}): $\nu_{\text{NO}} = 1749$ s; also 2966 w, 2932 w, 2870 w, 1578 w, 1470 m, 1451 m, 1375 w, 1315 w, 1265 m, 1230 vw, 1154 m, 1111 w, 1057 m, 1021 m, 994 m, 963 m, 867 vw, 843 m, 740 m, 702 w, 689 w. ^1H NMR (CDCl_3 , δ): 10.20 (s, 4H, *meso*-H of OEP), 6.25 (t, $J = 7$, 1H, *p*-H of SPh), 5.84 (t, $J = 7$, 2H, *m*-H of SPh), 5.28 (s, CH_2Cl_2), 4.12 (q, $J = 8$, 16H, CH_3CH_2 of OEP), 2.82 (d, $J = 7$, 2H, *o*-H of SPh), 1.99 (t, $J = 8$, 24H, CH_3CH_2 of OEP). Low-resolution mass spectrum (FAB): m/z 863 $[(\text{OEP})\text{Os}(\text{NO})(\text{SPh})]^+$ (5%), 833 $[(\text{OEP})\text{Os}(\text{SPh})]^+$ (23%), 754

$[(\text{OEP})\text{Os}(\text{NO})]^+$ (100%), 724 $[(\text{OEP})\text{Os}]^+$ (23%). UV-vis spectrum (λ , ϵ , $\text{mM}^{-1}\text{cm}^{-1}$), $1.40 \times 10^{-5}\text{ M}$ in CH_2Cl_2 : 363 (58), 451 (25), 555 (12), 589 (8) nm.

Preparation of $(\text{OEP})\text{Os}(\text{SPh})_2$.³¹ To a CH_2Cl_2 (20 mL) solution of $[(\text{OEP})\text{Os}]_2$ (0.040 g, 0.028 mmol) was added $\text{O}_2\text{NC}_6\text{H}_4\text{N}=\text{NSPh}$ ³² (0.030 g, 0.116 mmol). Effervescence (a white smoke) was seen right after mixing the reagents. The color of the solution changed from brown to purple over a 1 h period. The mixture was left to stir for another 1 h. All the solvent was then removed, the residue was redissolved in a benzene/hexane mixture (1:5), and the product was purified by neutral alumina column chromatography in air. Elution with hexane and then benzene/hexane (1:5) produced a yellow band which was discarded. Further elution with CH_2Cl_2 /hexane (1:3) produced a purple band, which was collected. The solvent was removed from the purple solution, and the product was dried in vacuo for 5 h to give the known $(\text{OEP})\text{Os}(\text{SPh})_2$ ³¹ (0.022 g, 0.023 mmol, 41% yield) which was identified by ^1H NMR spectroscopy and by X-ray crystallography. IR (KBr, cm^{-1}): 2964 w, 2931 w, 2865 w, 1725 w, 1576 w, 1536 w, 1470 m, 1447 m, 1436 w, 1372 w, 1316 w, 1266 m, 1226 w, 1149 m, 1111 w, 1084 w, 1056 m, 1020 s, 992 m, 961 m, 924 w, 865 w, 842 m, 740 s, 719 w, 700 w, 686 m.

A suitable crystal for structure determination was obtained by slow evaporation of a CH_2Cl_2 /toluene solution of the compound at room temperature under inert atmosphere.

Reaction of $[(\text{OEP})\text{Os}]_2(\text{PF}_6)_2$ with Isoamyl Thionitrite. To a CH_2Cl_2 (20 mL) solution of $[(\text{OEP})\text{Os}]_2(\text{PF}_6)_2$ (0.040 g, 0.023 mmol) was added excess isoamyl thionitrite (ca. 1.5 mmol). The color of the solution changed from brown to red. A solution IR spectrum of the reaction mixture after 10 min revealed the quantitative conversion of $[(\text{OEP})\text{Os}]_2(\text{PF}_6)_2$ to $[(\text{OEP})\text{Os}(\text{NO})](\text{PF}_6)$, indicated by the presence of a new band at 1829 cm^{-1} assigned to ν_{NO} and a band at 847 cm^{-1} assigned to ν_{PF_6} . The reaction mixture was stirred for an additional 20 min, and the mixture was

taken to dryness. An IR spectrum of the residue (as a KBr pellet) at this stage showed the presence of noticeable bands at 1816 and 1787 cm^{-1} and also at 840 cm^{-1} . Exposure of the solid to air for 30 h resulted in the formation of only one ν_{NO} band at 1808 cm^{-1} . The peak at 840 cm^{-1} assigned to ν_{PF_6} , also disappeared. Crystallization by slow solvent evaporation of a CH_2Cl_2 solution of the solid gives $(\text{OEP})\text{Os}(\text{NO})(\text{O}_2\text{PF}_2)$, which was identified by single-crystal X-ray crystallographic analysis (A suitable crystal of $(\text{OEP})\text{Os}(\text{NO})(\text{O}_2\text{PF}_2)$ for structure determination was grown from a saturated solution of $[(\text{OEP})\text{Os}]_2(\text{PF}_6)_2$ and isoamyl thionitrite in CH_2Cl_2 left under nitrogen for 25 days, followed by slow evaporation of the solution in a dry box for 2 days.).

Alternate Preparation of $(\text{OEP})\text{Os}(\text{NO})(\text{O}_2\text{PF}_2)$. $(\text{OEP})\text{Os}(\text{CO})$ (0.060 g, 0.080 mmol) and NOPF_6 (0.015 g, 96%, 0.082 mmol) were dissolved in CH_2Cl_2 (20 mL). A solution IR spectrum of the reaction mixture showed the disappearance of the starting $(\text{OEP})\text{Os}(\text{CO})$ ($\nu_{\text{CO}} = 1883 \text{ cm}^{-1}$) and the formation of $[(\text{OEP})\text{Os}(\text{NO})]\text{PF}_6$ ($\nu_{\text{NO}} = 1833 \text{ cm}^{-1}$; $\nu_{\text{PF}_6} = 848 \text{ cm}^{-1}$). The mixture was left to stir for 40 min and exposed to air for 3 days. The mixture was then filtered through a neutral alumina column in air with CH_2Cl_2 as eluent. All the solvent was removed from the filtrate thus obtained, and the resulting solid was dried in vacuo overnight to give $(\text{OEP})\text{Os}(\text{NO})(\text{O}_2\text{PF}_2)$ (0.019 g, 0.022 mmol, 28% yield). A sample for elemental analyses was obtained from crystallization of a CH_2Cl_2 /hexane solution by slow evaporation of the solvent mixture at room temperature and drying the crystalline solid in vacuo for 5 h. Anal. Calcd for $\text{C}_{36}\text{H}_{44}\text{O}_3\text{P}_1\text{F}_2\text{N}_5\text{Os}_1 \cdot 0.2\text{hexane}$: C, 51.29; H, 5.41; N, 8.04. Found: C, 51.58; H, 5.41; N, 7.92. IR (CH_2Cl_2 , cm^{-1}): $\nu_{\text{NO}} = 1820$. IR (KBr, cm^{-1}): $\nu_{\text{NO}} = 1808$ s; also 2969 w, 2932 w, 2872 w, 1464 w, 1451 w, 1383 w, 1374 w, 1324 s, 1275 w, 1260 w, 1229 w, 1156 m, 1116 m, 1105 m, 1058 m, 1022 m, 996 m, 964 m, 887 m, 856 m, 847 m. ^1H NMR (CDCl_3 , δ): 10.47 (s, 4H, *meso*-H of OEP), 4.20 (q, $J = 8$, 16H, CH_3CH_2 of OEP), 2.01 (t, $J = 8$, 24H,

CH_2CH_2 of OEP), 1.25 (hexane). ^{31}P NMR ($CDCl_3$, 400MHz, δ): -27.85 (t, $J_{P,F} = 985$). ^{19}F NMR ($CDCl_3$, 400MHz, δ): -89.49 (d, $J_{P,F} = 985$). Low-resolution mass spectrum (FAB): m/z 855 [(OEP)Os(NO)(O₂PF₂)]⁺ (11%), 754 [(OEP)Os(NO)]⁻ (13%). UV-vis spectrum (λ (ϵ , mM⁻¹ cm⁻¹), 1.66 x 10⁻⁵ M in benzene): 347 (42), 374 (44), 421 (62), 539 (14), 575 (24) nm.

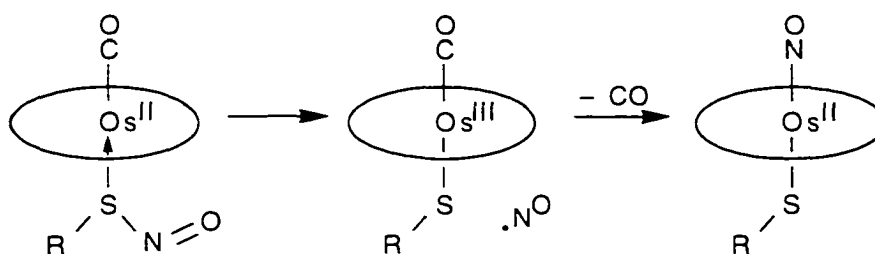
The analogous compound (OEP)Os(NS)(O₂PF₂) was prepared via the following route:³³ To a CH₂Cl₂ (20 mL) solution of (OEP)Os(NS)Cl (0.040g, 0.050 mmol) was added H₂O (1.4 μ L, 0.078 mmol) and AgPF₆ (0.013g, 0.051 mmol). The mixture was left to stir under nitrogen for 48 h, and the solution was filtered under nitrogen and dried in vacuo for 3h to give (OEP)Os(NS)(O₂PF₂) (0.043g, 0.048 mmol, 98% yield).

The identity of the product is confirmed by a single-crystal X-ray crystallographic analysis. A suitable crystal for structure determination was obtained by slow evaporation of a saturated CH₂Cl₂ solution under nitrogen for 4 days.

Results and Discussion

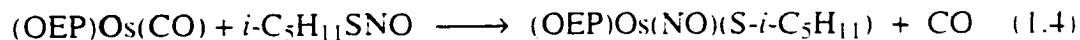
In this chapter, we will provide spectroscopic and chemical evidence to support the process outlined in Scheme 1.1. We propose that RSNO compounds add to Os^{II} porphyrins via an initial S-binding of RSNO, followed by homolytic S-NO bond cleavage and subsequent displacement of CO by NO. We propose a similar reaction pathway for RONO compounds as well.

Scheme 1.1



The first part of this Results and Discussion section deals with RSNO additions to the (OEP)Os(CO) compound (RONO additions will also be included). *Trans* additions of RSNO and RONO to the non-carbonyl-containing [(OEP)Os]₂ dimer will also be discussed. This will be followed by additional successful reactions that shed chemical insight on the general reaction pathway outlined in Scheme 1.1. Finally, the reaction of isoamyl thionitrite with a cationic (OEP)Os^{III} complex will be discussed.

Addition of RSNO to (OEP)Os(CO). The reaction of (OEP)Os(CO) with isoamyl thionitrite in CH₂Cl₂ at room temperature gives, after workup, the (OEP)Os(NO)(S-*i*-C₅H₁₁) *trans* addition product in 33% non-optimized yield (eq 1.4).

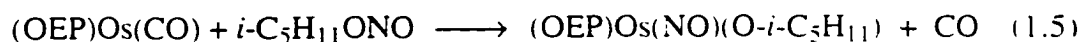


This red nitrosyl thiolate product is moderately air-stable, showing no signs of decomposition in air (as judged by ^1H NMR and IR spectroscopy) for at least 5 h in solution and several days in the solid state. This nitrosyl thiolate is freely soluble in CH_2Cl_2 but only slightly soluble in hexane. The ^1H NMR spectrum of $(\text{OEP})\text{Os}(\text{NO})(\text{S-}i\text{-C}_5\text{H}_{11})$ in CDCl_3 shows sharp peaks for the OEP macrocycle and the thiolate ligand, consistent with the diamagnetic nature of this formally d^6 Os^{II} complex. The IR spectrum of the complex (as a KBr pellet) shows a band at 1751 cm^{-1} assigned to ν_{NO} . This value of ν_{NO} is consistent with this $\{\text{Os}(\text{NO})\}^6$ complex having a linear $\text{Os}-\text{NO}$ linkage according to the Enemark–Feltham notation.³⁴ The UV–vis spectrum of the complex in CH_2Cl_2 reveals four bands at 354 (69), 441 (38), 551 (15) and 584 (11) nm, corresponding to a *hypso/hyper* metalloporphyrin.³⁵

The related reaction of $(\text{OEP})\text{Os}(\text{CO})$ with PhSNO in CH_2Cl_2 generates the $(\text{OEP})\text{Os}(\text{NO})(\text{SPh})$ thiophenolate product in 45% isolated yield. This dark-red product has similar solubility properties as the $(\text{OEP})\text{Os}(\text{NO})(\text{S-}i\text{-C}_5\text{H}_{11})$ analog. In contrast to $(\text{OEP})\text{Os}(\text{NO})(\text{S-}i\text{-C}_5\text{H}_{11})$, however, this nitrosyl thiophenolate complex is air-sensitive. The sharp peaks in the ^1H NMR spectrum of $(\text{OEP})\text{Os}(\text{NO})(\text{SPh})$ is also consistent with its diamagnetic nature. Only one triplet and one quartet for the ethyl groups of the OEP macrocycle were observed, indicating a fast rotation of the ethyl groups (of OEP) on the ^1H NMR timescale at room temperature. The FAB mass spectrum shows the formation of the parent ion $[(\text{OEP})\text{Os}(\text{NO})(\text{SPh})]^+$, and the $[(\text{OEP})\text{Os}(\text{SPh})]^+$ and $[(\text{OEP})\text{Os}(\text{NO})]^+$ fragments. The ν_{NO} of 1766 cm^{-1} of $(\text{OEP})\text{Os}(\text{NO})(\text{SPh})$ in CH_2Cl_2 is 9 cm^{-1} higher than that of the related alkyl thiolate $(\text{OEP})\text{Os}(\text{NO})(\text{S-}i\text{-C}_5\text{H}_{11})$, although the ν_{NO} 's of both nitrosyl thiolates as KBr pellets are identical. The UV–vis spectrum in CH_2Cl_2 is similar to that of $(\text{OEP})\text{Os}(\text{NO})(\text{S-}i\text{-C}_5\text{H}_{11})$ and also corresponds to a *hypso/hyper* type of metalloporphyrin.³⁵

IR monitoring of the reaction of PhSNO with (OEP)Os(CO) in CH₂Cl₂ reveals that in addition to the ν_{CO} band of starting (OEP)Os(CO) at 1883 cm⁻¹ and the ν_{NO} band of the thiophenolate (OEP)Os(NO)(SPh) product at 1766 cm⁻¹, a new *higher* band at 1957 cm⁻¹ is observed. This new band is attributed (consistent with earlier similar results)^{23b} to an intermediate carbonyl Os^{III} complex (OEP)Os(CO)(SPh) (Figure 1.3). In time, only the product band remains. The higher ν_{CO} for the tentatively assigned (OEP)Os(CO)(SPh) relative to that of the starting (OEP)Os(CO) compound is consistent with the increased oxidation state of Os^{III} in the (OEP)Os^{III}(CO)(SPh) intermediate relative to Os^{II} in (OEP)Os(CO), resulting in less backbonding to carbonyl. Additional support for the Os^{III} formulation comes from a recent report by Gross who isolated authentic (TMP)Os(CO)(Br) (TMP = 5, 10, 15, 20-tetramesitylporphyrinato anion) which has a ν_{CO} of 1933 cm⁻¹, higher than that of the parent (TMP)Os(CO) at 1920 cm⁻¹.³⁶

Addition of RONO to (por)Os(CO). Interestingly, the RSNO addition reaction can be extended to include the related RONO compounds. Thus, the reaction of (OEP)Os(CO) with isoamyl nitrite in CH₂Cl₂ at room temperature gives (OEP)Os(NO)(O-*i*-C₅H₁₁) in 51% isolated yield (eq 1.5). This red nitrosyl alkoxide



product is moderately air-stable, showing no signs of decomposition for at least 8 h in solution and several days in the solid state. This compound has similar solubility properties as its thiolate analog described earlier. The ν_{NO} of 1747 cm⁻¹ (as a KBr pellet) is only 4 cm⁻¹ lower than that of the thiolate analog, although their ν_{NO} 's in CH₂Cl₂ solution are identical.

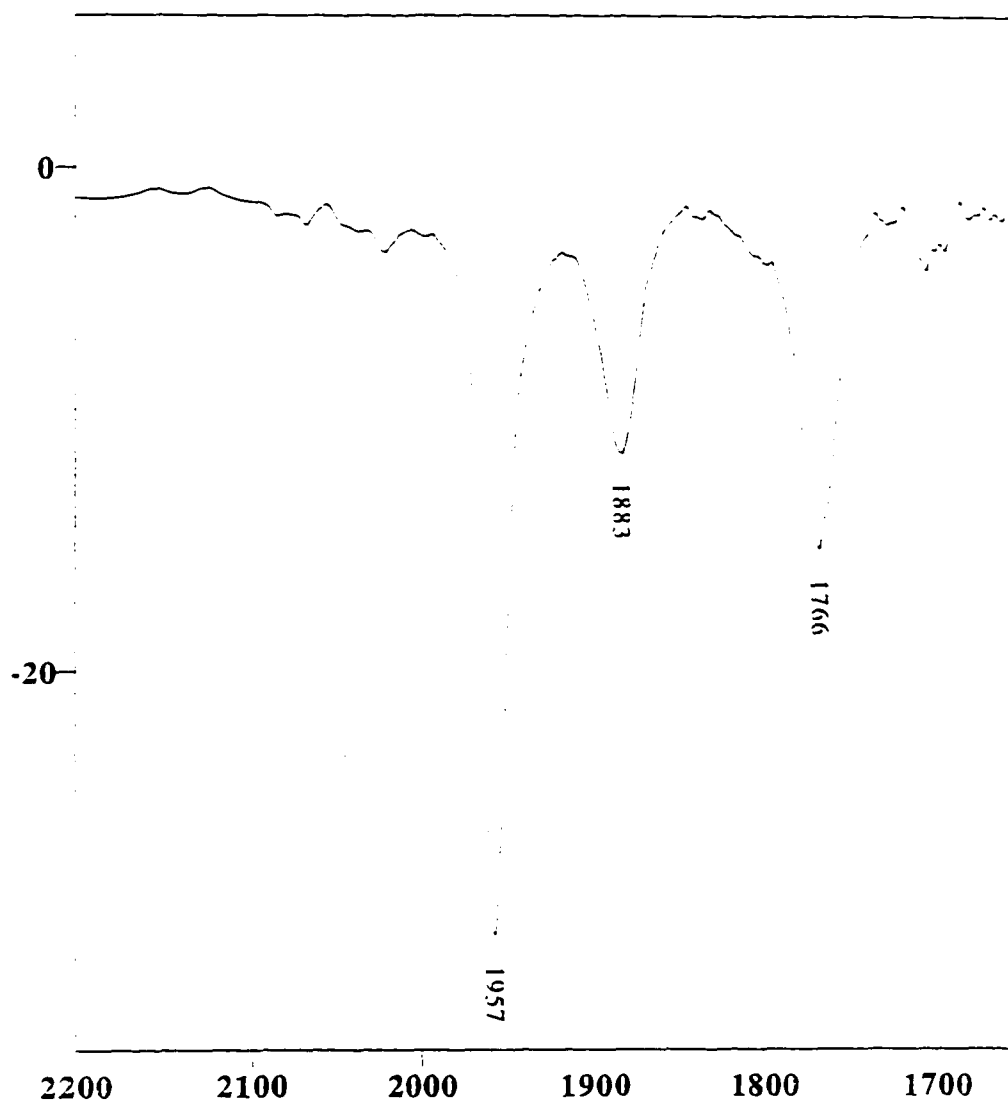


Figure 1.3. IR spectrum of the reaction solution (CH_2Cl_2) containing the starting $(\text{OEP})\text{Os}(\text{CO})$ ($\nu_{\text{CO}} = 1883 \text{ cm}^{-1}$), intermediate $(\text{OEP})\text{Os}(\text{CO})(\text{SPh})$ ($\nu_{\text{CO}} = 1957 \text{ cm}^{-1}$), and the final $(\text{OEP})\text{Os}(\text{NO})(\text{SPh})$ product ($\nu_{\text{NO}} = 1766 \text{ cm}^{-1}$).

The TTP analog, (TTP)Os(NO)(O-*i*-C₅H₁₁), is prepared in 57% isolated yield by the reaction of (TTP)Os(CO) with isoamyl nitrite. This red product has similar solubility and stability properties as its OEP analog. The UV-vis spectrum of the complex in CH₂Cl₂ gives four bands at 317 (37), 437 (277), 551 (36) and 588 (13) nm, also corresponding to a *hypo/hyper* type of metalloporphyrin.³⁵ The ν_{NO} for the product (as a KBr pellet, 1770 cm⁻¹) is higher than that of the OEP analog (1747 cm⁻¹). This is consistent with the TTP macrocycle acting as a better π acceptor than the OEP macrocycle, resulting in less backbonding to the NO ligand for (TTP)Os(NO)(O-*i*-C₅H₁₁) when compared with its OEP analog.

An intermediate for the reaction of (TTP)Os(CO) ($\nu_{\text{CO}} = 1898$ cm⁻¹) with isoamyl nitrite in CH₂Cl₂ is observed to form when the reaction is monitored by IR spectroscopy (Figure 1.4). A new band appears in the IR spectrum at 1968 cm⁻¹ in CH₂Cl₂ and is tentatively assigned as the ν_{CO} of the (TTP)Os(CO)(O-*i*-C₅H₁₁) intermediate complex. A third band at 1766 cm⁻¹ (CH₂Cl₂) is assigned as the ν_{NO} for the (TTP)Os(NO)(O-*i*-C₅H₁₁) product. In time, the ν_{CO} bands for both the intermediate and the starting material disappeared, and only the ν_{NO} band of the product remained.

We have found that other alkyl nitrites also add to (OEP)Os(CO). For example, the (OEP)Os(NO)(O-*n*-C₄H₉) compound was prepared in 58% isolated yield by the reaction of (OEP)Os(CO) with *n*-butyl nitrite. The IR spectrum of the complex (as a KBr pellet) shows a band at 1743 cm⁻¹ assigned to ν_{NO} . This value is similar to those of (OEP)Os(NO)(OMe)^{27b} (1745 cm⁻¹) and (OEP)Os(NO)(O-*i*-C₅H₁₁) (1747 cm⁻¹) and is indicative of the complex possessing a linear Os-NO linkage. Not surprisingly, the UV-vis spectra of the complexes (OEP)Os(NO)(O-*n*-C₄H₉) and (OEP)Os(NO)(O-*i*-C₅H₁₁) in CH₂Cl₂ are almost identical to that of previously reported (OEP)Os(NO)(OMe).^{26,27}

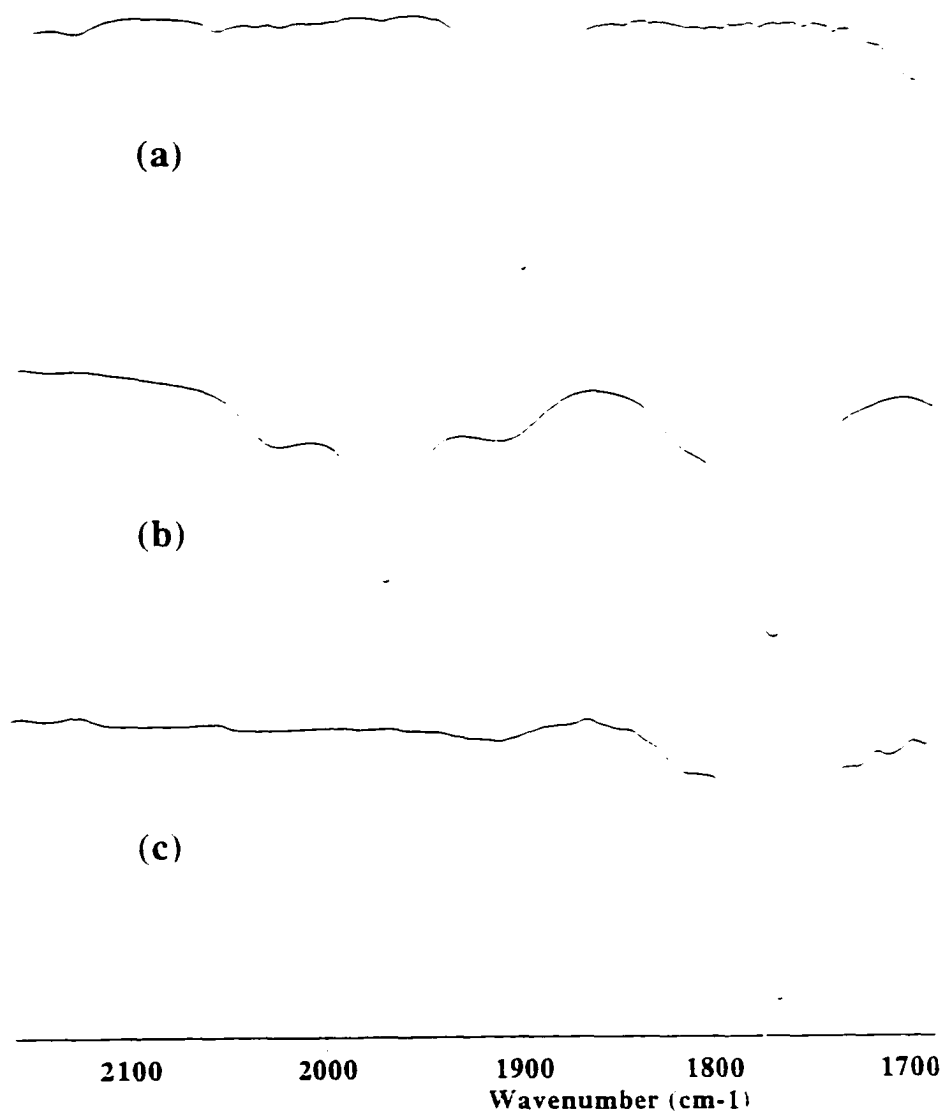


Figure 1.4. IR monitoring (in CH_2Cl_2) of the reaction of $(\text{TTP})\text{Os}(\text{CO})$ ($\nu_{\text{CO}} = 1898 \text{ cm}^{-1}$, spectrum a) with isoamyl nitrite to give $(\text{TTP})\text{Os}(\text{NO})(\text{O}-i\text{-C}_5\text{H}_{11})$ ($\nu_{\text{NO}} = 1766 \text{ cm}^{-1}$, spectrum c). spectrum b: after addition of isoamyl nitrite, showing the intermediate $(\text{TTP})\text{Os}(\text{CO})(\text{O}-i\text{-C}_5\text{H}_{11})$ ($\nu_{\text{CO}} = 1968 \text{ cm}^{-1}$) and the product $(\text{TTP})\text{Os}(\text{NO})(\text{O}-i\text{-C}_5\text{H}_{11})$.

The linearity of the Os–NO linkage in (OEP)Os(NO)(O-*n*-C₄H₉) was confirmed by a single-crystal X-ray crystallographic analysis of a suitable crystal of the compound (grown by slow evaporation of a CH₂Cl₂ solution of the complex at room temperature under nitrogen). The molecular structure of the compound is shown in Figure 1.5. The bond lengths and bond angles are listed in Tables 1.1 and 1.2. The NO group and the O-*n*-C₄H₉ group are *trans* to each other, with an N(5)–Os(1)–O(2) bond angle of 176.5(3)°. The butoxide C(37) nearly eclipses a porphyrin nitrogen, with an N(2)–Os(1)–O(2)–C(37) torsion angle of 18.4°. The Os–N(O) and N–O bond lengths of 1.833(8) and 1.173(11) Å are comparable with those of other structurally characterized osmium nitrosyl complexes (Table 1.3). The Os–N–O linkage is linear, with a bond angle of 172.8(8)°. The average Os–N(por) bond length of 2.056 Å is within the range for other structurally characterized osmium porphyrin complexes containing axial *O*- and *S*- donor ligands (Table 1.4). The axial Os–O distance of 1.877(7) Å appears short⁵⁴ relative to the 1.909(4)–2.200(7) Å previously observed for Os alkoxides;⁵⁵ however, it is longer than that observed for Os=O bonds in osmium porphyrins (Table 1.4, bottom). The Os–O–C alkoxide bond angle of 130.8(9)° falls within the 123.1(2)–133.8(8)° range seen for other Os alkoxides.⁵⁵

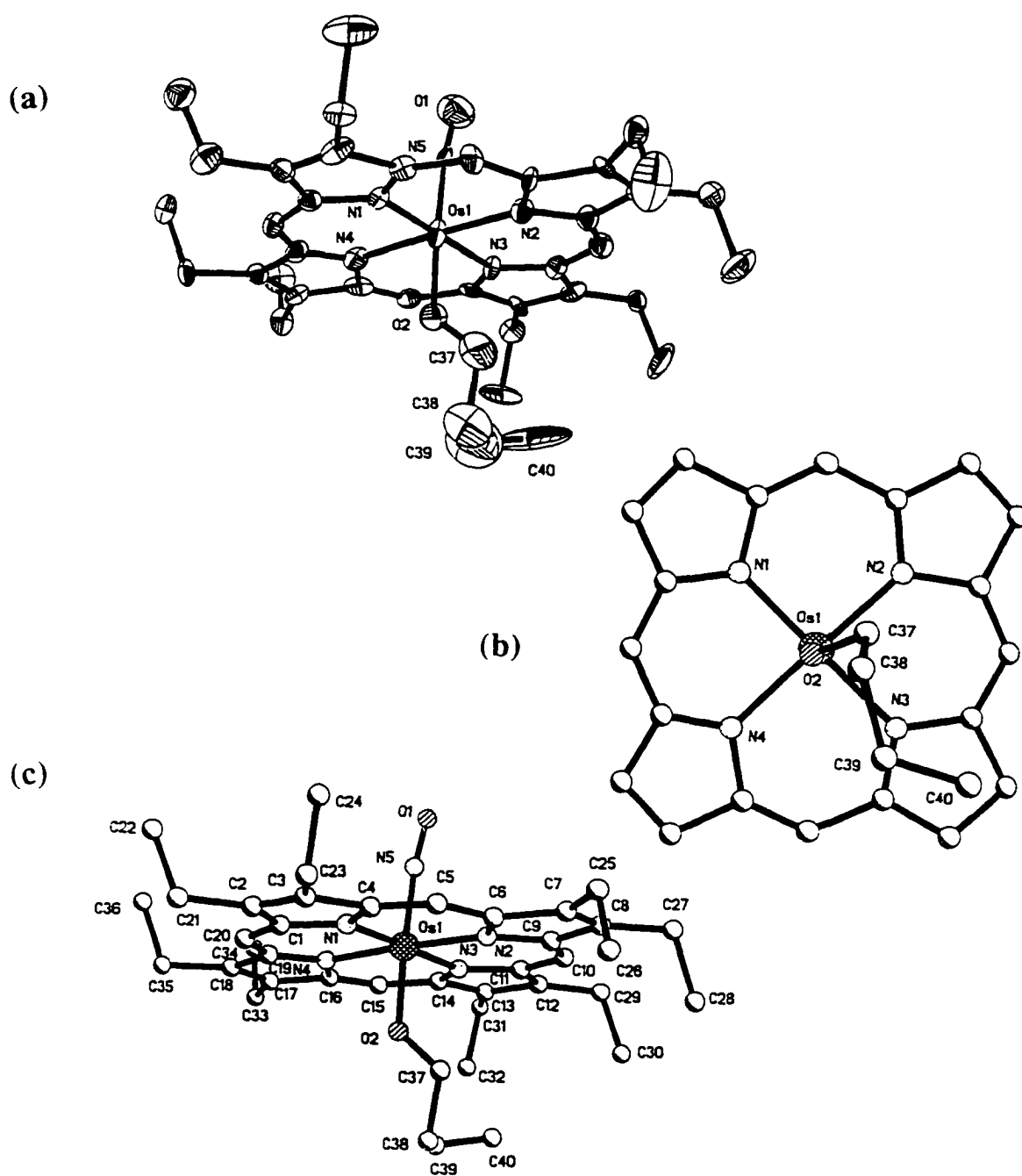


Figure 1.5. (a) Molecular structure of (OEP)Os(NO)(O-*n*-C₄H₉). (b) View along the O(2)–Os(1) bond showing the orientation of the axial *n*-C₄H₉ alkoxide ligand relative to the porphyrin core. (c) Ball and stick structure showing the labeling of the atoms.

Table 1.1. Bond Lengths (Å) for (OEP)Os(NO)(O-*n*-C₄H₉)

Os(1)-N(5)	1.833(8)	Os(1)-O(2)	1.877(7)
Os(1)-N(1)	1.986(9)	Os(1)-N(3)	2.051(7)
Os(1)-N(2)	2.078(8)	Os(1)-N(4)	2.109(8)
N(5)-O(1)	1.173(11)	O(2)-C(37)	1.26(2)
N(1)-C(1)	1.372(12)	N(1)-C(4)	1.435(12)
N(2)-C(6)	1.371(11)	N(2)-C(9)	1.398(12)
C(1)-C(20)	1.397(9)	C(1)-C(2)	1.435(12)
C(2)-C(3)	1.36(2)	C(2)-C(21)	1.467(14)
C(3)-C(23)	1.474(14)	C(3)-C(4)	1.49(2)
C(4)-C(5)	1.367(13)	C(5)-C(6)	1.394(12)
C(6)-C(7)	1.470(12)	C(7)-C(8)	1.328(13)
C(7)-C(25)	1.469(12)	C(8)-C(27)	1.474(14)
C(8)-C(9)	1.496(12)	C(9)-C(10)	1.366(13)
C(10)-C(11)	1.404(9)	C(21)-C(22)	1.509(14)
C(23)-C(24)	1.524(14)	C(25)-C(26)	1.53(2)
C(27)-C(28)	1.545(14)	N(3)-C(14)	1.356(12)
N(3)-C(11)	1.357(12)	N(4)-C(19)	1.300(12)
N(4)-C(16)	1.374(11)	C(11)-C(12)	1.445(12)
C(12)-C(13)	1.414(13)	C(12)-C(29)	1.490(13)
C(13)-C(14)	1.387(14)	C(13)-C(31)	1.523(13)
C(14)-C(15)	1.424(13)	C(15)-C(16)	1.319(13)
C(16)-C(17)	1.454(13)	C(17)-C(18)	1.334(13)
C(17)-C(33)	1.555(12)	C(18)-C(19)	1.448(11)
C(18)-C(35)	1.532(12)	C(19)-C(20)	1.380(13)
C(29)-C(30)	1.523(14)	C(31)-C(32)	1.537(14)

C(33)-C(34)	1.49(2)	C(35)-C(36)	1.526(14)
C(41)-Cl(1)	1.67(2)	C(41)-Cl(2)	1.71(2)
C(37)-C(38)	1.51(2)	C(38)-C(39)	1.48(2)
C(39)-C(40)	1.42(2)		

Table 1.2. Bond Angles ($^{\circ}$) for (OEP)Os(NO)(O-*n*-C₄H₉)

O(1)-N(5)-Os(1)	172.8(8)	C(37)-O(2)-Os(1)	130.8(9)
N(5)-Os(1)-O(2)	176.5(3)	N(5)-Os(1)-N(1)	92.9(3)
O(2)-Os(1)-N(1)	90.3(3)	N(5)-Os(1)-N(3)	87.5(3)
O(2)-Os(1)-N(3)	89.3(3)	N(1)-Os(1)-N(3)	179.6(2)
N(5)-Os(1)-N(2)	87.4(3)	O(2)-Os(1)-N(2)	91.1(2)
N(1)-Os(1)-N(2)	90.4(3)	N(3)-Os(1)-N(2)	89.6(2)
N(5)-Os(1)-N(4)	94.6(2)	O(2)-Os(1)-N(4)	86.8(3)
N(1)-Os(1)-N(4)	90.5(3)	N(3)-Os(1)-N(4)	89.6(3)
N(2)-Os(1)-N(4)	177.7(2)	C(1)-N(1)-C(4)	110.4(8)
C(1)-N(1)-Os(1)	125.6(6)	C(4)-N(1)-Os(1)	123.8(6)
C(6)-N(2)-C(9)	104.6(7)	C(6)-N(2)-Os(1)	128.4(6)
C(9)-N(2)-Os(1)	126.8(6)	N(1)-C(1)-C(20)	125.3(7)
N(1)-C(1)-C(2)	107.7(7)	C(20)-C(1)-C(2)	127.0(7)
C(3)-C(2)-C(1)	109.5(8)	C(3)-C(2)-C(21)	126.7(9)
C(1)-C(2)-C(21)	123.8(8)	C(2)-C(3)-C(23)	131.6(10)
C(2)-C(3)-C(4)	108.3(9)	C(23)-C(3)-C(4)	120.1(10)
C(5)-C(4)-N(1)	128.8(9)	C(5)-C(4)-C(3)	127.0(8)
N(1)-C(4)-C(3)	104.1(8)	C(4)-C(5)-C(6)	125.8(8)
N(2)-C(6)-C(5)	122.8(8)	N(2)-C(6)-C(7)	112.3(7)
C(5)-C(6)-C(7)	124.9(8)	C(8)-C(7)-C(25)	126.2(8)

C(8)-C(7)-C(6)	106.1(8)	C(25)-C(7)-C(6)	127.7(8)
C(7)-C(8)-C(27)	128.2(8)	C(7)-C(8)-C(9)	107.7(8)
C(27)-C(8)-C(9)	124.0(8)	C(10)-C(9)-N(2)	123.9(8)
C(10)-C(9)-C(8)	126.9(9)	N(2)-C(9)-C(8)	109.2(7)
C(9)-C(10)-C(11)	126.5(8)	C(2)-C(21)-C(22)	113.7(9)
C(3)-C(23)-C(24)	115.7(8)	C(7)-C(25)-C(26)	113.4(10)
C(8)-C(27)-C(28)	110.3(9)	C(14)-N(3)-C(11)	108.9(8)
C(14)-N(3)-Ost(1)	125.7(6)	C(11)-N(3)-Ost(1)	125.3(6)
C(19)-N(4)-C(16)	108.3(8)	C(19)-N(4)-Ost(1)	126.1(6)
C(16)-N(4)-Ost(1)	125.6(6)	N(3)-C(11)-C(10)	127.7(7)
N(3)-C(11)-C(12)	108.4(8)	C(10)-C(11)-C(12)	123.8(8)
C(13)-C(12)-C(11)	105.3(8)	C(13)-C(12)-C(29)	131.0(8)
C(11)-C(12)-C(29)	123.6(8)	C(14)-C(13)-C(12)	107.3(8)
C(14)-C(13)-C(31)	126.1(8)	C(12)-C(13)-C(31)	126.6(8)
N(3)-C(14)-C(13)	110.0(8)	N(3)-C(14)-C(15)	125.1(9)
C(13)-C(14)-C(15)	124.7(9)	C(16)-C(15)-C(14)	129.3(8)
C(15)-C(16)-N(4)	124.6(8)	C(15)-C(16)-C(17)	128.4(8)
N(4)-C(16)-C(17)	107.0(8)	C(18)-C(17)-C(16)	108.1(8)
C(18)-C(17)-C(33)	127.5(9)	C(16)-C(17)-C(33)	124.4(8)
C(17)-C(18)-C(19)	105.2(8)	C(17)-C(18)-C(35)	127.3(8)
C(19)-C(18)-C(35)	127.4(8)	N(4)-C(19)-C(20)	124.5(8)
N(4)-C(19)-C(18)	111.4(8)	C(20)-C(19)-C(18)	124.1(8)
C(19)-C(20)-C(1)	127.9(8)	C(12)-C(29)-C(30)	110.9(9)
C(13)-C(31)-C(32)	113.6(8)	C(34)-C(33)-C(17)	111.8(8)
C(36)-C(35)-C(18)	110.7(8)	Cl(1)-C(41)-Cl(2)	121.0(11)
O(2)-C(37)-C(38)	118.1(14)	C(39)-C(38)-C(37)	104(2)
C(40)-C(39)-C(38)	124(2)		

Table 1.3. Structural Parameters (in Å and °) for Osmium Nitrosyl Complexes^a

compound	coord no.	M–N(O)	N–O	M–N–O
(OEP)Os(NO)(O- <i>n</i> -Bu) ^b	6	1.833(8)	1.173(11)	172.8(8)
(OEP)Os(NO)(O ₂ PF ₂) ^b	6	1.711(6)	1.179(8)	174.3(6)
[(OEP)Os(NO)] ₂ (μ-O) ^c	6	1.778(11)	1.143(13)	180.0
(TTP)Os(NO)(S- <i>i</i> -C ₅ H ₁₁) ^{2,3b}	6	2.041(7)	1.086(10)	172.0(9)
[(η ⁵ C ₅ H ₅)Os(NO)(PMe ₃) ₂](PF ₆) ₂ ³⁷	6	1.747(11)	1.17(2)	179.8(15)
Os(NO)(η ² -O,O-ON=C(O)CF ₃)- (O ₂ CCF ₃)(PPh ₃) ₂ ³⁸	6	1.726(7)	1.209(9)	176.1(6)
Os(NO)(Cl) ₂ (CF ₃)(PPh ₃) ₂ ³⁹	6	1.741(9)	1.175(12)	180.0
<i>trans</i> -[Os(NO)(tpy)(Cl) ₂](BF ₄) ⁴⁰	6	1.704(14)	1.188(19)	176.6(10)
Os(NO)(Cl) ₂ (η ¹ -CH=C=CPh ₂)(P ^t Pr ₃) ₂ ⁴¹	6	1.733(6)	1.106(8)	174.4(5)
[(DMSO) ₂ H][Os(NO)(DMSO)(Cl) ₄] ^{42a}	6	1.717(8)	1.16(1)	179.2(8)
Cs{ <i>mer</i> [Os(NO)Cl ₃ (acac)]} ^{42b}	6	1.729(9)	1.16(1)	177(1)
Os(NO){η ² -C,O-CH ₂ CH ₂ - S(O)NSO ₂ tol}(Cl)(PPh ₃) ₂ ^{43a}	6	1.706(9)	1.179	174.7
Os(NO)(=CH ₂)(Cl)(PPh ₃) ₂ ^{43b}	5	1.93(1) ^d	0.915 ^d	155.4(2)
Os(NO)Br ₃ (Et ₂ S)(Et ₂ SO) ⁴⁴	6	1.712(22)	1.148(31)	174.3(29)
Os(NO)Cl ₂ (OCH ₂ CH ₂ OMe)(PPhEt ₂) ₂ ⁴⁴	6	1.837(10)	1.098(14)	177.3(8)
[MePPh ₃][Os(NO)(Cl) ₄] ⁴⁵	5	1.89(2)	0.90(3)	177(2)
[Os(NO) ₂ (OH)(PPh ₃) ₂](PF ₆) ⁴⁶	5	1.63(1)	1.24(2)	178(1)
		1.86(1) ^d	1.17(2) ^d	134(1)

^a All of these complexes appear to contain Os^{II}, with the exception of [(DMSO)₂H][Os(NO)(DMSO)(Cl)₄] which contains Os^{III}. ^b this work. ^c chapter 3.

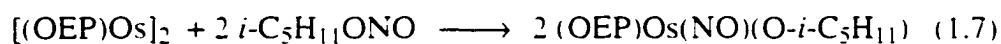
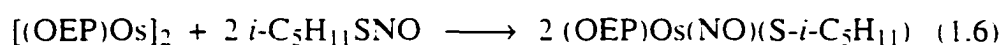
^d bent NO.

Table 1.4. Structurally Characterized Monometallic Osmium Porphyrins
with O- and S- Donor Ligands⁴⁷

compound	oxid. state	Os-N _p (Å)	Os-X (Å) (axial)	Os-X-Y (°)
<i>nitrosyl</i>				
(OEP)Os(NO)(O- <i>n</i> -Bu) ^a	II	1.986(9), 2.078(8) 2.051(7), 2.109(8)	1.877(7)	130.8(9)
(OEP)Os(NO)(O ₂ PF ₂) ^a	II	2.060(6), 2.053(5) 2.065(6), 2.067(6)	2.046(5)	138.7(3)
(TTP)Os(NO)(S- <i>i</i> - C ₅ H ₁₁) ^{23b}	II	2.035(5), 2.074(8) 2.076(9), 2.049(6)	2.209(3)	111.8(5)
<i>non-nitrosyl</i>				
(OEP)Os(OPPh ₃) ₂ ⁴⁸	II	2.031(8), 2.027(8)	2.036(7)	154.2(5)
(OEP)Os(PMS) ₂ ^{b, 49}	II	2.057(5), 2.044(5)	2.352(2)	110.3(3) 110.4(3)
[(OEP)Os(PMS) ₂]- (PF ₆) ^{b, 49}	III	2.047(4), 2.044(4)	2.382(2)	109.94(20) 109.81(21)
(OEP)Os(SPh) ₂ ^a	IV	2.047(4), 2.050(4)	2.295(1)	110.9(2)
(TTP)Os(SC ₆ F ₄ H) ₂ ⁵⁰	IV	2.041(6), 2.057(6)	2.294(3)	107.8(3)
(TPP)Os(OR) ₂ ⁵¹	IV			
R = Et		2.046(5), 2.038(5)	1.915(4)	128.2(5)
R = <i>i</i> -Pr		2.042(3), 2.040(3)	1.909(4)	127.0(3)
R = Ph		2.042(3), 2.038(2)	1.938(2)	127.5(2)
(OEP)Os(O) ₂ ⁵²	VI	2.052(6)	1.745(5)	
(TTP)Os(O) ₂ ⁵³	VI	2.065(4), 2.067(4)	1.743(3)	

^a this work. ^b Data from Supporting Material obtained via the Internet.

Addition of RSNO and RONO to [(OEP)Os]₂. The non-carbonyl-containing [(OEP)Os]₂ was employed as a reagent in the isoamyl thionitrite and isoamyl nitrite addition reactions in order to determine whether the presence of the carbonyl ligand in (OEP)Os(CO) is needed for the activation of the RSNO and RONO compounds. Interestingly, the same formal *trans* addition products are also obtained from the reactions of [(OEP)Os]₂ with isoamyl thionitrite (eq 1.6) and isoamyl nitrite (eq 1.7). Importantly, the success of eqs 1.6 and 1.7 implies that the presence of the



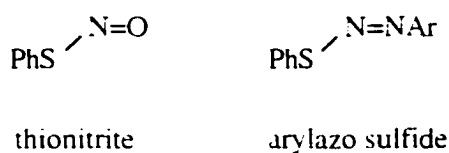
carbonyl ligand (e.g., in eqs 1.4 and 1.5) is not required for the activation of the RSNO and RONO compounds towards formal *trans* addition across the metal center.

Further Investigation of the Reaction Pathway for RSNO Addition. We propose that alkyl nitrites and thionitrites react with Os^{II} porphyrins via *O,S*-coordination of the RONO/RSNO groups (e.g. Scheme 1.1), followed by homolytic cleavage of the RO–NO or RS–NO bonds. In this pathway, rapid diffusion of the stable NO radical to the metal site (intra- and/or intermolecularly) results in a substitution of CO to give the final nitrosyl alkoxide and thiolate products.

This reaction pathway is supported by the IR spectral observations of (i) the reaction of (OEP)Os(CO) ($\nu_{\text{CO}} = 1883 \text{ cm}^{-1}$, in CH₂Cl₂) with PhSNO to give (OEP)Os^{III}(CO)(SPh) ($\nu_{\text{CO}} = 1957 \text{ cm}^{-1}$, CH₂Cl₂), followed by the replacement of CO by NO to give the final (OEP)Os(NO)(SPh) product ($\nu_{\text{NO}} = 1766 \text{ cm}^{-1}$, CH₂Cl₂), and (ii) the reaction of (TTP)Os(CO) ($\nu_{\text{CO}} = 1898 \text{ cm}^{-1}$, in CH₂Cl₂) with isoamyl nitrite to first generate the (TTP)Os^{III}(CO)(OR) intermediate ($\nu_{\text{CO}} = 1968 \text{ cm}^{-1}$, CH₂Cl₂).

followed by the replacement of CO by NO to give the final (TTP)Os(NO)(OR) product ($\nu_{\text{NO}} = 1766 \text{ cm}^{-1}$, CH_2Cl_2).

We continue to explore the reaction pathway for RSNO addition to metalloporphyrins. In particular, the well-used concept of the “element displacement principle”⁵⁶ was invoked to investigate the nature of RSNO additions to Os^{II} porphyrins. PhSNO is valence isoelectronic with compounds of the form PhSN=NAr (phenyl arylazo sulfides),³²⁻⁵⁷ where a simple formal replacement of the O atom in PhSNO with the valence isoelectronic NAr group will generate the “equivalent” phenyl arylazo sulfide. This concept has been utilized successfully in metal–nitrosyl (M–NO)



and metal–arylazo (M–N₂Ar) comparisons.⁵⁸ For example, both nitrosyl and arylazo groups can act as one- or three-electron donors in their transition metal complexes. Furthermore, the structural and electronic properties of metal–arylazo complexes are also similar to their nitrosyl analogs.

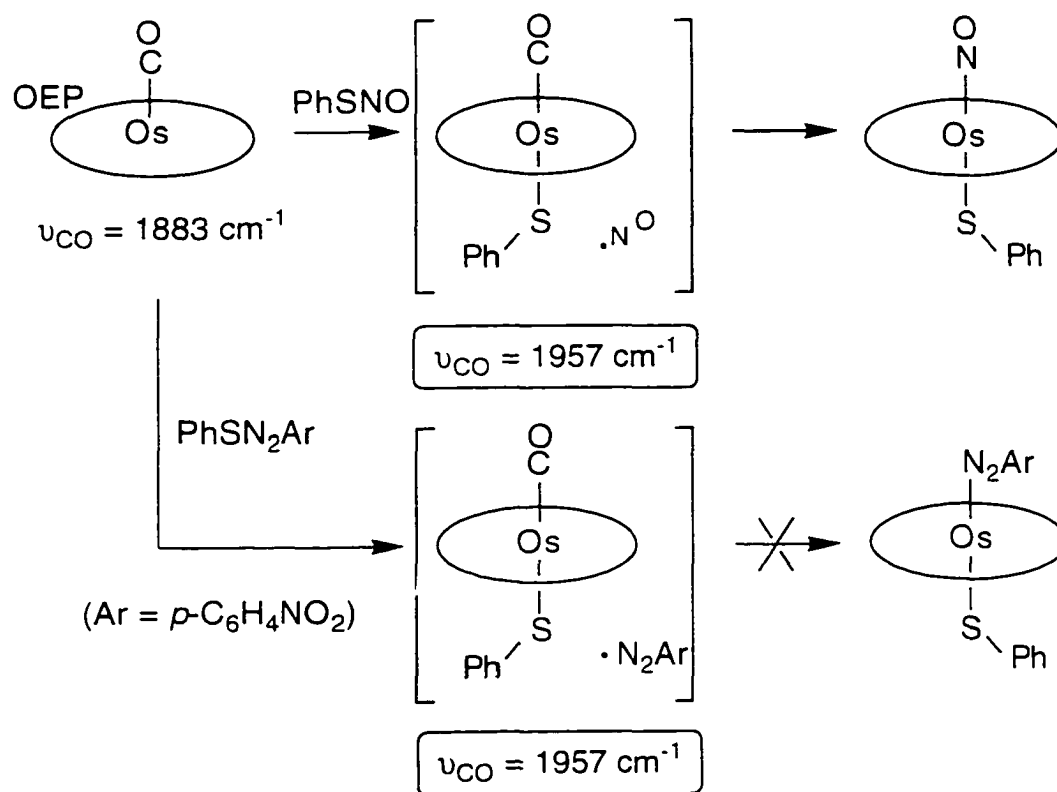
For the purpose of examining the sequence of reactions described in Scheme 1.1, the valence isoelectronic PhSN=NC₆H₄(*p*-NO₂) compound was employed in place of PhSNO, and the outcomes of these two reactions are compared (Scheme 1.2). It is conceivable that the success of the proposed Scheme 1.1 depends on the known stability of the NO radical, enabling it to diffuse rapidly to displace the bound carbonyl from the osmium center. Since the ·N₂Ar radical is generally not stable,⁵⁹ it would not be expected to survive the reaction conditions to displace CO (Scheme 1.2, bottom) to form the (OEP)Os(N₂Ar)(SPh) addition product.⁶⁰ If this is so, then any observed band in the carbonyl region of the IR spectrum should be due to ν_{CO} and not ν_{NO} , since there is no NO present in the reaction mixture when the phenyl arylazo sulfide is used.

Indeed, IR monitoring of the reaction of (OEP)Os(CO) with PhSN=NC₆H₄(*p*-NO₂) reveals the formation of the band at 1957 cm⁻¹ assigned to the intermediate carbonyl (OEP)Os(CO)(SPh) complex (Scheme 1.2, bottom). We have not been able to isolate this thermally unstable intermediate. However, reaction of this intermediate with NO gas (2 min) gives a 1:1 mixture of (OEP)Os(NO)(SPh) and the known (OEP)Os(NO)₂^{27b} (by IR spectroscopy). This latter compound forms from the reaction of NO with unreacted (OEP)Os(CO)^{27b} and (OEP)Os(NO)(SPh). In time, the intensity of the IR band for the dinitrosyl compound increases while the intensity of the IR band for the (OEP)Os(NO)(SPh) compound decreases.

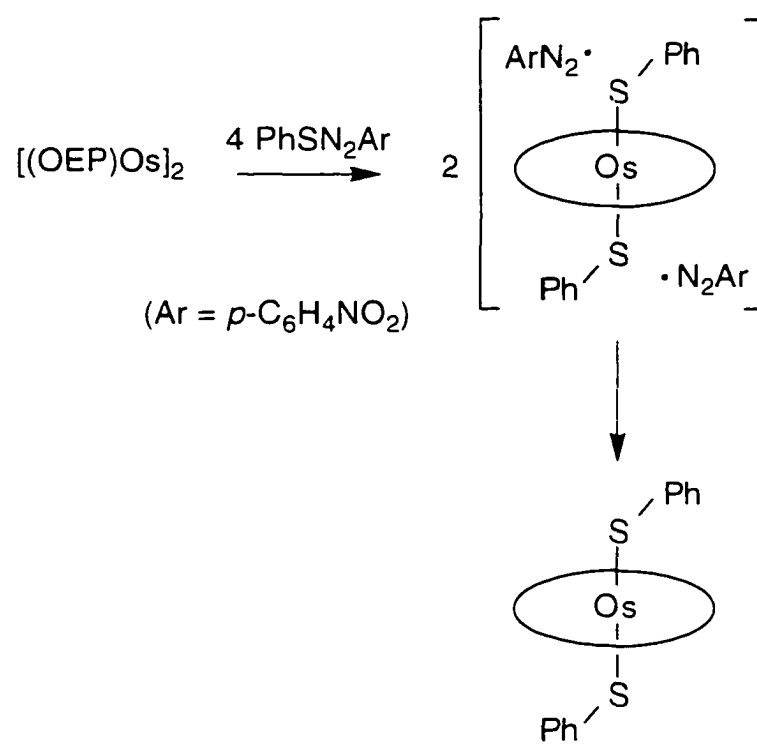
To further confirm the similarity of *S*-binding of PhSNO and PhSN=NAr to give the (OEP)Os(CO)(SR) thiolate intermediate, the non-carbonyl-containing [(OEP)Os]₂ dimer was employed instead of (OEP)Os(CO), with the intention of incorporating two *S*-bound ligands on opposite sides of the Os center. Remarkably, the reaction of [(OEP)Os]₂ with 4 equiv of PhSN=NAr (i.e., 2 equiv per Os center) gives the known compound (OEP)Os(SPh)₂ in 41% isolated yield,³¹ presumably via a bis-adduct intermediate which undergoes homolytic cleavage of the *S*-N bonds to give the known bis-thiolate species³¹ (Scheme 1.3). Importantly, the success of the reaction in Scheme 1.3 provides further chemical evidence for the *S*-binding of RSNO to Os^{II} porphyrins.

A suitable crystal of the moderately air-stable bis-thiolate Os^{IV} porphyrin complex was successfully obtained by slow evaporation of a CH₂Cl₂/toluene solution of the compound for a single-crystal X-ray crystallographic analysis. The molecular structure of the complex is shown in Figure 1.6. The bond lengths and bond angles are listed in Tables 1.5 and 1.6.

Scheme 1.2



Scheme 1.3



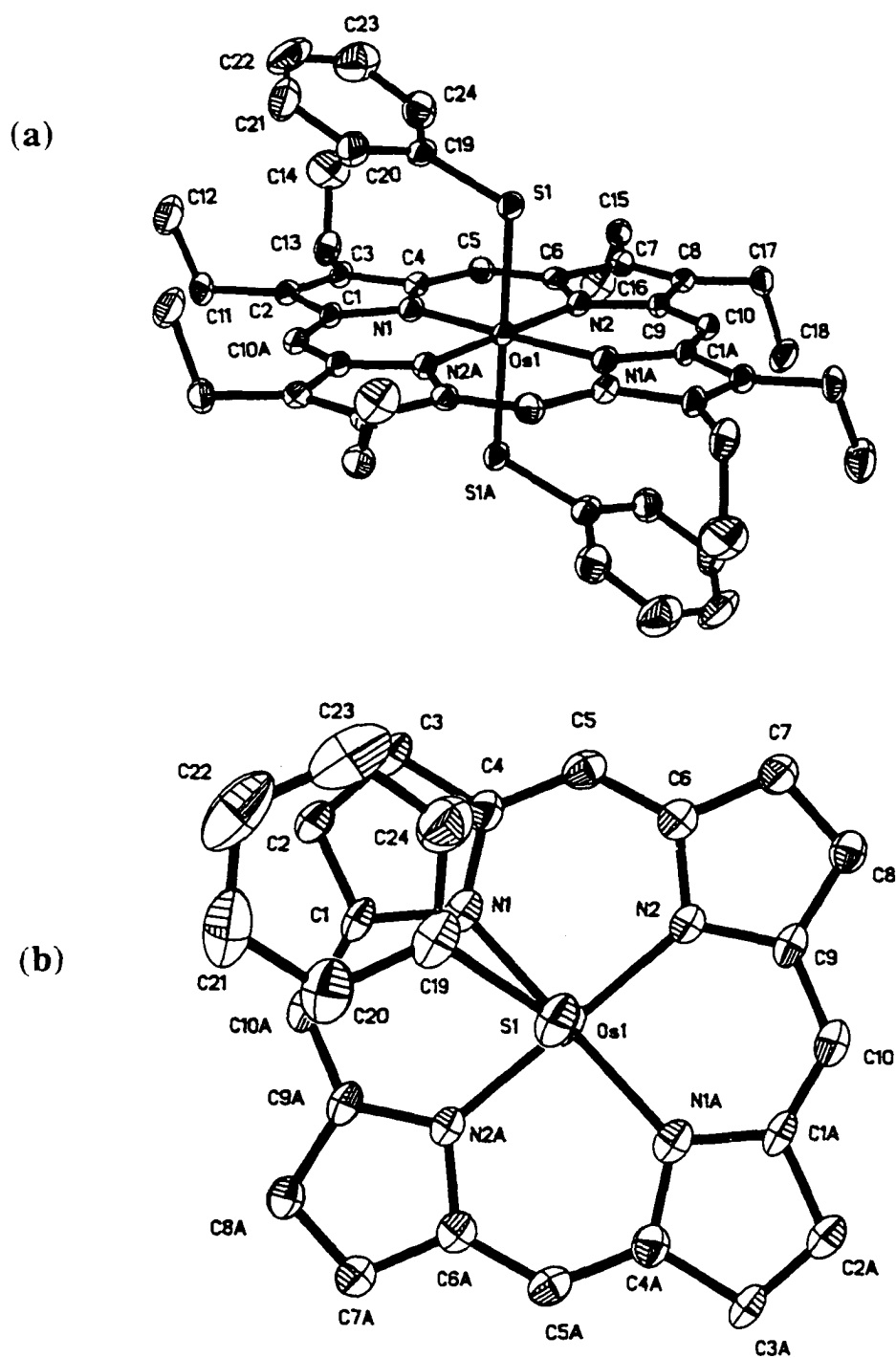


Figure 1.6. (a) Molecular structure of $(\text{OEP})\text{Os}(\text{SPh})_2$. (b) View of the thiolate orientation relative to the porphyrin core, with the view along the $\text{S}(1)\text{--Os}(1)$ bond.

Table 1.5. Bond Lengths (Å) for (OEP)Os(SPh)₂

Os(1)-N(1)	2.047(4)	Os(1)-N(1)A	2.047(4)
Os(1)-N(2)	2.050(4)	Os(1)-N(2)A	2.050(4)
Os(1)-S(1)	2.2952(12)	Os(1)-S(1)A	2.2953(12)
S(1)-C(19)	1.782(5)	N(1)-C(4)	1.370(6)
N(1)-C(1)	1.389(6)	N(2)-C(9)	1.379(5)
N(2)-C(6)	1.381(6)	C(1)-C(10)A	1.373(7)
C(1)-C(2)	1.445(6)	C(2)-C(3)	1.361(7)
C(2)-C(11)	1.501(7)	C(3)-C(4)	1.460(6)
C(3)-C(13)	1.494(7)	C(4)-C(5)	1.388(6)
C(5)-C(6)	1.388(6)	C(6)-C(7)	1.444(7)
C(7)-C(8)	1.368(7)	C(7)-C(15)	1.511(7)
C(8)-C(9)	1.446(7)	C(8)-C(17)	1.500(6)
C(9)-C(10)	1.388(7)	C(10)-C(1)A	1.373(7)
C(11)-C(12)	1.504(8)	C(13)-C(14)	1.485(8)
C(15)-C(16)	1.507(7)	C(17)-C(18)	1.515(8)
C(19)-C(24)	1.371(9)	C(19)-C(20)	1.394(7)
C(20)-C(21)	1.394(8)	C(21)-C(22)	1.364(10)
C(22)-C(23)	1.387(10)	C(23)-C(24)	1.377(10)

Table 1.6. Bond Angles (°) for (OEP)Os(SPh)₂

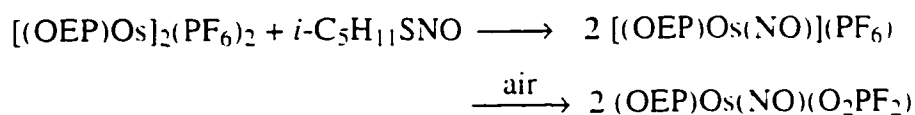
N(1)A-Os(1)-N(1)	180.0	N(1)A-Os(1)-N(2)A	90.4(2)
N(1)-Os(1)-N(2)A	89.6(2)	N(1)A-Os(1)-N(2)	89.6(2)
N(1)-Os(1)-N(2)	90.4(2)	N(2)A-Os(1)-N(2)	179.998(2)
N(1)A-Os(1)-S(1)	86.88(11)	N(1)-Os(1)-S(1)	93.12(11)

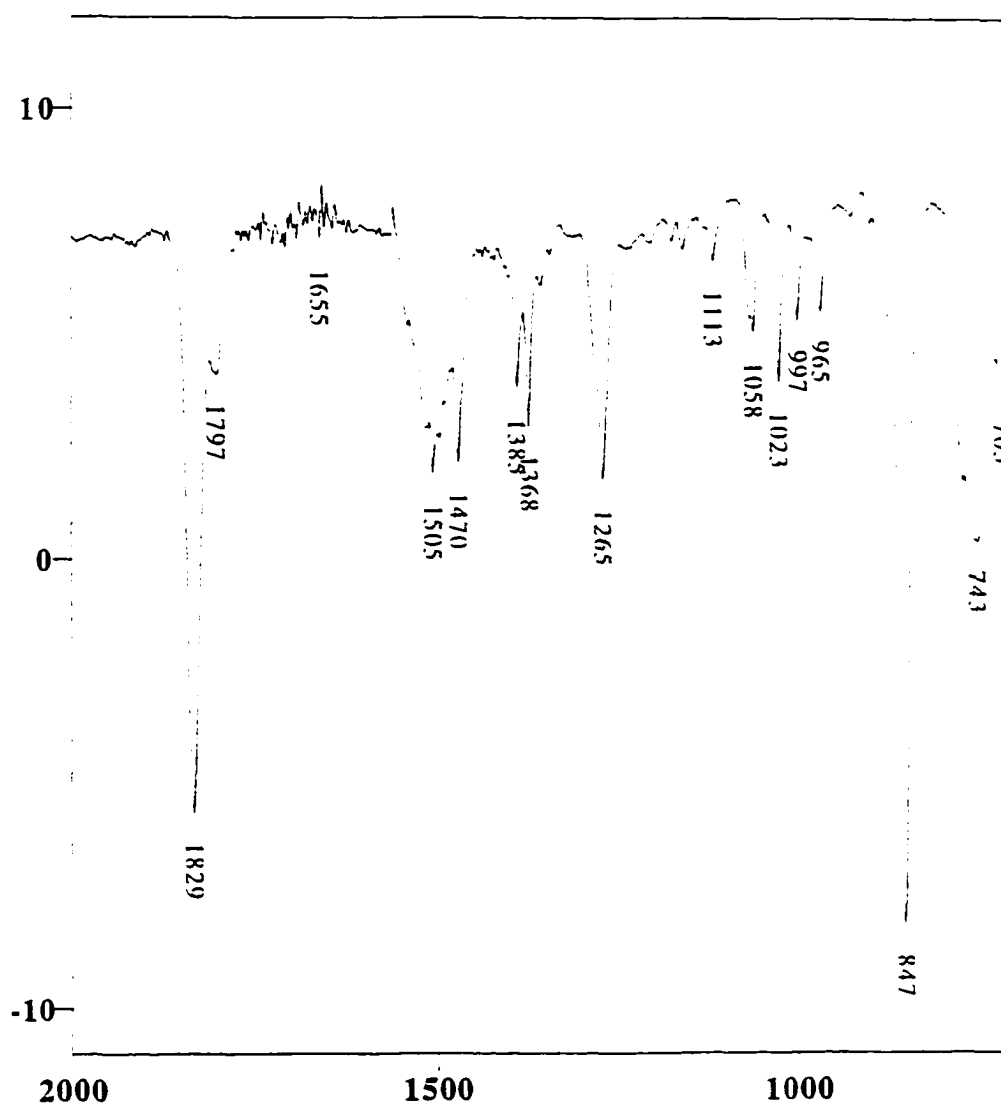
N(2)A-Os(1)-S(1)	90.71(11)	N(2)-Os(1)-S(1)	89.29(11)
N(1)A-Os(1)-S(1)A	93.12(11)	N(1)-Os(1)-S(1)A	86.88(11)
N(2)A-Os(1)-S(1)A	89.29(11)	N(2)-Os(1)-S(1)A	90.71(11)
S(1)-Os(1)-S(1)A	180.0	C(19)-S(1)-Os(1)	110.9(2)
C(4)-N(1)-C(1)	106.8(4)	C(4)-N(1)-Os(1)	126.4(3)
C(1)-N(1)-Os(1)	126.8(3)	C(9)-N(2)-C(6)	107.2(4)
C(9)-N(2)-Os(1)	126.7(3)	C(6)-N(2)-Os(1)	126.1(3)
C(10)A-C(1)-N(1)	124.4(4)	C(10)A-C(1)-C(2)	126.2(4)
N(1)-C(1)-C(2)	109.4(4)	C(3)-C(2)-C(1)	107.3(4)
C(3)-C(2)-C(11)	127.9(4)	C(1)-C(2)-C(11)	124.7(4)
C(2)-C(3)-C(4)	106.9(4)	C(2)-C(3)-C(13)	128.5(4)
C(4)-C(3)-C(13)	124.5(4)	N(1)-C(4)-C(5)	124.6(4)
N(1)-C(4)-C(3)	109.5(4)	C(5)-C(4)-C(3)	125.8(4)
C(6)-C(5)-C(4)	128.2(4)	N(2)-C(6)-C(5)	124.3(4)
N(2)-C(6)-C(7)	109.1(4)	C(5)-C(6)-C(7)	126.5(4)
C(8)-C(7)-C(6)	107.3(4)	C(8)-C(7)-C(15)	127.7(4)
C(6)-C(7)-C(15)	125.0(4)	C(7)-C(8)-C(9)	107.1(4)
C(7)-C(8)-C(17)	128.0(5)	C(9)-C(8)-C(17)	124.7(4)
N(2)-C(9)-C(10)	124.6(4)	N(2)-C(9)-C(8)	109.2(4)
C(10)-C(9)-C(8)	126.1(4)	C(1)A-C(10)-C(9)	127.9(4)
C(12)-C(11)-C(2)	112.6(4)	C(14)-C(13)-C(3)	112.9(4)
C(16)-C(15)-C(7)	115.2(4)	C(8)-C(17)-C(18)	110.9(4)
C(24)-C(19)-C(20)	118.7(5)	C(24)-C(19)-S(1)	121.3(4)
C(20)-C(19)-S(1)	119.8(4)	C(21)-C(20)-C(19)	119.4(6)
C(22)-C(21)-C(20)	120.7(6)	C(21)-C(22)-C(23)	120.2(6)
C(24)-C(23)-C(22)	118.8(7)	C(19)-C(24)-C(23)	122.1(6)

The thiolate ligands nearly eclipse diagonal porphyrin nitrogens, with an N(1)–Os(1)–S(1)–C(19) torsion angle of 14.2°. The average Os–N(por) bond length of 2.048 Å is within the range for osmium porphyrins containing *O/S*–donor ligands (Table 1.4). The Os–S distance of 2.295(1) Å in this formally Os^{IV} complex is identical to that of the other porphyrin Os^{IV} thiolate complex (TTP)Os(SC₆F₄H)₂ (2.294(3) Å), but is shorter than those of the Os^{II} (OEP)Os(PMS)₂ (PMS = pentamethylene sulfide (CH₂)₅S) and Os^{III} [(OEP)Os(PMS)₂](PF₆) complexes. The Os–S–C thiolate angle is 110.9(2)° and is within the range found for other osmium aryl thiolates (107.0–123.9°)^{50,61} or alkyl thiolates (102.5–111.8°).^{23b,62} The structure is essentially similar to that of the related (TTP)Os(SC₆F₄H)₂ reported by Collman and synthesized by the reaction of (TTP)Os(O)₂ with thiol.⁵⁰

Reaction of RSNO with an Os^{III} Porphyrin. We were only able to isolate a nitrosyl complex (with no thiolate or thiol ligands) when isoamyl thionitrite was reacted with a cationic (OEP)Os^{III} complex, although isoamyl thionitrite adds *trans* to Os^{II} porphyrins to give isolable nitrosyl thiolate products as described earlier. The reaction of the known [(OEP)Os^{III}]₂(PF₆)₂ complex with isoamyl thionitrite in CH₂Cl₂ resulted in the observation (by IR spectroscopy, Figure 1.7) of the [(OEP)Os(NO)](PF₆) intermediate ($\nu_{\text{NO}} = 1829 \text{ cm}^{-1}$, $\nu_{\text{PF}_6} = 847 \text{ cm}^{-1}$), which subsequently underwent anion hydrolysis by adventitious moisture upon attempted crystallization to give the isolable difluorophosphate (OEP)Os(NO)(O₂PF₂) derivative (Scheme 1.4). Our attempts to isolate [(OEP)Os(NO)](PF₆) have so far not been successful.

Scheme 1.4





Transmittance / Wavenumber (cm-1)

Figure 1.7. IR spectrum of the reaction (10 min) of $[(\text{OEP})\text{Os}^{\text{III}}]_2(\text{PF}_6)_2$ with isoamyl thionitrite in CH_2Cl_2 .

The hydrolysis of the PF₆ anion is a common feature in coordination chemistry^{64,65} and is known to occur even for the AgPF₆ salt (which was used to prepare the [(OEP)Os^{III}]₂(PF₆)₂ reagent).³³ We also synthesized [(OEP)Os(NO)](PF₆) independently by reacting (OEP)Os(CO) with NOPF₆.⁶³ Exposure of this product in solution to air also transforms it to (OEP)Os(NO)(O₂PF₂). In this study, neither the AgPF₆ nor the [(OEP)Os^{III}]₂(PF₆)₂ starting compound contained the difluorophosphate group (by IR spectroscopy).

Not surprisingly, the red (OEP)Os(NO)(O₂PF₂) product is air-stable. The ν_{NO} of 1808 cm⁻¹ (KBr) is higher than those displayed by the related osmium nitrosyl alkoxide or thiolate complexes. The IR spectrum also contains bands attributable to a monodentate difluorophosphate group ($\nu_{\text{PF}_2} = 887$ (ν_{as}) and 856 (ν_{s}) cm⁻¹; $\nu_{\text{PO}_2} = 1324$ cm⁻¹).^{66,67} A porphyrin band at 1156 cm⁻¹ probably obscures the expected ν_{s} (PO₂) band of the O₂PF₂ anion.⁶⁶ The locations of these bands are similar to those for other monodentate difluorophosphate groups in structurally characterized iridium⁶⁴ and palladium³³ and other η^1 -difluorophosphate complexes.⁶⁸ The FAB mass spectrum shows the presence of the parent ion [(OEP)Os(NO)(O₂PF₂)]⁺ and the [(OEP)Os(NO)]⁺ fragment. The ³¹P NMR (-27.85 ppm, triplet) and ¹⁹F NMR spectra (-89.49 ppm, doublet) are also similar to those of other monodentate difluorophosphate compounds. The $J_{\text{P-F}}$ coupling constant of 985 Hz is within the range commonly found for difluorophosphoric acid and its salts.^{33,69} The UV-vis spectrum of (OEP)Os(NO)(O₂PF₂) in benzene gives five bands at 347 (42), 374 (44), 421 (62), 539 (14) and 575 (24) nm. Not surprisingly, the UV-vis spectrum of (OEP)Os(NO)(O₂PF₂) is similar to that of (OEP)Os(NO)(OCIO₃).^{27a}

The molecular structure of (OEP)Os(NO)(O₂PF₂) is shown in Figure 1.8. The bond lengths and angles are listed in Tables 1.7 and 1.8. The Os-N-O bond is essentially linear with a bond angle of 174.3(6)°. The NO group and O₂PF₂ group are *trans* to each other with an N(5)-Os-O(2) bond angle of 178.4(3)°. The P atom of the

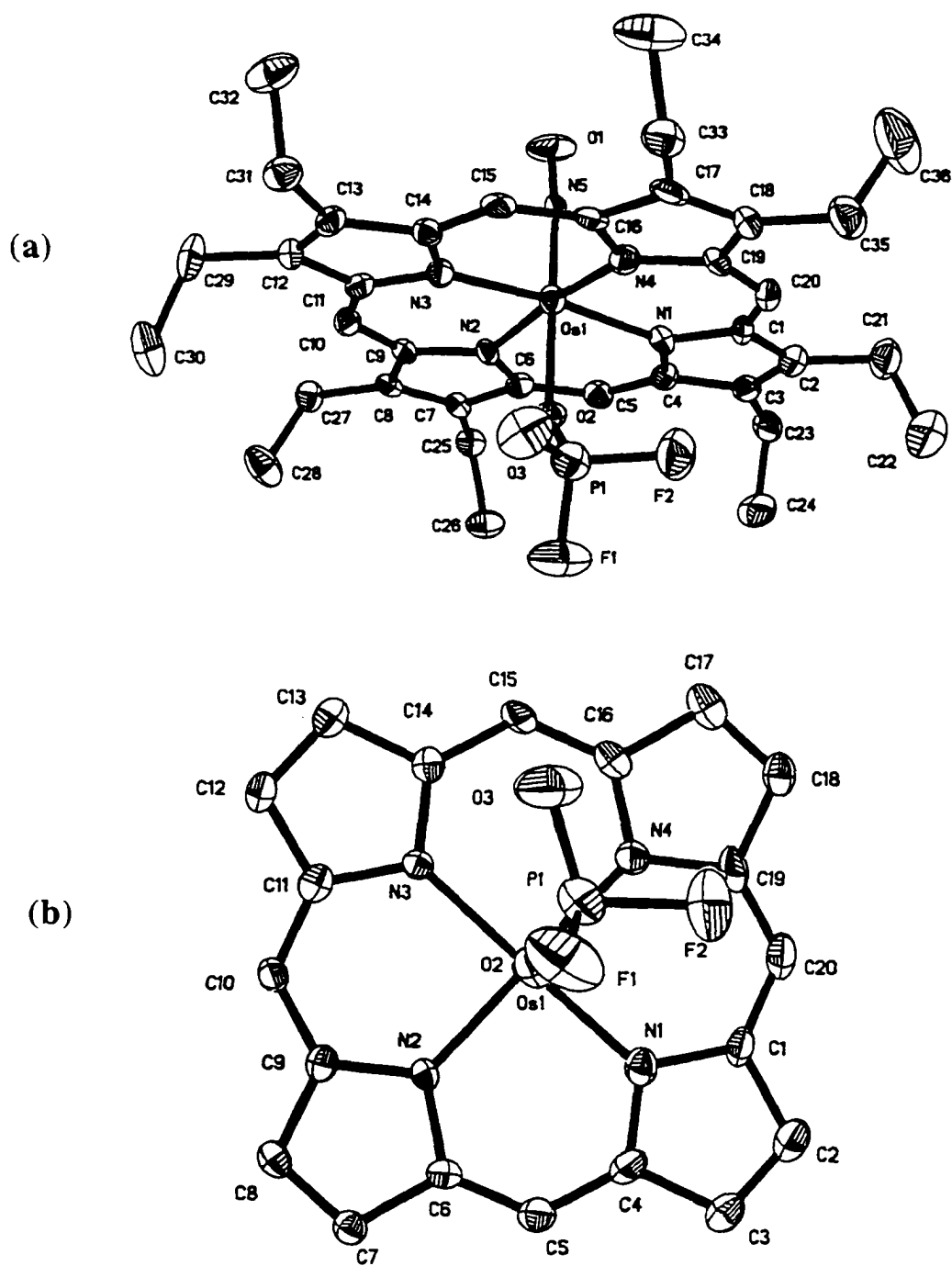


Figure 1.8. (a) Molecular structure of $(\text{OEP})\text{Os}(\text{NO})(\text{O}_2\text{PF}_2)$. (b) View of the O_2PF_2 ligand relative to the porphyrin core, with the view along the $\text{O}(2)\text{--Os}(1)$ bond.

Table 1.7. Bond Lengths (Å) for (OEP)Os(NO)(O₂PF₂)

Os(1)-N(5)	1.711(6)	Os(1)-O(2)	2.046(5)
Os(1)-N(2)	2.053(5)	Os(1)-N(1)	2.060(6)
Os(1)-N(3)	2.065(6)	Os(1)-N(4)	2.067(6)
P(1)-O(3)	1.454(7)	P(1)-O(2)	1.477(5)
P(1)-F(1)	1.511(6)	P(1)-F(2)	1.531(5)
O(1)-N(5)	1.179(8)	N(1)-C(4)	1.367(9)
N(1)-C(1)	1.371(9)	N(2)-C(6)	1.375(8)
N(2)-C(9)	1.376(8)	N(3)-C(14)	1.370(9)
N(3)-C(11)	1.375(9)	N(4)-C(16)	1.372(9)
N(4)-C(19)	1.374(9)	C(1)-C(20)	1.377(11)
C(1)-C(2)	1.465(10)	C(2)-C(3)	1.344(11)
C(2)-C(21)	1.521(11)	C(3)-C(4)	1.446(10)
C(3)-C(23)	1.502(10)	C(4)-C(5)	1.378(10)
C(5)-C(6)	1.383(10)	C(6)-C(7)	1.446(9)
C(7)-C(8)	1.355(10)	C(7)-C(25)	1.496(9)
C(8)-C(9)	1.439(9)	C(8)-C(27)	1.497(9)
C(9)-C(10)	1.374(10)	C(10)-C(11)	1.394(10)
C(11)-C(12)	1.439(10)	C(12)-C(13)	1.365(10)
C(12)-C(29)	1.505(9)	C(13)-C(14)	1.450(9)
C(13)-C(31)	1.491(10)	C(14)-C(15)	1.404(9)
C(15)-C(16)	1.390(10)	C(16)-C(17)	1.453(9)
C(17)-C(18)	1.368(11)	C(17)-C(33)	1.489(11)
C(18)-C(19)	1.450(10)	C(18)-C(35)	1.512(10)
C(19)-C(20)	1.381(11)	C(21)-C(22)	1.502(13)
C(23)-C(24)	1.507(11)	C(25)-C(26)	1.510(10)

C(27)-C(28)	1.518(11)	C(29)-C(30)	1.552(13)
C(31)-C(32)	1.490(11)	C(33)-C(34)	1.512(11)
C(35)-C(36)	1.471(14)		

Table 1.8. Bond Angles ($^{\circ}$) for (OEP)Os(NO)(O₂PF₂)

O(1)-N(5)-Os(1)	174.3(6)	N(5)-Os(1)-O(2)	178.4(3)
O(3)-P(1)-O(2)	118.4(4)	O(3)-P(1)-F(1)	111.2(4)
O(2)-P(1)-F(1)	108.2(3)	O(3)-P(1)-F(2)	108.3(4)
O(2)-P(1)-F(2)	108.2(3)	F(1)-P(1)-F(2)	101.1(4)
P(1)-O(2)-Os(1)	138.7(3)	N(5)-Os(1)-N(2)	94.0(3)
O(2)-Os(1)-N(2)	84.8(2)	N(5)-Os(1)-N(1)	94.3(3)
O(2)-Os(1)-N(1)	84.7(2)	N(2)-Os(1)-N(1)	89.9(2)
N(5)-Os(1)-N(3)	94.2(3)	O(2)-Os(1)-N(3)	86.8(2)
N(2)-Os(1)-N(3)	89.8(2)	N(1)-Os(1)-N(3)	171.4(2)
N(5)-Os(1)-N(4)	94.7(3)	O(2)-Os(1)-N(4)	86.5(2)
N(2)-Os(1)-N(4)	171.3(2)	N(1)-Os(1)-N(4)	89.7(2)
N(3)-Os(1)-N(4)	89.3(2)	C(4)-N(1)-C(1)	108.5(6)
C(4)-N(1)-Os(1)	125.8(5)	C(1)-N(1)-Os(1)	125.7(5)
C(6)-N(2)-C(9)	107.3(5)	C(6)-N(2)-Os(1)	126.0(4)
C(9)-N(2)-Os(1)	126.5(4)	C(14)-N(3)-C(11)	107.2(6)
C(14)-N(3)-Os(1)	127.1(4)	C(11)-N(3)-Os(1)	125.6(4)
C(16)-N(4)-C(19)	108.0(6)	C(16)-N(4)-Os(1)	126.1(5)
C(19)-N(4)-Os(1)	125.9(5)	N(1)-C(1)-C(20)	125.9(7)
N(1)-C(1)-C(2)	107.4(6)	C(20)-C(1)-C(2)	126.7(7)
C(3)-C(2)-C(1)	108.0(6)	C(3)-C(2)-C(21)	127.4(7)
C(1)-C(2)-C(21)	124.6(7)	C(2)-C(3)-C(4)	107.1(6)

C(2)-C(3)-C(23)	129.0(7)	C(4)-C(3)-C(23)	123.8(7)
N(1)-C(4)-C(5)	125.3(6)	N(1)-C(4)-C(3)	109.0(6)
C(5)-C(4)-C(3)	125.7(7)	C(4)-C(5)-C(6)	127.8(7)
N(2)-C(6)-C(5)	124.7(6)	N(2)-C(6)-C(7)	109.1(6)
C(5)-C(6)-C(7)	126.2(6)	C(8)-C(7)-C(6)	106.9(6)
C(8)-C(7)-C(25)	128.6(6)	C(6)-C(7)-C(25)	124.5(6)
C(7)-C(8)-C(9)	107.8(6)	C(7)-C(8)-C(27)	128.3(6)
C(9)-C(8)-C(27)	124.0(6)	C(10)-C(9)-N(2)	124.5(6)
C(10)-C(9)-C(8)	126.6(6)	N(2)-C(9)-C(8)	108.9(6)
C(9)-C(10)-C(11)	128.0(6)	N(3)-C(11)-C(10)	125.0(6)
N(3)-C(11)-C(12)	109.1(6)	C(10)-C(11)-C(12)	126.0(6)
C(13)-C(12)-C(11)	107.9(6)	C(13)-C(12)-C(29)	127.2(7)
C(11)-C(12)-C(29)	124.9(7)	C(12)-C(13)-C(14)	106.0(6)
C(12)-C(13)-C(31)	128.1(6)	C(14)-C(13)-C(31)	125.7(7)
N(3)-C(14)-C(15)	124.5(6)	N(3)-C(14)-C(13)	109.8(6)
C(15)-C(14)-C(13)	125.7(6)	C(16)-C(15)-C(14)	126.7(6)
N(4)-C(16)-C(15)	125.8(6)	N(4)-C(16)-C(17)	109.2(6)
C(15)-C(16)-C(17)	125.0(7)	C(18)-C(17)-C(16)	106.6(7)
C(18)-C(17)-C(33)	127.9(7)	C(16)-C(17)-C(33)	125.5(7)
C(17)-C(18)-C(19)	107.5(6)	C(17)-C(18)-C(35)	127.9(7)
C(19)-C(18)-C(35)	124.7(7)	C(20)-C(19)-N(4)	125.3(7)
C(20)-C(19)-C(18)	126.0(7)	N(4)-C(19)-C(18)	108.7(6)
C(19)-C(20)-C(1)	127.2(7)	C(22)-C(21)-C(2)	111.6(8)
C(3)-C(23)-C(24)	113.5(7)	C(7)-C(25)-C(26)	113.2(6)
C(8)-C(27)-C(28)	114.1(6)	C(12)-C(29)-C(30)	112.9(7)
C(13)-C(31)-C(32)	114.3(7)	C(17)-C(33)-C(34)	113.2(7)
C(36)-C(35)-C(18)	115.2(8)		

O₂PF₂ group essentially eclipses a porphyrin nitrogen, with an N(4)–Os(1)–O(2)–P(1) torsion angle of 10.3°. The average Os–N(por) bond length of 2.061 Å is within the range observed for other (OEP)Os^{II} complexes (see Table 2.3). The Os atom is displaced by 0.16 Å from the four-nitrogen porphyrin plane towards the NO ligand, and the Os–O (difluorophosphate) bond length of 2.046(5) Å is longer than that of (OEP)Os(NO)(O-*n*-C₄H₉) described earlier, but is similar to the Os–O bond lengths of (OEP)Os(OPPh₃)₂ (2.036(7) Å), and is shorter than the Os–O bond length of (TTP)Os(CO)(Et₂NNO) (2.200(7) Å, chapter 2). It is also longer than the observed axial Os–O bond lengths for the structurally characterized Os^{IV} porphyrin alkoxides (1.909(4)–1.938(2) Å) or Os^{VI} porphyrin dioxo derivatives (1.745(5) Å) (Table 1.4, bottom). The Os–N(O) bond length of 1.711(6) Å is shorter than those of (OEP)Os(NO)(O-*n*-C₄H₉) (1.833(8) Å) and (TTP)Os(NO)(S-*i*-C₅H₁₁) (2.041(7) Å). However, it is within the range of 1.63(1)–1.89(2) Å found for other Os^{II} linear nitrosyl complexes (Table 1.3). The N–O bond length of 1.179(8) Å is similar to those of other structurally characterized osmium nitrosyl complexes. The P–O(2) bond length of 1.477(5) Å is longer than the P–O(3) bond length of 1.454(7) Å, corresponding to the double bond character between the O(3) and P atoms. The O–P–O bond angle of 118.4(4)° is larger than the F–P–F angle of 101.1(4)°, and this observation is typical for transition metal difluorophosphate complexes (Table 1.9).

Importantly, although the difluorophosphate anion forms complexes with other transition metals,^{33,64,65,70,71} main group metals,^{72–75} the ammonium cation,⁷⁶ and even the nitrosonium cation,⁷⁷ to the best of our knowledge, this is the first reported example of a metalloporphyrin difluorophosphate derivative.

Table 1.9. Metric Parameters (in Å and °) for Transition Metal η^1 -OP(=O)F₂ Complexes

	(OEP)Os(NO) (O ₂ PF ₂) ^a	Ir(O ₂ PF ₂)(PPh ₃) ₂ (H)(Cl)(CO) ^b	Pd(O ₂ PF ₂)(η^3 -2-MeC ₃ H ₄) (PCy ₃) ^{c,d}
M–O	2.046(5)	2.201(8)	2.314(6) [2.126(5)]
O–P	1.477(5)	1.456(7)	1.471(5) [1.455(5)]
P–F	1.511(6), 1.531(5)	1.499(10), 1.529(12)	
P=O	1.454(7)	1.421(8)	1.468(8) [1.441(8)]
M–O–P	138.7(3)	127.0(4)	125.4(3) [124.7(3)]
O–P=O	118.4(4)	122.1(6)	123.3(4) [122.1(4)]
F–P–F	101.1(4)	95.4(7)	97.2(5) [96.0(4)]
O–P–F	108.2(3)	108.3(4), 107.4(5)	
O=P–F	111.2(4), 108.3(4)	112.1(5), 108.3(6)	

^a This work. ^b reference 64. ^c reference 33. ^d There are two independent molecules present. The data in brackets are for the second molecule.

We have also prepared the analogous thionitrosyl (OEP)Os(NS)(O₂PF₂) compound via the hydrolysis of [(OEP)Os(NS)](PF₆) under nitrogen. A suitable crystal for structure determination was grown by slow evaporation of a saturated CH₂Cl₂ solution of the compound under nitrogen. The molecular structure of (OEP)Os(NS)(O₂PF₂) is shown in Figure 1.9. The bond angles and bond lengths are listed in Tables 1.10 and 1.11. To the best of our knowledge, there are only three (por)Os(NS)-containing compounds that have been structurally characterized, namely, (OEP)Os(NS)(Cl) (chapter 3), (OEP)Os(NS)(Me) (chapter 3) and now (OEP)Os(NS)(O₂PF₂). Unfortunately, due to the nature of disorder of the axial NS and O₂PF₂ ligands and the inherent limited accuracy of the axial bond lengths and bond angles, a meaningful comparison of bond lengths and bond angles with (OEP)Os(NO)(O₂PF₂) is not possible. Nevertheless, the structure clearly indicates the NS coordination to osmium center and the η¹-O binding of the difluorophosphate ligand. The NS group and the O₂PF₂ group are *trans* to each other with an O(1)–Os(1)–N(5) bond angle of 163.9(5)°. The Os–N–S bond is linear with a bond angle of 170.9(7)°. As before, the average Os–N(por) bond length of 2.041 Å is comparable to other (por)Os^{II} complexes containing O- and S-donor ligands (Table 1.4).

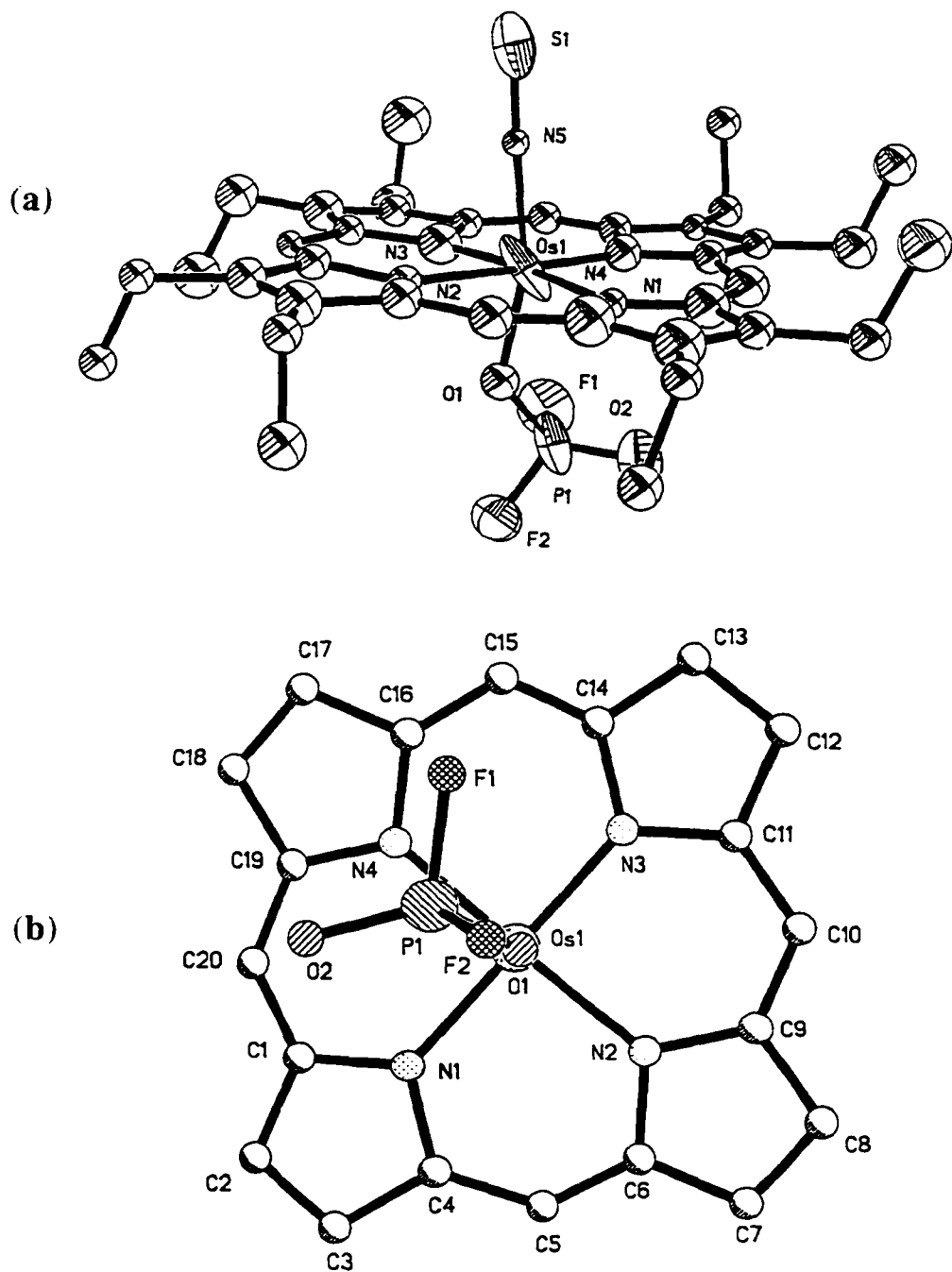


Figure 1.9. (a) Molecular structure of $(\text{OEP})\text{Os}(\text{NS})(\text{O}_2\text{PF}_2)$. (b) View of the O_2PF_2 ligand relative to the porphyrin core, with the view along the O(1)-Os(1) bond.

Table 1.10. Bond Lengths (Å) for (OEP)Os(NS)(O₂PF₂)

Os(1)-O(1)	1.877(9)	Os(1)-N(5)	1.960(8)
Os(1)-N(4)	2.001(10)	Os(1)-N(1)	2.028(8)
Os(1)-N(3)	2.034(10)	Os(1)-N(2)	2.100(9)
S(1)-N(5)	1.520(9)	P(1)-O(2)	1.42(2)
P(1)-F(2)	1.463(13)	P(1)-F(1)	1.507(11)
P(1)-O(1)	1.521(12)	N(1)-C(1)	1.377(14)
N(1)-C(4)	1.412(13)	C(1)-C(20)	1.38(2)
C(1)-C(2)	1.443(13)	C(2)-C(3)	1.37(2)
C(2)-C(21)	1.51(2)	C(3)-C(4)	1.45(2)
C(3)-C(23)	1.501(14)	C(4)-C(5)	1.403(14)
C(5)-C(6)	1.391(14)	N(2)-C(9)	1.395(13)
N(2)-C(6)	1.406(12)	C(6)-C(7)	1.44(2)
C(7)-C(8)	1.370(14)	C(7)-C(25)	1.526(14)
C(8)-C(9)	1.442(13)	C(8)-C(27)	1.502(14)
C(9)-C(10)	1.376(12)	C(10)-C(11)	1.396(13)
N(3)-C(14)	1.392(13)	N(3)-C(11)	1.393(13)
C(11)-C(12)	1.445(13)	C(12)-C(13)	1.38(2)
C(12)-C(29)	1.50(2)	C(13)-C(14)	1.431(13)
C(13)-C(31)	1.51(2)	C(14)-C(15)	1.342(14)
C(15)-C(16)	1.361(14)	N(4)-C(19)	1.364(14)
N(4)-C(16)	1.387(13)	C(16)-C(17)	1.440(13)
C(17)-C(18)	1.377(13)	C(17)-C(33)	1.518(14)
C(18)-C(19)	1.454(13)	C(18)-C(35)	1.49(2)
C(19)-C(20)	1.369(14)	C(21)-C(22)	1.53(2)
C(23)-C(24)	1.528(14)	C(25)-C(26)	1.51(2)

C(27)-C(28)	1.521(14)	C(29)-C(30)	1.54(2)
C(31)-C(32)	1.53(2)	C(33)-C(34)	1.532(14)
C(35)-C(36)	1.52(2)		

Table 1.11. Bond Angles ($^{\circ}$) for (OEP)Os(NS)(O₂PF₂)

S(1)-N(5)-Os(1)	170.9(7)	P(1)-O(1)-Os(1)	131.6(8)
O(2)-P(1)-F(2)	114.9(9)	O(2)-P(1)-F(1)	111.6(9)
F(2)-P(1)-F(1)	102.4(8)	O(2)-P(1)-O(1)	118.0(8)
F(2)-P(1)-O(1)	103.5(7)	F(1)-P(1)-O(1)	104.7(7)
O(1)-Os(1)-N(5)	163.9(5)	O(1)-Os(1)-N(4)	95.5(5)
N(5)-Os(1)-N(4)	95.6(4)	O(1)-Os(1)-N(1)	95.4(4)
N(5)-Os(1)-N(1)	95.7(4)	N(4)-Os(1)-N(1)	92.0(4)
O(1)-Os(1)-N(3)	80.7(5)	N(5)-Os(1)-N(3)	87.9(4)
N(4)-Os(1)-N(3)	89.4(5)	N(1)-Os(1)-N(3)	176.0(4)
O(1)-Os(1)-N(2)	84.2(4)	N(5)-Os(1)-N(2)	83.9(4)
N(4)-Os(1)-N(2)	176.3(4)	N(1)-Os(1)-N(2)	91.7(4)
N(3)-Os(1)-N(2)	86.9(4)	C(1)-N(1)-C(4)	106.9(8)
C(1)-N(1)-Os(1)	126.2(7)	C(4)-N(1)-Os(1)	126.3(7)
N(1)-C(1)-C(20)	120.8(12)	N(1)-C(1)-C(2)	110.1(8)
C(20)-C(1)-C(2)	129.1(12)	C(3)-C(2)-C(1)	106.5(8)
C(3)-C(2)-C(21)	128.6(11)	C(1)-C(2)-C(21)	124.9(11)
C(2)-C(3)-C(4)	108.3(8)	C(2)-C(3)-C(23)	130.9(12)
C(4)-C(3)-C(23)	120.7(12)	C(5)-C(4)-N(1)	121.1(12)
C(5)-C(4)-C(3)	131.2(12)	N(1)-C(4)-C(3)	107.7(8)
C(6)-C(5)-C(4)	134.7(14)	C(9)-N(2)-C(6)	104.7(8)
C(9)-N(2)-Os(1)	128.3(7)	C(6)-N(2)-Os(1)	125.7(7)

C(5)-C(6)-N(2)	119.8(11)	C(5)-C(6)-C(7)	130.3(11)
N(2)-C(6)-C(7)	109.5(8)	C(8)-C(7)-C(6)	107.6(8)
C(8)-C(7)-C(25)	139.5(12)	C(6)-C(7)-C(25)	112.9(11)
C(7)-C(8)-C(9)	106.6(8)	C(7)-C(8)-C(27)	126.0(10)
C(9)-C(8)-C(27)	127.3(10)	C(10)-C(9)-N(2)	123.6(10)
C(10)-C(9)-C(8)	125.1(11)	N(2)-C(9)-C(8)	110.6(8)
C(9)-C(10)-C(11)	125.7(12)	C(14)-N(3)-C(11)	106.2(8)
C(14)-N(3)-Os(1)	124.5(8)	C(11)-N(3)-Os(1)	128.3(8)
N(3)-C(11)-C(10)	125.6(10)	N(3)-C(11)-C(12)	109.1(8)
C(10)-C(11)-C(12)	125.0(10)	C(13)-C(12)-C(11)	107.3(8)
C(13)-C(12)-C(29)	128.7(12)	C(11)-C(12)-C(29)	124.0(12)
C(12)-C(13)-C(14)	107.0(8)	C(12)-C(13)-C(31)	123.9(13)
C(14)-C(13)-C(31)	129.0(13)	C(15)-C(14)-N(3)	128.7(11)
C(15)-C(14)-C(13)	121.6(11)	N(3)-C(14)-C(13)	109.7(8)
C(14)-C(15)-C(16)	123.5(13)	C(19)-N(4)-C(16)	107.6(9)
C(19)-N(4)-Os(1)	125.1(8)	C(16)-N(4)-Os(1)	126.9(8)
C(15)-C(16)-N(4)	126.7(11)	C(15)-C(16)-C(17)	124.5(10)
N(4)-C(16)-C(17)	108.5(8)	C(18)-C(17)-C(16)	107.7(7)
C(18)-C(17)-C(33)	116.8(11)	C(16)-C(17)-C(33)	135.4(11)
C(17)-C(18)-C(19)	106.2(8)	C(17)-C(18)-C(35)	129.6(11)
C(19)-C(18)-C(35)	124.3(11)	N(4)-C(19)-C(20)	123.1(12)
N(4)-C(19)-C(18)	109.5(8)	C(20)-C(19)-C(18)	126.3(12)
C(19)-C(20)-C(1)	132(2)	C(2)-C(21)-C(22)	114.9(13)
C(3)-C(23)-C(24)	116.5(11)	C(26)-C(25)-C(7)	119.1(11)
C(8)-C(27)-C(28)	113.8(11)	C(12)-C(29)-C(30)	109(2)
C(13)-C(31)-C(32)	107.0(14)	C(17)-C(33)-C(34)	108.5(11)
C(18)-C(35)-C(36)	109.3(13)		

Conclusion

In summary, we have provided new chemical insight into the reactions of thionitrites and alkyl nitrites with osmium porphyrins. By using the valence isoelectronic phenyl arylazo sulfide in place of PhSNO, we have been able to isolate and characterize the bis-thiolate adduct with the loss of the arylazo fragments, thereby giving more spectroscopic and chemical evidence that RSNO binds through the sulfur atom to the Os^{II} porphyrin center. Whereas nitrosyl thiolates and alkoxides are produced in the reactions of thionitrites and alkyl nitrites with Os^{II} porphyrins, only the osmium nitrosyl difluorophosphate complex is isolated in the case of a Os^{III} porphyrin. This work also adds to the sparse structural data currently available for osmium nitrosyl porphyrins: prior to this work, only one other osmium nitrosyl porphyrin (reported from our laboratory^{23b}) had been structurally characterized.

References and Notes

- (1) (a) Moncada, S.; Palmer, R. M. J.; Higgs, E. A. *Pharmacol. Rev.* **1991**, *43*, 109. (b) Ignarro, L. J. *Annu. Rev. Pharmacol. Toxicol.* **1990**, *30*, 535.
- (2) (a) Deinum, G.; Stone, J. R.; Babcock, G. T.; Marletta, M. A. *Biochemistry* **1996**, *35*, 1540. (b) Stone, J. R.; Marletta, M. A. *Biochemistry* **1994**, *33*, 5636. (c) Yu, A. E.; Hu, S.; Spiro, T. G.; Burstyn, J. N. *J. Am. Chem. Soc.* **1994**, *116*, 4117. (d) Craven, P. A.; DeRubertis, F. R. *Biochem. Biophys. Acta* **1983**, *745*, 310. (e) Craven, P. A.; DeRubertis, F. R. *J. Biol. Chem.* **1978**, *253*, 8433.
- (3) (a) Marletta, M. A. *J. Biol. Chem.* **1993**, *268*, 12231. (b) Crane, B. R.; Arvai, A. S.; Gachhui, R.; Wu, C.; Ghosh, D. K.; Getzoff, E. D.; Stuehr, D. J.; Tainer, J. A. *Science* **1997**, *278*, 425.
- (4) Williams, D. L. H. *Chem. Commun.* **1996**, 1085.
- (5) Butler, A. R.; Flitney, F. W.; Williams, D. L. H. *Trends Pharmacol. Sci.* **1995**, *16*, 18.
- (6) Upchurch, G. R., Jr.; Welch, G. N.; Loscalzo, J. *Adv. Pharmacol.* **1995**, *34*, 343.
- (7) Stamler, J. S. In *Current Topics in Microbiology and Immunology*; Koprowski, H.; Maeda, H., Eds.; Springer-Verlag: Berlin, 1995; Vol. 196, p 19.
- (8) Stamler, J. S. *Cell* **1994**, *78*, 931.
- (9) Mathews, W. R.; Kerr, S. W. *J. Pharmacol. Exp. Ther.* **1993**, *267*, 1529.
- (10) Kerr, S. W.; Buchanan, L. V.; Bunting, S.; Mathews, W. R. *J. Pharmacol. Exp. Ther.* **1992**, *263*, 285.
- (11) Myers, P. R.; Minor, R. L., Jr.; Guerra, R., Jr.; Bates, J. N.; Harrison, D. G. *Nature* **1990**, *345*, 161.
- (12) (a) Kowaluk, E. A.; Fung, H.-L. *J. Pharmacol. Exp. Ther.* **1990**, *255*, 1256. (b) Gaston, B.; Reilly, J.; Drazen, J. M.; Fackler, J.; Ramdev, P.; Arnette, D.;

- Mullins, M. E.; Sugarbaker, D. J.; Chee, C.; Singel, D. J.; Loscalzo, J.; Stamler, J. S. *Proc. Natl. Acad. Sci. U.S.A.* **1993**, *90*, 10957.
- (13) Bannenberg, G.; Xue, J.; Engman, L.; Cotgreave, I.; Moldéus, P.; Ryrfeldt, Å. *J. Pharmacol. Exp. Ther.* **1995**, *272*, 1238.
- (14) (a) Simon, D. I.; Mullins, M. E.; Jia, L.; Gaston, B.; Singel, D. J.; Stamler, J. S. *Proc. Natl. Acad. Sci. U.S.A.* **1996**, *93*, 4736. (b) Keshive, M.; Singh, S.; Wishnok, J. S.; Tannenbaum, S. R.; Deen, W. M. *Chem. Res. Toxicol.* **1996**, *9*, 988. (c) Park, J.-W. *Biochem. Biophys. Res. Commun.* **1988**, *152*, 916. (d) Stamler, J. S.; Simon, D. I.; Osborne, J. A.; Mullins, M. E.; Jaraki, O.; Michel, T.; Singel, D. J.; Loscalzo, J. *Proc. Natl. Acad. Sci. U.S.A.* **1992**, *89*, 444. (e) Stamler, J. S.; Simon, D. I.; Jaraki, O.; Osborne, J. A.; Francis, S.; Mullins, M.; Singel, D.; Loscalzo, J. *Proc. Natl. Acad. Sci. U.S.A.* **1992**, *89*, 8087.
- (15) (a) Jia, L.; Bonaventura, C.; Bonaventura, J.; Stamler, J. S. *Nature* **1996**, *380*, 221. (b) Gow, A. J.; Stamler, J. S. *Nature* **1998**, *391*, 169.
- (16) Stone, J. R.; Marletta, M. A. *Biochemistry* **1995**, *34*, 16397.
- (17) Stone, J. R.; Marletta, M. A. *Biochemistry* **1996**, *35*, 1093.
- (18) McAninly, J.; Williams, D. L. H.; Askew, S. C.; Butler, A. R.; Russell, C. J. *Chem. Soc., Chem. Commun.* **1993**, 1758.
- (19) (a) Dicks, A. P.; Swift, H. R.; Williams, D. L. H.; Butler, A. R.; Al-Sa'doni, H. H.; Cox, B. G. *J. Chem. Soc., Perkin Trans. 2* **1996**, 481. (b) Dicks, A. P.; Williams, D. L. H. *Chem. Biol.* **1996**, *3*, 655. (c) Askew, S. C.; Barnett, D. J.; McAninly, J.; Williams, D. L. H. *J. Chem. Soc., Perkin Trans. 2* **1995**, 741. (d) Gordge, M. P.; Meyer, D. J.; Hothersall, J.; Neild, G. H.; Payne, N. N.; Noronha-Dutra, A. *Brit. J. Pharmacol.* **1995**, *114*, 1083. (e) Williams, D. L. H. *Transition Met. Chem. (London)* **1996**, *21*, 189.

- (20) (a) Yi, G.-B.; Khan, M. A.; Richter-Addo, G. B. *J. Am. Chem. Soc.* **1995**, *117*, 7850. (b) Yi, G.-B.; Khan, M. A.; Richter-Addo, G. B. *Inorg. Chem.* **1996**, *35*, 3453. (c) Chen, L.; Yi, G.-B.; Wang, L.-S.; Dharmawardana, U. R.; Dart, A. C.; Khan, M. A.; Richter-Addo, G. B. *Inorg. Chem.* Submitted.
- (21) Yi, G.-B.; Khan, M. A.; Richter-Addo, G. B. *Inorg. Chem.* **1995**, *34*, 5703.
- (22) (a) Wang, L.-S.; Chen, L.; Khan, M. A.; Richter-Addo, G. B. *Chem. Commun.* **1996**, 323. (b) Fox, S. J. S.; Chen, L.; Khan, M. A.; Richter-Addo, G. B. *Inorg. Chem.* **1997**, *36*, 6465. (c) We have successfully extended *N*-binding of nitrosoarenes to osmium porphyrins (chapter 2).
- (23) (a) Yi, G.-B.; Khan, M. A.; Richter-Addo, G. B. *Chem. Commun.* **1996**, 2045. (b) Yi, G.-B.; Chen, L.; Khan, M. A.; Richter-Addo, G. B. *Inorg. Chem.* **1997**, *36*, 3876.
- (24) (a) Miranda, K. M.; Bu, X.; Lorkovic, I.; Ford, P. C. *Inorg. Chem.* **1997**, *36*, 4838. (b) Kadish, K. M.; Adamian, V. A.; Van Caemelbecke, E.; Tan, Z.; Tagliatesta, P.; Bianco, P.; Boschi, T.; Yi, G.-B.; Khan, M. A.; Richter-Addo, G. B. *Inorg. Chem.* **1996**, *35*, 1343. (c) Bohle, D. S.; Goodson, P. A.; Smith, B. D. *Polyhedron* **1996**, *15*, 3147. (d) Bohle, D. S.; Hung, C.-H.; Powell, A. K.; Smith, B. D.; Wocadlo, S. *Inorg. Chem.* **1997**, *36*, 1992. (e) Srivastava, T. S.; Hoffman, L.; Tsutsui, M. *J. Am. Chem. Soc.* **1972**, *94*, 1385.
- (25) (a) Hodge, S. J.; Wang, L.-S.; Khan, M. A.; Young, V. G., Jr.; Richter-Addo, G. B. *Chem. Commun.* **1996**, 2283. (b) Massoudipour, M.; Pandey, K. K. *Inorg. Chim. Acta* **1989**, *160*, 115.
- (26) Antipas, A.; Buchler, J. W.; Gouterman, M.; Smith, P. D. *J. Am. Chem. Soc.* **1978**, *100*, 3015.

- (27) (a) Antipas, A.; Buchler, J. W.; Gouterman, M.; Smith, P. D. *J. Am. Chem. Soc.* **1980**, *102*, 198. (b) Buchler, J. W.; Smith, P. D. *Chem. Ber.* **1976**, *109*, 1465.
- (28) Che, C.-M.; Poon, C.-K.; Chung, W.-C.; Gray, H. B. *Inorg. Chem.* **1985**, *24*, 1277.
- (29) (a) Collman, J. P.; Barnes, C. E.; Woo, L. K. *Proc. Natl. Acad. Sci. USA* **1983**, *80*, 7684. (b) Collman, J. P.; Prodoliet, J. W.; Leidner, C. R. *J. Am. Chem. Soc.* **1986**, *108*, 2916.
- (30) Bonnett, R.; Nicolaidou, P. *J. Chem. Soc., Perkin Trans. I* **1979**, 1969.
- (31) Che, C.-M.; Leung, W.-H.; Chung, W.-C. *Inorg. Chem.* **1990**, *29*, 1841.
- (32) Sakla, A. B.; Masoud, N. K.; Sawiris, Z.; Ebaid, W. S. *Helv. Chim. Acta* **1974**, *57*, 481.
- (33) Fernández-Galán, R.; Manzano, B. R.; Otero, A.; Lanfranchi, M.; Pellinghelli, M. A. *Inorg. Chem.* **1994**, *33*, 2309.
- (34) Feltham, R. D.; Enemark, J. H. *Topics Stereochem.* **1981**, *12*, 155.
- (35) Buchler, J. W.; Kokisch, W.; Smith, P. D. *Struct. Bonding* **1978**, *34*, 79.
- (36) Gross, Z.; Mahammed, A. *Inorg. Chem.* **1996**, *35*, 7260.
- (37) Bruce, M. I.; Tomkins, B.; Wong, F. S.; Skelton, B. W.; White, A. H. *J. Chem. Soc., Dalton Trans.* **1982**, 687.
- (38) Boyar, E. B.; Dobson, A.; Robinson, S. D.; Haymore, B. L.; Huffman, J. C. *J. Chem. Soc., Dalton Trans.* **1985**, 621.
- (39) Clark, G. R.; Greene, T. R.; Roper, W. R. *Aust. J. Chem.* **1986**, *39*, 1315.
- (40) Williams, D. S.; Meyer, T. J.; White, P. S. *J. Am. Chem. Soc.* **1995**, *117*, 823.
- (41) Werner, H.; Flügel, R.; Windmüller, B.; Michenfelder, A.; Wolf, J. *Organometallics* **1995**, *14*, 612.

- (42) (a) Rudnitskaya, O. V.; Buslaeva, T. M.; Stash, A. I.; Kisin, A. V. *Russ. J. Coord. Chem.* **1995**, *21*, 136. (b) Ooyama, D.; Nagao, N.; Nagao, H.; Sugimoto, Y.; Howell, F. S.; Mukaida, M. *Inorg. Chim. Acta* **1997**, *261*, 45.
- (43) (a) Herberhold, M.; Hill, A. F.; Clark, G. R.; Rickard, C. E. F.; Roper, W. R.; Wright, A. H. *Organometallics* **1989**, *8*, 2483. (b) Hill, A. F.; Roper, W. R.; Waters, J. M.; Wright, A. H. *J. Am. Chem. Soc.* **1983**, *105*, 5939.
- (44) Fergusson, J. E.; Robinson, W. T.; Coll, R. K. *Inorg. Chim. Acta* **1991**, *181*, 37.
- (45) Czeska, B.; Dehnicke, K.; Fenske, D. *Z. Naturforsch. B.* **1983**, *38*, 1031.
- (46) Clark, G. R.; Waters, J. M.; Whittle, K. R. *J. Chem. Soc., Dalton Trans.* **1975**, 463.
- (47) Other structurally characterized osmium porphyrins: (a) (OEP)Os(PPh₃)₂: reference 48. (b) (OEPMe₂)Os(CO)(py): Buchler, J. W.; Lay, K. L.; Smith, P. D.; Scheidt, W. R.; Rupprecht, G. A.; Kenny, J. E. *J. Organomet. Chem.* **1976**, *110*, 109. (c) (TTP)Os(4-pic)₂: Djukic, J.-P.; Young, V. G., Jr.; Woo, L. K. *Organometallics* **1994**, *13*, 3995. (d) (TTP)Os(Cl)₂: Smieja, J. A.; Omberg, K. M.; Busuego, L. N.; Breneman, G. L. *Polyhedron* **1994**, *13*, 339. (e) (TTP)Os(CH₂SiMe₃)₂: Leung, W.-H.; Hun, T. S. M.; Wong, K.-Y.; Wong, W.-T. *J. Chem. Soc., Dalton Trans.* **1994**, 2713. (f) (TTP)Os(*p*-NC₆H₄NO₂)₂: Smieja, J. A.; Omberg, K. M. *Inorg. Chem.* **1994**, *33*, 614. (g) Woo, L. K.; Smith, D. A.; Young, V. G., Jr. *Organometallics* **1991**, *10*, 3977.
- (48) Che, C.-M.; Lai, T.-F.; Chung, W.-C.; Schaefer, W. P.; Gray, H. B. *Inorg. Chem.* **1987**, *26*, 3907.
- (49) Scheidt, W. R.; Nasri, H. *Inorg. Chem.* **1995**, *34*, 2190.
- (50) Collman, J. P.; Bohle, D. S.; Powell, A. K. *Inorg. Chem.* **1993**, *32*, 4004.
- (51) Che, C.-M.; Huang, J.-S.; Li, Z.-Y.; Poon, C.-K.; Tong, W.-F.; Lai, T.-F.; Cheng, M.-C.; Wang, C.-C.; Wang, Y. *Inorg. Chem.* **1992**, *31*, 5220.

- (52) Nasri, H.; Scheidt, W. R. *Acta Crystallogr.* **1990**, *C46*, 1096.
- (53) Che, C.-M.; Chung, W.-C.; Lai, T.-F. *Inorg. Chem.* **1988**, *27*, 2801.
- (54) The short Os–O contact should be treated with caution due to the limited accuracy of this bond length.
- (55) Structurally characterized Os alkoxides: (a) Cheng, W.-K.; Wong, K.-Y.; Tong, W.-F.; Lai, T.-F.; Che, C.-M. *J. Chem. Soc., Dalton Trans.* **1992**, 91. (b) Masuda, H.; Taga, T.; Osaki, K.; Sugimoto, H.; Mori, M. *Bull. Chem. Soc. Jpn.* **1984**, *57*, 2345. (c) Hinckley, C. C.; Ali, I. A.; Robinson, P. D. *Acta Crystallogr.* **1990**, *C46*, 697. (d) reference 44. (e) reference 51.
- (56) Haas, A. *Adv. Inorg. Chem. Radiochem.* **1984**, *28*, 167.
- (57) Dell'Erba, C.; Houmam, A.; Morin, N.; Novi, M.; Petrillo, G.; Pinson, J.; Rolando, C. *J. Org. Chem.* **1996**, *61*, 929.
- (58) Sutton, D. *Chem. Soc. Rev.* **1975**, *4*, 443.
- (59) Suehiro, T.; Masuda, S.; Nakausa, R.; Taguchi, M.; Mori, A.; Koike, A.; Date, M. *Bull. Chem. Soc. Jpn.* **1987**, *60*, 3321.
- (60) Aryldiazonium adducts of metalloporphyrins are known: Farrell, N.; Neves, A. A. *Inorg. Chim. Acta* **1981**, *54*, L53.
- (61) (a) Che, C.-M.; Cheng, W.-K.; Mak, T. C. W. *Inorg. Chem.* **1986**, *25*, 703. (b) Cruz-Garriz, D.; Gelover, S.; Torrens, H.; Leal, J.; Richards, R. L. *J. Chem. Soc., Dalton Trans.* **1988**, 2393. (c) Cruz-Garriz, D.; Sosa, P.; Torrens, H.; Hills, A.; Hughes, D. L.; Richards, R. L. *J. Chem. Soc., Dalton Trans.* **1989**, 419. (d) Hills, A.; Hughes, D. L.; Richards, R. L.; Arroyo, M.; Cruz-Garriz, D.; Torrens, H. *J. Chem. Soc., Dalton Trans.* **1991**, 1281. (e) Arroyo, M.; Chamizo, J. A.; Hughes, D. L.; Richards, R. L.; Roman, P.; Sosa, P.; Torrens, H. *J. Chem. Soc., Dalton Trans.* **1994**, 1819.
- (62) Lynch, W. E.; Lintvedt, R. L.; Shui, X. Q. *Inorg. Chem.* **1991**, *30*, 1014.

- (63) The reaction of (OEP)Ru(CO) with NOBF₄ also generates [(OEP)Ru(NO)]BF₄, which is converted to [(OEP)Ru(NO)(H₂O)]BF₄ in air.^{20b}
- (64) Bauer, H.; Nagel, U.; Beck, W. *J. Organomet. Chem.* **1985**, 290, 219
- (65) Bruno, G.; Schiavo, S. L.; Piraino, P.; Faraone, F. *Organometallics* **1985**, 4, 1098.
- (66) Bühler, K.; Bues, W. *Z. Anorg. Allg. Chem.* **1961**, 308, 62.
- (67) Schmutzler, R. In *Advances In Fluorine Chemistry*; Stacey, M.; Tatlow, J. C.; Sharpe, A. G., eds; Butterworths: London, 1965, Vol. 5, p 252.
- (68) The Cp₂Rh₂(μ-CO)(μ-dppm)(μ-AgO₂PF₂) complex contains disordered O and F atoms in the O₂PF₂ group.⁶⁵
- (69) Schmutzler, R. In *Advances In Fluorine Chemistry*; Stacey, M.; Tatlow, J. C.; Sharpe, A. G., eds; Butterworths: London, 1965, Vol. 5, p 262.
- (70) Begley, M. J.; Dove, M. F. A.; Hibbert, R. C.; Logan, N.; Nunn, M.; Sowerby, D. B. *J. Chem. Soc., Dalton Trans.* **1985**, 2433.
- (71) Legzdins, P.; Oxley, J. C. *Inorg. Chem.* **1984**, 23, 1053.
- (72) Powell, J.; Horvath, M. J.; Lough, A. *J. Chem. Soc., Dalton Trans.* **1996**, 1669.
- (73) Granier, P. W.; Durand, J.; Cot, L.; Galigné, J. L. *Acta Crystallogr.* **1975**, B31, 2506.
- (74) Tan, T. H.; Dalziel, J. R.; Yeats, P. A.; Sams, J. R.; Thompson, R. C.; Aubke, F. *Can. J. Chem.* **1972**, 50, 1843.
- (75) Thompson, R. C.; Reed, W. *Inorg. Nucl. Chem. Lett.* **1969**, 5, 581.
- (76) Harrison, R. W.; Trotter, J. *J. Chem. Soc. A* **1969**, 1783.
- (77) Babaeva, V. P.; Rosolovskii, V. Y. *Russ. J. Inorg. Chem.* **1971**, 16 (4), 471.

Chapter 2. Nitrosamine and Nitrosoarene Complexes of Metalloporphyrins

Introduction

Nitrosamines ($R_2NN=O$) belong to the family of *N*-nitroso compounds, and they are generally considered to be carcinogenic.¹⁻⁷ They are metabolized by cytochrome P450, and final metabolized products may result from initial hydroxylation or denitrosation of the nitrosamine.⁸⁻¹⁰ Two types of interactions of nitrosamines with cytochrome P450 have been proposed (Figure 2.1). The first is the interaction of the nitrosamine with the substrate pocket (Type I) prior to the enzyme-catalyzed oxidation,^{8,9} and the second is the direct interaction of the nitrosamine with the iron center of the heme (Type II) in the enzyme.^{8,11} This variable binding of nitrosamines to the heme pocket of cytochrome P450 contributes to the rather complex metabolic pathways of nitrosamine activation.

Although nitrosamines are known to form complexes with some metals,¹²⁻¹⁹ the nature of nitrosamine binding to heme or heme models had not been reported prior to our study. Interestingly, it has been documented that *N*-hydroxyethylprotoporphyrin IX forms in the livers of mice after diethylnitrosamine treatment, although the mechanism of such formation remains unclear.²⁰ Some iron nitrosyl porphyrins also nitrosate secondary amines to form nitrosamines.^{21,22} Our research group is interested in investigating the coordination chemistry of nitrosamines with heme models, since nitrosamine interactions with cytochrome P450 lead to activation and/or denitrosation of the nitrosamine. Specifically, we were interested in (i) preparing discrete adducts of nitrosamines with heme models, and (ii) determining the nature of nitrosamine binding to the metal center in such heme models.

Prior to our work, only a handful of structurally characterized nitrosamine metal complexes were reported. The structure of $(Me_2NNO)(SbCl_5)^{12}$ was reported very

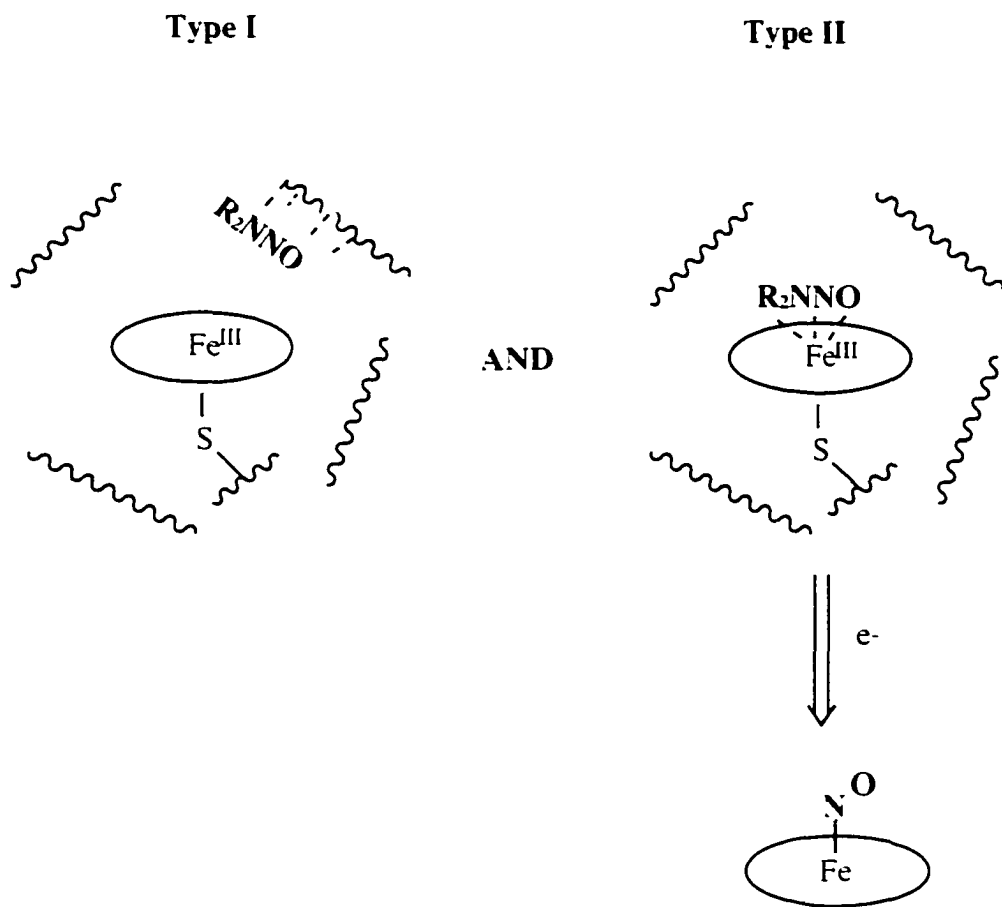


Figure 2.1. Proposed interactions of nitrosamine with the heme site of cytochrome P450.

recently, and it shows an η^1 -O binding mode of the nitrosamine ligand, while in transition metal $(\text{Me}_2\text{NNO})\text{CuCl}_2$ ¹⁵ and $((\text{CH}_2)_5\text{NNO})\text{CuCl}_2$ complexes.¹² both O-binding and N-binding of the nitrosamines are present. Structures of palladium and platinum complexes with cyclometallated C, N-bound nitrosamines are also known.²³

Our research group recently reported the synthesis and X-ray crystallographic characterization of the first isolable nitrosamine metalloporphyrin complex $[(\text{TPP})\text{Fe}(\text{Et}_2\text{NNO})_2](\text{ClO}_4)$ (TPP = 5, 10, 15, 20-tetraphenylporphyrinato dianion).^{24a,c} The X-ray crystal structure of the complex reveals that the two Et_2NNO ligands are η^1 -O bound to the iron center. The η^1 -O binding mode of nitrosamines was successfully extended to Ru^{II} porphyrins.^{24b,c} In this chapter, we will show the successful extension of the coordination chemistry of Et_2NNO to other Fe^{III} and Os^{II} porphyrin complexes.

Nitrosoalkanes and nitrosoarenes (C-nitroso compounds, RNO/ArNO) are known to bind to heme-containing biomolecules such as hemoglobin (Hb), myoglobin (Mb), cytochrome P450 and guanylyl cyclase.²⁵⁻²⁷ Nitrosobenzene (PhNO) binding to Hb has long been associated with PhNO_2 poisoning.²⁸ It has also been proposed that nitrosoalkane monomers bind to cytochrome P450 during the oxidative metabolism of amphetamine, phenylalkylamines and N-hydroxyamphetamine or during the reduction of nitroamphetamine^{29,30} (Figure 2.2). Furthermore, primary and secondary aliphatic nitro compounds react with Hb, Mb and cytochrome P450 under reducing conditions to produce Fe^{II} -nitrosoalkane complexes.^{26b,31} Previous studies also show the similarities of the C-nitroso compounds (RNO) to dioxygen (O_2): the low-lying π^* orbitals of dioxygen and C-nitroso compounds can easily accept electron density via metal-ligand backbonding.³²

There are three binding modes of C-nitroso ligands that have been established in mononuclear metal complexes (Figure 2.3).³³ All three binding modes have been

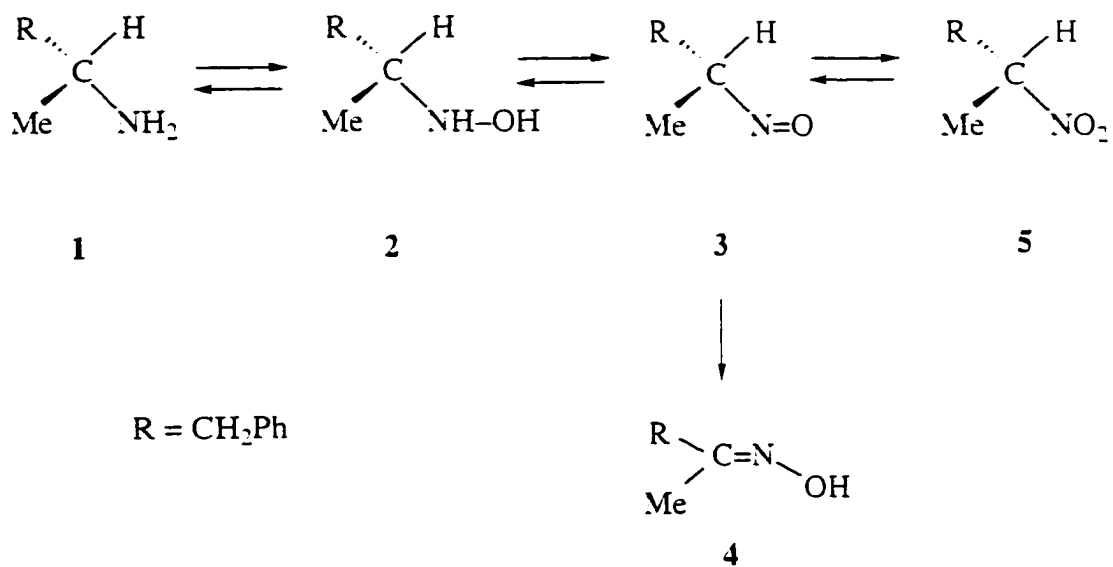


Figure 2.2 Possible redox intermediates between amphetamine **1** and its corresponding nitro compound **5**.²⁹

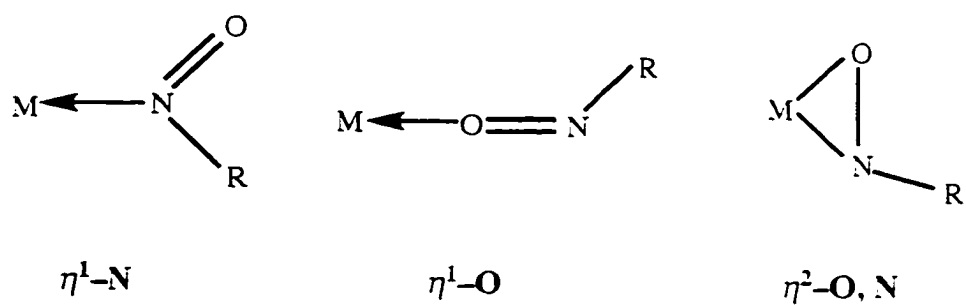


Figure 2.3. Coordination modes of C-nitroso ligands to monometallic centers.

confirmed by single-crystal X-ray crystallographic studies. The majority of metal-RNO complexes display η^1 -N binding of the C-nitroso ligands to the metal centers. Examples of η^1 -N binding include $\text{W}(\text{CO})_5(\text{}^t\text{BuNO})$ (d^6),³⁴ $\text{RhCl}(\text{cod})(2\text{-Me-4-Me}_2\text{NC}_6\text{H}_3\text{NO})$ (d^8),³⁵ $\text{PdCl}_2(\text{PhNO})_2$ (d^8),³⁶ $\text{PtCl}_2(\text{}^t\text{BuNO})_2$ (d^8)³⁷ and $[\text{CoCl}_2(\text{NODMA})_2]$ (d^7)³⁸ (NODMA = *N,N*-dimethyl-4-nitrosoaniline). Although there is ample precedent for the existence of nitrosoalkane and nitrosoarene complexes of hemes, there were only a handful of synthetic metalloporphyrin complexes containing C-nitroso compounds as ligands. The structurally characterized nitrosoalkane complex $(\text{TPP})\text{Fe}(\text{}^i\text{PrNO})(\text{}^i\text{PrNH}_2)$ displays the η^1 -N binding of the nitrosoalkane ligand to the formal Fe^{II} d^6 center.³² Our research group recently reported³⁹ that the structurally characterized $(\text{TPP})\text{Fe}(\text{PhNO})_2$ complex also displays the η^1 -N binding of the two nitrosobenzene ligands to the formal Fe^{II} d^6 metalloporphyrin center. James et al⁴⁰ have shown (by IR and NMR spectroscopy) that nitrosobenzene binds via its *N* atom to related formal Ru^{II} d^6 porphyrins. Some transition metal coordination (non-porphyrin) complexes containing bidentate C-nitroso ligands have also been reported.⁴¹

Surprisingly, the η^1 -O binding mode of C-nitroso monomers to monometallic complexes was only shown (by X-ray diffraction studies) in two metal complexes, namely, $\text{SnCl}_2\text{Me}_2(\text{NODMA})_2$ ^{42a} and $\text{ZnCl}_2(\text{NODMA})_2$,^{42b} with both metals having a formal d^{10} electronic configuration. The dimeric C-nitroso ligands also act as bidentate O-donors to various metals, such as Fe, Ti, Pb and Sn.⁴³ Based on structural data available, it was proposed that such an η^1 -O binding of C-nitroso monomers was indeed restricted to d^{10} metals.³³ We have since utilized our results with η^1 -O nitrosamine binding (to group 8 metalloporphyrins) to design appropriate reactions to prepare targeted η^1 -O nitrosoarene complexes of iron and manganese porphyrins.^{39,44} We have also extended the η^1 -N nitrosoarene binding to several Os^{II} porphyrins. Prior to our work, only one other Os-RNO complex had been reported in the literature.⁴⁵

Experimental Section

All reactions were performed under an atmosphere of prepurified nitrogen (Airgas, Inc.) using standard Schlenk techniques and/or in an Innovative Technology Labmaster 100 Dry Box unless stated otherwise. Solvents were distilled from appropriate drying agents under nitrogen just prior to use: CH_2Cl_2 (CaH_2), THF (Na/benzophenone), hexane (Na/benzophenone/tetraglyme), benzene (Na), and toluene (Na).

Chemicals. *N*-nitrosodiethylamine (Et_2NNO , >99%) was purchased from Fluka. The compounds NOBF_4 , diethylamine (98%), sodium nitrite (97%), AgSbF_6 (98%), PhNO (97%), *o*-tolNO (97%), *N,N*-dimethyl-4-nitrosoaniline ($\text{Me}_2\text{NC}_6\text{H}_4\text{NO}$, 97%), and *N,N*-diethyl-4-nitrosoaniline ($\text{Et}_2\text{NC}_6\text{H}_4\text{NO}$, 97%) were purchased from Aldrich Chemical Co. [^{18}O]water was purchased from Isotec. Anhydrous HCl gas was obtained from Matheson Gas Co. The (por)FeCl compounds (por = TPP, TTP; TTP = 5, 10, 15, 20-tetra-*p*-tolylporphyrinato dianion) were prepared by following the reported procedures.^{46,47} The (por)Os(CO)⁺⁸ compounds were prepared by literature methods (por = TPP, TTP, OEP, TMP⁴⁹; OEP = 2, 3, 7, 8, 12, 13, 17, 18-octaethylporphyrinato dianion, TMP = 5, 10, 15, 20-tetramesitylporphyrinato dianion). Chloroform-*d* (99.8%), methylene-*d*₂ chloride (99.9%), benzene-*d*₆ (99.6%) and toluene-*d*₈ (99.6%) were obtained from Cambridge Isotope Laboratories, subjected to three freeze-pump-thaw cycles, and stored over Linde 4Å molecular sieves. Elemental analyses were performed by Atlantic Microlab, Norcross, GA. Nitric oxide (98%, Matheson Gas) was passed through KOH pellets and a cold trap (Dry Ice/acetone, -78 °C) to remove higher nitrogen oxides.

Instrumentation. Infrared spectra were recorded on a Bio-Rad FT-155 FTIR spectrometer. ¹H NMR spectra were obtained on a Varian XL-300 spectrometer and the signals were referenced to the residual signal of the solvent employed. All chemical shifts are in ppm. All coupling constants are in Hz. FAB mass spectra were

obtained on a VG-ZAB-E mass spectrometer. UV-vis spectra were recorded on a Hewlett-Packard HP8453 Diode Array instrument. Solution magnetic susceptibilities were measured using the Evan's NMR method in C₆D₆ at room temperature.⁵⁰

***N*-Nitroso (Nitrosamine) Complexes**

Synthesis of [¹⁸O]Et₂NNO. This procedure is a slight modification of a published procedure for the preparation of the analogous Me₂NN¹⁸O.⁵¹ Sodium nitrite (0.154 g) was dissolved in [¹⁸O]water (1 g) and the mixture was deaerated by repeated freeze-pump-thaw cycles. The sample was placed under nitrogen and immersed in an ice bath. Anhydrous HCl gas was passed through the mixture for several minutes until the weight increase was ca. 0.2 g and a yellow precipitate was observed to form. The sample was left to stir for an additional 7 h. Cold diethylamine (0.35 g, ice bath) was then added, and the mixture was stirred overnight under nitrogen. The resulting mixture was extracted with CH₂Cl₂ (15 mL), and the extract was dried over anhydrous MgSO₄ to remove any remaining [¹⁸O]water. The solution was filtered into another container, and the solvent was removed by passage of nitrogen gas through the solution. Low-resolution mass spectrum (EI): *m/z* 104 [Et₂NN¹⁸O]⁺ (100%), 102 [Et₂NNO]⁺ (14%).

Preparation of [(TTP)Fe(THF)₂](SbF₆). To a THF (20 mL) solution of (TTP)FeCl (0.31 g, 0.41 mmol) was added AgSbF₆ (98%, 0.15g, 0.43 mmol). The mixture was heated to gently reflux for 30 min, and the color of the reaction mixture turned from brown to red. The solution was filtered to another reaction container. The volume of the solution was reduced to ca. 15 mL and hexane (45 mL) was added. The mixture was stored at -20 °C overnight. The supernatant was discarded, and the black purple solid was dried in vacuo for 2 h to give [(TTP)Fe(THF)₂](SbF₆) (0.42 g, 0.38 mmol, 93%). Anal. Calcd for C₅₆H₅₂O₂N₄FeSbF₆: C, 60.89; H, 4.74; N, 5.07. Found: C, 59.91; H, 4.63; N, 5.33. IR (KBr, cm⁻¹): $\nu_{\text{SbF}_6}^{52} = 657$ vs; also 3025 w.

2972 w, 2921 w, 2870 w, 1508 w, 1488 w, 1457 w, 1405 w, 1338 w, 1201 m, 1183 m, 1109 w, 1067 m, 1028 w, 1002 s, 917 w, 861 w, 847 m, 799 s, 746 w, 724 m, 567 w, 522 m. $\mu_{\text{eff}} = 5.7$.

Preparation of [(TTP)Fe(Et₂NNO)₂](SbF₆). To a stirred CH₂Cl₂ solution (10 mL) of [(TTP)Fe(THF)₂](SbF₆) (0.100 g, 0.090 mmol) was added excess Et₂NNO (0.5 mL, ca. 5 mmol). The solution was left to stir for 30 min. Hexane (20 mL) was then added. The product mixture was stored at -22 °C overnight. Precipitation of the solid was enhanced by mixing of the CH₂Cl₂/hexane solution, and the supernatant solution was discarded. The solid product remaining was washed with hexane (3 x 10 mL) and dried in vacuo for 10 min to give analytically pure [(TTP)Fe(Et₂NNO)₂](SbF₆) as dark purple crystalline solid (0.073 g, 0.063 mmol, 70% yield). Anal. Calcd for C₅₆H₅₆O₂N₈FeSbF₆: C, 57.75; H, 4.85; N, 9.62. Found: C, 57.73; H, 4.87; N, 9.57. IR (KBr, cm⁻¹): ν_{NO} = 1271 m, ν_{NN} = 1256 m; ν_{SbF_6} = 657 s; also 3025 w, 2986 w, 2943 w, 2921 w, 1511 w, 1476 w, 1451 w, 1379 w, 1331 w, 1200 w, 1182 w, 1128 w, 1108 w, 1098 w, 1073 w, 1004 s, 953 w, 849 w, 843 w, 805 s, 724 m, 680 w, 595 w, 567 w, 527 w, 517 w, 426 w. Low-resolution mass spectrum (FAB): m/z 724 [(TTP)Fe]⁺ (100%), 103 [Et₂NNO + H]⁺ (4%). Low-resolution mass spectrum (70 eV EI): m/z 102 [Et₂NNO]⁺ (100%). $\mu_{\text{eff}} = 6.0$. UV-vis spectrum (λ (ϵ , mM⁻¹ cm⁻¹), 9.46 x 10⁻⁶ M in C₆H₆): 415 (66), 516 (7), 572 (3), 613 (2) nm.

[(TTP)Fe(Et₂N¹⁵NO)₂](SbF₆). IR (KBr, cm⁻¹): ν_{NO} = 1263, ν_{NN} = 1248.

Attempted Preparation of [(TTP)Fe(NO)(Et₂NNO)](SbF₆). NO (g) was bubbled through a CH₂Cl₂ (10 mL) solution of [(TTP)Fe(Et₂NNO)₂](SbF₆) (0.056 g, 0.048 mmol). The color of the solution turned from purple red to red. All the solvent was then removed to result in a red powdery solid. IR (KBr, cm⁻¹): Et₂NNO: $\nu_{\text{NO/NN}}$ = 1263 m; nitrosyl: ν_{NO} = 1922 m, 1903 m; ν_{SbF_6} = 658 s. No

satisfactory elemental analysis was obtained. The compound is thermally unstable, similar to the TPP analog.^{24c}

Preparation of (TTP)Os(CO)(Et₂NNO). To a CH₂Cl₂ (10 mL) solution of (TTP)Os(CO) (0.035 g, 0.039 mmol) was added excess Et₂NNO (0.2 mL, ca. 2 mmol). The solution was gently heated and left to stir for 20 min. No substantial color change was observed. The product was recrystallized from CH₂Cl₂ (1 mL) and hexane (2 mL) at -20 °C overnight. The supernatant was discarded. The black purple crystalline solid was washed with hexane (3 x 10 mL) and dried in vacuo for 2 h to give (TTP)Os(CO)(Et₂NNO)·0.5 hexane (0.030 g, 0.029 mmol, 74% yield). Anal. Calcd for C₅₃H₄₆O₂N₆Os₁·0.5C₆H₁₄: C, 65.16; H, 5.17; N, 8.14. Found: C, 65.13; H, 5.20; N, 8.53. IR (KBr, cm⁻¹): ν_{NO} = 1292 m, ν_{NN} = 1251 w; ν_{CO} = 1902 s (compare: ν_{CO} for (TTP)Os(CO) = 1916); also 3021 w, 2955 w, 2920 w, 2870 w, 1799 w, 1609 w, 1571 w, 1531 m, 1513 w, 1454 w, 1437 w, 1412 w, 1380 w, 1352 m, 1307 w, 1208 w, 1180 m, 1118 w, 1107 w, 1069 m, 1011 s, 953 w, 798 s, 714 m, 675 w, 644 w, 596 w, 561 w, 525 m, 453 w. ¹H NMR (CDCl₃, ca. 20°C, δ): 8.50 (s, 8H, *pyr*-H of TTP), 8.11 (d, *J* = 8, 4H, *o*-H of TTP), 7.86 (d, *J* = 8, 4H, *o'*-H of TTP), 7.50 (d, *J* = 8, 4H, *m*-H of TTP), 7.44 (d, *J* = 8, 4H, *m'*-H of TTP), 2.65 (s, 12H, CH₃ of TTP), 1.25 (b, C₆H₁₄), 0.86 (t, C₆H₁₄). No apparent CH₃CH₂ peaks from Et₂NNO were observed at room temperature. ¹H NMR (CD₂Cl₂, -10°C, δ): 8.56 (s, 8H, *pyr*-H of TTP), 8.14 (d, *J* = 7, 4H, *o*-H of TTP), 7.87 (d, *J* = 7, *o'*-H of TTP), 7.57 (d, *J* = 7, *m*-H of TTP), 7.51 (d, *J* = 7, *m'*-H of TTP), 2.68 (s, 12H, CH₃ of TTP), 2.19 (q, *J* = 7, 2H, (CH₃CH₂)₂NNO), 1.27 (b, hexane), 1.03 (q, *J* = 7, 2H, (CH₃CH₂)₂NNO), 0.88 (t, hexane), 0.057 (t, *J* = 7, 3H, (CH₃CH₂)₂NNO), -1.26 (t, *J* = 7, 3H, (CH₃CH₂)₂NNO). Low-resolution mass spectrum (FAB): *m/z* 888 [(TTP)Os(CO)]⁺ (47%), 860 [(TTP)Os]⁺ (56%). Low-resolution mass spectrum (70 eV EI): *m/z* 102 [Et₂NNO]⁺ (100%). UV-vis spectrum (λ (ε, mM⁻¹ cm⁻¹), 3.54 x 10⁻⁶ M in CH₂Cl₂): 312 (36), 408 (323), 519 (25), 582 (12) nm.

A suitable crystal for structure determination was grown by recrystallization of the compound from a CH₂Cl₂/hexane mixture at -20 °C.

(TTP)Os(CO)(Et₂N¹⁵NO). IR (KBr, cm⁻¹): $\nu_{\text{N}^{15}\text{O}} = 1275$, $\nu_{\text{N}^{15}\text{N}} = 1246$.

Preparation of (OEP)Os(CO)(Et₂NNO). This product was prepared in 66% yield in a manner analogous to the TTP derivative described above. Anal. Calcd for C₄₁H₅₄O₂N₆Os₁: C, 57.72; H, 6.38; N, 9.85. Found: C, 57.61; H, 6.40; N, 8.59. IR (KBr, cm⁻¹): $\nu_{\text{NO}} = 1294$ w, $\nu_{\text{NN}} = 1208$ w; $\nu_{\text{CO}} = 1883$ s (compare: ν_{CO} for (OEP)Os(CO) = 1894); also 2962 w, 2933 w, 2870 w, 1585 w, 1544 w, 1537 w, 1488 w, 1464 s, 1453 s, 1374 m, 1354 w, 1336 w, 1315 w, 1273 m, 1231 m, 1220 m, 1149 m, 1111 w, 1056 s, 1018 s, 992 m, 958 s, 859 w, 842 m, 826 w, 744 s, 712 m, 707 m, 685 w, 654 w, 600 w. ¹H NMR (CDCl₃, ca. 20 °C, δ): 9.68 (s, 4H, *meso*-H of OEP), 3.93 (m, 16H, CH₃CH₂ of OEP), 1.85 (t, $J = 8$, 24H, CH₃CH₂ of OEP). No apparent CH₃CH₂ peaks from Et₂NNO were observed at room temperature. ¹H NMR (CD₂Cl₂, -40 °C, δ): 9.76 (s, 4H, *meso*-H of OEP), 3.98 (m, 16H, CH₃CH₂ of OEP), 1.85 (t, $J = 8$, 24H, CH₃CH₂ of OEP), 1.85 (q, 2H, (CH₃CH₂)₂NNO, overlapping with CH₃CH₂ of OEP), 0.68 (q, $J = 7$, 2H, (CH₃CH₂)₂NNO), -0.11 (t, $J = 7$, 3H, (CH₃CH₂)₂NNO), -1.69 (t, $J = 7$, 3H, (CH₃CH₂)₂NNO). Low-resolution mass spectrum (FAB): m/z 752 [(OEP)Os(CO)]⁺ (18%), 724 [(OEP)Os]⁺ (12%), 102 [Et₂NNO]⁺ (1%). Low-resolution mass spectrum (70 eV EI): m/z 102 [Et₂NNO]⁺ (100%). UV-vis spectrum (λ (ϵ , mM⁻¹cm⁻¹), 5.28 x 10⁻⁶ M in CH₂Cl₂): 370 (sh, 60), 389 (218), 507 (13), 539 (18) nm.

(OEP)Os(CO)(Et₂N¹⁵NO). IR (KBr, cm⁻¹): $\nu_{\text{N}^{15}\text{O}} = 1256$, $\nu_{\text{N}^{15}\text{N}} = 1203$.

Preparation of [(OEP)Os(NO)(Et₂NNO)](BF₄). To a CH₂Cl₂ solution of (OEP)Os(CO)(Et₂NNO) (0.114 g, 0.134 mmol) was added NOBF₄ (0.016 g, 0.137 mmol). The color of the solution turned from dark red to bright red. The

solution was left to stir for 30 min. All the solvent was then removed. ^1H NMR spectrum indicates the quantitative nature of the reaction to form $[(\text{OEP})\text{Os}(\text{NO})(\text{Et}_2\text{NNO})](\text{BF}_4)$. Anal. Calcd for $\text{C}_{40}\text{H}_{54}\text{O}_2\text{N}_7\text{Os}_1\text{B}_1\text{F}_4$: C, 51.01; H, 5.78; N, 10.41. ($\text{C}_{40}\text{H}_{54}\text{O}_2\text{N}_7\text{Os}_1\text{B}_1\text{F}_4 \cdot \text{H}_2\text{O}$: C, 50.05; H, 5.88; N, 10.21.) Found: C, 49.75; H, 5.75; N, 9.45. IR (KBr, cm^{-1}): Et_2NNO : ν_{NO} = 1241 m, ν_{NN} = 1198 m; nitrosyl: ν_{NO} = 1800 s; also 2969 w, 2935 w, 2874 w, 1501 w, 1469 m, 1455 m, 1435 m, 1375 w, 1317 w, 1272 m, 1155m, 1111 m, 1056 s, 1021 m, 996 m, 965 m, 851 m, 832 w, 749 m, 732 w, 716 m, 684 m, 625 w, 520 w. ^1H NMR (CDCl_3 , δ): 10.51 (s, 4H, *meso*-H of OEP), 4.22 (q, $J = 8$, 16H, CH_3CH_2 of OEP), 1.99 (t, $J = 8$, 24H, CH_3CH_2 of OEP), 1.99 (2H, $(\text{CH}_3\text{CH}_2)_2\text{NNO}$, overlapping with CH_3CH_2 of OEP), 0.58 (q, $J = 7$, 2H, $(\text{CH}_3\text{CH}_2)_2\text{NNO}$), -0.52 (t, $J = 7$, 3H, $(\text{CH}_3\text{CH}_2)_2\text{NNO}$), -2.01 (t, $J = 7$, 3H, $(\text{CH}_3\text{CH}_2)_2\text{NNO}$). Low-resolution mass spectrum (FAB): m/z 856 $[(\text{OEP})\text{Os}(\text{NO})(\text{Et}_2\text{NNO})]^+$ (6%), 754 $[(\text{OEP})\text{Os}(\text{NO})]^+$ (31%), 724 $[(\text{OEP})\text{Os}]^+$ (5%), 102 $[\text{Et}_2\text{NNO}]^+$ (1%). Low-resolution mass spectrum (70 eV EI): m/z 102 $[\text{Et}_2\text{NNO}]^+$ (100%). UV-vis spectrum (λ (ϵ , $\text{mM}^{-1}\text{cm}^{-1}$), 1.26×10^{-5} M in CH_2Cl_2): 348 (45), 370 (51), 418 (40), 542 (11), 579 (17) nm.

C-Nitroso Complexes

$[(\text{TPP})\text{Fe}(\text{ONC}_6\text{H}_4\text{Me}_2)_2](\text{SbF}_6)$ was first prepared by Dr. Li-Sheng Wang of our research group at the time.³⁹ IR (KBr, cm^{-1}): ν_{NO} = 1364 m, ν_{CN} = 1336 m; ν_{SbF_6} = 657 vs. μ_{eff} = 6.1.

Preparation of $[(\text{TPP})\text{Fe}(\text{O}^{15}\text{NC}_6\text{H}_4\text{NMe}_2)_2](\text{SbF}_6)$. $[(\text{TPP})\text{Fe}(\text{THF})_2](\text{SbF}_6) \cdot \text{THF}$ ³⁹ (0.030g, 0.027 mmol) and $\text{Me}_2\text{NC}_6\text{H}_4^{15}\text{NO}$ (0.014 g, 0.093 mmol)⁵³ were dissolved in CH_2Cl_2 (5 mL). The reaction mixture was left to stir for 30 min. All the solvent was then removed, the residual solid was washed with hexane (2 x 5 mL) and dried in vacuo for 2 h. IR (KBr, cm^{-1}): $\nu_{^{15}\text{NO}}$ = 1359, $\nu_{\text{C}^{15}\text{N}}$ = 1323;

$\nu_{\text{SbF}_6} = 657$ vs. UV-vis spectrum (λ (ϵ , $\text{mM}^{-1} \text{cm}^{-1}$), $8.71 \times 10^{-6} \text{ M}$ in C_6H_6): 413 (116), 508 (9), 569 (6), 610 (3), 659 (2) nm.

Preparation of [(TPP)Fe(ONC₆H₄NEt₂)₂](SbF₆)·0.3CH₂Cl₂. To a CH₂Cl₂ (15 mL) solution of [(TPP)Fe(THF)₂](SbF₆)·THF (0.10 g, 0.089 mmol) was added excess Et₂NC₆H₄NO (0.075g, 0.42 mmol). No substantial color change was observed. The solution was stirred for 30 min and the volume of the solution was reduced to ca. 8 mL. Hexane (10 mL) was added and the mixture was stored at -20°C overnight. The supernatant was discarded, and the purple crystalline solid was washed with hexane (2 x 5 mL) and dried in vacuo for 4 h to give [(TPP)Fe(ONC₆H₄NEt₂)₂](SbF₆)·0.3CH₂Cl₂ (0.095 g, 0.074 mmol, 83%). Anal. Calcd for C₆₄H₅₆O₂N₈FeSbF₆·0.3CH₂Cl₂: C, 60.04; H, 4.44; N, 8.71; Cl, 1.65. Found: C, 60.02; H, 4.54; N, 8.76; Cl, 1.61. IR (KBr, cm^{-1}): $\nu_{\text{SbF}_6} = 656$ s; also 3052 vw, 2981 vw, 2935 vw, 1614 s, 1602 s, 1575 sh, 1548 m, 1481 w, 1441 w, 1419 m, 1381 w, 1370 w, 1330 s, 1304 m, 1281 w, 1269 w, 1201 s, 1190 s, 1167 w, 1149 s, 1121 m, 1073 m, 1005 m, 996 m, 835 m, 797 s, 759 m, 752 m, 737 m, 715 m, 703 s, 632 m, 606 m, 566 m, 497 w, 432 w. Low-resolution mass spectrum (FAB): m/z 668 [(TPP)Fe]⁺ 100%, 179 [ONC₆H₄NEt₂ + H]⁺ 86%. $\mu_{\text{eff}} = 6.0$. UV-vis spectrum (λ (ϵ , $\text{mM}^{-1} \text{cm}^{-1}$), $7.30 \times 10^{-6} \text{ M}$ in C_6H_6): 413 (173), 512 (16) nm.

[(TPP)Fe(ONC₆H₄NEt₂)₂](SbF₆)·0.3CH₂Cl₂ (0.100g) was redissolved in CH₂Cl₂ to make a saturated solution which was kept at -20°C for 5 days. After some dark purple crystals came out, the mother solution was transferred to another schlenk tube and kept at -20°C for 3 more days. A crystal coming out from the mother solution was used for structure determination.

A suitable crystal of the Mn^{III} analog [(TPP)Mn(ONC₆H₄NEt₂)₂](SbF₆) for structure determination was obtained from a CH₂Cl₂/hexane solution at -20°C .

Preparation of [(TTP)Fe(ONC₆H₄NMe₂)₂](SbF₆). The [(TTP)Fe(ONC₆H₄NMe₂)₂](SbF₆) complex was prepared by similar procedures for [(TPP)Fe(ONC₆H₄NEt₂)₂](SbF₆)·0.3CH₂Cl₂ in 59% yield. Anal. Calcd for C₆₄H₅₆O₂N₈FeSbF₆: C, 60.97; H, 4.48; N, 8.89. Found: C, 60.87; H, 4.65; N, 8.67. IR (KBr, cm⁻¹): ν_{N=O} = 1363 m, ν_{CN} = 1334 m; ν_{SbF₆} = 657 vs; also 1605 m, 1445 w, 1398 m, 1303 m, 1203 w, 1182 w, 1151 m, 1120 m, 1001 m, 839 m, 801 s, 724 s, 632 s, 605 m, 568 m, 521 m. Low-resolution mass spectrum (FAB): *m/z* 724 [(TTP)Fe]⁺ (100%), 151 [Me₂NC₆H₄NO + H]⁺ (4%). μ_{eff} = 4.8. UV-vis spectrum (λ (ε, mM⁻¹ cm⁻¹), 7.94 x 10⁻⁶ M in C₆H₆): 322 (24), 413 (109), 572 (6), 613 (3) nm.

Preparation of [(TTP)Fe(ONC₆H₄NEt₂)₂](SbF₆)·0.5CH₂Cl₂. The [(TTP)Fe(ONC₆H₄NEt₂)₂](SbF₆)·0.5CH₂Cl₂ complex was prepared by similar procedures in 55% yield. Anal. Calcd for C₆₈H₆₄O₂N₈FeSbF₆·0.5CH₂Cl₂: C, 60.53; H, 4.82; N, 8.24; Cl, 2.61. Found: C, 60.53; H, 4.85; N, 8.24; Cl, 2.62. IR (KBr, cm⁻¹): ν_{SbF₆} = 659 vs; also 1615 m, 1602 m, 1548 w, 1472 w, 1447 w, 1422 w, 1381 w, 1329 m, 1303 m, 1202 m, 1190 w, 1150 m, 1123 w, 1074 w, 1002 m, 839 m, 826 w, 802 s, 738 w, 724 w, 707 s, 629 s, 607 m, 568 m, 520 m, 496 m, 427 m. Low-resolution mass spectrum (FAB): *m/z* 724 [(TTP)Fe]⁺ (100%), 179 [Et₂NC₆H₄NO + H]⁺ (33%). μ_{eff} = 5.0. UV-vis spectrum (λ (ε, mM⁻¹ cm⁻¹), 6.08 x 10⁻⁶ M in C₆H₆): 415 (127), 511 (12), 611(3) nm.

Reaction of [(TPP)Fe(ONC₆H₄NMe₂)₂](SbF₆) with THF. The [(TPP)Fe(ONC₆H₄NMe₂)₂](SbF₆) compound (0.021 g, 0.017 mmol) was dissolved in THF (10 mL) and left to stir for 1h. Hexane (15 mL) was added, and the mixture was kept at -20 °C overnight. The supernatant was filtered off, and the purple crystalline solid was dried in vacuo for 15 min to give [(TPP)Fe(THF)₂](SbF₆)·THF by IR spectroscopy (0.014 g, 0.012 mmol, 71% yield).

Preparation of (TTP)Os(PhNO)₂. Two methods were employed:

Method I. To a toluene (20 mL) solution of (TTP)Os(CO) (0.040 g, 0.045 mmol) was added excess PhNO (0.011 g, 0.10 mmol). The solution was heated to reflux for 30 min whereby the color of the solution changed from orange-red to brown (the reaction takes 5-6 h at room temperature). The volume of the solution was reduced to ca. 2 mL. The product was precipitated out by adding hexane (4 mL) to the solution and keeping the mixture at ca. -20 °C overnight. The supernatant was discarded, and the purple-brown crystalline solid was dried in vacuo for 3 h to give (TTP)Os(PhNO)₂ (0.030 g, 0.028 mmol, 62% yield). Anal. Calcd for C₆₀H₄₆O₂N₆Os₁: C, 67.15; H, 4.32; N, 7.83. Found: C, 67.69; H, 4.78; N, 7.39. IR (KBr, cm⁻¹): ν_{NO} = 1291 s; also 3022 vw, 2917 vw, 1570 w, 1527 w, 1512 w, 1496 w, 1451 w, 1350 w, 1312 s, 1212 w, 1180 m, 1150 vw, 1107 w, 1071 w, 1014 s, 868 m, 831 w, 797 s, 766 m, 730 vw, 717 m, 691 m, 670 w, 662 w, 632 w, 524 m. ¹H NMR (CDCl₃, δ): 8.48 (s, 8H, *pyr*-H of TTP), 7.96 (d, *J* = 8, 8H, *o*-H of TTP), 7.50 (d, *J* = 8, 8H, *m*-H of TTP), 6.40 (t, *J* = 8, 2H, *p*-H of PhNO), 5.92 (t, *J* = 8, 4H, *m*-H of PhNO), 2.67 (s, 12H, CH₃ of TTP), 2.43 (d, *J* = 8, 4H, *o*-H of PhNO). Low-resolution mass spectrum (FAB): 967 [(TTP)Os(PhNO)]⁺ (14%), 860 [(TTP)Os]⁺ (24%), 107 [PhNO]⁺ (21%). UV-vis spectrum (λ (ϵ , mM⁻¹ cm⁻¹), 8.40 x 10⁻⁶ M in CH₂Cl₂): 314 (29), 408 (136), 655 (6) nm.

A suitable crystal of (TTP)Os(PhNO)₂ for structure determination was grown from a toluene/hexane mixture at ca. -20 °C.

Method II. To a CH₂Cl₂ (15 mL) solution of (TTP)Os(CO) (0.047 g, 0.053 mmol) was added PhNO (0.007 g, 0.065 mmol). The color of the solution changed from orange-red to a dirty dark brown. The mixture was left to stir for 20 min, and the volume of the solution was reduced to ca. 2 mL. The product mixture was precipitated out by adding hexane (4 mL) to the solution and keeping the mixture at ca. -20 °C overnight. The supernatant was discarded, and the solid was dried in vacuo for 3 h to

give a mixture of (TTP)Os(PhNO)₂ (major) and (TTP)Os(CO)(PhNO) (minor) in a 3:1 ratio. The IR spectrum of the mixture (as a KBr pellet) contained a band at 1972 cm⁻¹ attributed to ν_{CO} of (TTP)Os(CO)(PhNO). Low-resolution mass spectrum (FAB) of mixture: m/z 967 [(TTP)Os(PhNO)]⁺ (22%), 888 [(TTP)Os(CO)]⁺ (14%), 860 [(TTP)Os]⁺ (40%), 107 [PhNO]⁺ (41%). Further reaction of this product mixture with PhNO in refluxing toluene produces (TTP)Os(PhNO)₂ exclusively (0.023 g, 0.021 mmol, 40% overall yield).

A suitable crystal of (TTP)Os(CO)(PhNO) for structure determination was adventitiously grown from a reaction mixture of (TTP)Os(CO) and crude Me₂NC₆H₄NO (97%) which had been kept at -20 °C for 30 days.

Preparation of (TPP)Os(PhNO)₂. An analogous procedure to **Method I** above was used to synthesize (TPP)Os(PhNO)₂. No satisfactory elemental analysis was obtained in this case. IR of mixture (KBr, cm⁻¹): ν_{NO} = 1295 s; also 3054 vw, 3022 vw, 1597 w, 1575 w, 1530 w, 1506 w, 1489 w, 1478 w, 1450 sh, 1441 m, 1350 m, 1311 s, 1209 w, 1177 m, 1156 w, 1071 m, 1015 s, 1000 m, 920 w, 871 m, 832 w, 795 m, 767 m, 752 s, 735 w, 715 w, 701 s, 695 s, 666 m, 636 w, 527 w. Low-resolution mass spectrum (FAB): m/z 911 [(TPP)Os(PhNO)]⁺ (11%), 804 [(TPP)Os]⁺ (19%), 107 [PhNO]⁺ (52%).

Although an analytically pure bulk sample was not obtained, a suitable crystal for structure determination was grown from CH₂Cl₂/hexane at -20 °C.

Preparation of (TMP)Os(PhNO)₂. To a toluene (20 mL) solution of (TMP)Os(CO) (0.058 g, 0.058 mmol) was added excess PhNO (0.020 g, 0.19 mmol). The mixture was heated to reflux for 25 min. The color of the solution turned from light red to light brown. All the solvent was then removed in vacuo. The product was filtered through a neutral alumina column in air with CH₂Cl₂ as eluent. The brown filtrate was taken to dryness, and the product was dried in vacuo for 5 h to give (TMP)Os(PhNO)₂ (0.052 g, 0.044 mmol, 76% yield). Anal. Calcd for

$C_{68}H_{62}O_2N_6Os_1$: C, 68.90; H, 5.27; N, 7.09. Found: C, 68.39; H, 5.50; N, 6.75. IR (KBr, cm^{-1}): $\nu_{NO} = 1276$ s; also 2917 vw, 2850 vw, 1610 vw, 1586 vw, 1525 vw, 1478 w, 1452 w, 1436 m, 1380 w, 1344 w, 1324 w, 1310 w, 1206 w, 1181 w, 1155 w, 1063 m, 1015 s, 919 m, 868 m, 853 w, 833 m, 797 m, 765 w, 730 s, 720 s, 686 m, 671 w, 644 w, 635 w, 561 w. 1H NMR ($CDCl_3$, δ): 8.26 (s, 8H, *p*-H of TMP), 7.20 (s, 8H, *m*-H of TMP), 6.29 (t, $J = 8$, 2H, *p*-H of PhNO), 5.81 (t, $J = 8$, 4H, *m*-H of PhNO), 2.79 (d, $J = 8$, 4H, *o*-H of PhNO), 2.56 (s, 12H, *p*- CH_3 of TMP), 1.86 (s, 24H, *o*- CH_3 of TMP). Low-resolution mass spectrum (FAB): m/z 1080 [(TMP)Os(PhNO) + H]⁺ (3%), 972 [(TMP)Os]⁺ (4%). UV-vis spectrum (λ (ϵ , $mM^{-1} cm^{-1}$), 3.72×10^{-6} M in CH_2Cl_2): 315 (42), 408 (163), 658 (10) nm.

A suitable crystal for structure determination was grown by slow solvent evaporation under inert atmosphere.

Preparation of (OEP)Os(PhNO)₂. (OEP)Os(PhNO)₂ was prepared by similar procedures as for (TMP)Os(PhNO)₂ in 45% isolated yield. Anal. Calcd for $C_{48}H_{54}O_2N_6Os_1$: C, 61.52; H, 5.81; N, 8.97. Found: C, 61.35; H, 5.87; N, 8.92. IR (KBr, cm^{-1}): $\nu_{NO} = 1286$ s; also 2964 w, 2932 w, 2864 w, 1588 w, 1468 w, 1451 w, 1447 w, 1378 w br, 1304 m, 1231 w, 1177 w, 1152 m, 1112 w, 1057 m, 1019 m, 993 m, 960 m, 870 w, 840 w, 766 m, 747 w, 738 w, 718 w, 689 m, 670 w, 666 w, 657 w, 625 w. 1H NMR ($CDCl_3$, δ): 9.93 (s, 4H, *meso*-H of OEP), 6.18 (t, $J = 8$, 2H, *p*-H of PhNO), 5.68 (t, $J = 8$, 4H, *m*-H of PhNO), 3.99 (q, $J = 8$, 16H, CH_3CH_2 of OEP), 1.99 (d, $J = 8$, 4H, *o*-H of PhNO), 1.83 (t, $J = 8$, 24H, CH_3CH_2 of OEP). Low-resolution mass spectrum (FAB): m/z 938 [(OEP)Os(PhNO)₂]⁺ (3%), 831 [(OEP)Os(PhNO)]⁺ (22%), 724 [(OEP)Os]⁺ (56%), 107 [PhNO]⁺ (20%). UV-vis spectrum (λ (ϵ , $mM^{-1} cm^{-1}$), 5.93×10^{-6} M in CH_2Cl_2): 328 (sh, 41), 377 (124), 498 (26), 658 (9) nm.

Preparation of (OEP)Os(*o*-tolNO)₂. (OEP)Os(*o*-tolNO)₂ was prepared by similar procedures as for (OEP)Os(PhNO)₂ and (TMP)Os(PhNO)₂ in 49% isolated yield. Anal. Calcd for C₅₀H₅₈O₂N₆Os₁: C, 62.22; H, 6.06; N, 8.71. Found: C, 62.30; H, 6.06; N, 8.62. IR (KBr, cm⁻¹): ν_{N-O} = 1290 s; also 2963 w, 2931 w, 2868 w, 1480 w, 1468 w, 1464 w, 1447 m, 1379 w, 1317 m, 1274 s, 1231 w, 1152 m, 1111 w, 1056 m, 1018 m, 992 m, 959 m, 886 m, 868 w, 859 w, 839 m, 749 s, 738 w, 718 m, 706 w, 664 w, 648 w, 626 w. ¹H NMR (toluene-*d*₈, δ): 10.02 (s, 4H, *meso*-H of OEP), 5.81 (app t, *J* = 7/8, 2H, *p*-H of *o*-tolNO), 5.45 (app t, *J* = 8/8, 2H, *m*-H of *o*-tolNO), 5.31 (d, *J* = 7, 2H, *m'*-H of *o*-tolNO), 3.91 (q, *J* = 7, 16H, CH₃CH₂ of OEP), 1.82 (t, *J* = 7, 24H, CH₃CH₂ of OEP), 1.51 (d, *J* = 8, 2H, *o*-H of *o*-tolNO), -1.26 (s, 6H, CH₃ of *o*-tolNO). ¹H NMR (CDCl₃, δ): 9.91 (s, 4H, *meso*-H of OEP), 5.99 (app t, *J* = 7/8, 2H, *p*-H of *o*-tolNO), 5.49 (app t, *J* = 7/8, 4H, *m*-H of *o*-tolNO), 3.99 (q, *J* = 8, 16H, CH₃CH₂ of OEP), 1.82 (t, *J* = 8, 24H, CH₃CH₂ of OEP), 1.19 (d, *J* = 8, 2H, *o*-H of *o*-tolNO), -1.46 (s, 6H, CH₃ of *o*-tolNO). Low-resolution mass spectrum (FAB): *m/z*: 845 [(OEP)Os(*o*-tolNO)]⁺ (3%), 724 [(OEP)Os]⁺ (49%), 121 [*o*-tolNO]⁺ (6%). UV-vis spectrum (λ (ε, mM⁻¹ cm⁻¹), 1.62 x 10⁻⁵ M in CH₂Cl₂): 322 (sh, 28), 383 (76), 499 (18) nm.

A suitable crystal of (OEP)Os(*o*-tolNO)₂ for X-ray structure determination was grown by slow evaporation of the toluene-*d*₈ mixture of the reaction of (OEP)Os(PhNO)₂ with excess *o*-tolNO (NMR tube reaction).

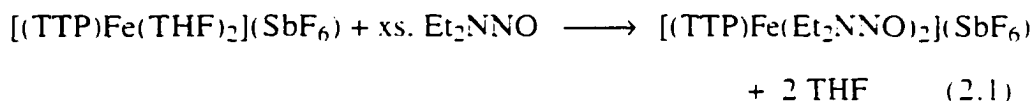
NMR Monitoring of the Substitution Reaction of (OEP)Os(PhNO)₂ with Excess *o*-tolNO. To a toluene-*d*₈ solution of (OEP)Os(PhNO)₂ (0.005 g) was added six equivalents of *o*-tolNO. ¹H NMR spectrum was taken after 30 min at room temperature. The spectrum only indicated the presence of (OEP)Os(PhNO)₂ and free *o*-tolNO ligand peaks. The mixture was then heated. ¹H NMR spectra were taken at the certain times and temperatures listed below. The peak at -1.26 is for the *o*-Me of the *o*-tolNO in (OEP)Os(*o*-tolNO)₂, the peak at

-1.15 is presumed for the *o*-Me of the *o*-tolNO in (OEP)Os(*o*-tolNO)(PhNO). The compounds' ratios from ¹H NMR integration's for the two singlet peaks at -1.15 and -1.26 are also listed below.

temperature and time	(OEP)Os(<i>o</i> -tolNO) (PhNO)	(OEP)Os(<i>o</i> -tolNO) ₂
50°C. 10 min	1	0.73
50°C. 20 min	1	1.27
50°C. 20 min then 75°C. 15 min	1	1.35
50°C. 20 min then 75°C. 25 min	1	1.28
50°C. 20 min then 75°C. 55 min	1	1.33
50°C. 20 min then 75°C. 7 h	1	1.31

Results and Discussion

Synthesis and Characterization of Nitrosamine Complexes of Iron and Osmium Porphyrins. Our research group recently reported the preparation and solid-state structure of [(TTP)Fe(Et₂NNO)₂](ClO₄).^{24a} The reaction of [(TTP)Fe(THF)₂](SbF₆) with excess Et₂NNO in CH₂Cl₂ generates the bis-nitrosamine [(TTP)Fe(Et₂NNO)₂](SbF₆) complex in 70% isolated yield (eq 2.1). The purple



product is moderately air-stable in solid state but is air-sensitive in solution. The product is freely soluble in CH₂Cl₂, moderately soluble in benzene but is only slightly soluble in hexane. The IR spectrum (as a KBr pellet) shows two new bands at 1271 cm⁻¹ and 1256 cm⁻¹ which are assigned as ν_{NO} and ν_{NN} for the coordinated Et₂NNO, respectively. These two bands shift to 1263 cm⁻¹ and 1248 cm⁻¹ when Et₂N¹⁵NNO is used in the reaction (Figure 2.4). The strong band at 657 cm⁻¹ is assigned as the ν_{SbF_6} of the complex.⁵² Unlike those of the [(TTP)Fe(Et₂NNO)₂](ClO₄)^{24a,c} ($\nu_{NO/NN}$ = 1270 cm⁻¹) complex, the ν_{NO} and ν_{NN} of [(TTP)Fe(Et₂NNO)₂](SbF₆) are distinguishable in the IR spectrum. The FAB mass spectrum shows peaks for [(TTP)Fe]⁺ and [Et₂NNO + H]⁺. The complementary EI mass spectrum reveals the presence of the Et₂NNO ligand. The μ_{eff} of 6.0 in C₆D₆ solution indicates a *d*⁵ high-spin state of the formal Fe^{III} center. The UV-vis spectrum in C₆H₆ gives a strong Soret band at 415 nm.

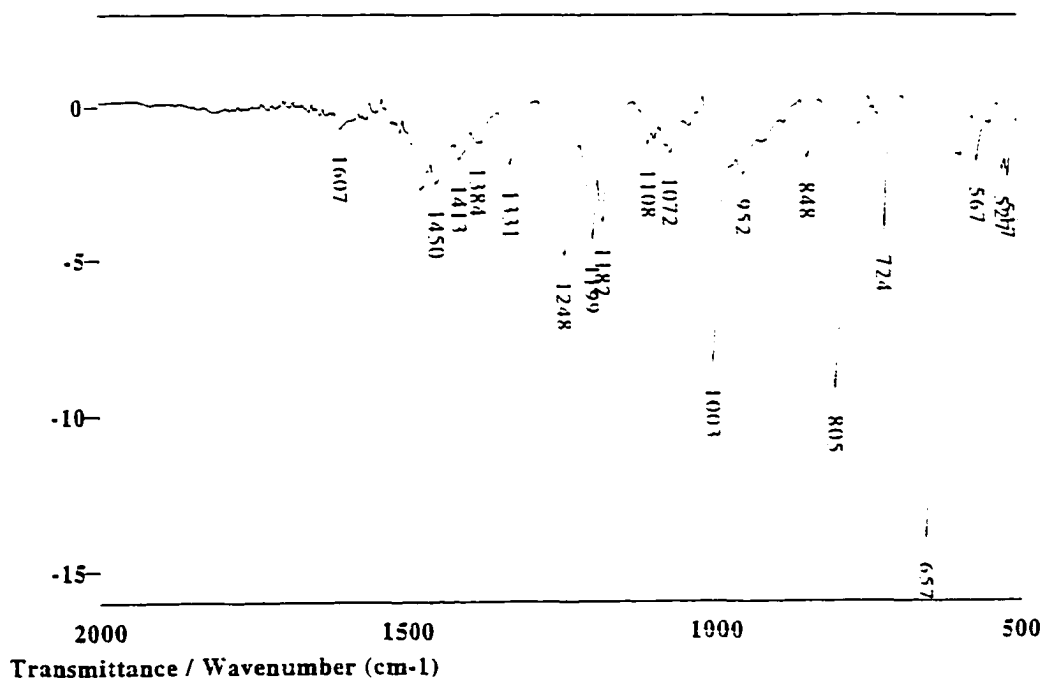
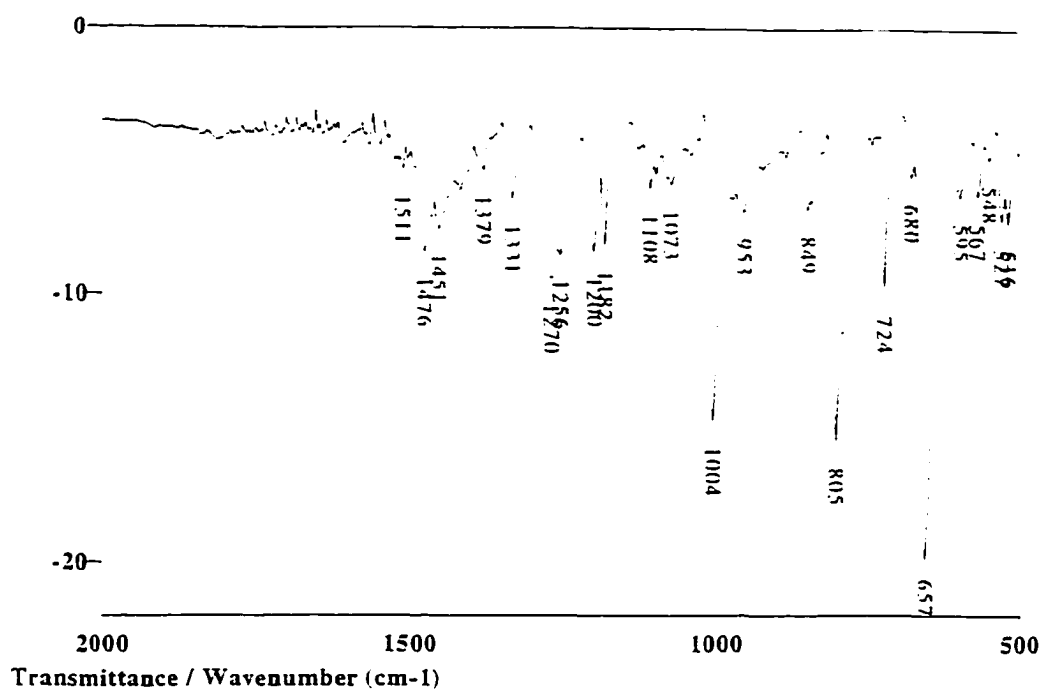
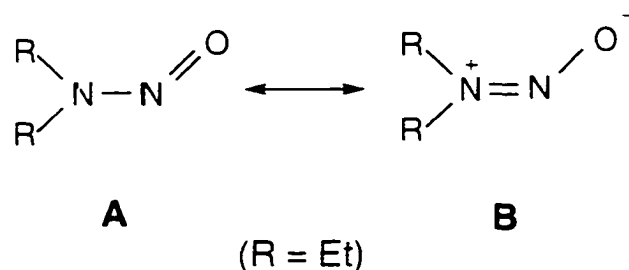


Figure 2.4. IR spectra of $[(\text{TTP})\text{Fe}(\text{Et}_2\text{NNO})_2](\text{SbF}_6)$ (top) and $[(\text{TTP})\text{Fe}(\text{Et}_2\text{N}^{15}\text{NO})_2](\text{SbF}_6)$ (bottom).

The complexed Et_2NNO can be represented by a resonance hybrid having a significant contribution from structure **B** as indicated by the N–N bond length of 1.282



Å and the N–O bond length of 1.272 Å in the $[(\text{TPP})\text{Fe}(\text{Et}_2\text{NNO})_2](\text{ClO}_4)$ complex.^{24a,c} A similar contribution from the dipolar structure **B** (R = Me) is noted in the low temperature X-ray structure of Me_2NNO .⁵⁴

Attempts were made to investigate the nature of nitrosamine binding to the related $(\text{por})\text{Fe}^{\text{II}}$ metal centers. In particular, complexes with the form of $[(\text{por})\text{Fe}(\text{NO})(\text{Et}_2\text{NNO})]^+$ (por = TPP^{24c}, TTP) were prepared. The linear NO ligand (regarded formally as NO^+) would then generate the required formal Fe^{II} center. The reaction of $[(\text{TTP})\text{Fe}(\text{Et}_2\text{NNO})_2](\text{SbF}_6)$ with NO gas in CH_2Cl_2 results in the formation of a proposed nitrosyl nitrosamine $[(\text{TTP})\text{Fe}(\text{NO})(\text{Et}_2\text{NNO})](\text{SbF}_6)$ complex based on its IR spectrum (as a KBr pellet, Figure 2.5). The ν_{NO} and ν_{NN} bands (1271 cm^{-1} and 1256 cm^{-1}) converged to a broad band at 1263 cm^{-1} with a decreased intensity. The similarity of the $\nu_{\text{NO/NN}}$ value in the nitrosyl nitrosamine $[(\text{TTP})\text{Fe}(\text{NO})(\text{Et}_2\text{NNO})](\text{SbF}_6)$ complex to the ν_{NO} and ν_{NN} values of the precursor bis-nitrosamine $[(\text{TTP})\text{Fe}(\text{Et}_2\text{NNO})](\text{SbF}_6)$ complex in the coordinated nitrosamine region suggests that the $\eta^1\text{-O}$ binding mode of the nitrosamine is not altered for the $[(\text{por})\text{Fe}^{\text{II}}(\text{NO})(\text{Et}_2\text{NNO})]^+$ complexes. Two new bands appear at higher wavenumbers 1922 cm^{-1} and 1903 cm^{-1} with comparable intensity. The new bands are assigned as the ν_{NO} of the nitrosyl ligand, and the presence of two bands might be due

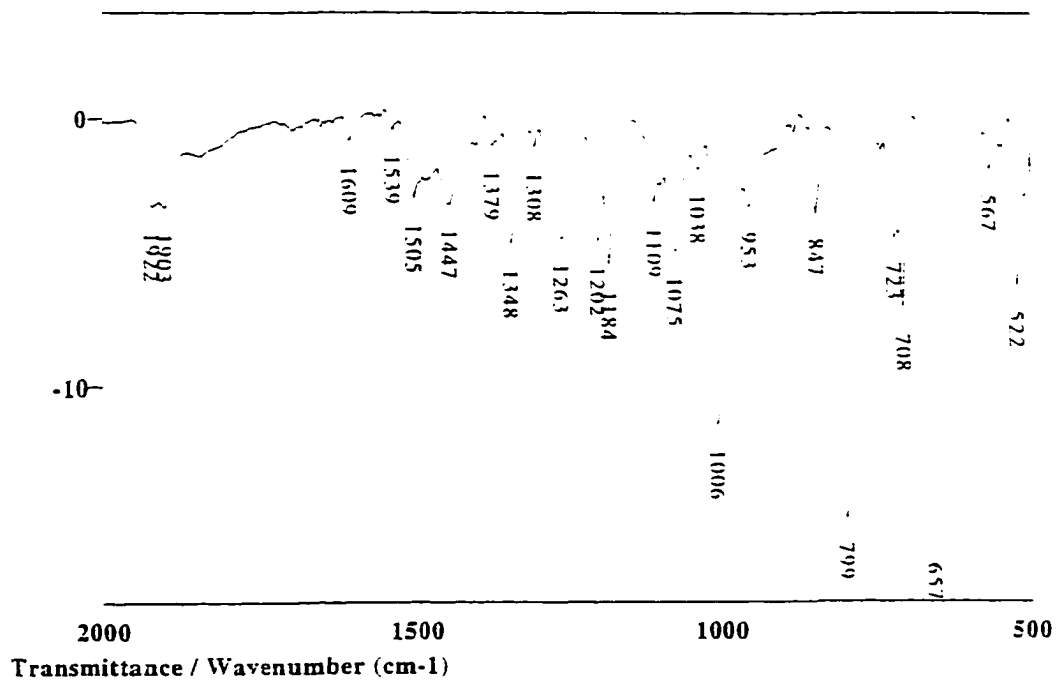
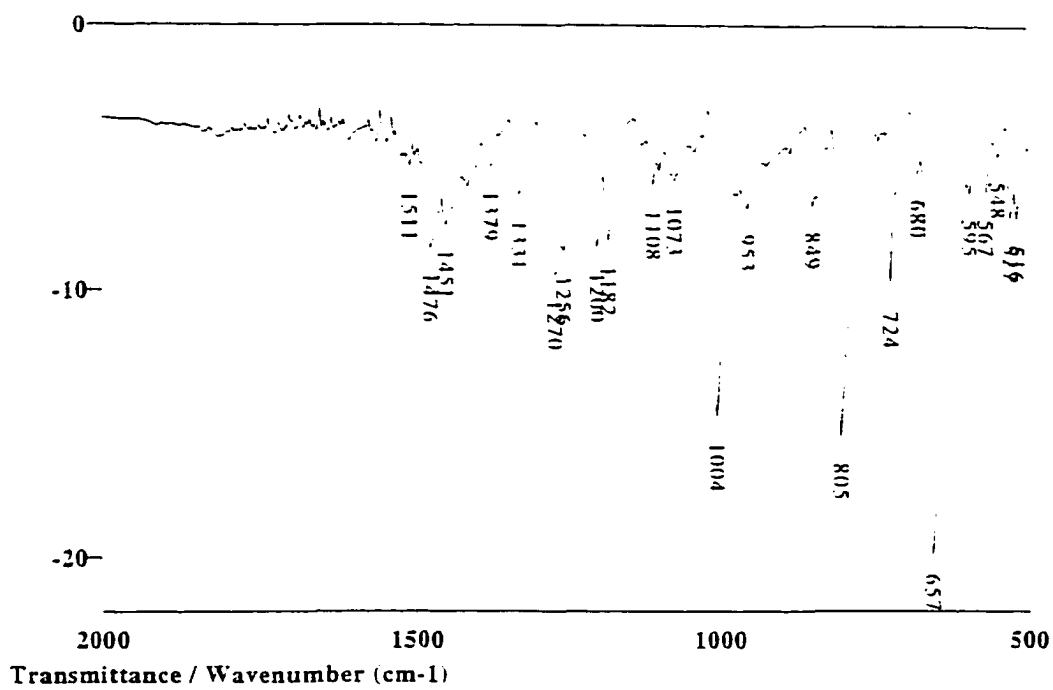
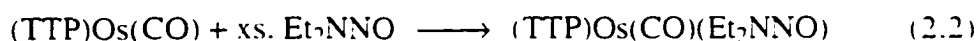


Figure 2.5. IR spectra (KBr) of $[(TTP)Fe(Et_2NNO)_2](SbF_6)$ (top) and proposed $[(TTP)Fe(NO)(Et_2NNO)](SbF_6)$ (bottom).

to the presence of different conformations of the complex in the solid state.⁵⁵ Attempts to grow crystals for an X-ray structural analysis have not been successful due to the thermal instability of the compound (it loses the axial NO ligand).

The instabilities of the [(por)Fe^{II}(NO)(Et₂NNO)]⁺ complexes prompted us to prepare the analogous (por)Ru^{II} and (por)Os^{II} complexes, in an attempt to generate more thermally stable (and possibly isolable) complexes. Geun-Bae Yi of our research group had successfully extended the nitrosamine coordination chemistry to ruthenium porphyrins.^{24b} We were interested in the further extension of the nitrosamine binding to osmium porphyrins. Prior to our work, no osmium nitrosamine complexes were known.⁵⁶⁻⁵⁸

The reaction of (TTP)Os(CO) with excess Et₂NNO in CH₂Cl₂ gives, after workup, (TTP)Os(CO)(Et₂NNO) in 74% isolated yield (eq 2.2). The product is



moderately air-stable, showing no signs of decomposition after several days in solid state and several hours in solution. The product is freely soluble in CH₂Cl₂ and benzene but is only slightly soluble in hexane. ¹H NMR in CDCl₃ shows the presence of sharp peaks for TTP macrocycle, consistent with the diamagnetic nature of the compound. The ethyl peaks of Et₂NNO are not observed at room temperature. However, a ¹H NMR spectrum of the complex in CD₂Cl₂ at -10 °C gives the expected sharp peaks for the TTP macrocycle, two triplets for the methyl groups of Et₂NNO and two quartets for the methylene groups of Et₂NNO. The methyl peaks of Et₂NNO are upfield with respect to the methylene peaks of Et₂NNO. The IR spectrum (as a KBr pellet, Figure 2.6, bottom) shows two new bands at 1292 cm⁻¹ and 1251 cm⁻¹ which are assigned as the ν_{NO} and ν_{NN} for the coordinated Et₂NNO ligand. The use of

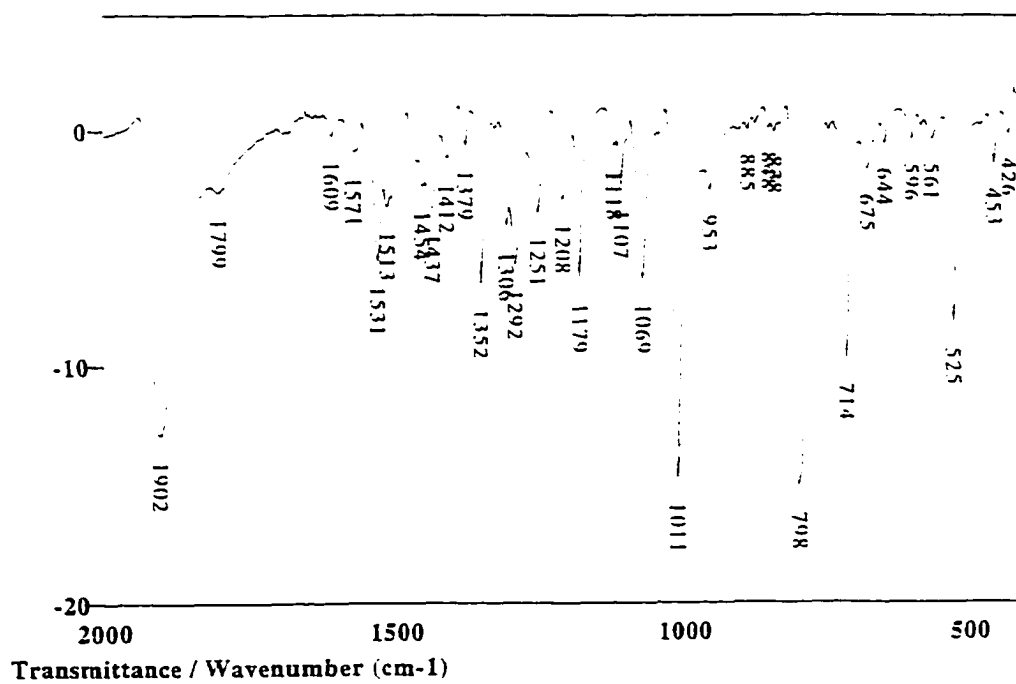
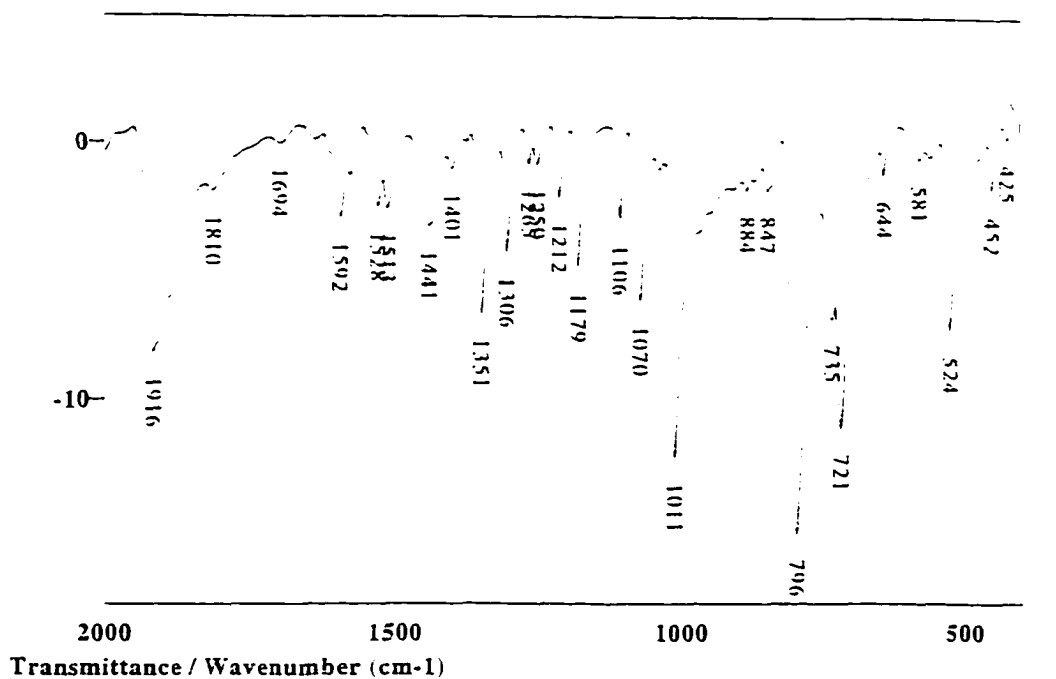


Figure 2.6. IR spectra (KBr) of (TTP)Os(CO) (top) and (TTP)Os(CO)(Et₂NNO) (bottom).

Et₂N¹⁵N¹⁸O in the reaction shifts these bands to 1275 and 1246 cm⁻¹. The larger $\Delta\nu$ (i.e., $|\nu_{\text{N}^{18}\text{O}} - \nu_{\text{N}^{15}\text{O}}|$) in the Os^{II} nitrosamine complexes compared to the smaller $\Delta\nu$ for [(TTP)Fe(Et₂NNO)₂](SbF₆) suggests a decreased contribution of the dipolar resonance structure **B** (see page 78) of the coordinated nitrosamine in the osmium complexes. The IR spectrum (as a KBr pellet) also shows a strong band at 1902 cm⁻¹ which is assigned to ν_{CO} . This value is lower than that of the starting (TTP)Os(CO) complex (1916 cm⁻¹), consistent with Et₂NNO acting as a σ -donor to strengthen the backbonding from the Os^{II} center to the π^* orbitals of the carbonyl ligand, thus decreasing the ν_{CO} value. The FAB mass spectrum of (TTP)Os(CO)(Et₂NNO) indicates the presence of the [(TTP)Os(CO) + H]⁺ and [(TTP)Os + H]⁺ fragments. The EI mass spectrum shows the presence of Et₂NNO ligand. The UV-vis spectrum of the complex in CH₂Cl₂ gives four bands at 312 (36), 408 (323), 519 (25) and 582 (12) nm. The solid-state structure of the compound was determined by an X-ray crystallographic study (Figure 2.7). Selected bond lengths and bond angles are listed in Tables 2.1 and 2.2.

As is observed in Figure 2.7, the nitrosamine ligand is bound to the Os^{II} center in an η^1 -O fashion. The axial Os-O (nitrosamine) distance of 2.200(7) Å is identical to the related Ru-O (axial) distance in (OEP)Ru(CO)(Et₂NNO) (2.200(8) Å).^{24c} The nitrosamine O-N and N-N bond lengths are 1.241(13) and 1.294(14) Å, respectively, and the nitrosamine O-N-N bond angle is 113.3(12)°. These data are similar to those found in (OEP)Ru(CO)(Et₂NNO).^{24c} The nitrosamine functionality in (TTP)Os(CO)(Et₂NNO) is essentially planar, with O(2)-N(5)-N(6)-C(52) and O(2)-N(5)-N(6)-C(50) torsion angles of 6.4 and 179.6°, respectively. The nitrosamine ligand nearly eclipses a porphyrin nitrogen, with an N(4)-Os(1)-O(2)-N(5) torsion angle of -20.2° (Figure 2.7b). The average Os-N(por) bond length in (TTP)Os(CO)(Et₂NNO) is 2.055 Å, and lies within the 2.029–2.067 Å range observed for other reported Os^{II} porphyrins (Table 2.3).

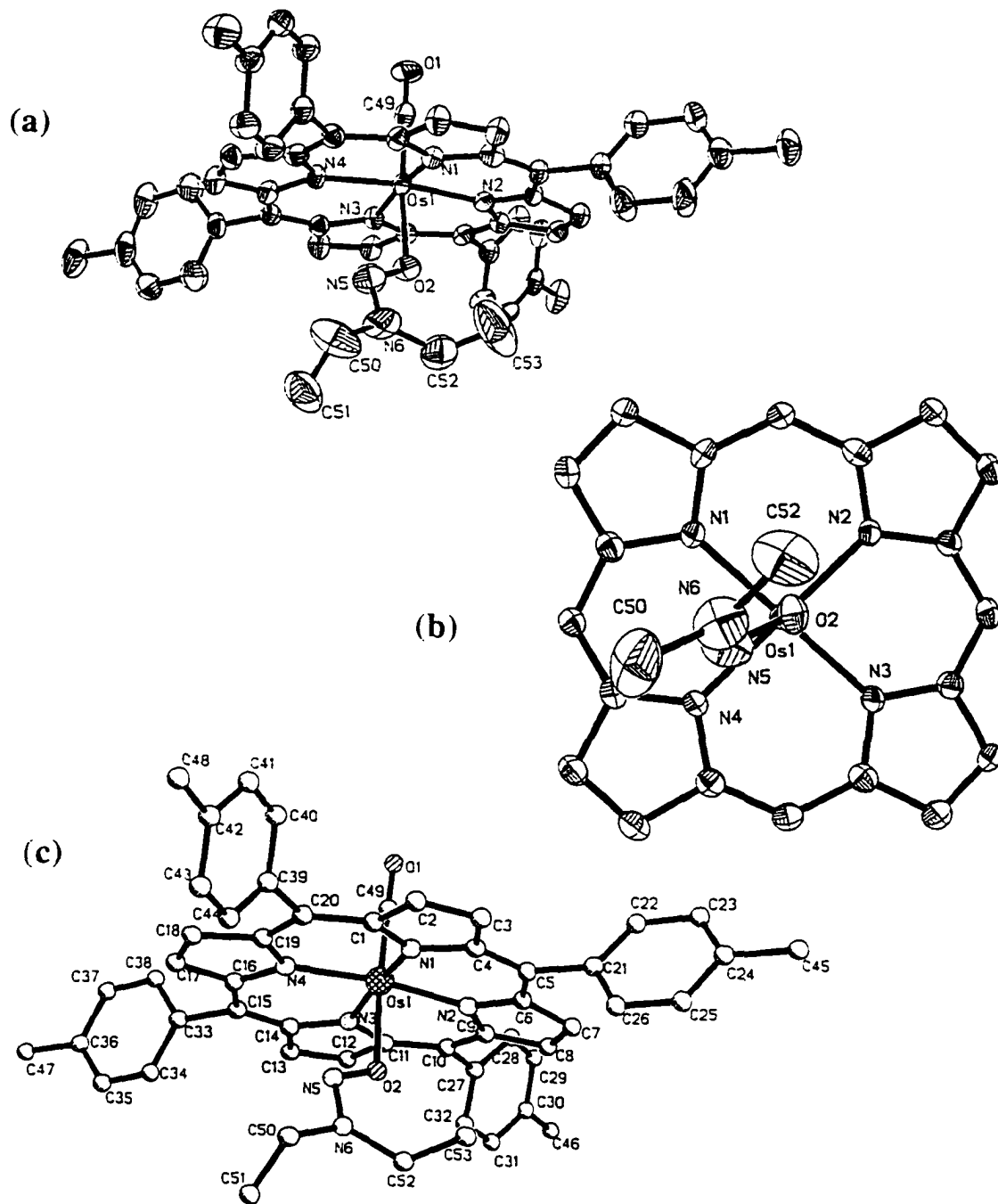


Figure 2.7. (a) Molecular structure of $(\text{TTP})\text{Os}(\text{CO})(\text{Et}_2\text{NNO})$. (b) View along the O(2)–Os(1) bond showing the nitrosamine orientation relative to the porphyrin core. (c) Ball and stick structure showing the atom labelings.

Table 2.1. Selected Bond Lengths (Å) for (TTP)Os(CO)(Et₂NNO)

Os(1)-C(49)	1.818(11)	Os(1)-N(2)	2.044(7)
Os(1)-N(1)	2.052(7)	Os(1)-N(3)	2.057(7)
Os(1)-N(4)	2.068(7)	Os(1)-O(2)	2.200(7)
O(1)-C(49)	1.140(12)	O(2)-N(5)	1.241(13)
N(5)-N(6)	1.294(14)	N(6)-C(52)	1.43(2)
N(6)-C(50)	1.47(2)	C(50)-C(51)	1.41(2)
C(52)-C(53)	1.47(3)	N(1)-C(4)	1.372(10)
N(1)-C(1)	1.375(10)	C(1)-C(20)	1.416(12)
C(1)-C(2)	1.432(12)	C(2)-C(3)	1.355(12)
C(3)-C(4)	1.457(11)	C(4)-C(5)	1.395(12)
C(5)-C(6)	1.382(12)	N(2)-C(9)	1.368(10)
N(2)-C(6)	1.381(10)	C(6)-C(7)	1.450(11)
C(7)-C(8)	1.356(12)	C(8)-C(9)	1.442(11)
C(9)-C(10)	1.412(12)	C(10)-C(11)	1.405(12)
N(3)-C(11)	1.373(10)	N(3)-C(14)	1.380(10)
C(11)-C(12)	1.457(11)	C(12)-C(13)	1.343(12)
C(13)-C(14)	1.433(11)	C(14)-C(15)	1.404(12)
C(15)-C(16)	1.398(13)	N(4)-C(19)	1.365(10)
N(4)-C(16)	1.380(10)	C(16)-C(17)	1.449(11)
C(17)-C(18)	1.364(13)	C(18)-C(19)	1.455(11)
C(19)-C(20)	1.392(13)		

Table 2.2. Selected Bond Angles ($^{\circ}$) for (TTP)Os(CO)(Et₂NNO)

O(1)-C(49)-Os(1)	177.9(10)	N(5)-O(2)-Os(1)	115.0(7)
O(2)-N(5)-N(6)	113.3(12)	N(5)-N(6)-C(52)	121.5(13)
N(5)-N(6)-C(50)	114.2(14)	C(52)-N(6)-C(50)	123.9(14)
C(51)-C(50)-N(6)	114(2)	N(6)-C(52)-C(53)	120(2)
C(49)-Os(1)-O(2)	174.6(4)	C(49)-Os(1)-N(2)	93.4(4)
C(49)-Os(1)-N(1)	92.9(4)	C(49)-Os(1)-N(3)	94.4(4)
C(49)-Os(1)-N(4)	94.1(4)	N(2)-Os(1)-N(1)	89.9(3)
N(1)-Os(1)-N(3)	172.8(3)	N(2)-Os(1)-N(3)	89.5(3)
N(2)-Os(1)-N(4)	172.5(3)	N(1)-Os(1)-N(4)	89.7(3)
N(3)-Os(1)-N(4)	89.9(3)	N(2)-Os(1)-O(2)	83.3(3)
N(1)-Os(1)-O(2)	83.0(3)	N(3)-Os(1)-O(2)	89.8(3)
N(4)-Os(1)-O(2)	89.3(3)	C(4)-N(1)-C(1)	107.1(7)
C(4)-N(1)-Os(1)	126.3(5)	C(1)-N(1)-Os(1)	126.7(6)
N(1)-C(1)-C(20)	125.2(8)	N(1)-C(1)-C(2)	109.2(7)
C(20)-C(1)-C(2)	125.7(8)	C(3)-C(2)-C(1)	108.3(7)
C(2)-C(3)-C(4)	106.1(7)	N(1)-C(4)-C(5)	125.2(8)
N(1)-C(4)-C(3)	109.4(7)	C(5)-C(4)-C(3)	125.4(8)
C(6)-C(5)-C(4)	127.0(9)	C(9)-N(2)-C(6)	106.2(7)
C(9)-N(2)-Os(1)	127.1(6)	C(6)-N(2)-Os(1)	126.7(5)
N(2)-C(6)-C(5)	124.8(8)	N(2)-C(6)-C(7)	109.7(7)
C(5)-C(6)-C(7)	125.5(8)	C(8)-C(7)-C(6)	106.7(7)
C(7)-C(8)-C(9)	107.2(7)	N(2)-C(9)-C(10)	126.1(8)
N(2)-C(9)-C(8)	110.2(7)	C(10)-C(9)-C(8)	123.6(8)
C(11)-C(10)-C(9)	123.5(8)	C(11)-N(3)-C(14)	106.8(7)
C(11)-N(3)-Os(1)	125.8(6)	C(14)-N(3)-Os(1)	127.2(5)

N(3)-C(11)-C(10)	127.0(8)	N(3)-C(11)-C(12)	108.4(7)
C(10)-C(11)-C(12)	124.6(8)	C(13)-C(12)-C(11)	107.8(7)
C(12)-C(13)-C(14)	107.0(7)	N(3)-C(14)-C(15)	124.1(8)
N(3)-C(14)-C(13)	109.8(7)	C(15)-C(14)-C(13)	126.1(8)
C(16)-C(15)-C(14)	127.2(9)	C(19)-N(4)-C(16)	107.9(7)
C(19)-N(4)-Os(1)	126.2(6)	C(16)-N(4)-Os(1)	125.9(6)
N(4)-C(16)-C(15)	125.5(8)	N(4)-C(16)-C(17)	108.8(7)
C(15)-C(16)-C(17)	125.7(8)	C(18)-C(17)-C(16)	107.1(7)
C(17)-C(18)-C(19)	107.1(7)	N(4)-C(19)-C(20)	126.1(8)
N(4)-C(19)-C(18)	109.0(7)	C(20)-C(19)-C(18)	124.9(8)
C(19)-C(20)-C(1)	125.7(8)		

Table 2.3. Os–N(por) Bond Lengths (Å) for Os^{II} Porphyrin Complexes

compounds	Os–N _p	Os–N _p (av)
(TTP)Os(CO)(PhNO) ₂ ^a	2.073(7), 2.082(6)	2.078
(TTP)Os(PhNO) ₂ ^a	2.053(9), 2.050(9), 2.058(9), 2.107(9)	2.067
(TPP)Os(PhNO) ₂ ^a	2.053(3), 2.057(3), 2.052(3), 2.067(3)	2.057
(TMP)Os(PhNO) ₂ ^a	2.037(10), 2.055(9), 2.059(9), 2.058(9)	2.052
(TTP)Os(CO)(Et ₂ NNO) ^a	2.052(7), 2.044(7), 2.057(7), 2.068(7)	2.055
(TTP)Os(NO)(S- <i>i</i> -C ₅ H ₁₁) ⁵⁹	2.035(5), 2.074(8), 2.076(9), 2.049(6)	2.058
(TPP)Os(PPh ₃) ₂ ⁶⁰		
molecule A	2.037(4), 2.047(4)	2.042
molecule B	2.045(4), 2.045(4)	2.045
(TTP)Os(4-pic) ₂ ⁶¹	2.034(3)	2.034
(OEP)Os(<i>o</i> -tolNO) ₂ ^a	2.051(5), 2.068(5)	2.060
(OEP)Os(NO)(O- <i>n</i> -C ₄ H ₉) ⁶²	1.986(9), 2.078(8), 2.051(7), 2.109(8)	2.056
(OEP)Os(NO)(O ₂ PF ₂) ⁶²	2.060(6), 2.053(5), 2.065(6), 2.067(6)	2.061
(OEP)Os(OPPh ₃) ₂ ⁶⁰	2.031(8), 2.027(8)	2.029
(OEP)Os(PMS) ₂ ⁶³	2.057(5), 2.044(5)	2.050
(OEP)Os(NS)(O ₂ PF ₂) ⁶⁴	1.986(9), 2.078(8), 2.051(7), 2.109(8)	2.056
[(OEP)Os(NO)] ₂ (μ-O) ⁶⁵	2.066(5)	2.066
(OEP)Os(NS)(Cl) ⁶⁵	2.050(7), 2.072(6), 2.075(9), 2.063(5)	2.065
(OEP)Os(NS)(Me) ⁶⁵	2.056(7), 2.057(7)	2.056
(OEPMe ₂)Os(CO)(py) ⁶⁶	2.069(3), 2.065(3)	2.067

^a this chapter

Selected bond lengths and bond angles for (por)Os(CO)-containing structures are listed in Table 2.4. The Os–C(O) bond length of 1.818(11) Å for (TTP)Os(CO)(Et₂NNO) is similar to that of (OEPMe₂)Os(CO)(py), but is shorter than that of (TTP)Os(CO)(PhNO) (see later) with a π -acceptor as *trans* ligand. The Os–C–O bond is virtually linear with a bond angle of 177.9(10)^o. The related phthalocyanine (Pc)Os(CO)(py) complex also has similar Os–CO dimensions (Os–C = 1.83(1) Å, C–O = 1.17(1) Å, Os–C–O = 177(1)^o).⁶⁷

Table 2.4. Structural Parameters (in Å and ^o) for (por)Os^{II}(CO)(L) complexes

compounds	Os–C(O)	C–O	Os–C–O	ref
(TTP)Os(CO)(PhNO)	1.93(2)	1.144(5)	175(4)	this chapter
(TTP)Os(CO)(Et ₂ NNO)	1.818(11)	1.140(12)	177.9(10)	this chapter
(OEPMe ₂)Os(CO)(py)	1.828(5)	1.151(7)	178.9(14)	66

The related reaction of (OEP)Os(CO) with excess Et₂NNO results in the formation of (OEP)Os(CO)(Et₂NNO) in 66% isolated yield. The reaction is quantitative as determined by ¹H NMR spectroscopy. This red purple product has similar solubility and stability properties as its TTP analog. Also, (and similar to the TTP analog), no coordinated Et₂NNO peaks are observed in the ¹H NMR spectrum at room temperature for (OEP)Os(CO)(Et₂NNO), and the coordinated Et₂NNO peaks are only observed at low temperature. The methylene and methyl peaks of the coordinated Et₂NNO in (OEP)Os(CO)(Et₂NNO) in CD₂Cl₂ are more upfield with respect to free Et₂NNO than those in (TTP)Os(CO)(Et₂NNO). This suggests that the (OEP)Os(CO) fragment has stronger effect on the coordinated Et₂NNO than does the (TTP)Os(CO) fragment. Its IR spectrum (as a KBr pellet, Figure 2.8) shows two new bands at 1294

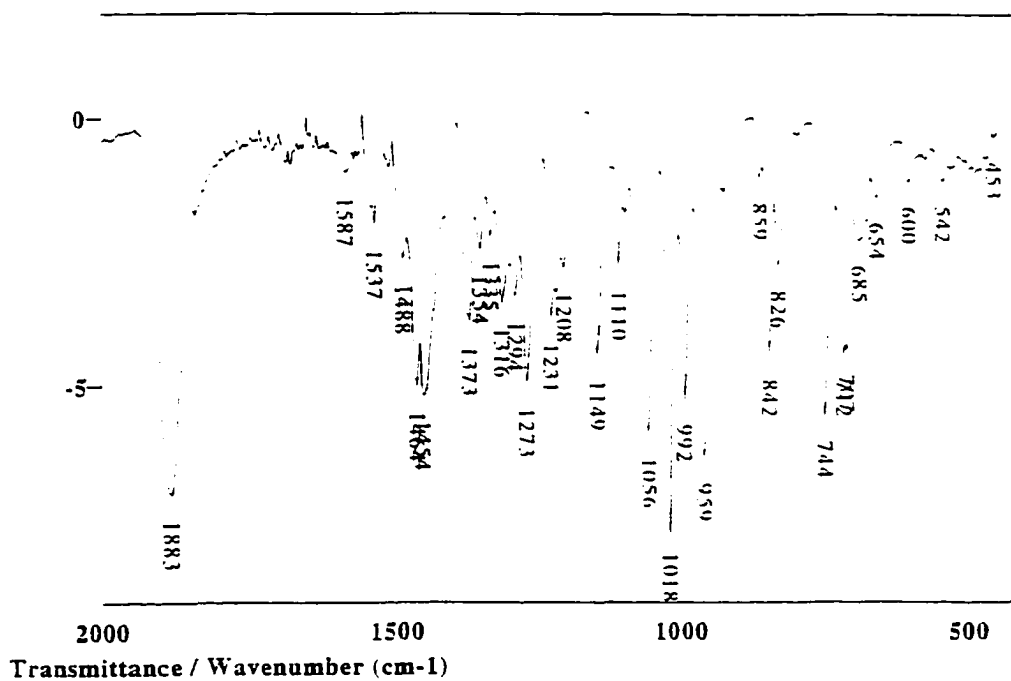
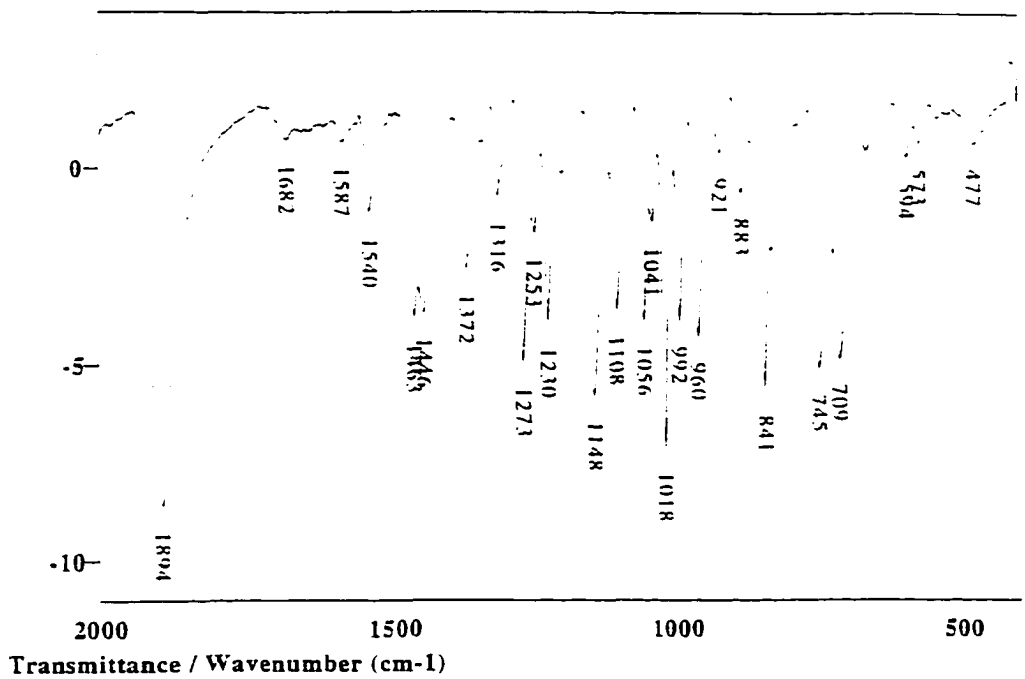
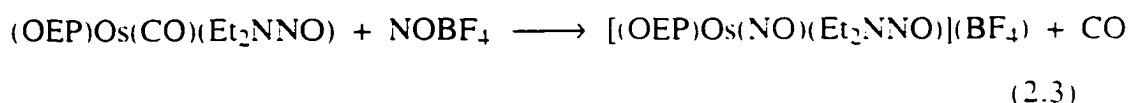


Figure 2.8. IR spectra (KBr) of (OEP)Os(CO) (top) and (OEP)Os(CO)(Et₂NNO) (bottom).

cm⁻¹ and 1208 cm⁻¹ which were assigned as the ν_{NO} and ν_{NN} for the coordinated Et₂NNO ligand. The assignment was further confirmed by the use of Et₂¹⁵NNO (ν_{NO} = 1256 cm⁻¹ and ν_{NN} = 1203 cm⁻¹). The IR spectrum (as a KBr pellet) also gives a strong band at 1883 cm⁻¹ which is assigned as ν_{CO} . This value is lower than that of the TTP analog, consistent with the greater π -acidity of the TTP macrocycle compared with the OEP macrocycle. The ν_{CO} value is 28 cm⁻¹ lower than that of (OEP)Ru(CO)(Et₂NNO),^{24b,c} consistent with the greater π -backbonding capacity of Os→CO than Ru→CO. The σ -donor ability of the Et₂NNO ligand is also indicated in the small decrease in ν_{CO} for (OEP)Os(CO)(Et₂NNO) with respect to the starting (OEP)Os(CO) complex (1894 cm⁻¹). The UV-vis spectrum in CH₂Cl₂ also gives four bands (370 sh (60), 389 (218), 507 (13), 539 (18) nm). The UV-vis spectra of both (TTP)Os(CO)(Et₂NNO) and (OEP)Os(Et₂NNO) belong to the *hypso/hyper* type.⁶⁸

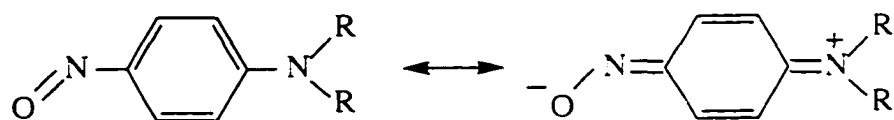
The nitrosylation of (OEP)Os(CO)(Et₂NNO) results in the replacement of the carbonyl ligand by the isoelectronic NO⁺ ligand in quantitative yield to give [(OEP)Os(NO)(Et₂NNO)](BF₄) (eq 2.3). This red solid has similar solubility and



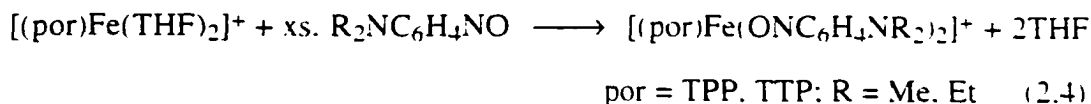
stability properties as the red purple carbonyl analog. The coordinated Et₂NNO peaks in [(OEP)Os(NO)(Et₂NNO)](BF₄), however, are observed in the ¹H NMR spectrum in CDCl₃ at room temperature. The magnitude of δ_{meso} in the ¹H NMR spectrum of a (OEP)Os complex is a good indicator for the *cis*-influence of axial ligands on the OEP macrocycle.⁶⁸ The δ_{meso} for (OEP)Os(CO)(Et₂NNO) in CDCl₃ is upfield with respect to that for [(OEP)Os(NO)(Et₂NNO)](BF₄), indicating a difference in the *cis*-influence of the axial CO/Et₂NNO and NO⁺/Et₂NNO pairs on the OEP macrocycle due to a change in π -backbonding from Os^{II}→OEP. Generally, CO is a weaker π -acceptor than

NO⁺,⁶⁹ making more electron density available at the Os^{II} center for π -backbonding to OEP macrocycle in the case of (OEP)Os(CO)(Et₂NNO). The IR spectrum of [(OEP)Os(NO)(Et₂NNO)]⁺ (as a KBr pellet) shows two new bands at 1241 cm⁻¹ and 1198 cm⁻¹ which are assigned as the ν_{NO} and ν_{NN} for the coordinated Et₂NNO ligand. The strong band at 1800 cm⁻¹ is assigned as the ν_{NO} of the nitrosyl ligand. The lower nitrosyl ν_{NO} for [(OEP)Os(NO)(Et₂NNO)]⁺ than that for [(OEP)Ru(NO)(Et₂NNO)]⁺,^{24c} is also consistent with the greater π -backbonding capacity of Os \rightarrow NO. The UV-vis spectrum of the [(OEP)Os(NO)(Et₂NNO)](BF₄) complex is similar to those of (OEP)Os(NO)(O₂PF₂)⁶³ and (OEP)Os(NO)(OCIO₃).⁷⁰

Extension of the η^1 -O Nitrosamine Binding Feature to the Preparation of the First Transition Metal η^1 -O Bound Nitrosoarene Complexes. The ferrous (TPP)Fe(PhNO)₂ displays an η^1 -N binding mode, and was obtained previously via the reaction of (TPP)Fe^{II} with excess PhNO.³⁹ The attempts to obtain the ferric analog [(TPP)Fe^{III}(PhNO)₂]⁺ were not successful. However, as has been mentioned earlier, the dipolar structure of nitrosamines might play a significant role in stabilizing the η^1 -O binding of Et₂NNO to the cationic Fe^{III} porphyrin in the [(por)Fe(Et₂NNO)₂]⁺ complexes. We reasoned that the correct choice of nitrosoarene ligands (e.g., with similar dipolar resonance structures) might enable the stabilization of an η^1 -O binding to a (por)Fe^{III} cation.



Gratifyingly, the use of the *para*-dialkylamino substituted nitrosoarenes (R₂NC₆H₄NO, R = Me, Et) resulted in the formation of the desired η^1 nitroso-O bound ferric compounds as shown in eq 2.4. Thus, the reactions of the *para*-dialkylamino substituted nitrosoarenes (R = Me, Et) with the [(por)Fe(THF)₂]⁺ cations



in CH_2Cl_2 generate the bis-nitrosoarene complexes $[(\text{por})\text{Fe}(\text{ONC}_6\text{H}_4\text{NR}_2)_2]^+$ in 55–83% isolated yields. The $[(\text{TPP})\text{Fe}(\text{ONC}_6\text{H}_4\text{Me}_2)_2](\text{SbF}_6)$ complex was first synthesized by Dr. Li-Sheng Wang (of our research group at the time).³⁹ All the compounds are freely soluble in CH_2Cl_2 , moderately soluble in benzene but are only slightly soluble in hexane. The excess organic nitrosoarene compounds are freely soluble in hexane and can be easily removed by washing the products with hexane. The purple crystalline products are moderately air-stable in the solid state but are air-sensitive in solution. The assignment of the IR ν_{NO} and ν_{CN} bands of these Fe^{III} nitrosoarene complexes is ambiguous. The bands at 1366 cm^{-1} and 1338 cm^{-1} for the free $\text{Me}_2\text{NC}_6\text{H}_4\text{NO}$ shift to 1361 and 1334 cm^{-1} for the ^{15}N labeled $\text{Me}_2\text{NC}_6\text{H}_4^{15}\text{NO}$. The bands at 1366 and 1338 cm^{-1} were assigned as ν_{NO} and ν_{CN} , respectively, for the free ligand.⁷¹ Upon coordination of the $\text{Me}_2\text{NC}_6\text{H}_4\text{NO}$ ligand to the $(\text{por})\text{Fe}^{\text{III}}$ center, the changes in ν_{NO} and ν_{CN} are negligible ($\nu_{\text{NO}} = 1364 \text{ cm}^{-1}$, $\nu_{\text{CN}} = 1336 \text{ cm}^{-1}$ for TPP; $\nu_{\text{NO}} = 1363 \text{ cm}^{-1}$, $\nu_{\text{CN}} = 1334 \text{ cm}^{-1}$ for TTP). Such a small frequency change upon coordination of the $\text{Me}_2\text{NC}_6\text{H}_4\text{NO}$ ligand is not uncommon.⁷¹ The assignments of the ν_{NO} and ν_{CN} bands are confirmed by the use of $\text{Me}_2\text{NC}_6\text{H}_4^{15}\text{NO}$. The ν_{NO} and ν_{CN} bands for the *para*-diethylamino substituted nitrosoarene $(\text{por})\text{Fe}^{\text{III}}$ complexes cannot be assigned unambiguously due to the complexity of the IR spectra. In general, IR spectroscopy is not a useful tool in the assignment of $\text{R}_2\text{NC}_6\text{H}_4\text{NO}$ coordination.^{33,71,72} The IR spectra (as a KBr pellet) give very strong bands at ca. 657 cm^{-1} , which are assigned as the uncoordinated ν_{SbF_6} bands.

The two $\text{Me}_2\text{NC}_6\text{H}_4\text{NO}$ ligands in $[(\text{TPP})\text{Fe}(\text{ONC}_6\text{H}_4\text{Me}_2)_2](\text{SbF}_6)$ are weakly coordinated and are easily substituted by THF to give the bis-solvated complex.

Magnetic Susceptibility. According to Walker,⁷³ Reed and Scheidt,⁷⁴ there are four possible spin states for a d^5 Fe^{III} porphyrin complex (Table 2.5).

Table 2.5. Spin States for (por)Fe^{III} Complexes

d orbitals	H.S. ($S = 5/2$)	admixed I.S. ($S = 3/2, 5/2$)	I.S. ($S = 3/2$)	L.S. ($S = 1/2$)
x^2-y^2	\uparrow	\uparrow	—	—
z^2	\uparrow	\uparrow	\uparrow	—
xz, yz	$\uparrow \uparrow$	$\uparrow \uparrow$	$\uparrow \uparrow$	$\uparrow\downarrow \uparrow$
xy	\uparrow	$\uparrow\downarrow$	$\uparrow\downarrow$	$\uparrow\downarrow$

Magnetic susceptibility measurements by the ¹H NMR Evans's⁵⁰ method gives μ_{eff} of 6.1 and 6.0, respectively, for the [(TPP)Fe(ONC₆H₄NMe₂)₂](SbF₆) and [(TPP)Fe(ONC₆H₄NEt₂)₂](SbF₆) complexes. These μ_{eff} values indicate the presence of 5 unpaired electrons, corresponding to a d^5 high-spin state of the metal center. However, the μ_{eff} values for [(TTP)Fe(ONC₆H₄NMe₂)₂](SbF₆) and [(TTP)Fe(ONC₆H₄NEt₂)₂](SbF₆) are 4.8 and 5.0, respectively, corresponding to the values expected for an admixed spin state ($S = 3/2, 5/2$). Walker⁷³ has also pointed out that, for *para*-substituted [(T(*p*-X)P)Fe(OCIO₃)] derivatives, electron donating substituents on the porphyrin phenyl rings favor the $S = 3/2$ ground state. For the [(TTP)Fe(ONC₆H₄NMe₂)₂](SbF₆) and [(TTP)Fe(ONC₆H₄NEt₂)₂](SbF₆) complexes, the *p*-Me substituent on the porphyrin phenyl rings has greater electron donating ability than the H atom (in the TPP case), and this appears to cause these complexes to have the admixed spin state of $S = 3/2, 5/2$, whereas the tetraphenylporphyrinato analogs have pure $S = 5/2$ spin state.

The UV-vis spectra of the (por)Fe^{III} nitrosoarene complexes all give very strong Soret bands at ca. 413 nm in C₆H₆ (Figure 2.9). Not surprisingly, all the Fe^{III} bis-nitrosoarene complexes display virtually the same purple color in solution.

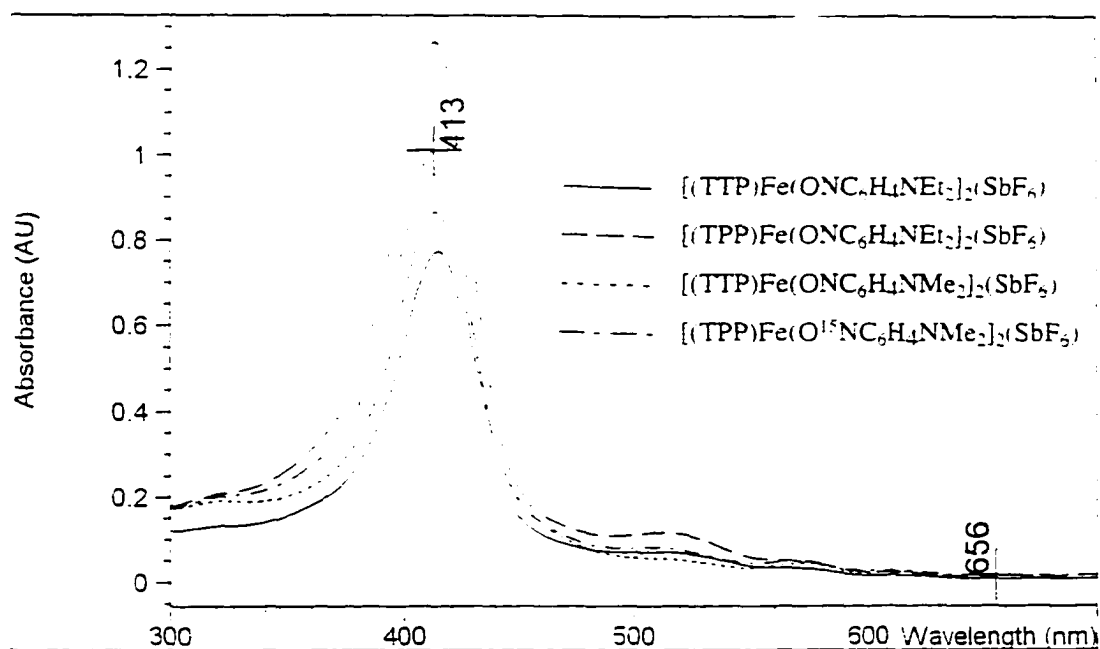


Figure 2.9. UV-vis spectra of the Fe^{III} bis-nitrosoarene complexes in C₆H₆.

Contrary to the earlier proposal³³ that the η^1 -O binding mode of *C*-nitroso ligands was restricted to d^{10} *para*-dialkylamino substituted nitrosoarene complexes, the X-ray structure of [(TPP)Fe(ONC₆H₄NEt₂)₂](SbF₆) reveals a distinct η^1 nitroso-O binding of the Et₂NC₆H₄NO ligands to the cationic Fe^{III} center (Figure 2.10). Importantly, this was the first time that the sole η^1 nitroso-O binding of *C*-nitroso ligands was ever observed in non- d^{10} transition metal complexes.³⁹ In the cation, the phenyl rings and the N(3) atoms of the Et₂NC₆H₄NO ligand are disordered at two sites. Selected bond lengths and bond angles are listed in Tables 2.6 and 2.7. The Et₂NC₆H₄NO moiety is essentially planar with the O(1)-N(3Y)-C(1Y)-C(2Y) and O(1)-N(3Z)-C(1Z)-C(2Z) torsion angles of 176.8° and 8.2°, respectively, and the amido nitrogen N(4) is also essentially planar with the sum of angles around it being ca. 360°. The average Fe-N(por) bond length of 2.008(3) Å is lower than that normally associated with a six-coordinated high-spin Fe^{III} center (2.045(8) Å) but is higher than that for a six-coordinated intermediate spin state Fe^{III} center (1.995(3) Å).^{74a} The axial Fe-O distance of 1.950(3) Å is shorter than those of other six-coordinated porphyrin Fe^{III} d^5 complexes containing O-donor ligands.⁷⁵⁻⁸² It is also shorter than those of [(TPP)Fe(Et₂NNO)₂](ClO₄)^{24a,c} and [(TPP)Fe(THF)₂](ClO₄)^{24c}, which are also six-coordinated high-spin d^5 Fe^{III} complexes reported by our research group. The origin of this unusual shortening is unclear, and we are hesitant to over-interpret the accuracy of the bond lengths and angles in this highly disordered nitroso fragment. The bond lengths of O(1)-N(3Y) (1.157(6) Å) and N(3Y)-C(1Y) (1.323(11) Å) are both shorter than those previously reported for the free ligand which was also disordered.⁸³ The bond length of N(4)-C(4Y) (1.35(3) Å) appears essentially unaffected by the coordination of the ligands. Due to the nature of the disorder in the cation, caution must be taken when interpreting specific bond lengths and angles in [(TPP)Fe(ONC₆H₄NEt₂)₂]⁺.

The dipolar resonance structure of the *para*-dialkylamino substituted nitrosoarene appears to play a role in the stabilization of the η^1 nitroso-O binding to the cationic Fe^{III} porphyrin. The planarity around the amido N atom in the complex is consistent with this view. To complement our studies on iron porphyrins, we were interested in determining whether indeed, such an η^1 -O binding mode could be expanded to include metals whose configurations were those other than d^{10} or d^5 . Together with Shelia Jean (Schultze) Fox (of our research group at the time), I was able to successfully obtain a suitable crystal of the air sensitive Mn^{III} analog [(TPP)Mn(ONC₆H₄NEt₂)₂](SbF₆)⁴⁺ for a single-crystal X-ray crystallographic analysis.

The X-ray structure of the cation of [(TPP)Mn(ONC₆H₄NEt₂)₂](SbF₆)⁴⁺ is shown in Figure 2.11. Selected bond lengths and bond angles are listed in Tables 2.8 and 2.9. The structure is almost identical to that of [(TPP)Fe(ONC₆H₄NEt₂)₂](SbF₆). This structure also clearly shows the η^1 nitroso-O binding of the two Et₂NC₆H₄NO ligands. The (O)NC₆H₄ fragment of the nitrosoarene ligand is also disordered over two positions. The disordered nitroso groups are essentially staggered or eclipsed with respect to the porphyrin nitrogen atoms (Figure 2.11b), with the N(3)-O(1)-Mn(1)-N(1) torsion angles being 47° (for N(3Y)) and 98° (for N(3Z)). The O(1)-N(3Y)-C(1Y)-C(2Y), O(1)-N(3Z)-C(1Z)-C(2Z), C(25)-N(4)-C(4Y)-C(3Y), and C(25)-N(4)-C(4Z)-C(3Z) torsion angles are 175.23°, 4.22°, 172.69° and 173.66°, respectively, and the sum of the angles around amido N atom is ca. 360°, indicating the essential planarity of the Et₂NC₆H₄NO moiety.

The nitroso O-N bond length (av 1.083 Å) is unusually short for a coordinated C-nitroso compound, and is significantly shorter than the reported value of 1.27(1) Å for the free ligand (which was also disordered),⁸³ or the reported values for the related d^{10} complexes of *dimethyl* derivative (1.218(4) Å for SnCl₂Me₂(*p*-ONC₆H₄NMe₂)₂)⁴² 1.305 Å for ZnCl₂(*p*-ONC₆H₄NMe₂)₂)⁴³, and is shorter than that for the analogous

Fe^{III} complex (av 1.110 Å). The shortening of the O–N bond length is also observed in 3,5-di-*tert*-butyl-4-nitrosopyrazole.⁸⁴ The structure of this organic compound is also disordered on two sites. Its N–O bond lengths are 1.053(10) Å and 1.048(11) Å respectively. The authors⁸⁴ argue that the reason for the abnormal shortening of the N–O bond length in 3,5-di-*tert*-butyl-4-nitrosopyrazole may be associated with the considerable twist of the nitroso group out of the pyrazole ring plane. In our cases, the O(1)–N(3Y)–C(1Y)–C(6Y) torsion angle is 176.57° for [(TPP)Fe(ONC₆H₄NEt₂)₂](SbF₆) and the O(1)–N(3Y)–C(1Y)–C(2Y) torsion angle is 175.23° for [(TPP)Mn(ONC₆H₄NEt₂)₂](SbF₆), indicating that the N–O groups are essentially coplanar with the phenyl plane in both cases. Again, since there is a high disorder in the [(TPP)Mn(ONC₆H₄NEt₂)₂](SbF₆) structure, it is uncertain whether the unusual shortening of the N–O bond length is a real effect or due to the nature of the disorder in the cation. The (O)N–C bond length of 1.36 Å is, however, comparable to the reported values for the free ligand (1.38(1) Å),⁸³ or the *d*¹⁰ complexes containing the *dimethyl* derivative (1.398(6) Å for SnCl₂Me₂(*p*-ONC₆H₄NMe₂)₂;⁴² 1.342 Å for ZnCl₂(*p*-ONC₆H₄NMe₂)₂;⁴³).

The axial Mn–O distance of 2.211(4) Å is long, and may be compared with the axial Mn–O distances in related Mn^{III} complexes of the form [(TPP)Mn(L)₂](ClO₄) (L = DMF (2.217(4) Å), MeOH (2.252(2) and 2.270(2) Å), 2,6-lutidine-N-oxide (2.263(4) and 2.264(4) Å)).⁸⁵ It is longer than the axial Mn–O distances in the {[(TPP)Mn]₂(μ-OH)}(ClO₄) complex.⁸⁶ The average Mn–N(por) bond length of 2.016 Å is within the range normally expected for six-coordinate Mn^{III} porphyrins.^{85,87} The long axial Mn–O bond lengths relative to Mn–N(por) for [(TPP)Mn(ONC₆H₄NEt₂)₂](SbF₆) are consistent with a tetragonal elongation expected for a singly occupied antibonding *d*_{z² orbital in the high-spin Mn^{III} center.⁸⁵⁻⁸⁸}

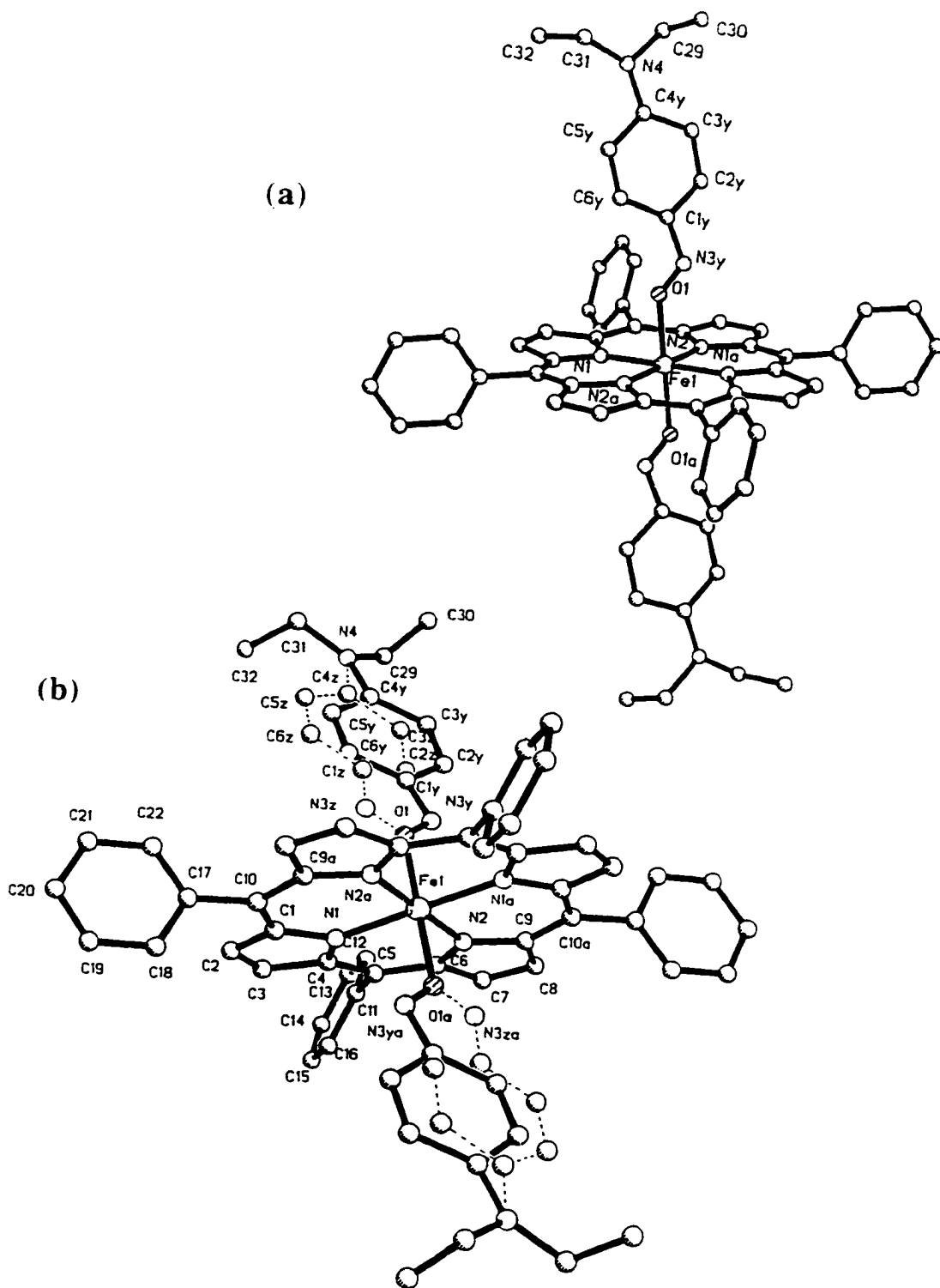


Figure 2.10. (a) Molecular structure of $[(\text{TPP})\text{Fe}(\text{ONC}_6\text{H}_4\text{NEt}_2)_2]^+$.

(b) Disorder of the ligands.

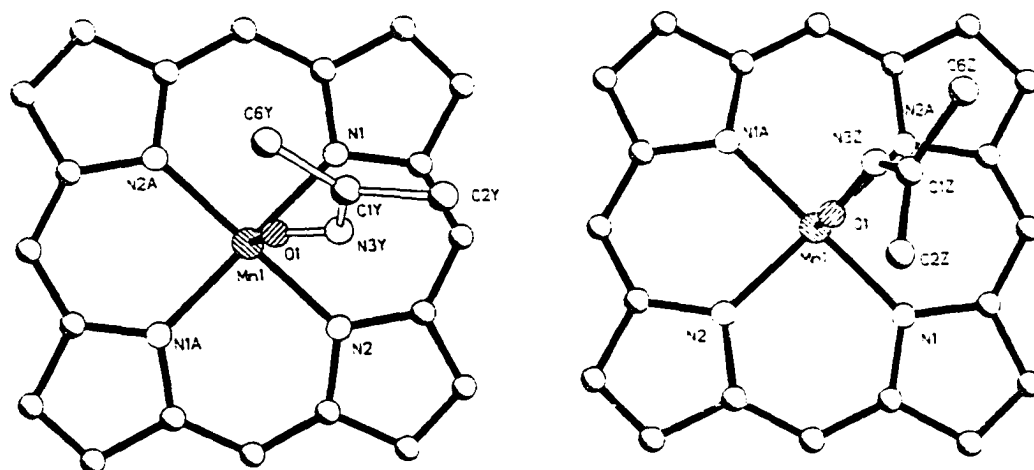
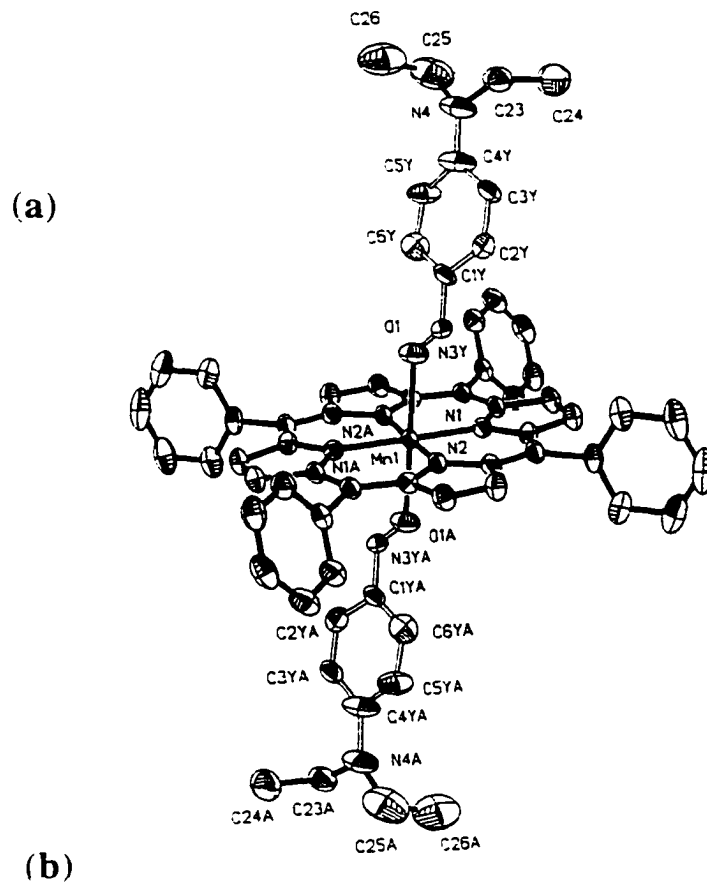


Figure 2.11. (a) Molecular structure of $[(\text{TPP})\text{Mn}(\text{ONC}_6\text{H}_4\text{NEt}_2)_2]^+$. (b) View of ligand orientations relative to the porphyrin core, with the view along the O(1)–Mn(1) bond (two orientations due to the disorder of the ligands).

Table 2.6. Selected Bond Lengths (Å) for [(TPP)Fe(ONC₆H₄NEt₂)₂]⁺

Fe(1)-O(1)	1.950(3)	Fe-O(1)A	1.950(3)
Fe(1)-N(2)A	2.006(3)	Fe(1)-N(2)	2.006(3)
Fe(1)-N(1)	2.010(3)	Fe(1)-N(1)A	2.010(3)
O(1)-N(3Z)	1.062(8)	O(1)-N(3Y)	1.157(6)
N(3Y)-C(1Y)	1.323(11)	C(1Y)-C(6Y)	1.426(14)
C(1Y)-C(2Y)	1.451(11)	C(4Y)-N(4)	1.35(2)
C(2Y)-C(3Y)	1.380(13)	C(3Y)-C(4Y)	1.46(2)
C(4Y)-C(5Y)	1.45(2)	C(5Y)-C(6Y)	1.331(13)
N(3Z)-C(1Z)	1.413(13)	C(1Z)-C(2Z)	1.35(2)
C(1Z)-C(6Z)	1.392(14)	C(2Z)-C(3Z)	1.49(2)
C(3Z)-C(4Z)	1.43(2)	C(4Z)-N(4)	1.38(2)
C(4Z)-C(5Z)	1.46(2)	C(5Z)-C(6Z)	1.34(2)
N(4)-C(31)	1.450(6)	N(4)-C(29)	1.649(12)
C(29)-C(30)	1.365(11)	C(31)-C(32)	1.502(6)
N(1)-C(1)	1.375(4)	N(1)-C(4)	1.381(4)
N(2)-C(6)	1.373(4)	N(2)-C(9)	1.376(4)
C(1)-C(10)	1.380(5)	C(1)-C(2)	1.442(5)
C(2)-C(3)	1.341(5)	C(3)-C(4)	1.436(5)
C(4)-C(5)	1.390(5)	C(5)-C(6)	1.394(5)
C(6)-C(7)	1.446(5)	C(7)-C(8)	1.351(5)
C(8)-C(9)	1.431(5)	C(9)-C(10)A	1.396(5)
C(10)-C(9)A	1.396(5)		

Table 2.7. Selected Bond Angles ($^{\circ}$) for $[(\text{TPP})\text{Fe}(\text{ONC}_6\text{H}_4\text{NEt}_2)_2]^+$

O(1)-Fe(1)-O(1)A	180.000(1)	O(1)-Fe(1)-N(2)A	91.22(12)
O(1)A-Fe(1)-N(2)A	88.78(12)	O(1)-Fe(1)-N(2)	88.78(12)
O(1)A-Fe(1)-N(2)	91.22(12)	O(1)-Fe(1)-N(1)	86.37(12)
O(1)A-Fe(1)-N(1)	93.63(11)	O(1)-Fe(1)-N(1)A	93.63(12)
O(1)A-Fe(1)-N(1)A	86.37(11)	N(2)A-Fe(1)-N(2)	180.0
N(2)A-Fe(1)-N(1)	90.45(11)	N(2)-Fe(1)-N(1)	89.55(11)
N(2)A-Fe(1)-N(1)A	89.55(11)	N(2)-Fe(1)-N(1)A	90.45(11)
N(1)-Fe(1)-N(1)A	180.000(1)	O(1)-N(3Y)-C(1Y)	118.7(7)
N(3Y)-O(1)-Fe(1)	127.7(3)	C(4Y)-N(4)-C(31)	134.5(7)
C(4Y)-N(4)-C(29)	109.5(8)	C(31)-N(4)-C(29)	116.0(4)
C(30)-C(29)-N(4)	97.7(8)	N(4)-C(31)-C(32)	111.1(4)
N(3Y)-C(1Y)-C(6Y)	128.8(9)	N(3Y)-C(1Y)-C(2Y)	114.3(9)
C(6Y)-C(1Y)-C(2Y)	116.9(9)	C(3Y)-C(2Y)-C(1Y)	123.5(8)
C(2Y)-C(3Y)-C(4Y)	117.1(11)	C(5Y)-C(4Y)-C(3Y)	119(2)
N(4)-C(4Y)-C(5Y)	114.2(11)	N(4)-C(4Y)-C(3Y)	127.0(13)
C(6Y)-C(5Y)-C(4Y)	122.3(11)	C(5Y)-C(6Y)-C(1Y)	121.4(8)
O(1)-N(3Z)-C(1Z)	121.8(9)	N(3Z)-O(1)-Fe(1)	133.5(5)
C(4Z)-N(4)-C(31)	112.3(9)	C(4Z)-N(4)-C(29)	130.9(9)
C(6Z)-C(1Z)-N(3Z)	112.5(11)	C(2Z)-C(1Z)-N(3Z)	121.8(13)
C(2Z)-C(1Z)-C(6Z)	125.6(13)	C(1Z)-C(2Z)-C(3Z)	119.0(13)
C(4Z)-C(3Z)-C(2Z)	114.8(14)	N(4)-C(4Z)-C(3Z)	114.1(13)
N(4)-C(4Z)-C(5Z)	124.5(14)	C(3Z)-C(4Z)-C(5Z)	121(2)
C(6Z)-C(5Z)-C(4Z)	120.8(13)	C(5Z)-C(6Z)-C(1Z)	118.3(12)
C(1)-N(1)-C(4)	106.1(3)	C(1)-N(1)-Fe(1)	126.1(2)
C(4)-N(1)-Fe(1)	127.3(2)	C(6)-N(2)-C(9)	106.0(3)

C(6)-N(2)-Fe(1)	127.2(2)	C(9)-N(2)-Fe(1)	126.8(2)
N(1)-C(1)-C(10)	126.8(3)	N(1)-C(1)-C(2)	109.4(3)
C(10)-C(1)-C(2)	123.6(3)	C(3)-C(2)-C(1)	107.4(3)
C(2)-C(3)-C(4)	107.4(3)	N(1)-C(4)-C(5)	125.6(3)
N(1)-C(4)-C(3)	109.6(3)	C(5)-C(4)-C(3)	124.8(3)
C(4)-C(5)-C(6)	123.7(3)	N(2)-C(6)-C(5)	126.2(3)
N(2)-C(6)-C(7)	109.8(3)	C(5)-C(6)-C(7)	124.0(3)
C(8)-C(7)-C(6)	106.7(3)	C(7)-C(8)-C(9)	107.4(3)
N(2)-C(9)-C(10)A	125.8(3)	N(2)-C(9)-C(8)	110.1(3)
C(10)A-C(9)-C(8)	124.1(3)	C(1)-C(10)-C(9)A	124.1(3)

Table 2.8. Selected Bond Lengths (Å) for [(TPP)Mn(ONC₆H₄NEt₂)₂]⁺

Mn(1)-N(2)	2.015(4)	Mn(1)-N(2)A	2.015(4)
Mn(1)-N(1)	2.017(3)	Mn(1)-N(1)A	2.017(3)
Mn(1)-O(1)A	2.211(4)	Mn(1)-O(1)	2.211(4)
O(1)-N(3Y)	1.057(10)	O(1)-N(3Z)	1.109(8)
N(4)-C(4Y)	1.391(14)	N(4)-C(4Z)	1.352(13)
N(4)-C(23)	1.473(9)	N(4)-C(25)	1.535(12)
C(23)-C(24)	1.492(9)	C(25)-C(26)	1.426(13)
N(3Y)-C(1Y)	1.36(2)	C(1Y)-C(6Y)	1.39(2)
C(1Y)-C(2Y)	1.409(14)	C(2Y)-C(3Y)	1.35(2)
C(3Y)-C(4Y)	1.41(2)	C(4Y)-C(5Y)	1.42(2)
C(5Y)-C(6Y)	1.38(2)	N(3Z)-C(1Z)	1.356(13)
C(1Z)-C(2Z)	1.409(14)	C(1Z)-C(6Z)	1.413(14)
C(2Z)-C(3Z)	1.353(13)	C(3Z)-C(4Z)	1.41(2)
C(4Z)-C(5Z)	1.42(2)	C(5Z)-C(6Z)	1.350(14)

N(1)-C(4)	1.363(6)	N(1)-C(1)	1.380(6)
N(2)-C(6)	1.377(6)	N(2)-C(9)	1.378(6)
C(1)-C(10)A	1.404(6)	C(1)-C(2)	1.427(6)
C(2)-C(3)	1.338(7)	C(3)-C(4)	1.445(6)
C(4)-C(5)	1.387(6)	C(5)-C(6)	1.391(6)
C(6)-C(7)	1.421(7)	C(7)-C(8)	1.349(7)
C(8)-C(9)	1.429(7)	C(9)-C(10)	1.379(6)
C(10)-C(1)A	1.404(6)		

Table 2.9. Selected Bond Angles ($^{\circ}$) for $[(\text{TPP})\text{Mn}(\text{ONC}_6\text{H}_4\text{NEt}_2)_2]^+$

N(3Y)-O(1)-Mn(1)	133.4(7)	N(3Z)-O(1)-Mn(1)	126.2(5)
N(2)-Mn(1)-N(2)A	180.0	N(2)-Mn(1)-N(1)	90.37(14)
N(2)A-Mn(1)-N(1)	89.63(14)	N(2)-Mn(1)-N(1)A	89.63(14)
N(2)A-Mn(1)-N(1)A	90.37(14)	N(1)-Mn(1)-N(1)A	180.0
N(2)-Mn(1)-O(1)A	87.6(2)	N(2)A-Mn(1)-O(1)A	92.4(2)
N(1)-Mn(1)-O(1)A	95.7(2)	N(1)A-Mn(1)-O(1)A	84.3(2)
N(2)-Mn(1)-O(1)	92.4(2)	N(2)A-Mn(1)-O(1)	87.6(2)
N(1)-Mn(1)-O(1)	84.3(2)	N(1)A-Mn(1)-O(1)	95.7(2)
O(1)A-Mn(1)-O(1)	180.0	C(4Z)-N(4)-C(23)	132.2(9)
C(4Y)-N(4)-C(23)	108.6(10)	C(4Z)-N(4)-C(25)	111.0(9)
C(4Y)-N(4)-C(25)	134.5(10)	C(23)-N(4)-C(25)	116.7(6)
N(4)-C(23)-C(24)	112.6(7)	C(26)-C(25)-N(4)	104.5(9)
O(1)-N(3Z)-C(1Z)	122.0(9)	N(3Z)-C(1Z)-C(2Z)	126.6(12)
N(3Z)-C(1Z)-C(6Z)	115.9(11)	C(2Z)-C(1Z)-C(6Z)	117.5(10)
C(3Z)-C(2Z)-C(1Z)	121.2(10)	C(2Z)-C(3Z)-C(4Z)	121.8(11)
N(4)-C(4Z)-C(3Z)	115.9(12)	N(4)-C(4Z)-C(5Z)	127.0(12)

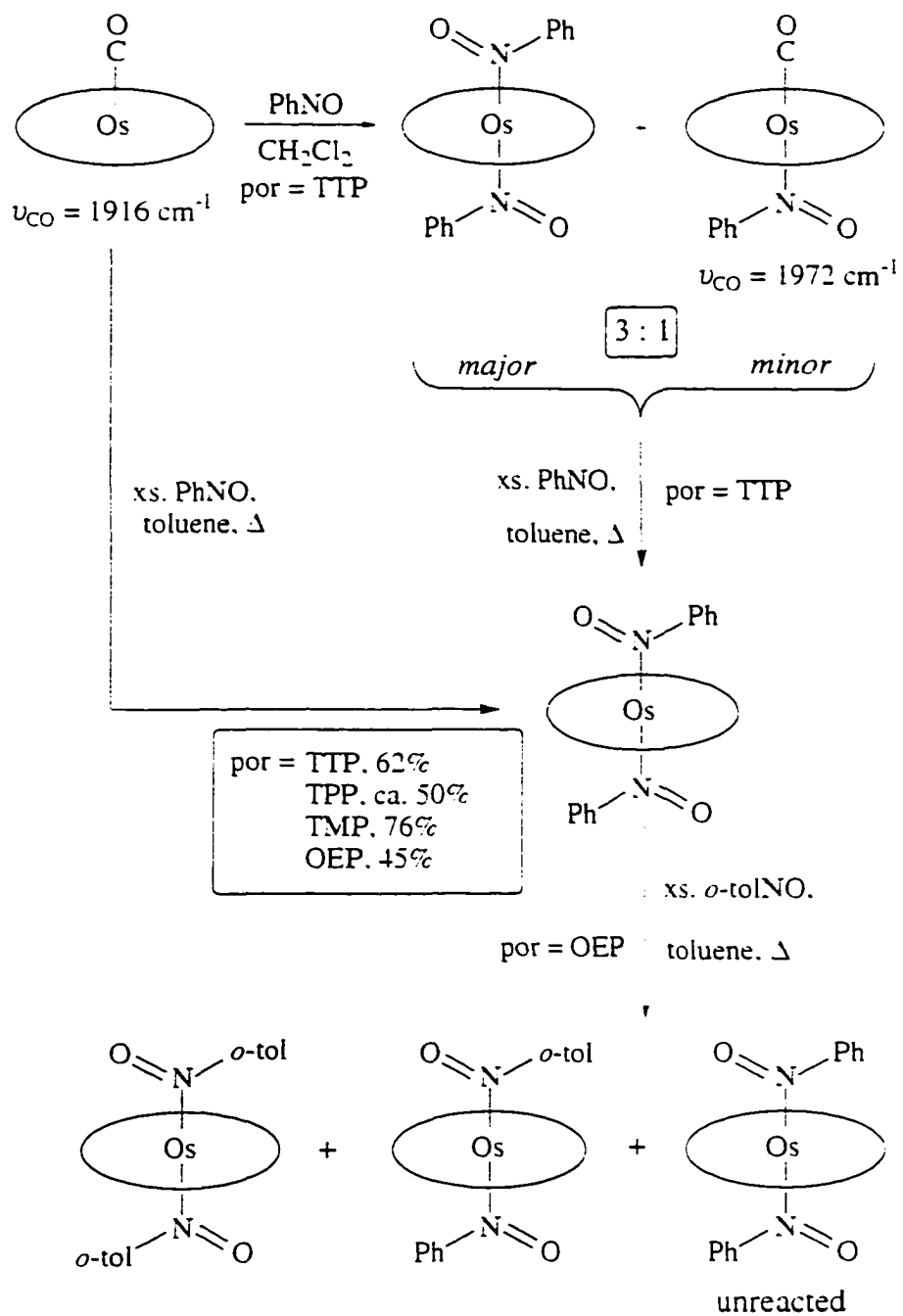
C(3Z)-C(4Z)-C(5Z)	116.8(10)	C(6Z)-C(5Z)-C(4Z)	121.5(11)
C(5Z)-C(6Z)-C(1Z)	121.0(10)	O(1)-N(3Y)-C(1Y)	121.9(12)
N(3Y)-C(1Y)-C(6Y)	125.9(14)	N(3Y)-C(1Y)-C(2Y)	114.8(13)
C(6Y)-C(1Y)-C(2Y)	119.4(12)	C(3Y)-C(2Y)-C(1Y)	120.0(12)
C(2Y)-C(3Y)-C(4Y)	122.7(12)	N(4)-C(4Y)-C(3Y)	129.1(14)
N(4)-C(4Y)-C(5Y)	114.8(14)	C(3Y)-C(4Y)-C(5Y)	115.9(12)
C(6Y)-C(5Y)-C(4Y)	121.5(13)	C(5Y)-C(6Y)-C(1Y)	119.8(13)
C(4)-N(1)-C(1)	106.6(4)	C(4)-N(1)-Mn(1)	125.9(3)
C(1)-N(1)-Mn(1)	127.0(3)	C(6)-N(2)-C(9)	106.2(4)
C(6)-N(2)-Mn(1)	126.6(3)	C(9)-N(2)-Mn(1)	127.2(3)
N(1)-C(1)-C(10)A	125.5(4)	N(1)-C(1)-C(2)	109.1(4)
C(10)A-C(1)-C(2)	125.4(4)	C(3)-C(2)-C(1)	108.0(4)
C(2)-C(3)-C(4)	107.0(4)	N(1)-C(4)-C(5)	127.2(4)
N(1)-C(4)-C(3)	109.3(4)	C(5)-C(4)-C(3)	123.3(4)
C(4)-C(5)-C(6)	124.1(4)	N(2)-C(6)-C(5)	125.8(4)
N(2)-C(6)-C(7)	109.7(4)	C(5)-C(6)-C(7)	124.5(4)
C(8)-C(7)-C(6)	107.3(4)	C(7)-C(8)-C(9)	107.5(4)
N(2)-C(9)-C(10)	126.1(4)	N(2)-C(9)-C(8)	109.2(4)
C(10)-C(9)-C(8)	124.7(4)	C(9)-C(10)-C(1)A	124.3(4)

The observation of the η^1 nitroso-O binding of the *para*-dialkylamino substituted nitrosoarene to the formal d^4 Mn^{III} center is interesting. This η^1 nitroso-O binding to a d^4 metal center is thus only the second example of such a binding to non- d^{10} transition metal centers, and suggests that this binding mode may indeed be more accessible than was previously thought.

The η^1 -N Binding of Nitrosoarenes to Os^{II} Porphyrins. Our laboratory previously reported the structurally characterized complex (TPP)Fe(PhNO)₂ with η^1 -N binding nitrosobenzene ligand.³⁹ James also reported the synthesis and spectroscopic characterization of (OEP)Ru(PhNO)₂.⁴⁰ However, no monometallic osmium porphyrin complexes with *C*-nitroso compounds as ligands was reported prior to our work. Hence, we were interested in extending the η^1 -N binding chemistry of nitrosoarenes to Os^{II} porphyrins.

The formation and reactions of (por)Os^{II} nitrosoarene complexes are summarized in Scheme 2.1. These are the first monomeric osmium *C*-nitroso complexes to be reported. The most important feature of this type of compounds is that the η^1 -N bound nitrosoarene ligands act as π acceptors in the complexes and their spectroscopic and structural properties are consistent with this notion. The (por)Os^{II} bis-nitrosobenzene complexes are prepared by the reaction of (por)Os(CO) with excess PhNO in toluene at refluxing temperature. Unlike (OEP)Ru(PhNO)₂,⁴⁰ which undergoes substitution reaction by pyridine to give (OEP)Ru(PhNO)(py) quantitatively at room temperature within 10 min, no substitution of the PhNO ligand by pyridine was observed for (OEP)Os(PhNO)₂ at room temperature for several hours. This result indicates that the PhNO ligand in (OEP)Os(PhNO)₂ is not as labile as in (OEP)Ru(PhNO)₂. The reaction of (OEP)Os(PhNO)₂ with excess *o*-tolNO was monitored by ¹H NMR spectroscopy in toluene-*d*₈. The ¹H NMR spectrum indicated that no substitution of PhNO occurred at room temperature over a 30 min period. However, after the reaction mixture was heated (Scheme 2.1, bottom), substitution

Scheme 2.1



occurred to give a mixture of (OEP)Os(PhNO)(*o*-tolNO), (OEP)Os(*o*-tolNO)₂ and some unreacted (OEP)Os(PhNO)₂. The ratio of (OEP)Os(*o*-tolNO)₂ to (OEP)Os(PhNO)(*o*-tolNO) increases with temperature and time until the reaction reaches an equilibrium (no further change in ratio).

All the bis-nitrosoarene Os^{II} porphyrin complexes are air-stable, showing no signs of decomposition after several months in the solid state. They are all freely soluble in CH₂Cl₂ and benzene but are rather insoluble in hexane. The ¹H NMR spectra of the analytically pure bis-nitrosoarene complexes consist of sharp peaks for both the ligands and the porphyrin macrocycles, consistent with the diamagnetic nature of the complexes. The two bis-nitrosoarene ligands are equivalent in solution as indicated by the ¹H NMR spectra of the complexes in CDCl₃.

The reaction of (TTP)Os(CO) with less than two equivalents of PhNO at room temperature gives the mixture of (TTP)Os(CO)(PhNO) and (TTP)Os(PhNO)₂ in 1:3 ratio (Scheme 2.1, top). The ν_{CO} changes from 1916 cm⁻¹ for the starting material (TTP)Os(CO) to 1972 cm⁻¹ for (TTP)Os(CO)(PhNO) (Figure 2.12). The shift to the higher energy for (TTP)Os(CO)(PhNO) is consistent with PhNO acting as a π -acceptor ligand towards the (TTP)Os(CO) fragment, withdrawing electron density from the Os^{II} center, thus making less electron density available for Os^{II}→CO backdonation, thereby raising the ν_{CO} . Further reaction of (TTP)Os(CO)(PhNO) with excess PhNO in refluxing toluene produces the (TTP)Os(PhNO)₂ derivative exclusively (but in 40% overall yield from (TTP)Os(CO)).

The molecular structures of the (por)Os^{II} nitrosoarene complexes (namely, (TTP)Os(PhNO)₂, (TTP)Os(CO)(PhNO), (TPP)Os(PhNO)₂, (TMP)Os(PhNO)₂ and (OEP)Os(*o*-tolNO)₂) are shown in Figures 2.13–2.17. Selected bond lengths and bond angles are listed in Tables 2.10–2.19.

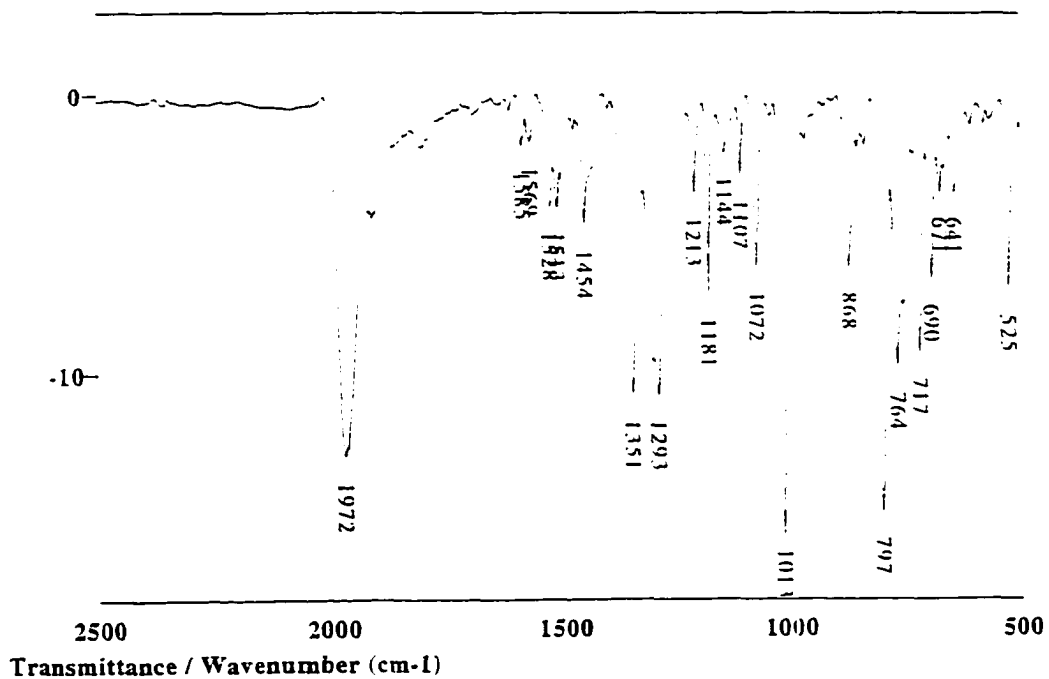
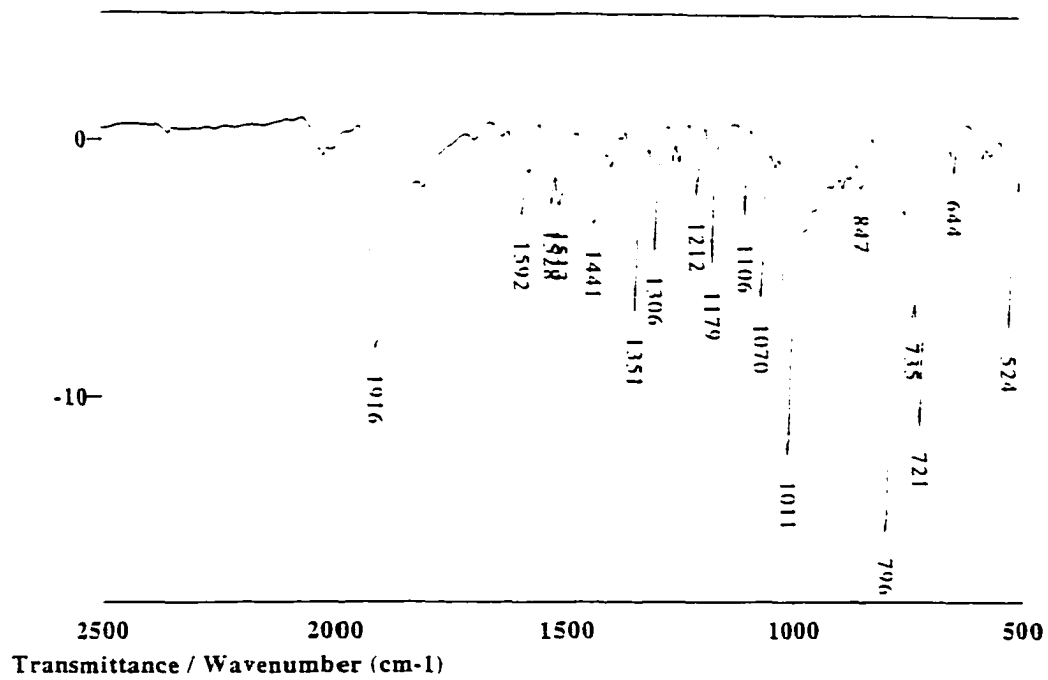


Figure 2.12. IR spectra (KBr) showing the ν_{CO} 's for (TTP)Os(CO) (top, 1916 cm⁻¹) and (TTP)Os(CO)(PhNO) (bottom, 1972 cm⁻¹).

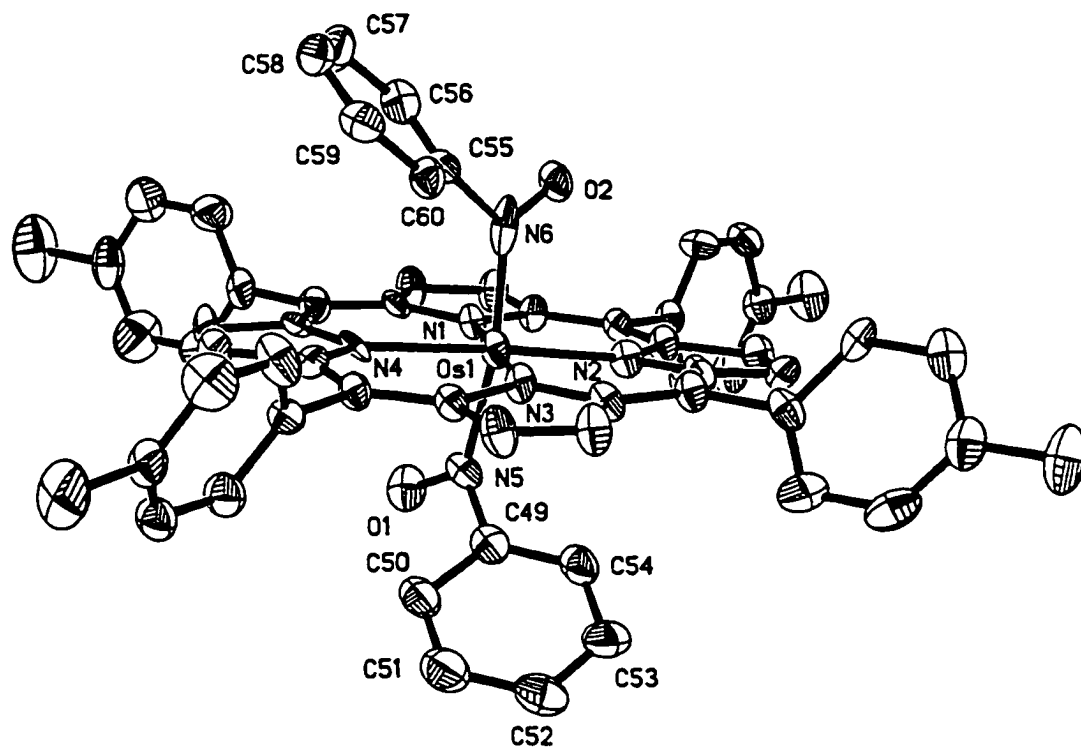


Figure 2.13. Molecular structure of $(\text{TTP})\text{Os}(\text{PhNO})_2$.

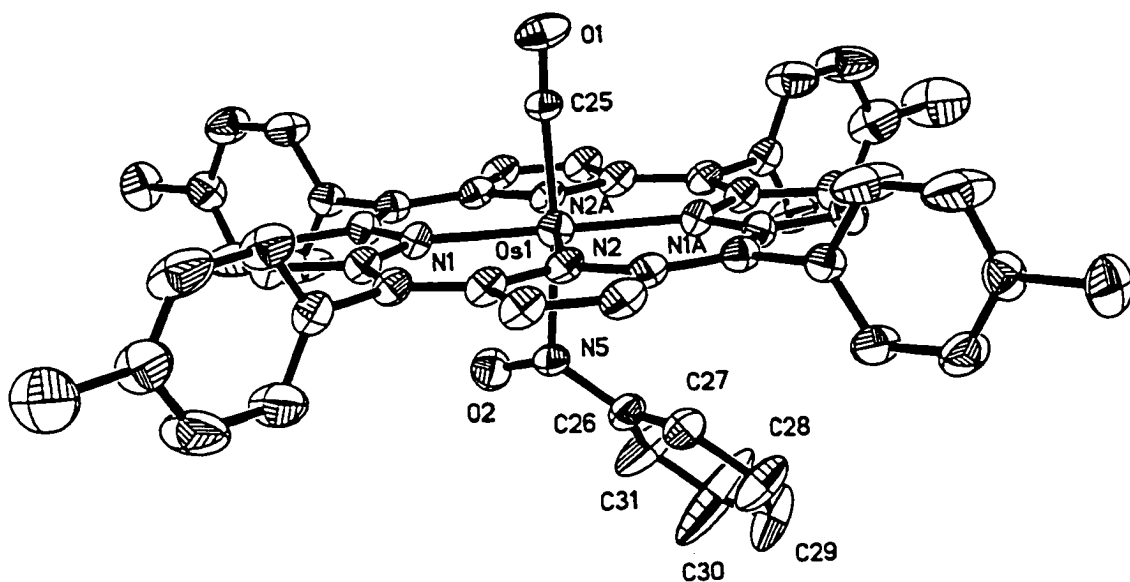


Figure 2.14. Molecular structure of (TTP)Os(CO)(PhNO).

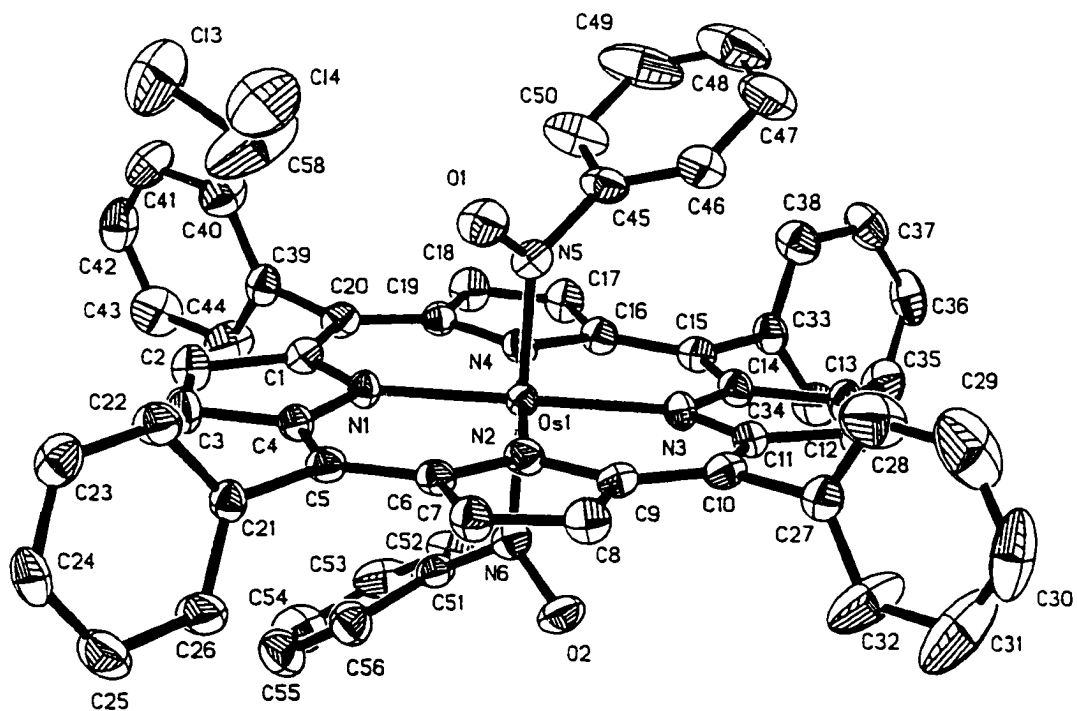


Figure 2.15. Molecular structure of $(\text{TPP})\text{Os}(\text{PhNO})_2$.

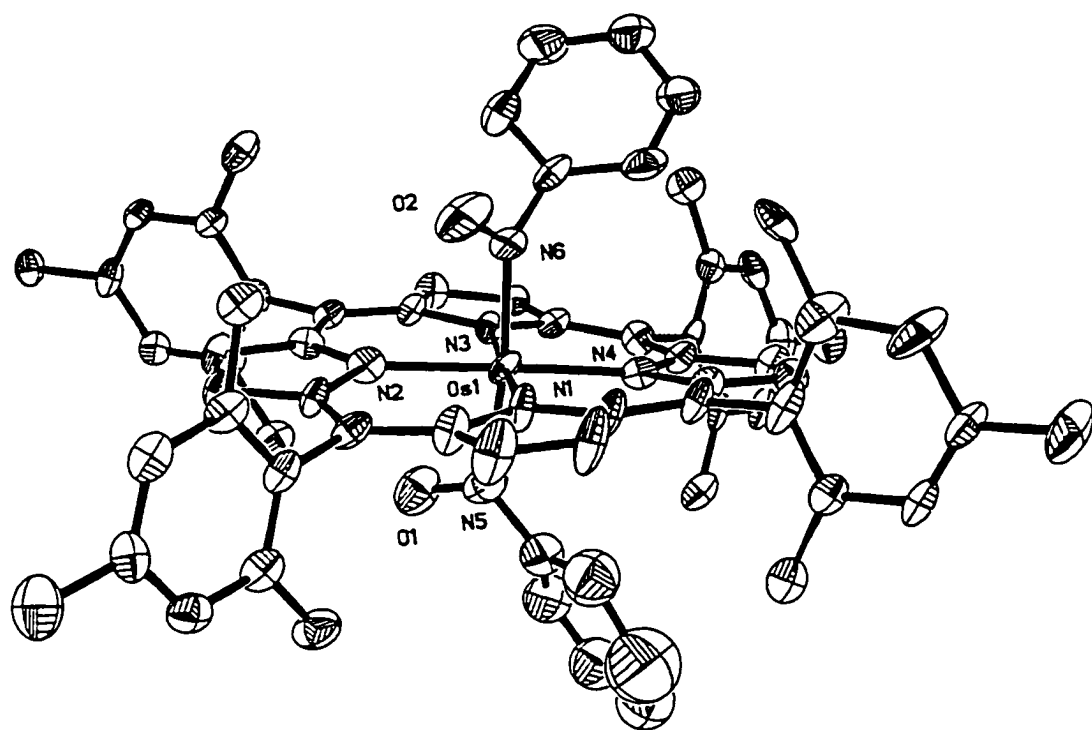


Figure 2.16. Molecular structure of (TMP)Os(PhNO)₂.

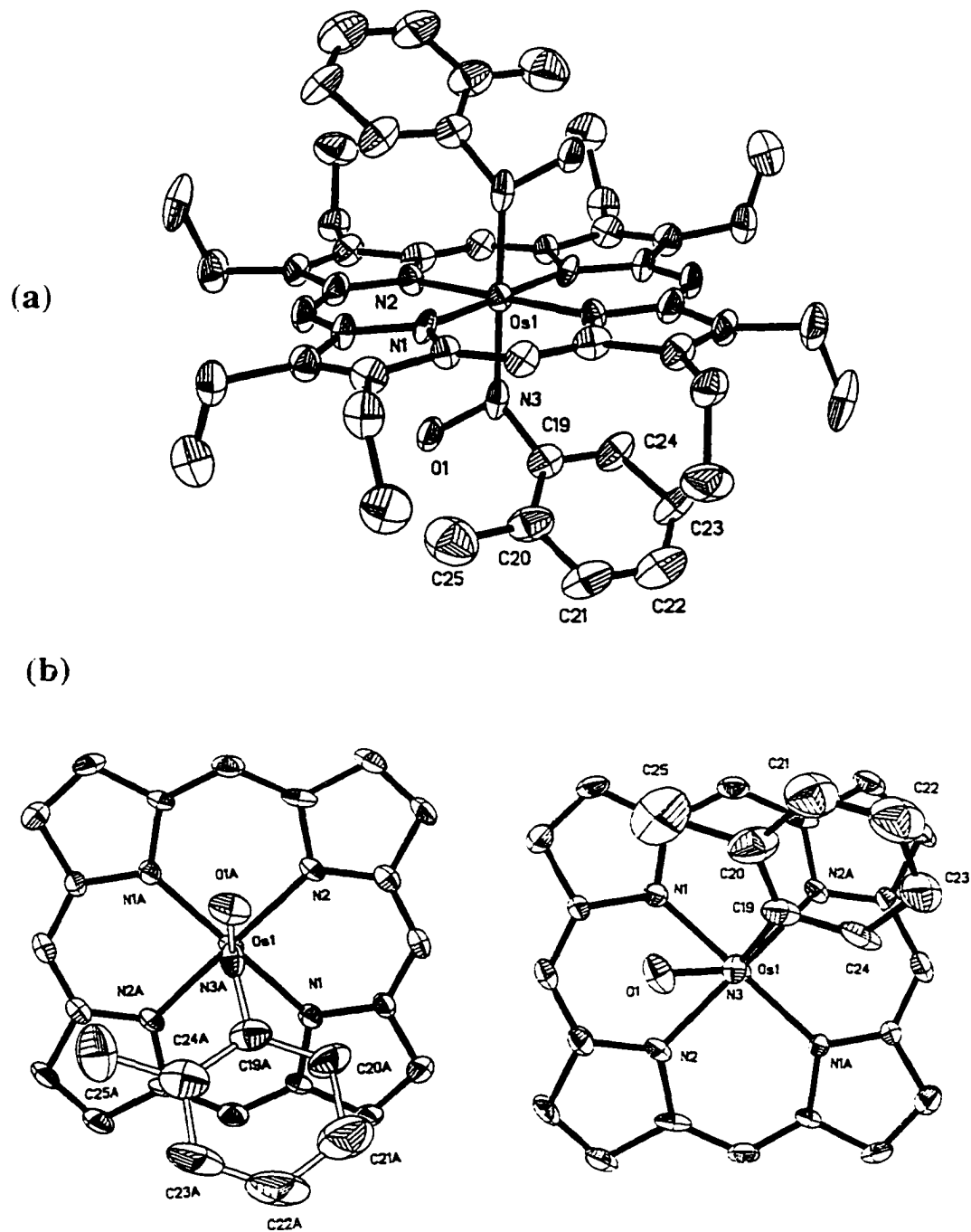


Figure 2.17. (a) Molecular structure $(\text{OEP})\text{Os}(\textit{o}\text{-tolNO})_2$. (b) View along the $\text{N}(3)\text{--Os}(1)$ bond showing the orientation of the axial $\textit{o}\text{-tolNO}$ ligand relative to the porphyrin core (two positions due to the disorder of the $\textit{o}\text{-tolNO}$ ligands).

Table 2.10. Selected Bond Lengths (Å) for (TTP)Os(PhNO)₂

Os(1)-N(6)	1.931(13)	Os(1)-N(5)	1.994(9)
Os(1)-N(2)	2.050(9)	Os(1)-N(1)	2.053(9)
Os(1)-N(3)	2.058(9)	Os(1)-N(4)	2.107(9)
N(5)-O(1)	1.278(12)	N(6)-O(2)	1.298(13)
N(5)-C(49)	1.43(2)	N(6)-C(55)	1.475(14)
C(49)-C(50)	1.40(2)	C(50)-C(51)	1.39(2)
C(51)-C(52)	1.43(2)	C(52)-C(53)	1.38(2)
C(53)-C(54)	1.37(2)	C(49)-C(54)	1.39(2)
C(55)-C(56)	1.36(2)	C(55)-C(60)	1.37(2)
C(56)-C(57)	1.38(2)	C(57)-C(58)	1.36(2)
C(58)-C(59)	1.37(2)	C(59)-C(60)	1.37(2)
N(1)-C(1)	1.355(13)	N(1)-C(4)	1.388(14)
N(2)-C(6)	1.382(14)	N(2)-C(9)	1.428(14)
N(3)-C(14)	1.367(13)	N(3)-C(11)	1.391(14)
N(4)-C(19)	1.328(14)	N(4)-C(16)	1.366(14)
C(1)-C(20)	1.38(2)	C(1)-C(2)	1.47(2)
C(2)-C(3)	1.35(2)	C(3)-C(4)	1.44(2)
C(4)-C(5)	1.39(2)	C(5)-C(6)	1.40(2)
C(6)-C(7)	1.43(2)	C(7)-C(8)	1.38(2)
C(8)-C(9)	1.40(2)	C(9)-C(10)	1.38(2)
C(10)-C(11)	1.39(2)	C(11)-C(12)	1.43(2)
C(12)-C(13)	1.34(2)	C(13)-C(14)	1.45(2)
C(14)-C(15)	1.38(2)	C(15)-C(16)	1.38(2)
C(16)-C(17)	1.45(2)	C(17)-C(18)	1.37(2)
C(18)-C(19)	1.49(2)	C(19)-C(20)	1.42(2)

Table 2.11. Selected Bond Angles ($^{\circ}$) for (TTP)Os(PhNO)₂

O(1)-N(5)-C(49)	113.2(10)	O(1)-N(5)-Os(1)	121.6(8)
C(49)-N(5)-Os(1)	123.7(8)	O(2)-N(6)-C(55)	109.3(11)
O(2)-N(6)-Os(1)	122.3(8)	C(55)-N(6)-Os(1)	127.3(8)
N(6)-Os(1)-N(5)	169.5(4)	N(6)-Os(1)-N(2)	91.3(4)
N(5)-Os(1)-N(2)	97.3(4)	N(6)-Os(1)-N(1)	85.0(4)
N(5)-Os(1)-N(1)	89.0(4)	N(2)-Os(1)-N(1)	90.4(3)
N(6)-Os(1)-N(3)	96.7(4)	N(5)-Os(1)-N(3)	89.3(4)
N(2)-Os(1)-N(3)	89.6(3)	N(1)-Os(1)-N(3)	178.4(4)
N(6)-Os(1)-N(4)	91.3(4)	N(5)-Os(1)-N(4)	80.0(4)
N(2)-Os(1)-N(4)	177.3(4)	N(1)-Os(1)-N(4)	89.1(4)
N(3)-Os(1)-N(4)	90.8(4)	C(54)-C(49)-C(50)	120.3(13)
C(54)-C(49)-N(5)	121.9(12)	C(50)-C(49)-N(5)	117.8(11)
C(51)-C(50)-C(49)	117.9(13)	C(50)-C(51)-C(52)	121(2)
C(53)-C(52)-C(51)	120(2)	C(54)-C(53)-C(52)	119(2)
C(53)-C(54)-C(49)	121.9(13)	C(56)-C(55)-C(60)	120.9(11)
C(56)-C(55)-N(6)	119.4(10)	C(60)-C(55)-N(6)	119.7(11)
C(55)-C(56)-C(57)	118.8(12)	C(58)-C(57)-C(56)	121.1(13)
C(57)-C(58)-C(59)	119.4(12)	C(58)-C(59)-C(60)	120.1(12)
C(55)-C(60)-C(59)	119.6(12)	C(1)-N(1)-C(4)	107.6(9)
C(1)-N(1)-Os(1)	126.6(8)	C(4)-N(1)-Os(1)	125.7(7)
C(6)-N(2)-C(9)	106.7(9)	C(6)-N(2)-Os(1)	126.6(8)
C(9)-N(2)-Os(1)	126.4(7)	C(14)-N(3)-C(11)	108.6(9)
C(14)-N(3)-Os(1)	125.0(7)	C(11)-N(3)-Os(1)	126.2(7)
C(19)-N(4)-C(16)	112.2(9)	C(19)-N(4)-Os(1)	124.6(7)
C(16)-N(4)-Os(1)	123.1(8)	N(1)-C(1)-C(20)	127.7(11)

N(1)-C(1)-C(2)	108.8(10)	C(20)-C(1)-C(2)	123.5(10)
C(3)-C(2)-C(1)	107.0(11)	C(2)-C(3)-C(4)	107.4(11)
C(5)-C(4)-N(1)	125.4(10)	C(5)-C(4)-C(3)	125.5(10)
N(1)-C(4)-C(3)	109.1(9)	C(4)-C(5)-C(6)	127.3(10)
N(2)-C(6)-C(5)	124.6(10)	N(2)-C(6)-C(7)	108.9(11)
C(5)-C(6)-C(7)	126.5(10)	C(8)-C(7)-C(6)	107.4(11)
C(7)-C(8)-C(9)	108.3(10)	C(10)-C(9)-C(8)	126.7(11)
C(10)-C(9)-N(2)	124.7(10)	C(8)-C(9)-N(2)	108.4(10)
C(9)-C(10)-C(11)	126.2(11)	C(10)-C(11)-N(3)	126.2(10)
C(10)-C(11)-C(12)	126.8(11)	N(3)-C(11)-C(12)	107.0(9)
C(13)-C(12)-C(11)	109.2(11)	C(12)-C(13)-C(14)	107.4(10)
N(3)-C(14)-C(15)	126.5(11)	N(3)-C(14)-C(13)	107.9(9)
C(15)-C(14)-C(13)	125.4(10)	C(14)-C(15)-C(16)	126.8(10)
N(4)-C(16)-C(15)	127.2(10)	N(4)-C(16)-C(17)	106.2(10)
C(15)-C(16)-C(17)	126.4(10)	C(18)-C(17)-C(16)	108.6(10)
C(17)-C(18)-C(19)	105.8(10)	N(4)-C(19)-C(20)	128.6(10)
N(4)-C(19)-C(18)	107.1(9)	C(20)-C(19)-C(18)	124.2(10)
C(1)-C(20)-C(19)	123.2(10)		

Table 2.12. Selected Bond Lengths (Å) for (TTP)Os(CO)(PhNO)

Os(1)-C(25)	1.93(2)	Os(1)-C(25)A	1.93(2)
Os(1)-N(1)	2.073(7)	Os(1)-N(1)A	2.073(7)
Os(1)-N(2)	2.082(6)	Os(1)-N(2)A	2.082(6)
Os(1)-N(5)A	2.18(2)	Os(1)-N(5)	2.18(2)
N(5)-O(2)	1.26(2)	C(25)-O(1)	1.144(5)
N(5)-C(26)	1.39(3)	C(26)-C(27)	1.31(3)

C(26)-C(31)	1.41(4)	C(27)-C(28)	1.42(3)
C(28)-C(29)	1.44(3)	C(29)-C(30)	1.30(4)
C(30)-C(31)	1.32(4)	N(1)-C(4)	1.375(11)
N(1)-C(1)	1.382(11)	N(2)-C(9)	1.360(12)
N(2)-C(6)	1.390(12)	C(1)-C(10)A	1.418(13)
C(1)-C(2)	1.455(14)	C(2)-C(3)	1.38(2)
C(3)-C(4)	1.449(14)	C(4)-C(5)	1.421(14)
C(5)-C(6)	1.385(14)	C(6)-C(7)	1.454(13)
C(7)-C(8)	1.34(2)	C(8)-C(9)	1.441(13)
C(9)-C(10)	1.407(14)	C(10)-C(10)A	1.418(13)

Table 2.13. Selected Bond Angles ($^{\circ}$) for (TTP)Os(CO)(Ph.NO)

C(25)-Os(1)-C(25)A	179.999(3)	O(1)-C(25)-Os(1)	175(4)
O(2)-N(5)-Os(1)	113(2)	O(2)-N(5)-C(26)	120(2)
C(26)-N(5)-Os(1)	122.1(12)	C(25)-Os(1)-N(1)	89.1(14)
C(25)A-Os(1)-N(1)	90.9(14)	C(25)-Os(1)-N(1)A	90.9(14)
C(25)A-Os(1)-N(1)A	89.1(14)	N(1)-Os(1)-N(1)A	180.0
C(25)-Os(1)-N(2)	91(2)	C(25)A-Os(1)-N(2)	89(2)
N(1)-Os(1)-N(2)	90.4(3)	N(1)A-Os(1)-N(2)	89.6(3)
C(25)-Os(1)-N(2)A	89(2)	C(25)A-Os(1)-N(2)A	91(2)
N(1)-Os(1)-N(2)A	89.6(3)	N(1)A-Os(1)-N(2)A	90.4(3)
N(2)-Os(1)-N(2)A	179.998(1)	N(1)-Os(1)-N(5)A	95.5(8)
N(1)A-Os(1)-N(5)A	84.5(9)	N(2)-Os(1)-N(5)A	84.7(9)
N(2)A-Os(1)-N(5)A	95.3(9)	N(1)-Os(1)-N(5)	84.5(9)
N(1)A-Os(1)-N(5)	95.5(8)	N(2)-Os(1)-N(5)	95.3(9)
N(2)A-Os(1)-N(5)	84.7(9)	N(5)A-Os(1)-N(5)	179.999(2)

C(4)-N(1)-C(1)	108.1(7)	C(4)-N(1)-Os(1)	125.7(6)
C(1)-N(1)-Os(1)	126.1(6)	C(9)-N(2)-C(6)	107.8(7)
C(9)-N(2)-Os(1)	127.0(6)	C(6)-N(2)-Os(1)	125.2(6)
N(1)-C(1)-C(10)A	125.9(8)	N(1)-C(1)-C(2)	108.7(8)
C(10)A-C(1)-C(2)	125.4(9)	C(3)-C(2)-C(1)	106.8(9)
C(2)-C(3)-C(4)	107.3(9)	N(1)-C(4)-C(5)	126.1(9)
N(1)-C(4)-C(3)	109.0(8)	C(5)-C(4)-C(3)	124.9(9)
C(6)-C(5)-C(4)	126.0(9)	C(5)-C(6)-N(2)	126.6(8)
C(5)-C(6)-C(7)	125.9(9)	N(2)-C(6)-C(7)	107.5(8)
C(8)-C(7)-C(6)	108.0(8)	C(7)-C(8)-C(9)	107.3(8)
N(2)-C(9)-C(10)	125.7(8)	N(2)-C(9)-C(8)	109.4(8)
C(10)-C(9)-C(8)	124.9(9)	C(9)-C(10)-C(1)A	125.7(8)
C(27)-C(26)-C(31)	118(2)	C(27)-C(26)-N(5)	124(2)
C(31)-C(26)-N(5)	118(2)	C(26)-C(27)-C(28)	125(2)
C(27)-C(28)-C(29)	115(2)	C(30)-C(29)-C(28)	117(3)
C(29)-C(30)-C(31)	128(3)	C(30)-C(31)-C(26)	118(3)

Table 2.14. Selected Bond Lengths (Å) for (TPP)Os(PhNO)₂

Os(1)-N(5)	1.961(3)	Os(1)-N(6)	1.971(3)
Os(1)-N(1)	2.053(3)	Os(1)-N(3)	2.052(3)
Os(1)-N(2)	2.057(3)	Os(1)-N(4)	2.067(3)
O(1)-N(5)	1.249(4)	O(2)-N(6)	1.259(5)
N(5)-C(45)	1.469(5)	N(6)-C(51)	1.458(5)
C(45)-C(50)	1.369(7)	C(45)-C(46)	1.383(7)
C(46)-C(47)	1.378(8)	C(47)-C(48)	1.377(10)
C(48)-C(49)	1.360(11)	C(49)-C(50)	1.391(8)
C(51)-C(56)	1.374(6)	C(51)-C(52)	1.392(6)

C(52)-C(53)	1.379(7)	C(53)-C(54)	1.387(8)
C(54)-C(55)	1.377(8)	C(55)-C(56)	1.382(7)
N(1)-C(1)	1.372(5)	N(1)-C(4)	1.376(5)
N(2)-C(9)	1.366(5)	N(2)-C(6)	1.366(5)
N(3)-C(14)	1.369(5)	N(3)-C(11)	1.376(5)
N(4)-C(19)	1.375(5)	N(4)-C(16)	1.376(5)
C(1)-C(20)	1.396(6)	C(1)-C(2)	1.444(6)
C(2)-C(3)	1.363(6)	C(3)-C(4)	1.442(6)
C(4)-C(5)	1.390(5)	C(5)-C(6)	1.399(6)
C(6)-C(7)	1.442(6)	C(7)-C(8)	1.361(6)
C(8)-C(9)	1.454(6)	C(9)-C(10)	1.400(6)
C(10)-C(11)	1.391(6)	C(11)-C(12)	1.443(6)
C(12)-C(13)	1.359(6)	C(13)-C(14)	1.453(6)
C(14)-C(15)	1.401(6)	C(15)-C(16)	1.388(6)
C(16)-C(17)	1.442(6)	C(17)-C(18)	1.356(7)
C(18)-C(19)	1.440(6)	C(19)-C(20)	1.396(6)

Table 2.15. Selected Bond Angles ($^{\circ}$) for (TPP)Os(PhNO)₂

N(5)-Os(1)-N(6)	174.59(14)	O(1)-N(5)-Os(1)	125.4(3)
O(1)-N(5)-C(45)	112.4(3)	C(45)-N(5)-Os(1)	122.0(3)
O(2)-N(6)-Os(1)	124.1(3)	O(2)-N(6)-C(51)	113.1(3)
C(51)-N(6)-Os(1)	122.2(3)	N(5)-Os(1)-N(1)	89.33(14)
N(6)-Os(1)-N(1)	89.93(14)	N(5)-Os(1)-N(3)	91.25(14)
N(6)-Os(1)-N(3)	89.52(14)	N(1)-Os(1)-N(3)	179.34(13)
N(5)-Os(1)-N(2)	88.06(13)	N(6)-Os(1)-N(2)	86.58(14)
N(1)-Os(1)-N(2)	89.75(14)	N(3)-Os(1)-N(2)	90.58(14)
N(5)-Os(1)-N(4)	91.69(13)	N(6)-Os(1)-N(4)	93.67(14)

N(1)-Os(1)-N(4)	90.10(13)	N(2)-Os(1)-N(4)	179.71(13)
N(3)-Os(1)-N(4)	89.57(14)	C(50)-C(45)-C(46)	121.1(5)
C(50)-C(45)-N(5)	119.8(4)	C(46)-C(45)-N(5)	119.1(4)
C(45)-C(46)-C(47)	119.2(6)	C(48)-C(47)-C(46)	119.6(6)
C(49)-C(48)-C(47)	121.2(6)	C(48)-C(49)-C(50)	119.7(6)
C(45)-C(50)-C(49)	119.3(6)	C(56)-C(51)-C(52)	121.2(4)
C(56)-C(51)-N(6)	119.5(4)	C(52)-C(51)-N(6)	119.3(4)
C(53)-C(52)-C(51)	118.9(5)	C(52)-C(53)-C(54)	120.5(5)
C(55)-C(54)-C(53)	119.6(5)	C(54)-C(55)-C(56)	120.8(5)
C(51)-C(56)-C(55)	119.1(5)	C(1)-N(1)-C(4)	108.1(3)
C(1)-N(1)-Os(1)	126.0(3)	C(4)-N(1)-Os(1)	125.8(3)
C(9)-N(2)-C(6)	108.0(3)	C(9)-N(2)-Os(1)	125.5(3)
C(6)-N(2)-Os(1)	126.5(3)	C(14)-N(3)-C(11)	108.1(3)
C(14)-N(3)-Os(1)	126.4(3)	C(11)-N(3)-Os(1)	125.5(3)
C(19)-N(4)-C(16)	108.3(3)	C(19)-N(4)-Os(1)	125.6(3)
C(16)-N(4)-Os(1)	126.1(3)	N(1)-C(1)-C(20)	126.4(4)
N(1)-C(1)-C(2)	109.0(4)	C(20)-C(1)-C(2)	124.5(4)
C(3)-C(2)-C(1)	106.7(4)	C(2)-C(3)-C(4)	108.0(4)
N(1)-C(4)-C(5)	126.4(4)	N(1)-C(4)-C(3)	108.2(3)
C(5)-C(4)-C(3)	125.4(4)	C(4)-C(5)-C(6)	125.3(4)
N(2)-C(6)-C(5)	125.9(4)	N(2)-C(6)-C(7)	108.9(4)
C(5)-C(6)-C(7)	125.2(4)	C(8)-C(7)-C(6)	107.7(4)
C(7)-C(8)-C(9)	106.4(4)	N(2)-C(9)-C(10)	126.2(4)
N(2)-C(9)-C(8)	109.0(4)	C(10)-C(9)-C(8)	124.7(4)
C(11)-C(10)-C(9)	125.8(4)	N(3)-C(11)-C(10)	126.1(4)
N(3)-C(11)-C(12)	108.7(4)	C(10)-C(11)-C(12)	125.2(4)
C(13)-C(12)-C(11)	107.5(4)	C(12)-C(13)-C(14)	107.2(4)

N(3)-C(14)-C(15)	126.5(4)	N(3)-C(14)-C(13)	108.6(3)
C(15)-C(14)-C(13)	124.8(4)	C(16)-C(15)-C(14)	125.0(4)
N(4)-C(16)-C(15)	126.4(4)	N(4)-C(16)-C(17)	108.0(4)
C(15)-C(16)-C(17)	125.6(4)	C(18)-C(17)-C(16)	107.9(4)
C(17)-C(18)-C(19)	107.4(4)	N(4)-C(19)-C(20)	126.2(4)
N(4)-C(19)-C(18)	108.4(4)	C(20)-C(19)-C(18)	125.3(4)
C(1)-C(20)-C(19)	125.4(4)		

Table 2.16. Selected Bond Lengths (Å) for (TMP)Os(PhNO)₂

Os(1)-N(6)	1.979(9)	Os(1)-N(5)	2.049(12)
O(1)-N(5)	1.31(2)	O(2)-N(6)	1.252(12)
Os(1)-N(2)	2.037(10)	Os(1)-N(1)	2.055(9)
Os(1)-N(4)	2.058(9)	Os(1)-N(3)	2.059(9)
N(5)-C(57)	1.40(2)	N(6)-C(63)	1.45(2)
C(57)-C(58)	1.39(2)	C(57)-C(62)	1.46(3)
C(58)-C(59)	1.30(2)	C(59)-C(60)	1.49(3)
C(60)-C(61)	1.46(3)	C(61)-C(62)	1.53(3)
C(63)-C(64)	1.39(2)	C(63)-C(68)	1.40(2)
C(64)-C(65)	1.37(2)	C(65)-C(66)	1.36(2)
C(66)-C(67)	1.38(2)	C(67)-C(68)	1.39(2)
N(1)-C(4)	1.373(14)	N(1)-C(1)	1.402(14)
N(2)-C(9)	1.398(14)	N(2)-C(6)	1.403(14)
N(3)-C(14)	1.402(14)	N(3)-C(11)	1.405(14)
N(4)-C(19)	1.381(14)	N(4)-C(16)	1.391(14)
C(1)-C(20)	1.41(2)	C(1)-C(2)	1.47(2)
C(2)-C(3)	1.32(2)	C(3)-C(4)	1.45(2)

C(4)-C(5)	1.42(2)	C(5)-C(6)	1.45(2)
C(6)-C(7)	1.45(2)	C(7)-C(8)	1.37(2)
C(8)-C(9)	1.42(2)	C(9)-C(10)	1.438(14)
C(10)-C(11)	1.39(2)	C(11)-C(12)	1.44(2)
C(12)-C(13)	1.37(2)	C(13)-C(14)	1.45(2)
C(14)-C(15)	1.39(2)	C(15)-C(16)	1.43(2)
C(16)-C(17)	1.47(2)	C(17)-C(18)	1.32(2)
C(18)-C(19)	1.46(2)	C(19)-C(20)	1.43(2)

Table 2.17. Selected Bond Angles ($^{\circ}$) for (TMP)Os(PhNO)₂

O(1)-N(5)-Os(1)	116.5(9)	O(1)-N(5)-C(57)	110.4(12)
C(57)-N(5)-Os(1)	131.8(11)	O(2)-N(6)-Os(1)	121.5(8)
O(2)-N(6)-C(63)	112.5(9)	C(63)-N(6)-Os(1)	125.9(8)
N(6)-Os(1)-N(2)	87.7(4)	N(6)-Os(1)-N(5)	171.0(5)
N(2)-Os(1)-N(5)	86.4(4)	N(6)-Os(1)-N(1)	87.6(4)
N(2)-Os(1)-N(1)	90.0(3)	N(5)-Os(1)-N(1)	99.1(5)
N(6)-Os(1)-N(4)	93.7(4)	N(2)-Os(1)-N(4)	178.6(4)
N(5)-Os(1)-N(4)	92.4(4)	N(1)-Os(1)-N(4)	89.7(3)
N(6)-Os(1)-N(3)	91.0(4)	N(2)-Os(1)-N(3)	90.4(3)
N(5)-Os(1)-N(3)	82.3(4)	N(1)-Os(1)-N(3)	178.6(4)
N(4)-Os(1)-N(3)	89.9(3)	C(58)-C(57)-N(5)	125(2)
C(58)-C(57)-C(62)	124(2)	N(5)-C(57)-C(62)	111(2)
C(59)-C(58)-C(57)	124(2)	C(58)-C(59)-C(60)	118(2)
C(61)-C(60)-C(59)	123(3)	C(60)-C(61)-C(62)	115(3)
C(57)-C(62)-C(61)	115(2)	C(64)-C(63)-C(68)	118.5(14)
C(64)-C(63)-N(6)	121.6(12)	C(68)-C(63)-N(6)	119.9(13)

C(65)-C(64)-C(63)	118.8(14)	C(66)-C(65)-C(64)	125(2)
C(65)-C(66)-C(67)	115(2)	C(66)-C(67)-C(68)	123(2)
C(67)-C(68)-C(63)	119(2)	C(4)-N(1)-C(1)	106.1(10)
C(4)-N(1)-Os(1)	127.4(8)	C(1)-N(1)-Os(1)	126.4(8)
C(9)-N(2)-Os(1)	127.3(7)	C(9)-N(2)-C(6)	105.1(9)
C(6)-N(2)-Os(1)	127.1(7)	C(14)-N(3)-C(11)	107.4(9)
C(14)-N(3)-Os(1)	126.2(7)	C(11)-N(3)-Os(1)	126.1(7)
C(19)-N(4)-C(16)	106.5(9)	C(19)-N(4)-Os(1)	126.6(7)
C(16)-N(4)-Os(1)	126.6(8)	N(1)-C(1)-C(20)	126.0(11)
N(1)-C(1)-C(2)	108.1(10)	C(20)-C(1)-C(2)	125.8(11)
C(3)-C(2)-C(1)	107.8(12)	C(2)-C(3)-C(4)	107.9(12)
N(1)-C(4)-C(5)	125.8(11)	N(1)-C(4)-C(3)	110.0(11)
C(5)-C(4)-C(3)	124.1(11)	C(4)-C(5)-C(6)	124.3(11)
N(2)-C(6)-C(5)	124.5(10)	N(2)-C(6)-C(7)	109.8(10)
C(5)-C(6)-C(7)	125.5(10)	C(8)-C(7)-C(6)	106.4(10)
C(7)-C(8)-C(9)	108.3(10)	N(2)-C(9)-C(8)	110.1(9)
N(2)-C(9)-C(10)	124.6(10)	C(8)-C(9)-C(10)	125.2(11)
C(11)-C(10)-C(9)	125.4(11)	C(10)-C(11)-N(3)	126.1(10)
C(10)-C(11)-C(12)	125.9(10)	N(3)-C(11)-C(12)	107.9(9)
C(13)-C(12)-C(11)	109.0(10)	C(12)-C(13)-C(14)	106.9(10)
C(15)-C(14)-N(3)	126.5(10)	C(15)-C(14)-C(13)	124.8(10)
N(3)-C(14)-C(13)	108.7(10)	C(14)-C(15)-C(16)	124.5(10)
N(4)-C(16)-C(15)	125.7(11)	N(4)-C(16)-C(17)	108.7(10)
C(15)-C(16)-C(17)	125.7(11)	C(18)-C(17)-C(16)	107.7(11)
C(17)-C(18)-C(19)	107.8(11)	N(4)-C(19)-C(20)	126.4(10)
N(4)-C(19)-C(18)	109.0(9)	C(20)-C(19)-C(18)	124.5(11)
C(1)-C(20)-C(19)	123.7(11)		

Table 2.18. Selected Bond Lengths (Å) for (OEP)Os(*o*-tolNO)₂

Os(1)-N(3A)	1.985(10)	Os(1)-N(3A)A	1.985(10)
Os(1)-N(3)	2.012(11)	Os(1)-N(3)A	2.012(11)
Os(1)-N(1)	2.051(5)	Os(1)-N(1)A	2.051(5)
Os(1)-N(2)	2.068(5)	Os(1)-N(2)A	2.068(5)
N(3)-O(1)	1.273(13)	N(3A)-O(1A)	1.219(12)
N(3)-C(19)	1.481(14)	N(3A)-C(19A)	1.441(14)
C(19)-C(20)	1.380(14)	C(19)-C(24)	1.385(13)
C(20)-C(21)	1.404(14)	C(20)-C(25)	1.52(3)
C(21)-C(22)	1.40(2)	C(22)-C(23)	1.39(2)
C(23)-C(24)	1.420(14)	C(19A)-C(20A)	1.373(14)
C(19A)-C(24A)	1.374(14)	C(20A)-C(21A)	1.42(2)
C(21A)-C(22A)	1.40(2)	C(22A)-C(23A)	1.39(2)
C(23A)-C(24A)	1.41(2)	C(24A)-C(25A)	1.53(2)
N(1)-C(1)	1.383(7)	N(1)-C(4)	1.384(8)
N(2)-C(6)	1.375(9)	N(2)-C(9)	1.385(8)
C(1)-C(10)A	1.355(9)	C(1)-C(2)	1.460(9)
C(2)-C(3)	1.356(10)	C(3)-C(4)	1.465(9)
C(4)-C(5)	1.376(9)	C(5)-C(6)	1.391(10)
C(6)-C(7)	1.438(9)	C(7)-C(8)	1.362(10)
C(8)-C(9)	1.443(10)	C(9)-C(10)	1.389(10)
C(10)-C(1)A	1.355(9)		

Table 2.19. Selected Bond Angles ($^{\circ}$) for (OEP)Os(*o*-tolNO)₂

O(1)-N(3)-C(19)	108.8(9)	O(1)-N(3)-Os(1)	124.5(8)
C(19)-N(3)-Os(1)	125.1(8)	O(1A)-N(3A)-C(19A)	116.9(10)
O(1A)-N(3A)-Os(1)	125.1(9)	C(19A)-N(3A)-Os(1)	117.4(8)
N(3A)-Os(1)-N(3A)A	180.0	N(3)-Os(1)-N(3A)	180.0
N(3A)-Os(1)-N(1)	94.3(3)	N(3A)A-Os(1)-N(1)	85.7(3)
N(3)-Os(1)-N(1)	80.7(4)	N(3A)-Os(1)-N(1)	99.3(4)
N(3A)-Os(1)-N(1A)	85.7(3)	N(3A)A-Os(1)-N(1A)	94.3(3)
N(3)-Os(1)-N(1A)	99.3(4)	N(3A)-Os(1)-N(1A)	80.7(4)
N(1)-Os(1)-N(1A)	180.0	N(3A)-Os(1)-N(2A)	93.2(4)
N(3A)A-Os(1)-N(2A)	86.8(4)	N(3)-Os(1)-N(2A)	91.7(3)
N(3A)-Os(1)-N(2A)	88.3(3)	N(1)-Os(1)-N(2A)	90.2(2)
N(1A)-Os(1)-N(2A)	89.8(2)	N(3A)-Os(1)-N(2)	86.8(4)
N(3A)A-Os(1)-N(2)	93.2(4)	N(3)-Os(1)-N(2)	88.3(3)
N(3A)-Os(1)-N(2)	91.7(3)	N(1)-Os(1)-N(2)	89.8(2)
N(1A)-Os(1)-N(2)	90.2(2)	N(2A)-Os(1)-N(2)	180.0
C(20)-C(19)-C(24)	121.2(10)	C(20)-C(19)-N(3)	121.7(9)
C(24)-C(19)-N(3)	117.1(9)	C(19)-C(20)-C(21)	119.8(10)
C(19)-C(20)-C(25)	124.5(13)	C(21)-C(20)-C(25)	115.7(13)
C(22)-C(21)-C(20)	119.4(11)	C(23)-C(22)-C(21)	121.2(12)
C(22)-C(23)-C(24)	118.5(10)	C(19)-C(24)-C(23)	119.8(10)
C(20A)-C(19A)-C(24A)	122.5(11)	C(20A)-C(19A)-N(3A)	121.8(10)
C(24A)-C(19A)-N(3A)	115.6(10)	C(19A)-C(20A)-C(21A)	119.4(11)
C(22A)-C(21A)-C(20A)	118.1(12)	C(23A)-C(22A)-C(21A)	121.6(13)
C(22A)-C(23A)-C(24A)	118.7(12)	C(19A)-C(24A)-C(23A)	119.3(11)
C(19A)-C(24A)-C(25A)	126.4(13)	C(23A)-C(24A)-C(25A)	113.9(13)

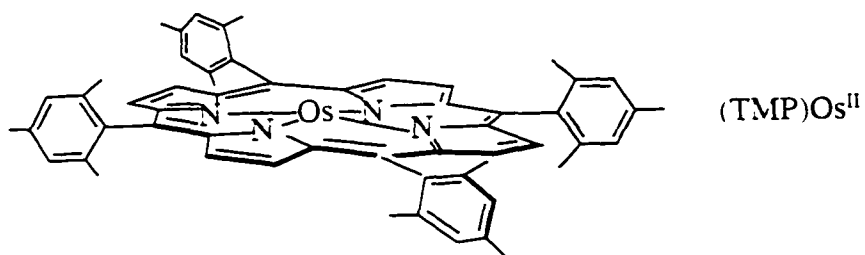
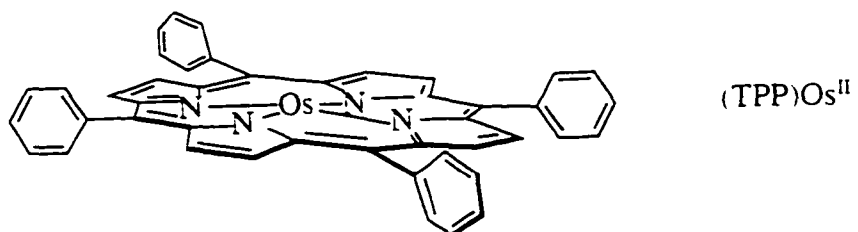
C(1)-N(1)-C(4)	107.9(5)	C(1)-N(1)-Os(1)	125.7(4)
C(4)-N(1)-Os(1)	126.2(4)	C(6)-N(2)-C(9)	108.7(5)
C(6)-N(2)-Os(1)	126.5(4)	C(9)-N(2)-Os(1)	124.8(5)
C(10)A-C(1)-N(1)	126.3(6)	C(10)A-C(1)-C(2)	125.3(6)
N(1)-C(1)-C(2)	108.3(5)	C(3)-C(2)-C(1)	108.1(5)
C(2)-C(3)-C(4)	107.0(6)	C(5)-C(4)-N(1)	124.9(6)
C(5)-C(4)-C(3)	126.3(6)	N(1)-C(4)-C(3)	108.7(5)
C(4)-C(5)-C(6)	128.3(6)	N(2)-C(6)-C(5)	124.1(6)
N(2)-C(6)-C(7)	108.3(6)	C(5)-C(6)-C(7)	127.6(6)
C(8)-C(7)-C(6)	107.5(6)	C(7)-C(8)-C(9)	108.0(6)
N(2)-C(9)-C(10)	126.0(6)	N(2)-C(9)-C(8)	107.4(6)
C(10)-C(9)-C(8)	126.6(6)	C(1)A-C(10)-C(9)	126.9(6)

The average Os–N(por) bond length of 2.078 Å for (TTP)Os(CO)(PhNO) appears longer than that for other Os^{II} tetraphenylporphyrin derivatives (Table 2.3). The Os–C(O) bond length of 1.93(2) Å is longer than those for (TTP)Os(CO)(Et₂NNO) and (OEPMe₂)Os(CO)(py) (Table 2.4), consistent with PhNO acting as a π acid to decrease the extent of backbonding from Os^{II} center to the *trans* carbonyl ligand, making Os–C(O) bond weaker and longer. The Os–C–O bond is virtually linear. The Os–N_{ax} distance for (TTP)Os(CO)(PhNO) of 2.18(2) Å is longer than the average Os–N_{ax} distance in (TTP)Os(PhNO)₂ (1.962 Å), consistent with the carbonyl ligand acting as a better π acceptor than the PhNO ligand, causing less π backbonding from Os^{II} to *trans* PhNO, and resulting in a weaker and longer *trans* Os–N bond.

The average Os–N(por) distances for all the (por)Os^{II} bis-nitrosoarene complexes are within the range observed for other (por)Os^{II} complexes (Table 2.3). The Os–N_{ax} distances are essentially the same for all four (por)Os^{II} bis-nitrosoarene complexes. The sum of the bond angles around the N atoms of the PhNO ligands in all five structures are ca. 360°, indicating the planarity around the nitroso N atoms.

The O–N–Os–N(por) torsion angles (α_1 and α_2) for the (por)Os^{II} nitrosoarene complexes are shown in Figures 2.18–2.21. Scheidt and coworkers⁸⁹ studied the ligand orientation in the [(T_{piv}PP)Fe(NO₂)(NO)]⁻ complex with *trans* π accepting axial ligands. The conclusion they reached was that “If both axial ligands were to exhibit strong π -accepting behavior, it is to be expected that two axial ligands should be found in planes orthogonal to each other, so as to maximize the M→L π -bonding.” In the case of the (por)Os^{II} bis-nitrosobenzene complexes, the sum of the indicated torsion angles ($\alpha_1 + \alpha_2$) is close to 90°, and suggests that the coordinated *trans* PhNO ligands are essentially orthogonal to each other in all three (por)Os^{II} bis-nitrosobenzene complexes (86.7° for TTP, 81.5° for TPP and 93.6° for TMP). This suggests that they are positioned in such a manner as to maximize the π interactions between the HOMO

of the formal d^6 (por)Os^{II} core (namely d_{xz} and d_{yz}) and the empty π^* orbitals of the PhNO ligands. The sterically demanding TMP was used to see if the sum of the indicated torsion angles ($\alpha_1 + \alpha_2$) could be forced to be smaller, but the results show that there is no significant effect.



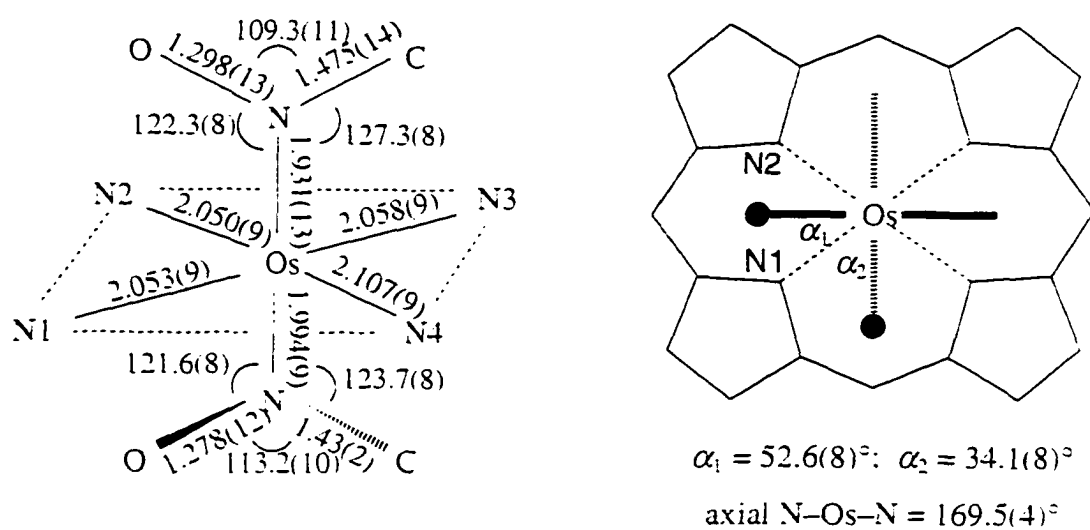
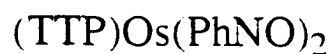


Figure 2.18. Structural data for (TTP)Os(PhNO)₂: selected bond lengths and bond angles are shown on the left. Also shown are the O—N—Os—N(1) torsion angles on the right: the solid line represents the nitroso group of the PhNO ligand above the plane and the dashed line represents the equivalent nitroso group below the plane.

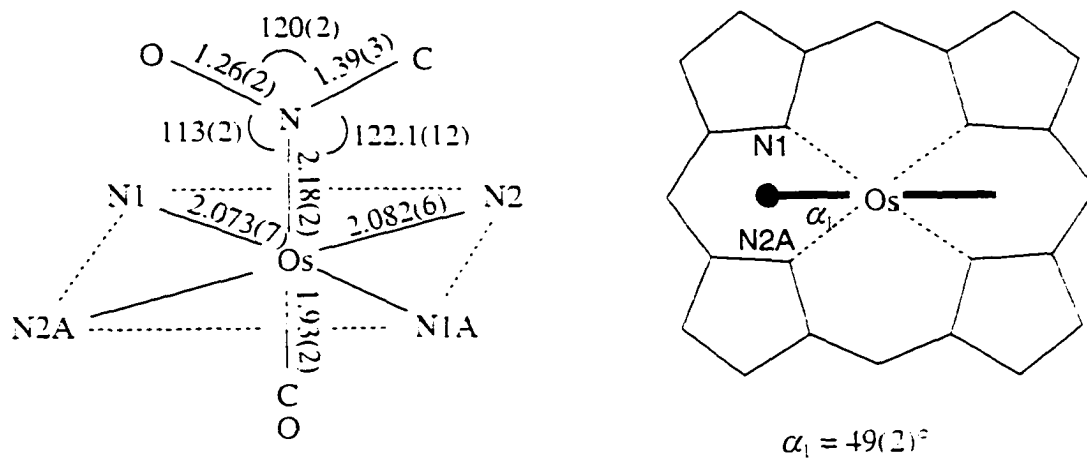


Figure 2.19. Structural data for (TTP)Os(CO)(PhNO): selected bond lengths and bond angles are shown on the left. Also shown is the O-N-Os-N(2A) torsion angle on the right.

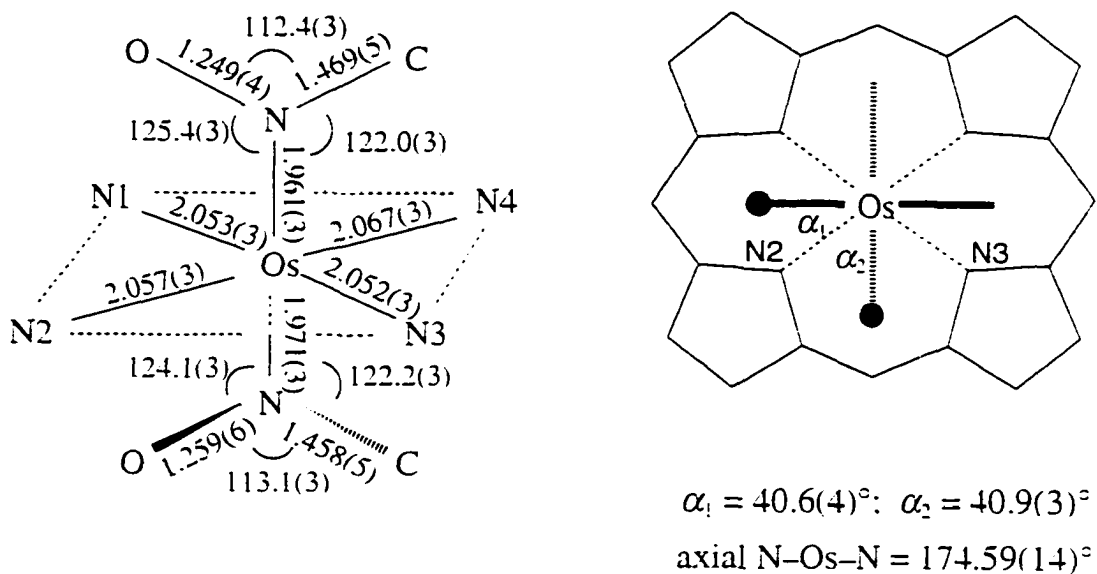
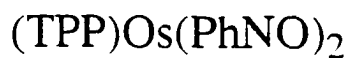


Figure 2.20. Structural data for (TPP)Os(PhNO)₂: selected bond lengths and bond angles are shown on the left. Also shown are the O—N—Os—N(2) torsion angles on the right: the solid line represents the nitroso group of the PhNO ligand above the plane and the dashed line represents the equivalent nitroso group below the plane.

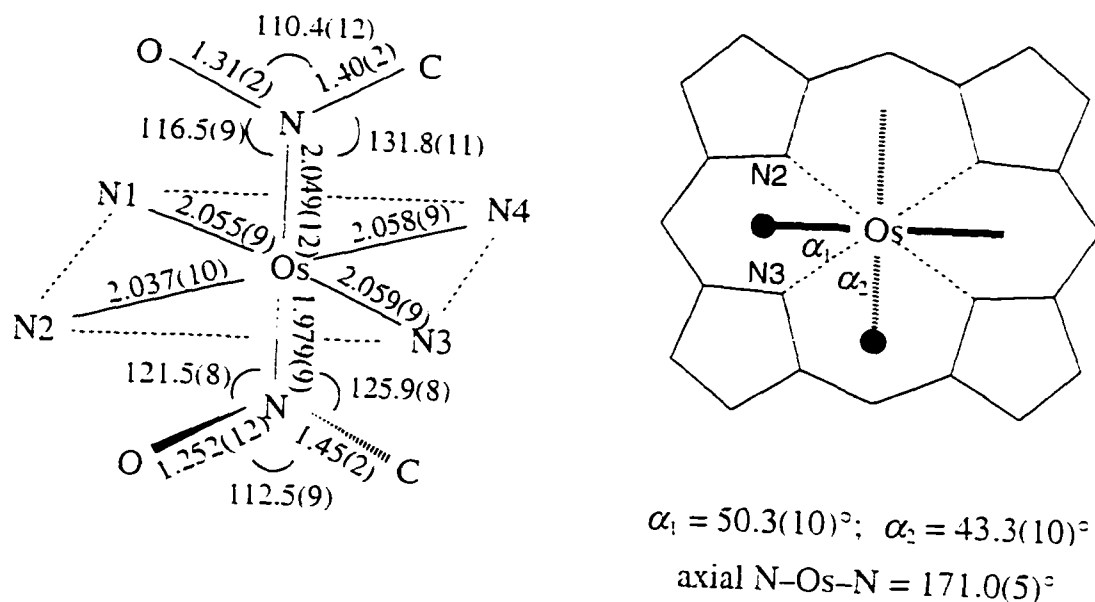
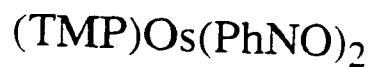


Figure 2.21. Structural data for (TMP)Os(PhNO)₂: selected bond lengths and bond angles are shown on the left. Also shown are the O—N—Os—N(3) torsion angles on the right: the solid line represents the nitroso group of the PhNO ligand above the plane and the dashed line represents the equivalent nitroso group below the plane.

Conclusion

This study shows the extension of the η^1 -O binding of the diethylnitrosamine ligand to $\text{Fe}^{\text{III}} d^5$ and $\text{Os}^{\text{II}} d^6$ porphyrins. This study also provides the first examples of η^1 -O binding of the specially designed C-nitroso ligands to non- d^{10} transition metals. It has been shown that the binding mode of the C-nitroso ligands is determined by the nature of the metal center as well as the nature of the ligands. The resonance structures of the nitrosamine and the C-nitroso ligands might play a very important role in the η^1 -O binding. The first examples of nitrosoarene binding to (por)Os^{II} in an η^1 -N binding mode have been synthesized and structurally characterized. Prior to this study, only a few (por)Os^{II} structures were published. This work provides six (por)Os^{II} structures, which will make good structural comparisons for future work. Most importantly, the Et₂NNO ligand exhibits weak σ -donating character in the (por)Os^{II} nitrosamine complexes whereas the PhNO ligand acts as a strong π -acceptor in the (por)Os^{II} nitrosobenzene complexes. The two *trans* PhNO ligands are oriented orthogonal to each other to maximize the M→L π backbonding. The effects of PhNO acting as a π acceptor and Et₂NNO as a weak σ donor are also well represented by the increase of ν_{CO} for (TTP)Os(CO)(PhNO) and decrease of ν_{CO} for (TTP)Os(CO)(Et₂NNO) with respect to (TTP)Os(CO).

References and Notes

- (1) Preussman, R.; Stewart, B. W. In *Chemical Carcinogens*; 2nd ed.; C. E. Searle, Ed.; American Chemical Society: Washington, D.C., 1984; Vol. 2; pp 643–828.
- (2) *Nitrosamines: Toxicology and Microbiology*; Hill, M. J., Ed.; VCH Ellis Horwood Ltd.: Chichester (England), 1988.
- (3) Lijinsky, W. *Chemistry and Biology of N-Nitroso Compounds*; Cambridge University Press: Cambridge, U. K. 1992.
- (4) Cadogan, J. I. G. *Acc. Chem. Res.* **1971**, *4*, 186.
- (5) Fridman, A. L.; Mukhametshin, F. M.; Novikov, S. S. *Russ. Chem. Rev. (Engl. Trans.)* **1971**, *40*, 34.
- (6) *Safety Evaluation of Nitrosatable Drugs and Chemicals*; Gibson, G. G.; Ioannides, C., Ed.; Taylor and Francis Ltd.: London, 1981.
- (7) Saavedra, J. E. *Org. Prep. Proced. Int.* **1987**, *19*, 83.
- (8) Ioannides, C.; Gibson, G. G. In *Safety Evaluation of Nitrosatable Drugs and Chemicals*; G. G. Gibson and C. Ioannides, Ed.; Taylor and Francis: London, 1981; pp 257–278.
- (9) Guttenplan, J. B. *Mutation Research* **1987**, *186*, 81.
- (10) *Nitrosamines and Related N-Nitroso Compounds. Chemistry and Biochemistry*; Loepky, R. N.; Michejda, C. J., Ed.; American Chemical Society: Washington, D.C., 1994; Vol. 553.
- (11) Appel, K. E.; Ruf, H. H.; Mahr, B.; Schwarz, M.; Rickart, R.; Kunz, W. *Chem.-Biol. Interac.* **1979**, *28*, 17.
- (12) Schmidpeter, A.; Nöth, H. *Inorg. Chim. Acta* **1998**, *269*, 7.
- (13) Asaji, T.; Sakai, H.; Nakamura, D. *Inorg. Chem.* **1983**, *22*, 202.
- (14) Schmidpeter, A. *Chem. Ber.* **1963**, *96*, 3275.

- (15) (a) Klement, U.; Schmidpeter, A. *Angew. Chem. Int. Ed. Engl.* **1968**, *7*, 470.
(b) Klement, U. *Acta Crystallogr.* **1969**, *B25*, 2460.
- (16) Brown, R. D.; Coates, G. E. *J. Chem. Soc.* **1962**, 4723.
- (17) Willett, R. D. *Acta Crystallogr.* **1988**, *B44*, 503.
- (18) Asaji, T.; Ikeda, R.; Inoue, M.; Nakamura, D. *J. Mol. Struct.* **1980**, *58*, 315.
- (19) Khan, M. I.; Agarwala, U. C. *Bull. Chem. Soc. Jpn.* **1986**, *59*, 1285.
- (20) White, I. N. H.; Smith, A. G.; Farmer, P. B. *Biochem. J.* **1983**, *212*, 599.
- (21) Bonnett, R.; Charalambides, A. A.; Martin, R. A. *J. Chem. Soc., Perkin Trans. I* **1978**, 974.
- (22) Bonnett, R.; Charalambides, A. A.; Martin, R. A.; Sales, K. D.; Fitzsimmons, B. W. *J. Chem. Soc., Chem. Commun.* **1975**, 884.
- (23) (a) Albinati, A.; Affolter, S.; Pregosin, P. S. *J. Organomet. Chem.* **1990**, *395*, 231. (b) Constable, A. G.; McDonald, W. S.; Shaw, B. L. *J. Chem. Soc., Dalton Trans.* **1980**, 2282.
- (24) (a) Yi, G.-B.; Khan, M. A.; Richter-Addo, G. B. *J. Am. Chem. Soc.* **1995**, *117*, 7850. (b) Yi, G.-B.; Khan, M. A.; Richter-Addo, G. B. *Inorg. Chem.* **1996**, *35*, 3453. (c) Chen, L.; Yi, G.-B.; Wang, L.-S.; Dharmawardana, U. R.; Dart, A. C.; Khan, M. A.; Richter-Addo, G. B. *Inorg. Chem.* Submitted.
- (25) (a) Hirota, K.; Itano, H. A. *J. Biol. Chem.* **1978**, *253*, 3477. (b) Gibson, Q. H. *Biochem. J.* **1960**, *77*, 519. and references therein.
- (26) (a) Mansuy, D.; Rouer, E.; Bacot, C.; Gans, P.; Chottard, J. C.; Lerouz, J. P. *Biochem. Pharmacol.* **1978**, *27*, 1229. (b) Mansuy, D.; Chottard, J. C.; Chottard, G. *Eur. J. Biochem.* **1977**, *76*, 617.
- (27) Stone, J. R.; Marletta, M. A. *Biochemistry* **1995**, *34*, 16397.
- (28) Murayama, M. *J. Bio. Chem.* **1960**, *235*, 1024.
- (29) Mansuy, D.; Beaune, P.; Chottard, J. C.; Bartoli, J. F.; Gans, P. *Biochem. Pharmacol.* **1976**, *25*, 609.

- (30) Jonsson, J.; Lindeke, B.: *Acta Pharm. Suecica* **1976**, *13*, 313.
- (31) Mansuy, D.; Gans, P.; Chottard, J. C.; Bartoli, J. F. *Eur. J. Biochem.* **1977**, *76*, 607.
- (32) Mansuy, D.; Battioni, P.; Chottard, J.-C.; Riche, C.; Chiaroni, A. *J. Am. Chem. Soc.* **1983**, *105*, 455.
- (33) Cameron, M.; Gowenlock, B. G.; Vasapollo, G. *Chem. Soc. Rev.* **1990**, *19*, 355.
- (34) Pilato, R. S.; McGettigan, C.; Geoffroy, G. L. *Organometallics* **1990**, *9*, 312.
- (35) Matsubayashi, G.-E.; Tanaka, T. *J. Chem. Soc. Dalton Trans.* **1990**, 437.
- (36) Little, R. G.; Doedens, R. J. *Inorg. Chem.* **1973**, *12*, 537.
- (37) Mansuy, D.; Drême, M.; Chottard, J. C.; Guilhem, J. *J. Organomet. Chem.* **1978**, *161*, 207.
- (38) Sams, D. B.; Doedens, R. J. *Inorg. Chem.* **1979**, *18*, 153.
- (39) Wang, L.-S.; Chen, L.; Khan, M. A.; Richter-Addo, G. B. *Chem. Commun.* **1996**, 323.
- (40) Crotti, C.; Sishta, C.; Pacheco, A.; James, B. R. *Inorg. Chim. Acta* **1988**, *141*, 13.
- (41) (a) Liebeskind, L. S.; Sharpless, K. B.; Wilson, R. D.; Ibers, J. A. *J. Am. Chem. Soc.* **1978** *100*, 7061. (b) Skoog, S. J.; Campbell, J. P.; Gladfelter, W. L. *Organometallics* **1994**, *13*, 4137.
- (42) (a) Matsubayashi, G.-E.; Nakatsu, K. *Inorg. Chim. Acta* **1982**, *64*, L163. (b) Hu, S.; Thompson, D. M.; Ikekwere, P. O.; Barton, R. J.; Johnson, K. E.; Robertson, B. E. *Inorg. Chem.* **1989**, *28*, 4552.
- (43) Srivastava, R. S.; Khan, M. A.; Nicholas, K. M. *J. Am. Chem. Soc.* **1996**, *118*, 3311, and references therein.
- (44) Fox, S. J. S.; Chen, L.; Khan, M. A.; Richter-Addo, G. B. *Inorg. Chem.* **1997**, *36*, 6465.

- (45) Ang, H. G.; Kwik, W. L.; Ong, K. K. *J. Fluor. Chem.* **1993**, *60*, 43.
- (46) Adler, A. D.; Longo, F. R.; Finarelli, J. D.; Goldmacher, J.; Assour, J.; Korsakoff, L. *J. Org. Chem.* **1967**, *32*, 476.
- (47) Fleischer, E. B.; Palmer, J. M.; Srivastava, T. S.; Chatterjee, A. *J. Am. Chem. Soc.* **1971**, *93*, 3162.
- (48) Che, C.-M.; Poon, C.-K.; Chung, W.-C.; Gray, H. B. *Inorg. Chem.* **1985**, *24*, 1277.
- (49) (a) Lindsey, J. S.; Wagner, R. W. *J. Org. Chem.* **1989**, *54*, 828. (b) Safo, M. K.; Gupta, G. P.; Walker, F. A.; Scheidt, W. R.; *J. Am. Chem. Soc.* **1991**, *113*, 5497.
- (50) Grant, D. H. *J. Chem. Ed.* **1995**, *72*, 39, and references therein.
- (51) Keefer, L. K.; Hrabie, J. A.; Hilton, B. D.; Wilbur, D. *J. Am. Chem. Soc.* **1988**, *110*, 7459.
- (52) Nakamoto, K. *Infrared and Raman Spectra of Inorganic and Coordination Compounds*, 4th Ed.; Wiley-Interscience: New York, 1986; pp147–150.
- (53) Bennett, G. M.; Bell, E. V. *Org. Synth. Collec.* **1943**, *2*, 223.
- (54) Krebs, B.; Mandt, J. *Chem. Ber.* **1975**, *108*, 1130.
- (55) Richter-Addo, G. B.; Legzdins, P. *Metal Nitrosyls*; Oxford University Press: New York, 1992. p64-65, and references therein.
- (56) An earlier formulation of osmium nitrosamine complexes formed by oxidation of coordinated ammonia in the presence of secondary amines (ref 57) has been questioned by the same authors (ref 58).
- (57) Stershic, M. T.; Keefer, L. K.; Sullivan, B. P.; Meyer, T. J. *J. Am. Chem. Soc.* **1988**, *110*, 6884.
- (58) Coia, G. M.; White, P. S.; Meyer, T. J.; Wink, D. A.; Keefer, L. K.; Davis, W. M. *J. Am. Chem. Soc.* **1994**, *116*, 3649.

- (59) Yi, G.-B.; Chen, L.; Khan, M. A.; Richter-Addo, G. B. *Inorg. Chem.* **1997**, *36*, 3876.
- (60) Che, C.-M.; Lai, T.-F.; Chung, W.-C.; Schaefer, W. P.; Gray, H. B. *Inorg. Chem.* **1987**, *26*, 3907.
- (61) Djukic, J.-P.; Young, V. G., Jr.; Woo, L. K. *Organometallics* **1994**, *13*, 3995.
- (62) Chen, L.; Khan, M. A.; Richter-Addo, G. B. *Inorg. Chem.* **1998**, *37*, 533.
- (63) Scheidt, W. R.; Nasri, H. *Inorg. Chem.* **1995**, *34*, 2190.
- (64) Chapter 1.
- (65) chapter 3.
- (66) Buchler, J. W.; Lay, K. L.; Smith, P. D.; Scheidt, W. R.; Rupprecht, G. A.; Kenny, J. E. *J. Organomet. Chem.* **1976**, *110*, 109.
- (67) Omiya, S.; Tsutsui, M.; Meyer, E. F., Jr.; Bernal, I.; Cullen, D. L. *Inorg. Chem.* **1980**, *19*, 134.
- (68) Buchler, J. W.; Kokisch, W.; Smith, P. D. *Struct. Bonding* **1978**, *34*, 79.
- (69) Richter-Addo, G. B.; Legzdins, P. *Metal Nitrosyls*; Oxford University Press: New York, 1992. p19 and references therein.
- (70) Antipas, A.; Buchler, J. W.; Gouterman, M.; Smith, P. D. *J. Am. Chem. Soc.* **1980**, *102*, 198.
- (71) Cameron, M.; Gowenlock, B. G.; Vasapollo, G. *Polyhedron*. **1994**, *13*, 1371 and references therein.
- (72) Cameron, M.; Gowenlock, B. G.; Vasapollo, G. *J. Organomet. Chem.* **1989**, *378*, 493.
- (73) Walker, F. A.; Simonis U. In *Encyclopedia of Inorganic Chemistry*; R. B. King, Ed.; John Wiley and Sons: Chichester, 1994; Vol. 4; p 1785.

- (74) (a) Scheidt, W. R.; Reed, C. A. *Chem. Rev.* **1981**, *81*, 543. (b) Reed, C. A.; Mashiko, T.; Bentley, S. P.; Kastner, M. E.; Scheidt, W. R.; Spartalian, K.; Lang, G. *J. Am. Chem. Soc.* **1979**, *101*, 2948.
- (75) Serr, B. R.; Headford, C. E. L.; Anderson, O. P.; Elliot, C. M.; Spartalian, K.; Fainzilberg, V. E.; Hatfield, W. E.; Rohrs, B. R.; Eaton, S. S.; Eaton, G. R. *Inorg. Chem.* **1992**, *31*, 5450.
- (76) (a) Gans, P.; Buisson, G.; Duée, E.; Regnard, J.-R.; Marchon, J.-C. *J. Chem. Soc. Chem. Commun.* **1979**, 393. (b) Scheidt, W. R.; Geiger, D. K.; Lee, Y. J.; Gans, P.; Marchon, J.-C. *Inorg. Chem.* **1992**, *31*, 2660.
- (77) Scheidt, W. R.; Lee, Y. J.; Hatano, K. *J. Am. Chem. Soc.* **1984**, *106*, 3191.
- (78) Scheidt, W. R.; Cohen, I. A.; Kastner, M. E. *Biochemistry* **1979**, *18*, 3546.
- (79) Mashiko, T.; Kastner, M. E.; Spartalian, K.; Scheidt, W. R.; Reed, C. A. *J. Am. Chem. Soc.* **1978**, *100*, 6354.
- (80) Senge, M. O. *Acta Crystallogr.* **1996**, *C52*, 302.
- (81) Einstein, F. W. B.; Willis, A. C. *Inorg. Chem.* **1978**, *17*, 3040.
- (82) Kellett, P. J.; Pawlik, M. J.; Taylor, L. F.; Thompson, R. G.; Levstik, M. A.; Anderson, O. P.; Strauss, S. H. *Inorg. Chem.* **1989**, *28*, 440.
- (83) Talberg, H. J. *Acta Chem. Scand. A* **1977**, *31*, 743.
- (84) Fletcher, D. A.; Gowenlock, B. G.; Orrell, K. G.; Sik, V.; Hibbs, D. E.; Hursthouse, M. B.; Malik, K. M. A. *J. Chem. Soc., Perkin Trans. 2* **1997**, 721.
- (85) (a) Hill, C. L.; Williamson, M. M. *Inorg. Chem.* **1985**, *24*, 2836. (b) Hatano, K.; Anzai, K.; Iitaka, Y. *Bull. Chem. Soc. Jpn.* **1983**, *56*, 422. (c) Hill, C. L.; Williamson, M. M. *Inorg. Chem.* **1985**, *24*, 3024.
- (86) Cheng, B.; Fries, P. H.; Marchon, J.-C.; Scheidt, W. R. *Inorg. Chem.* **1996**, *35*, 1024 and references therein.
- (87) Scheidt, W. R. *Acc. Chem. Res.* **1977**, *10*, 339.

- (88) The UV-Vis spectrum of $[(\text{TPP})\text{Mn}(\text{ONC}_6\text{H}_4\text{NEt}_2)_2]\text{SbF}_6$ (1.0×10^{-5} M in toluene, ϵ in units of $\text{mM}^{-1}\text{cm}^{-1}$) shows peaks at 392 (126), 413 (106, sh), 480 (56), 570 (15), and 603 (11) nm. The spectrum is almost identical to the spectrum of $[(\text{TPP})\text{Mn}(\text{DMF})_2]\text{ClO}_4$ ^{85a} which has been fully characterized as a d^4 high-spin system.
- (89) Scheidt, W. R.; Chipman, D. M. *J. Am. Chem. Soc.* **1986**, *108*, 1163.

Chapter 3. Synthesis and Characterization of Osmium Nitrosyl Porphyrins Containing Organo, Chloro and μ -Oxo Ligands, and Extension to the First Organoosmium Thionitrosyl Porphyrin

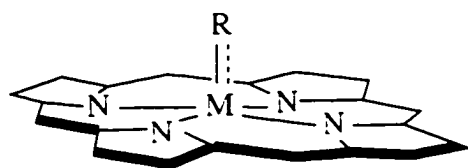
Introduction

Interest in the study of organometallic porphyrin complexes containing a direct M–R interaction results from the detection and/or postulation of organometallic species in the natural and model chemistry of coenzyme B₁₂, cytochrome P450, and other heme-containing biomolecules.¹⁻⁴ In this regard, many Co model systems for coenzyme B₁₂ have been synthesized and studied.⁵⁻⁹

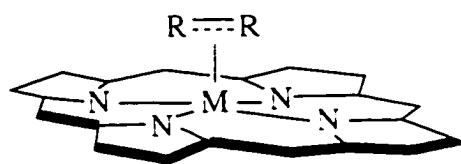
There are three types of organometallic porphyrins containing a direct M–R interaction (Chart 1). Organometallic porphyrins of Type **A** comprise those with metal–carbon(alkyl/aryl) single or multiple bonds. Dialkyl(aryl) complexes of the form (por)M(R)₂ have also been structurally characterized, and the σ -R ligands may either be located *cis* to each other (e.g., as in (OEP)Zr(Me)₂)^{10,11} or located *trans* to each other (e.g., as in (TTP)Os(CH₂SiMe₃)₂) (OEP = 2, 3, 7, 8, 12, 13, 17, 18-octaethylporphyrinato dianion, TTP = 5, 10, 15, 20-tetra-*p*-tolylporphyrinato dianion).^{12,13} Organometallic porphyrins of Type **B** include those with η^2 -alkene/alkyne or other π -bonded groups such as cyclopentadienyl or indenyl ligands.^{1,15-18} Type **C** complexes contain μ -N.M units in which the bridging alkyl (or carbene, vinyl, etc.) group maintains direct contact with the metal center.^{1,2,19,20}

The reported organometallic chemistry of group 8 metalloporphyrins has so far been focused on those of iron²¹⁻²⁵ and ruthenium.^{15,17,20,26-36} Surprisingly, only a handful of organoosmium porphyrins have been reported to date.^{12,17,30,36,37} Interestingly, some (por)Fe(R) complexes (of Type **A**) react with NO gas to form nitrosyl adducts (eq 3.1).^{39,40}

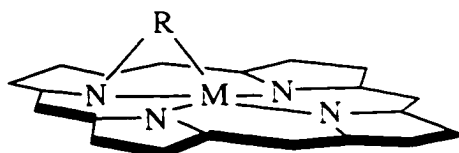
Chart 1



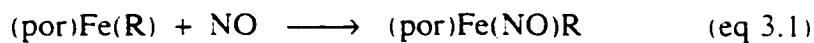
A



B

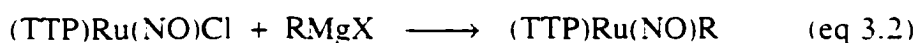


C



por = OEP, TPP; R = alkyl, aryl

In some cases, the known (por)Fe(NO) complexes are produced. Our research group recently reported the synthesis and characterization of analogous Ru complexes (Type **A**) via the reaction of the (TTP)Ru(NO)Cl precursors with Grignard reagents (eq 3.2).³¹



R = Me, *p*-C₆H₄F

The solid-state structure of (TTP)Ru(NO)(*p*-C₆H₄F) was also reported. Attempts were made to extend the reaction outlined in eq 3.2 to osmium porphyrins, but the desired organoosmium products were only obtained in very low (<5%) yields. Earlier work in our laboratory by Shelly Hodge revealed that the sequential reaction of (TTP)Os(CO) with NOPF₆, then (*p*-C₆H₄F)MgBr produced a compound formulated as (TTP)Os(NO)(*p*-C₆H₄F). We have since extended this finding to prepare isolable quantities of the desired (por)Os(NO)R (R = alkyl) complexes (Type **A**). The successful extension to the synthesis and structural characterization of osmium thionitrosyl porphyrins is also covered in this chapter.

Experimental Section

All reactions were performed under an atmosphere of prepurified nitrogen using standard Schlenk techniques and/or in an Innovative Technology Labmaster 100 Dry Box unless stated otherwise. All column chromatography was performed under nitrogen. Solvents were distilled from appropriate drying agents under nitrogen just prior to use: CH_2Cl_2 (CaH_2), THF (Na/benzophenone), hexane (Na/benzophenone/tetraglyme), and benzene (Na). Solutions for spectral studies were prepared under nitrogen and the spectra were recorded immediately.

Chemicals. $(\text{TTP})\text{Os}(\text{CO})$ and $(\text{OEP})\text{Os}(\text{CO})$ were prepared by literature methods.⁴² $(\text{NSCl})_3$ was prepared by the literature method.⁴³ The labeled (^{15}N) $(\text{NSCl})_3$ analog was prepared similarly using $^{15}\text{NH}_4\text{Cl}$ (Isotec). Nitrosyl chloride (ClNO) was prepared by the literature method.⁴⁴ NOPF_6 (96%) and all Grignard reagents used were purchased from Aldrich Chemical Co. Chloroform-*d* (99.8%) and benzene-*d*₆ (99.6%) were obtained from Cambridge Isotope Laboratories, subjected to three freeze-pump-thaw cycles and stored over Linde 4Å molecular sieves. Elemental analyses were performed by Atlantic Microlab, Norcross, GA.

Instrumentation. Infrared spectra were recorded on a Bio-Rad FT-155 FTIR spectrometer. ^1H NMR spectra were obtained either on a Varian XL-300 spectrometer or a Varian 400MHz spectrometer and the signals (in ppm) were referenced to the residual signals of the solvents employed. All couplings are in Hz. FAB mass spectra were obtained on a VG-ZAB-E mass spectrometer. UV-vis spectra were recorded on a Hewlett Packard Model 8452A diode array instrument.

Preparation of $(\text{OEP})\text{Os}(\text{NO})(\text{Me})$. To a CH_2Cl_2 (20 mL) solution of $(\text{OEP})\text{Os}(\text{CO})$ (0.060 g, 0.08 mmol) was added NOPF_6 (96%, 0.015 g, 0.082 mmol). The color of the solution changed from pink to dark red. The mixture was left to stir for 30 min. and all the solvent was removed. The solid was redissolved in THF (20 mL) and excess MeMgBr (0.7 mmol) was added. No substantial color change was

observed. The solvent was removed immediately after the addition of MeMgBr, and the residue was purified by filtration on a silica gel column with benzene as eluent. All the solvent was removed from the eluent, and the red solid was dried in vacuo for 5 h to give (OEP)Os(NO)(Me) (0.027 g, 0.035 mmol, 44% overall yield). IR (CH₂Cl₂, cm⁻¹): ν_{NO} = 1721. IR (KBr, cm⁻¹): ν_{NO} = 1732 s; also 2966 w, 2933 w, 2869 w, 1684 w, 1467 m, 1446 m, 1372 w, 1317 w, 1272 m, 1227 w, 1151 m, 1111 w, 1057 m, 1020 s, 994 m, 964 m, 838 m, 802 w, 745 m, 713 m, 518 w. ¹H NMR (CDCl₃, δ): 10.21 (s, 4H, *meso*-H of OEP), 4.12 (q, J = 8, 16H, CH₃CH₂ of OEP), 1.97 (t, J = 8, 24H, CH₃CH₂ of OEP), -8.10 (s, 3H, CH₃ of Me). Low-resolution mass spectrum (FAB): m/z 770 [(OEP)Os(NO)(Me) + H]⁺ (4%), 739 [(OEP)Os(CH₃)]⁺ (12%). UV-vis spectrum (λ (ϵ , mM⁻¹ cm⁻¹), 7.81 x 10⁻⁶ M in CH₂Cl₂): 351 (67), 445 (47), 552 (15), 584 (8) nm.

Preparation of (TTP)Os(NO)(Me). The (TTP)Os(NO)(Me) complex was prepared similarly in 35% overall yield from the sequential reaction of (TTP)Os(CO) with NOPF₆, then with excess MeMgCl as described above. IR (CH₂Cl₂, cm⁻¹): ν_{NO} = 1729. IR (KBr, cm⁻¹): ν_{NO} = 1732 m; also 1716 m, 1610 w, 1574 w, 1529 w, 1512 w, 1496 w, 1446 w, 1351 m, 1306 w, 1212 w, 1179 m, 1105 w, 1069 m, 1016 s, 796 s, 718 m, 525 m. ¹H NMR (CDCl₃, δ): 8.87 (s, 8H, *pyr*-H of TTP), 8.15 (d, J = 7, 4H, *o*-H of TTP), 8.06 (d, J = 8, 4H, *o'*-H of TTP), 7.55 (app t, J = 7/8, 8H, *m*-H of TTP), 2.70 (s, 12H, CH₃ of TTP), -7.35 (s, 3H, CH₃ of Me). UV-vis spectrum (λ (ϵ , mM⁻¹ cm⁻¹), 1.44 x 10⁻⁵ M in CH₂Cl₂): 345 (sh, 44), 361 (46), 408 (45), 454 (91), 573 (13), 616 (12) nm.

Preparation of (OEP)Os(NO)(*i*-Pr). (OEP)Os(NO)(*i*-Pr) was prepared similarly by the use of excess *i*-PrMgCl in 30% overall yield. The sample for elemental analysis was prepared by solvent evaporation of a CH₂Cl₂ solution of the compound and drying the residue in vacuo for two days. Anal. Calcd for C₃₉H₅₁N₅O₁Os₁·0.35CH₂Cl₂: C, 57.23; H, 6.31; N, 8.48; Cl, 3.01. Found: C, 57.34; H, 6.57; N,

7.73; Cl, 2.83. IR (CH₂Cl₂, cm⁻¹): $\nu_{\text{NO}} = 1703$. IR (KBr, cm⁻¹): $\nu_{\text{NO}} = 1715$ s; also 2965 w, 2928 w, 2868 w, 1700 m, 1684 w, 1609 m, 1534 w, 1464 m, 1446 m, 1372 m, 1316 w, 1273 s, 1218 m, 1151 s, 1110 w, 1056 m, 1019 s, 994 m, 962 s, 839 m, 803 m, 744 m, 713 m. ¹H NMR (CDCl₃, δ): 10.21 (s, 4H, *meso*-H of OEP), 5.28 (s, CH₂Cl₂), 4.12 (q, $J = 8$, 16H, CH₃CH₂ of OEP), 1.96 (t, $J = 8$, 24H, CH₃CH₂ of OEP), -4.63 (d, $J = 7$, 6H, (CH₃)₂CH of *i*-Pr), -7.12 (septet, $J = 7$, 1H, (CH₃)₂CH of *i*-Pr). Low-resolution mass spectrum (FAB): m/z 798 [(OEP)Os(NO)(*i*-Pr) + H]⁺ (6%), 767 [(OEP)Os(*i*-Pr)]⁺ (9%), 754 [(OEP)Os(NO)]⁺ (27%). UV-vis spectrum (λ (ε, mM⁻¹ cm⁻¹), 1.68 x 10⁻⁵ M in CH₂Cl₂): 359 (62), 446 (34), 552 (13), 582 (8) nm.

Preparation of a Mixture of (OEP)Os(NO)(Et) and (OEP)Os(Et)₂.

A 2:1 mixture of (OEP)Os(NO)(Et) and (OEP)Os(Et)₂ was produced similarly (using excess EtMgCl) in 39% overall yield. IR (CH₂Cl₂, cm⁻¹): $\nu_{\text{NO}} = 1710$. IR (KBr, cm⁻¹): $\nu_{\text{NO}} = 1716$ m. ¹H NMR (CDCl₃, δ) for (OEP)Os(NO)(Et): 10.21 (s, 4H, *meso*-H of OEP), 4.12 (q, $J = 8$, 16H, CH₃CH₂ of OEP), 1.96 (t, $J = 8$, 24H, CH₃CH₂ of OEP), -4.62 (t, $J = 8$, 3H, CH₃CH₂ of Et), -7.44 (q, $J = 8$, 2H, CH₃CH₂ of Et). Data for (OEP)Os(Et)₂: 9.23 (s, 4H, *meso*-H of OEP), 3.67 (q, $J = 8$, 16H, CH₃CH₂ of OEP), 1.73 (t, $J = 8$, 24H, CH₃CH₂ of OEP), -0.72 (q, $J = 7$, 4H, CH₃CH₂ of Et), -4.77 (t, $J = 7$, 6H, CH₃CH₂ of Et).

Preparation of (OEP)Os(NO)Cl and [(OEP)Os(NO)]₂(μ -O). To a CH₂Cl₂ (20 mL) solution of (OEP)Os(CO) (0.060 g, 0.080 mmol) was added ClNO (0.081 mmol in CH₂Cl₂) dropwise at room temperature. The reaction mixture was left to stir for 15 min. The color of the solution turned from pink red to bright red. The reaction mixture was transferred to the top of an alumina column and filtered using CH₂Cl₂ as eluent. The filtrate was collected and taken to dryness, and the red residue was dried in vacuo for 2 h to give (OEP)Os(NO)Cl (0.031 g, 0.039 mmol, 49% yield). The alumina column was then washed with THF, and a resulting second filtrate was collected. The solvent was removed, and the red residue was recrystallized from

CH_2Cl_2 (by slow solvent evaporation under nitrogen) to give $[(\text{OEP})\text{Os}(\text{NO})]_2(\mu\text{-O})$ (0.029 g, 0.019 mmol, 48% yield based on Os).

$(\text{OEP})\text{Os}(\text{NO})\text{Cl}$ and $[(\text{OEP})\text{Os}(\text{NO})]_2(\mu\text{-O})$ were also isolated and characterized independently from the reaction of crude $(\text{OEP})\text{Os}(\text{NO})(\text{PF}_6)$ with excess RMgCl by Dr. Lin Cheng of our research group.^{45a}

$(\text{OEP})\text{Os}(\text{NO})\text{Cl}$. IR (CH_2Cl_2 , cm^{-1}): $\nu_{\text{NO}} = 1799$. IR (KBr, cm^{-1}): $\nu_{\text{NO}} = 1788$ s. ^1H NMR (CDCl_3 , δ): 10.41 (s, 4H, *meso*-H of OEP), 4.16 (m, 16H, CH_3CH_2 of OEP), 2.02 (t, $J = 8$, 24H, CH_3CH_2 of OEP).

$[(\text{OEP})\text{Os}(\text{NO})]_2(\mu\text{-O})$. IR (CH_2Cl_2 , cm^{-1}): $\nu_{\text{NO}} = 1770$. IR (KBr, cm^{-1}): $\nu_{\text{NO}} = 1760$ s. ^1H NMR (CDCl_3 , δ): 10.35 (s, 4H, *meso*-H of OEP), 4.15 (m, 16H, CH_3CH_2 of OEP), 2.00 (t, $J = 8$, 24H, CH_3CH_2 of OEP).

Preparation of $(\text{OEP})\text{Os}(\text{NS})\text{Cl}$. To a THF (25 mL) solution of $(\text{OEP})\text{Os}(\text{CO})$ (0.060 g, 0.080 mmol) was added excess $(\text{NSCl})_3$ (0.014 g, 0.057 mmol). The mixture was heated to reflux for 30 min. The color of the solution changed from red to brown, then to green. The solvent was removed in vacuo, and the resulting green solid was purified by chromatography through neutral alumina with CH_2Cl_2 as eluent. The green fraction was collected, and all the solvent was removed. The resulting green solid was further purified by recrystallization from CH_2Cl_2 /hexane at -20 °C to give $(\text{OEP})\text{Os}(\text{NS})(\text{Cl})\cdot 0.9\text{CH}_2\text{Cl}_2$ (0.034 g, 0.039 mmol, 49% yield). Anal. Calcd for $\text{C}_{36}\text{H}_{44}\text{N}_5\text{Cl}_1\text{S}_1\text{Os}_1\cdot 0.9\text{CH}_2\text{Cl}_2$: C, 50.31; H, 5.24; N, 7.95; Cl, 11.27; S, 3.64. Found: C, 49.54; H, 5.13; N, 7.75; Cl, 10.84; S, 3.71. IR (KBr, cm^{-1}): $\nu_{\text{NS}} = 1270$ s; also 2967 w, 2930 w, 2869 w, 1470 m, 1444 m, 1372 w, 1362 w, 1317 w, 1226 w, 1152 s, 1111 m, 1054 m, 1020 s, 994 m, 963 m, 839 m, 744 s, 714 m. ^1H NMR (C_6D_6 , δ): 10.65 (s, 4H, *meso*-H of OEP), 4.26 (s, CH_2Cl_2), 4.00 (q, $J = 8$, 16H, CH_3CH_2 of OEP), 1.90 (t, $J = 8$, 24H, CH_3CH_2 of OEP). ^1H NMR (CDCl_3 , δ): 10.49 (s, 4H, *meso*-H), 5.28 (s, CH_2Cl_2), 4.20 (q, $J = 8$, 16H, CH_3CH_2 of OEP), 2.03 (t, $J = 8$, 24H, CH_3CH_2 of OEP). Low-resolution mass

spectrum (FAB): m/z 805 [(OEP)Os(NS)Cl]⁺ (58%), 770 [(OEP)Os(NS)]⁺ (53%). UV-vis spectrum (λ (ϵ , mM⁻¹ cm⁻¹), 1.24 x 10⁻⁵ M in CH₂Cl₂): 362 (75), 385 (sh, 63), 605 (6) nm.

A suitable crystal for structure determination was grown by slow evaporation of a CH₂Cl₂ solution of the compound in a dry box.

(OEP)Os(¹⁵NS)Cl. This compound was prepared (using (¹⁵NSCl)₃) by similar procedures as for the unlabeled analog. IR (KBr, cm⁻¹): $\nu_{15\text{NS}} = 1231$ s.

Preparation of a Mixture of (OEP)Os(NS)(Me) and (OEP)Os(Me)₂. To a THF (25 mL, heat to dissolve) solution of (OEP)Os(NS)Cl·0.9CH₂Cl₂ (0.032 g, 0.036 mmol) was added excess MeMgBr (0.28 mmol). The color of the solution changed from green to red brown. All the solvent was removed immediately after the addition of MeMgBr was complete, and the residue was purified by chromatography through silica gel with benzene as eluent. A red brown fraction was collected, all the solvent was removed in vacuo, and the red brown solid was dried in vacuo for 3 h to give a mixture of (OEP)Os(NS)(Me) (ca. 59%) and (OEP)Os(Me)₂ (ca. 41%) (0.013 g, 0.017 mmol, 47% overall yield). IR (KBr, cm⁻¹): $\nu_{\text{NS}} = 1194$ m. ¹H NMR (CDCl₃, δ) data for (OEP)Os(NS)(Me): 10.30 (s, 4H, *meso*-H of OEP), 4.14 (m, 16H, CH₃CH₂ of OEP), 1.97 (t, $J = 8$, 24H, CH₃CH₂ of OEP), -7.88 (s, 3H, CH₃ of Me). Data for (OEP)Os(Me)₂: 9.34 (s, 4H, *meso*-H of OEP), 3.70 (q, 16H, $J = 8$, CH₃CH₂ of OEP), 1.75 (t, $J = 8$, 24H, CH₃CH₂ of OEP), -1.16 (s, 6H, CH₃ of Me).

A suitable crystal of (OEP)Os(NS)(Me) for structure determination was grown by slow evaporation of a CH₂Cl₂ solution of the above mixture under nitrogen.

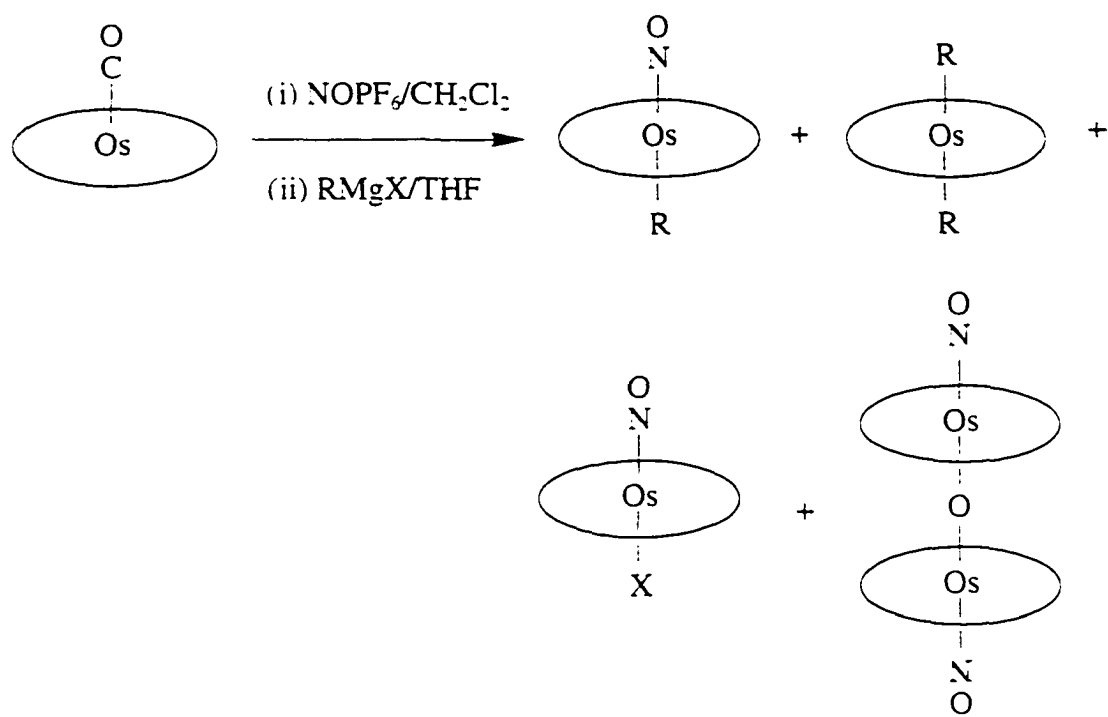
(OEP)Os(¹⁵NS)(Me). This compound was prepared similarly as the unlabeled analog. IR (KBr, cm⁻¹): $\nu_{15\text{NS}} = 1163$.

Results and Discussion

Synthesis and Characterization of Organoosmium Nitrosyl Porphyrin Complexes. Reactions of (por)Os(CO) (por = OEP, TTP) with NOPF₆ in CH₂Cl₂ generate the [(por)Os(NO)](PF₆) compounds. Some of the (por)Os(NO)(PF₆) compounds undergo fluorine extraction from the PF₆ anion unit to give (por)Os(NO)(F).⁴⁵ In any event, the reactions of crude [(por)Os(NO)](PF₆) with excess Grignard reagents (RMgX) at room temperature result in the formation of (por)Os(NO)R (R = Me for TTP; R = Me, *i*-Pr for OEP) in low to moderate overall yield (from 30% to 44%).⁴⁶ The related reaction of (OEP)Os(NO)((PF₆) with excess EtMgCl generates an isolable 2:1 mixture of (OEP)Os(NO)(Et) and (OEP)Os(Et)₂ in 39% yield. In general, the reaction conditions are very critical in obtaining pure samples of the (por)Os(NO)R compounds. The use of excess RMgX is necessary, since the reactions of crude (por)Os(NO)(PF₆) with one equivalent of RMgX are very slow, and a shorter reaction time (with excess Grignard reagent) favors the formation of (por)Os(NO)R, whereas a longer reaction time (with or without excess Grignard reagent) results in the decomposition of the nitrosyl alkyl product and the formation of the following by-products: (por)Os(NO)X (X = halide), (por)Os(R)₂ and the μ -oxo [(OEP)Os(NO)]₂(μ -O) dimer (Scheme 3.1). This partly explains the low yield we experienced in the synthesis of the organoosmium(II) nitrosyl porphyrin complexes. Dr. Lin Cheng of our research group has since performed some follow-up work and has succeeded in isolating these four products in low to moderate yields.^{45a} Interestingly, the same μ -oxo [(OEP)Os(NO)]₂(μ -O) dimer is generated from the reaction of (OEP)Os(CO) with one equivalent of ClNO (see later).

The (TTP)Os(NO)(Me) complex is green. However, all the (OEP)Os(NO)R complexes are red. All these organoosmium nitrosyl complexes are moderately air stable in solid state. They are all freely soluble in CH₂Cl₂ and benzene but are only slightly soluble in hexane. These compounds are generally characterized by ¹H NMR.

Scheme 3.1



IR, UV-vis spectroscopy, and by mass spectrometry. The (OEP)Os(NO)(*i*-Pr) compound has also been characterized by elemental analysis. ¹H NMR spectra of these (por)Os(NO)R complexes in CDCl₃ show the expected sharp peaks for the porphyrin macrocycles and the alkyl groups, consistent with the diamagnetic nature of the products. The ν_{NO} 's of the products are lower than the ν_{NO} 's of the corresponding osmium nitrosyl alkoxide and thiolate porphyrin complexes (chapter 1). The UV-vis spectra of (OEP)Os(NO)(Me) and (OEP)Os(NO)(*i*-Pr) are quite similar and are also similar to those of other (OEP)Os(NO)R complexes.^{45a} The IR ν_{NO} 's and ¹H NMR δ_{meso} and δ_{axial} data are listed in Table 3.1.

The greater π -accepting ability of the TTP macrocycle relative to the OEP macrocycle is reflected in (i) the higher ν_{NO} (in CH₂Cl₂ solution, due to less backbonding from Os^{II} to NO ligand) for (TTP)Os(NO)(Me) compared with (OEP)Os(NO)(Me), and (ii) a resulting downfield shift of the δ_{Me} for (TTP)Os(NO)(Me) (-7.35 ppm) relative to that of (OEP)Os(NO)(Me) (-8.10 ppm).

Buchler has demonstrated that the δ_{meso} 's in the ¹H NMR spectra of (OEP)Os complexes can be used to measure the relative extent of metal→OEP backbonding.⁴⁸ In general, a stronger metal→OEP backbonding will result in an upfield shift of δ_{meso} . The extent of Os→OEP backbonding is also determined, to some extent, by the electron donating/withdrawing properties of the axial ligands in (OEP)Os-containing complexes.

The ν_{NO} 's of the (OEP)Os(NO)R complexes in CH₂Cl₂ solution follow the trend: (OEP)Os(NO)(*i*-Pr) (1703 cm⁻¹) < (OEP)Os(NO)(Et) (1710 cm⁻¹) < (OEP)Os(NO)(Me) (1721 cm⁻¹), consistent with the increase in electron donating ability of the R groups. The insignificant changes in δ_{meso} in the ¹H NMR spectra of these compounds reflect the fact that the push-pull effect of the NO/alkyl pair leaves the electron density at the Os center in these (OEP)Os(NO)R complexes essentially unchanged. Thus, changing the alkyl group in the (OEP)Os(NO)R complexes from Me

Table 3.1. Selected Spectral Data for (OEP)Os(NE)X (E = O, S) and Related Compounds

compound	¹ H NMR (CDCl ₃ , ppm)		IR (cm ⁻¹)	
	δ _{meso}	δ _{axial}	ν _{NO} , CH ₂ Cl ₂	ν _{NS} , KBr
(TTP)Os(NO)(Me)	8.87	-7.35 (CH ₃)	1729	
	(pyr-H)			
(OEP)Os(NO)(Me)	10.21	-8.10 (CH ₃)	1721	
(OEP)Os(NO)(Et)	10.21	-7.44 (CH ₂ CH ₃) -4.62 (CH ₂ CH ₃)	1710	
(OEP)Os(NO)(<i>i</i> -Pr)	10.21	-7.12 (CH(CH ₃) ₂) -4.63 (CH(CH ₃) ₂)	1703	--
(OEP)Os(NO)Cl	10.41	--	1799	
[(OEP)Os(NO)] ₂ (μ-O)	10.35		1770	
(OEP)Os(NS)Cl	10.49	--	--	1270 (1231) ^a
(OEP)Os(NS)(Me)	10.30	-7.88 (CH ₃)	--	1194 (1163) ^a
(OEP)Os(Me) ₂	9.34	-1.16 (CH ₃)	--	--
(OEP)Os(Et) ₂	9.23	-4.77 (CH ₂ CH ₃) -0.72 (CH ₂ CH ₃)	--	--

^a ¹⁵N-labeled data are in brackets.

to Et to *i*-Pr results in a transmission of the electron-density change completely to the *trans* NO ligand, shifting ν_{NO} to lower wavenumbers, but not affecting δ_{meso} to any significant extent.

Both the δ_{meso} peaks in (OEP)Os(NO)(Me) and (OEP)Os(NO)(Et) are shifted dramatically downfield relative to these of the non-nitrosyl (OEP)Os(Me)₂ ($\Delta\delta_{\text{meso}} = 0.87$ ppm) and (OEP)Os(Et)₂ ($\Delta\delta_{\text{meso}} = 0.98$ ppm). This is consistent with the NO ligand acting as a strong π -acid to withdraw electron density from the Os^{II} center, resulting in less backbonding from Os^{II}→OEP, causing the downfield shift of the δ_{meso} 's for (OEP)Os(NO)(Me) and (OEP)Os(NO)(Et). The δ_{meso} for (OEP)Os(Et)₂ is 0.12 ppm upfield relative to that of (OEP)Os(Me)₂, consistent with the Et group acting as a better σ -donor relative to the Me group, causing stronger Os→OEP backbonding.

Synthesis and Characterization of Osmium Nitrosyl Porphyrin Chloro and μ -Oxo Dimer Complexes. The reaction of (OEP)Os(CO) with one equivalent of ClNO generates (OEP)Os(NO)Cl in 49% yield. To the best of our knowledge, the (OEP)Os(NO)Cl has not been reported previously in the literature, although the (OEP)Os(NO)F complex has been known for over 20 years.^{49,50} The (OEP)Os(NO)Cl complex is air-stable, showing no signs of decomposition in solution in air overnight. IR spectrum of (OEP)Os(NO)Cl in CH₂Cl₂ shows a band at 1799 cm⁻¹ which is assigned as the ν_{NO} of the complex. This ν_{NO} value is higher than those of the (OEP)Os(NO)R complexes described earlier (1703–1729 cm⁻¹). The δ_{meso} value in the ¹H NMR spectrum of (OEP)Os(NO)Cl in CDCl₃ is downfield with respect to those of the (OEP)Os(NO)R complexes (10.21 ppm, Table 3.1).

Surprisingly, a second product from the reaction of (OEP)Os(CO) with ClNO is the μ -oxo [(OEP)Os(NO)]₂(μ -O) dimer which is obtained in 48% yield. This same μ -oxo dimer can also be obtained in smaller yields via the reaction of crude [(OEP)Os(NO)](PF₆) with Grignard reagents.^{45a} IR spectrum of [(OEP)Os(NO)]₂(μ -O) in CH₂Cl₂ shows a peak at 1770 cm⁻¹ which is assigned as ν_{NO} . This ν_{NO} value is

lower than that of (OEP)Os(NO)Cl (1799 cm⁻¹), but is much higher than those of the (OEP)Os(NO)R complexes (1703–1729 cm⁻¹). It is slightly higher than those of (OEP)Os(NO)(O-*n*-C₄H₉) (1757 cm⁻¹) and (OEP)Os(NO)(O-*i*-C₅H₁₁) (1756 cm⁻¹), but is lower than those of (OEP)Os(NO)(O₂PF₂) (1820 cm⁻¹), all of which contain axial O-bound ligands *trans* to NO (chapter 1). The δ_{meso} peak is at 10.35 ppm, which is in-between those of (OEP)Os(NO)Cl (10.41 ppm) and the (OEP)Os(NO)R complexes (10.21 ppm, Table 3.1).

The identity of [(OEP)Os(NO)]₂(μ -O) was confirmed by single-crystal X-ray diffraction. The molecular structure of [(OEP)Os(NO)]₂(μ -O) is shown in Figure 3.1. To the best of our knowledge, this is the first reported example of a nitrosyl porphyrin μ -oxo dimer of any metal. Selected bond lengths and bond angles are listed in Tables 3.2 and 3.3. The Os–N(por) bond length of 2.066(5) Å is within the range found for other structurally characterized (OEP)Os^{II} complexes (Table 2.3). The Os–NO linkage is linear. The Os–N(O) (1.778(11) Å) and the N–O (1.143(13) Å) bond lengths for [(OEP)Os(NO)]₂(μ -O) are typical for osmium nitrosyl complexes with linear Os–NO linkage (Table 1.3). The Os–(μ -O)–Os linkage is also linear, similar to other group 8 oxo-bridged dimers. The Os–(μ -O) bond length, however, is longer than those for the structurally characterized Ru^{IV} and Os^{IV} porphyrin μ -oxo dimer complexes (Table 3.4).

The porphyrin core is domed, and the Os atom is displaced 0.23 Å from the 24-atom mean plane towards the axial nitrosyl ligand (Figure 3.1a). This observation is remarkable, since a common feature of porphyrin μ -oxo dimers is the displacement of the metal towards the μ -oxo ligand.⁶⁶ For example, the Os atom is displaced 0.07 Å from the 24-atom porphyrin core towards the μ -oxo ligand in the only other structurally characterized osmium porphyrin μ -oxo complex, namely [(OEP)Os(OCH₃)]₂(μ -O).^{51,65} The two porphyrin rings of [(OEP)Os(NO)]₂(μ -O) display a twist angle of 22.5° with respect to each other (Figure 3.1b).

Table 3.2. Selected Bond Lengths (Å) for [(OEP)Os(NO)]₂(μ-O)

Os(1)-N(2)	1.778(11)	O(1)-N(2)	1.143(13)
Os(1)-O(2)	2.0945(5)	O(2)-Os(2)	2.0945(5)
Os(1)-N(1)	2.066(5)	Os(1)-N(1A)	2.066(5)
Os(1)-N(1B)	2.066(5)	Os(1)-N(1C)	2.066(5)
N(1)-C(4)	1.346(8)	N(1)-C(1)	1.382(8)
C(1)-C(5)B	1.372(10)	C(1)-C(2)	1.456(9)
C(2)-C(3)	1.342(10)	C(3)-C(4)	1.454(10)
C(4)-C(5)	1.409(9)	C(5)-C(1)C	1.372(10)

Table 3.3. Selected Bond Angles (°) for [(OEP)Os(NO)]₂(μ-O)

O(1)-N(2)-Os(1)	180.000(1)	Os(1)-O(2)-Os(2)	180.0
N(2)-Os(1)-O(2)	180.0	N(1)-Os(1)-O(2)	85.8(2)
N(1A)-Os(1)-O(2)	85.8(2)	N(1B)-Os(1)-O(2)	85.8(2)
N(1C)-Os(1)-O(2)	85.8(2)	N(2)-Os(1)-N(1)	94.2(2)
N(2)-Os(1)-N(1A)	94.2(2)	N(2)-Os(1)-N(1B)	94.2(2)
N(2)-Os(1)-N(1C)	94.2(2)	N(1A)-Os(1)-N(1B)	89.70(2)
N(1A)-Os(1)-N(1C)	89.70(2)	N(1B)-Os(1)-N(1C)	171.6(3)
N(1A)-Os(1)-N(1)	171.6(3)	N(1B)-Os(1)-N(1)	89.70(2)
N(1C)-Os(1)-N(1)	89.69(2)	C(4)-N(1)-C(1)	107.9(6)
C(4)-N(1)-Os(1)	126.1(4)	C(1)-N(1)-Os(1)	126.0(4)
C(5)B-C(1)-N(1)	125.2(6)	C(5)B-C(1)-C(2)	126.5(6)
N(1)-C(1)-C(2)	108.2(6)	C(3)-C(2)-C(1)	107.2(6)
C(2)-C(3)-C(4)	107.3(6)	N(1)-C(4)-C(5)	125.9(6)
N(1)-C(4)-C(3)	109.4(6)	C(5)-C(4)-C(3)	124.6(6)
C(1)C-C(5)-C(4)	126.9(6)		

Table 3.4. Structural Parameters (in Å and °) for Group 8 Oxo-Bridged Dimers

compound	M-(μ -O)	M-O-M	reference
<i>Iron</i>			
[(OEP)Fe] ₂ (μ -O) triclinic	1.758(3)	172.2(2)	51
	1.754(3)		
	monoclinic	1.748(4)	176.21(23)
		1.762(4)	
[(TPP)Fe] ₂ (μ -O)	1.759(1)	176.1	52
[(T(<i>p</i> -Cl)PP) ₂ (μ -O)	1.743(3)	180.0	53
[(OEP)(NO ₂) ₂ Fe] ₂ (μ -O)	1.763(4)	167.9(3)	54
	1.751(4)		
[(T(F ₅)PP)Fe] ₂ (μ -O)	1.775(1)	178.4(5)	55
[(Me ₂ OEP)Fe] ₂ (μ -O)	1.752(1)	178.5(6)	56
[(TPC)Fe] ₂ (μ -O) ^a	1.747(5)	180.0	57
	1.763(5)		
[(T(<i>o</i> -F ₂)PP)Fe] ₂ (μ -O)	1.760(2)	178.5(8)	58
[(FF)Fe] ₂ (μ -O) ^b	1.800(6)	161.1(4)	59
	1.774(6)		
[(TMPyP)Fe] ₂ (μ -O)·(ClO ₄) ₈	1.750(2)	175.1(7)	60
[(<i>N</i> -CH ₃ TPP)Fe-O-Fe(TPP)]ClO ₄	1.740(4)	165.4(3)	61
	1.767(4)-TPP		
<i>Ruthenium</i>			
[(OEP)Ru(OH)] ₂ (μ -O)	1.847(13)	180.0	62
[(OEP)Ru(Cl)] ₂ (μ -O)	1.793(2)	180.0	63
[(TPP)Ru(<i>p</i> -OC ₆ H ₄ Me)] ₂ (μ -O)	1.787(11)	177.8(7)	64
	1.791(11)		
<i>Osmium</i>			
[(OEP)Os(OCH ₃)] ₂ (μ -O)	1.807(3)	177.4(17)	65
	[1.809(3)] ^c	[179.5(11)] ^c	
[(OEP)Os(NO)] ₂ (μ -O)	2.0945(5)	180.0	this work

^a TPC = tetraphenylchlorinato dianion. ^b FF = Face-to-face porphyrin. *N,N*-Bis(5-*o*-phenyl)-10.15.20-triphenylporphyrin urea. ^c Two independent dimers. The values for the second dimer are in brackets.

Synthesis and Characterization of Osmium Thionitrosyl Porphyrin Chloro and Methyl Complexes. Shelly Hodge of our research group prepared the related (TTP)Os(NS)Cl complex.^{45b} The related (TTP)Ru(NS)Cl has also been reported,⁶⁷ and the (TPP)Fe(NS) compound has been claimed.⁴¹ To the best of our knowledge, no thionitrosyl organoosmium porphyrin complexes has been reported.

The reaction of (OEP)Os(CO) with excess (NSCl)₃ in refluxing THF gives, after workup, (OEP)Os(NS)Cl in 49% isolated yield. The green product is moderately air-stable and can be handled in air in solution for short periods. The product is fairly soluble in CH₂Cl₂, moderately soluble in THF, poorly soluble in benzene and only slightly soluble in hexane. The ¹H NMR spectra of (OEP)Os(NS)Cl in both C₆D₆ and CDCl₃ give the expected sharp peaks for the OEP macrocycle, indicating the diamagnetic nature of this Os^{II} complex. The δ_{meso} in the ¹H NMR spectrum of (OEP)Os(NS)Cl in CDCl₃ is at 10.49 ppm, which is downfield from that of (OEP)Os(NO)Cl at 10.41 ppm. The IR spectrum (as a KBr pellet) shows a strong band at 1270 cm⁻¹ which is assigned as ν_{NS} of the product. This value is within the 1065–1390 cm⁻¹ range observed for other thionitrosyl compounds with linear Metal–NS linkages.⁶⁸ This assigned ν_{NS} band shifts to 1231 cm⁻¹ when (¹⁵NSCl)₃ is employed in the reaction, confirming the assignment of the band. The FAB mass spectrum shows the presence of the parent ion [(OEP)Os(NS)Cl]⁺, further confirming the identity of the product. The UV–vis spectrum in CH₂Cl₂ gives three bands at 362 (75), 385 (sh, 63), 605 (6) nm. The identity of the product is also confirmed by a single-crystal X-ray crystallographic analysis. The molecular structure of (OEP)Os(NS)Cl is shown in Figure 3.2. Selected bond lengths and bond angles are listed in Tables 3.5 and 3.6.

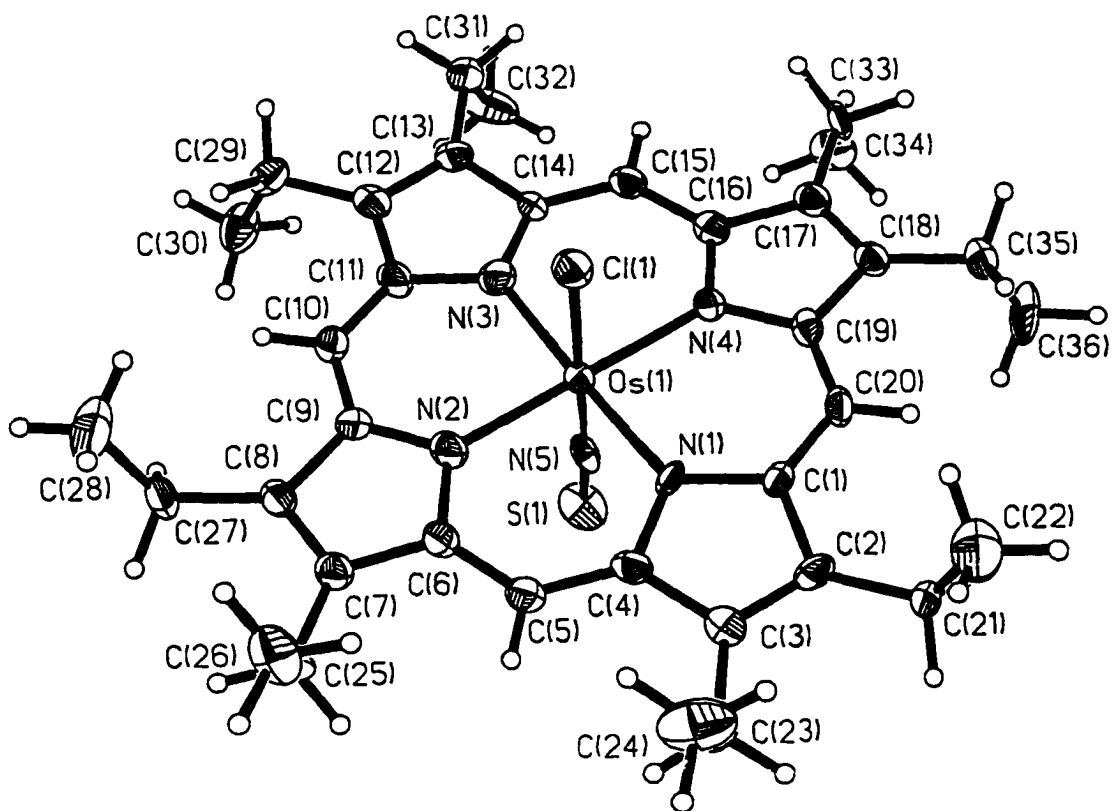


Figure 3.2. Molecular structure of (OEP)Os(NS)(Cl) (only one of the disordered NS/Cl orientations is shown).

Table 3.5. Selected Bond Lengths (Å) for (OEP)Os(NS)Cl

Cl(1)-Os(1)	2.329(3)	Os(1)-N(5)	1.832(13)
Cl(1')-Os(1)	2.327(4)	Os(1)-N(5')	1.834(13)
N(5)-S(1)	1.501(12)	N(5')-S(1')	1.502(12)
Os(1)-N(1)	2.050(7)	Os(1)-N(2)	2.072(6)
Os(1)-N(4)	2.063(5)	Os(1)-N(3)	2.075(9)
N(1)-C(1)	1.374(11)	N(1)-C(4)	1.396(10)
C(1)-C(20)	1.372(11)	C(1)-C(2)	1.481(11)
C(2)-C(3)	1.353(10)	C(3)-C(4)	1.463(10)
C(4)-C(5)	1.394(10)	C(5)-C(6)	1.405(10)
N(2)-C(9)	1.364(9)	N(2)-C(6)	1.366(9)
C(6)-C(7)	1.413(9)	C(7)-C(8)	1.377(11)
C(8)-C(9)	1.454(10)	C(9)-C(10)	1.396(10)
C(10)-C(11)	1.354(12)	N(3)-C(14)	1.352(11)
N(3)-C(11)	1.404(12)	C(11)-C(12)	1.443(13)
C(12)-C(13)	1.376(10)	C(13)-C(14)	1.461(10)
C(14)-C(15)	1.383(10)	C(15)-C(16)	1.400(11)
N(4)-C(16)	1.337(9)	N(4)-C(19)	1.378(9)

Table 3.6. Selected Bond Angles (°) for (OEP)Os(NS)Cl

S(1)-N(5)-Os(1)	174.5(14)	S(1')-N(5')-Os(1)	174(2)
N(5)-Os(1)-Cl(1)	177.7(7)	N(5')-Os(1)-Cl(1')	176.4(10)
N(5)-Os(1)-N(1)	92.1(6)	N(5')-Os(1)-N(1)	84.2(12)
N(5)-Os(1)-N(2)	91.6(7)	N(5')-Os(1)-N(2)	88(2)
N(5)-Os(1)-N(3)	91.6(7)	N(5')-Os(1)-N(3)	92.1(11)
N(5)-Os(1)-N(4)	92.1(7)	N(5')-Os(1)-N(4)	88(2)

N(1)-Os(1)-Cl(1)	89.7(3)	N(1)-Os(1)-Cl(1')	92.4(7)
N(2)-Os(1)-Cl(1)	90.0(2)	N(2)-Os(1)-Cl(1')	90.4(8)
N(3)-Os(1)-Cl(1)	86.7(2)	N(3)-Os(1)-Cl(1')	91.2(7)
N(4)-Os(1)-Cl(1)	86.4(2)	N(4)-Os(1)-Cl(1')	93.3(8)
N(1)-Os(1)-N(4)	89.8(2)	N(1)-Os(1)-N(2)	90.2(3)
N(1)-Os(1)-N(3)	176.3(4)	N(4)-Os(1)-N(2)	176.4(2)
N(4)-Os(1)-N(3)	89.6(3)	N(2)-Os(1)-N(3)	90.2(3)
C(1)-N(1)-C(4)	107.7(7)	C(1)-N(1)-Os(1)	127.0(6)
C(4)-N(1)-Os(1)	125.3(5)	C(20)-C(1)-N(1)	124.7(8)
C(20)-C(1)-C(2)	126.7(8)	N(1)-C(1)-C(2)	108.6(7)
C(3)-C(2)-C(1)	107.5(6)	C(2)-C(3)-C(4)	107.4(6)
C(5)-C(4)-N(1)	126.0(7)	C(5)-C(4)-C(3)	125.2(6)
N(1)-C(4)-C(3)	108.9(6)	C(4)-C(5)-C(6)	126.9(7)
C(9)-N(2)-C(6)	107.6(6)	C(9)-N(2)-Os(1)	125.3(5)
C(6)-N(2)-Os(1)	126.9(5)	N(2)-C(6)-C(5)	124.5(6)
N(2)-C(6)-C(7)	110.2(6)	C(5)-C(6)-C(7)	125.3(7)
C(8)-C(7)-C(6)	107.2(6)	C(7)-C(8)-C(9)	106.3(6)
N(2)-C(9)-C(10)	125.9(6)	N(2)-C(9)-C(8)	108.7(6)
C(10)-C(9)-C(8)	125.4(6)	C(11)-C(10)-C(9)	128.2(8)
C(14)-N(3)-C(11)	109.3(8)	C(14)-N(3)-Os(1)	125.5(6)
C(11)-N(3)-Os(1)	125.1(7)	C(10)-C(11)-N(3)	125.2(10)
C(10)-C(11)-C(12)	128.3(9)	N(3)-C(11)-C(12)	106.5(8)
C(13)-C(12)-C(11)	109.1(7)	C(12)-C(13)-C(14)	105.9(6)
N(3)-C(14)-C(15)	126.1(7)	N(3)-C(14)-C(13)	109.1(6)
C(16)-N(4)-C(19)	108.5(6)	C(16)-N(4)-Os(1)	126.4(5)
C(19)-N(4)-Os(1)	125.1(5)	N(4)-C(16)-C(15)	125.8(6)
N(4)-C(16)-C(17)	109.5(7)	C(15)-C(16)-C(17)	124.7(6)
N(4)-C(19)-C(20)	126.0(6)	N(4)-C(19)-C(18)	108.6(6)

Table 3.7. Selected Structural Data for Osmium and Ruthenium Thionitrosyl Complexes

Compound	M-N (Å)	N-S (Å)	M-N-S (°)	ref
<i>Osmium</i>				
(OEP)Os(NS)Cl	1.832(13)	1.501(12)	174.5(14)	this work
	1.834(13)	1.502(12)	174(2)	
(OEP)Os(NS)(Me)	1.999(8)	1.433(13)	163.0(8)	this work
(OEP)Os(NS)(O ₂ PF ₂)	1.960(8)	1.520(9)	170.9(7)	chapter 1
Os(NS)Cl ₃ (PPh ₃) ₂	1.779(9)	1.503(10)	180.0(1)	69
(PPh ₄)[Os(NS)Cl ₄ (H ₂ O)]	1.731(4)	1.514(5)	174.9(3)	70
(AsPh ₄)[Os(NS)(NSCl)Cl ₄] ^a	1.828(8)	1.46(1)	169.1(5)	71
<i>Ruthenium</i>				
(PPh ₄)[Ru(NS)Cl ₄ (H ₂ O)]	1.729(4)	1.504(4)	170.9(3)	72
(PPh ₄) ₂ [Ru(NS)Cl ₄] ₂ ·4CH ₂ Cl ₂	1.752(6)	1.466(7)	177.3(5)	73
(PPh ₄)[{Ru(NS)Br ₄] ₂ (μ-N ₂ S ₂)]·4CH ₂ X ₂ ^b	1.69(3)	1.51(3)	175(2)	74
(TTP)Ru(NS)Cl ^c	1.768(4)	1.489(5)	169.1(3)	67
	[1.85(3)]	[1.47(3)]	[170(3)]	

^a The Cl atom of NSCl is disordered over the NS and NSCl ligands. ^b Contains CH₂Cl₂ and CH₂Br₂ molecules (i.e., X = Cl, Br). ^c Two independent molecules. Data for the second (disordered) molecule are in brackets.

The average Os–N(por) bond length is 2.065 Å, and falls within the range observed for other structurally characterized (OEP)Os^{II} complexes (Table 2.3). The NS and Cl fragments are disordered. The Os–N(S) and (Os)N–S bond lengths of 1.83(1) and 1.50(1) Å are comparable with those of other structurally characterized Os–NS complexes (Table 3.7). The Os–N–S linkage is linear, as indicated by an Os–N–S bond angle of 174°.

Reaction of (OEP)Os(NS)Cl with excess MeMgBr results in the formation of an air-sensitive 3:2 mixture of (OEP)Os(NS)(Me) and (OEP)Os(Me)₂ in 47% yield. As with the nitrosyl derivatives, formation of (OEP)Os(NS)(Me) is favored over (OEP)Os(Me)₂ with a shorter reaction time by employing excess Grignard reagent. This reaction is very slow at room temperature even with excess Grignard reagent. The ¹H NMR spectrum of the mixture clearly indicates the presence of the expected peaks for the two diamagnetic compounds. The IR spectrum (as a KBr pellet) of the mixture shows a medium band at 1194 cm⁻¹ which is assigned as the ν_{NS} of (OEP)Os(NS)(Me). The mixture of (OEP)Os(¹⁵NS)(Me) and (OEP)Os(Me)₂ was prepared similarly by employing (OEP)Os(¹⁵NS)Cl. The IR band at 1194 cm⁻¹ shifts to 1163 cm⁻¹, confirming the assignment of the ν_{NS} band for (OEP)Os(NS)(Me). The δ_{meso} peak in the ¹H NMR spectrum of (OEP)Os(NS)(Me) (10.30 ppm) in CDCl₃ is shifted downfield from that of its nitrosyl analog (OEP)Os(NO)(Me) (10.21 ppm). Similar to the nitrosyl analogs, the ν_{NS} is higher for (OEP)Os(NS)Cl and its δ_{meso} peak is shifted downfield compared to (OEP)Os(NS)(Me) (Table 3.1). The δ_{meso} peak of (OEP)Os(NS)(Me) is also dramatically shifted downfield ($\Delta\delta_{\text{meso}} = 0.96$ ppm) relative to that of (OEP)Os(Me)₂. Similarly, the lower electron density at the Os center of the (OEP)Os(NS)(Me) complex is caused by the π -acid character of the NS ligand. The lower electron density at the Os center of (OEP)Os(NS)(Me) in turn causes less Os^{II}→OEP backbonding, resulting in the downfield shift of δ_{meso} . Attempts at generating other (OEP)Os(NS)R complexes have so far not been successful.

The molecular structure of (OEP)Os(NS)(Me) is shown in Figure 3.3. Selected bond lengths and bond angles are listed in Tables 3.8 and 3.9. The most important feature is the confirmation of the identity of the *trans* methyl and thionitrosyl ligands. The axial methyl and NS groups are disordered. Because of the nature of disorder of the axial ligands, a meaningful comparison of bond lengths and bond angles involving these axial groups is not possible. The Os–N(por) bond lengths of 2.056(7) and 2.055(7) Å are, however, within the range observed for other structurally characterized (OEP)Os^{II} complexes (Table 2.3).

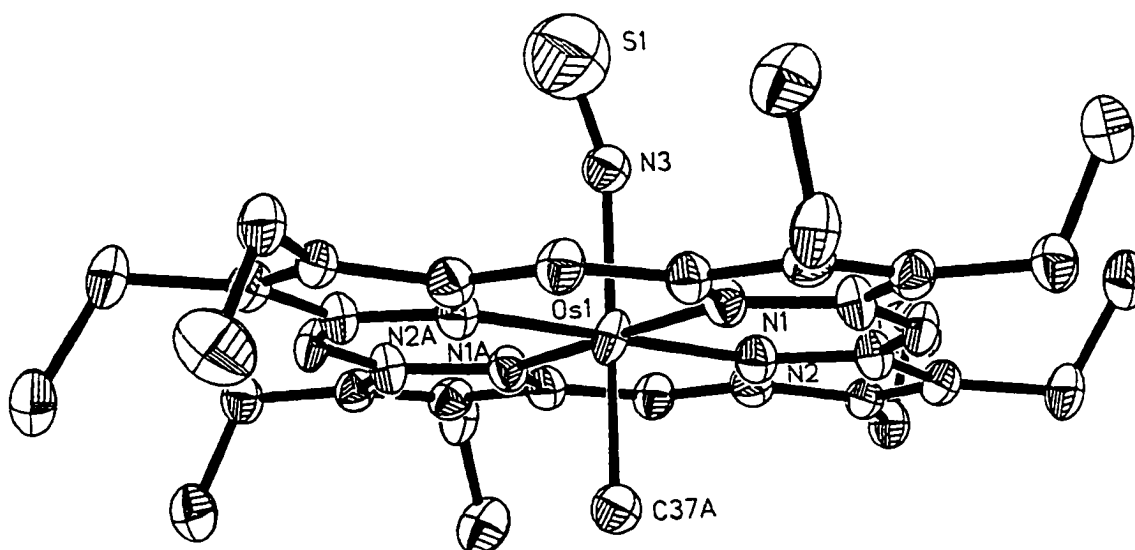


Figure 3.3. Molecular structure of (OEP)Os(NS)(Me) (only one of the disordered NS/Me orientations is shown).

Table 3.8. Selected Bond Lengths (Å) for (OEP)Os(NS)(Me)

Os(1)-C(37)A	1.999(8)	Os(1)-N(3)	1.999(8)
N(3)-S(1)	1.433(13)	Os(1)-N(2)	2.055(7)
Os(1)-N(2)A	2.055(7)	Os(1)-N(1)	2.056(7)
Os(1)-N(1)A	2.056(7)	N(1)-C(1)	1.372(11)
N(1)-C(4)	1.382(11)	N(2)-C(9)	1.367(12)
N(2)-C(6)	1.377(11)	C(1)-C(10)A	1.385(13)
C(1)-C(2)	1.446(12)	C(2)-C(3)	1.375(13)
C(3)-C(4)	1.450(12)	C(4)-C(5)	1.389(13)
C(5)-C(6)	1.388(13)	C(6)-C(7)	1.455(12)
C(7)-C(8)	1.379(13)	C(8)-C(9)	1.450(12)
C(9)-C(10)	1.400(13)	C(10)-C(1)A	1.385(13)

Table 3.9. Selected Bond Angles ($^{\circ}$) for (OEP)Os(NS) μ Me

S(1)-N(3)-Os(1)	163.0(8)	C(37)A-Os(1)-N(3)	180.0
C(37)A-Os(1)-N(2)	89.6(3)	C(37)A-Os(1)-N(1)	88.5(3)
C(37)A-Os(1)-N(1)A	91.5(3)	C(37)A-Os(1)-N(2)A	90.4(3)
N(3)-Os(1)-N(1)	91.5(3)	N(3)-Os(1)-N(1)A	88.5(3)
N(3)-Os(1)-N(2)	90.4(3)	N(3)-Os(1)-N(2)A	89.6(3)
N(2)-Os(1)-N(2)A	180.0	N(2)-Os(1)-N(1)A	89.6(3)
N(2)A-Os(1)-N(1)A	90.4(3)	N(2)-Os(1)-N(1)	90.4(3)
N(2)A-Os(1)-N(1)	89.6(3)	N(1)A-Os(1)-N(1)	180.0
C(1)-N(1)-C(4)	107.4(7)	C(1)-N(1)-Os(1)	126.6(6)
C(4)-N(1)-Os(1)	126.0(6)	C(9)-N(2)-C(6)	107.3(7)
C(9)-N(2)-Os(1)	126.6(6)	C(6)-N(2)-Os(1)	126.0(6)
N(1)-C(1)-C(10)A	125.1(8)	N(1)-C(1)-C(2)	109.2(8)
C(10)A-C(1)-C(2)	125.7(8)	C(3)-C(2)-C(1)	107.5(8)
C(2)-C(3)-C(4)	106.4(8)	N(1)-C(4)-C(5)	124.9(8)
N(1)-C(4)-C(3)	109.4(8)	C(5)-C(4)-C(3)	125.6(8)
C(4)-C(5)-C(6)	127.7(8)	N(2)-C(6)-C(5)	125.1(8)
N(2)-C(6)-C(7)	109.3(8)	C(5)-C(6)-C(7)	125.6(8)
C(8)-C(7)-C(6)	106.7(8)	C(7)-C(8)-C(9)	106.5(7)
N(2)-C(9)-C(10)	125.1(8)	N(2)-C(9)-C(8)	110.0(8)
C(10)-C(9)-C(8)	124.9(8)	C(1)A-C(10)-C(9)	126.8(8)

Conclusion

This study describes the synthesis and characterization of (i) novel osmium nitrosyl organo, chloro, μ -oxo porphyrin complexes, (ii) an osmium thionitrosyl chloro porphyrin complex, and (iii) the first organoosmium thionitrosyl porphyrin complex. In the (OEP)Os(NO)R complexes, changing the alkyl group from Me to Et to *i*-Pr appears to result in a transmission of the electron-density change almost completely to the *trans* NO ligand. The strong π -accepting properties of the NO and NS ligands result in less backbonding from Os \rightarrow OEP in the (OEP)Os(NO)R and (OEP)Os(NS)(Me) complexes compared to the corresponding (OEP)Os(R)₂ complexes. This study also provides the solid-state structure of the first reported example of a nitrosyl porphyrin μ -oxo dimer, namely [(OEP)Os(NO)₂]₂(μ -O), and the first structures of osmium thionitrosyl porphyrins, namely (OEP)Os(NS)Cl and (OEP)Os(NS)(Me).

References and Notes

- (1) Brothers, P. J.; Collman, J. P. *Acc. Chem. Res.* **1986**, *19*, 209.
- (2) Setsune, J.-I.; Dolphin, D. *Can. J. Chem.* **1987**, *65*, 459.
- (3) Mansuy, D. *Pure Appl. Chem.* **1987**, *59*, 759.
- (4) Kräutler, B. In *Encyclopedia of Inorganic Chemistry*; R. B. King, Ed.; John Wiley and Sons: Chichester, 1994; Vol. 2: pp 697-712.
- (5) Brown, K.; Cheng, S.; Zou, X.; Zubkowski, J. D.; Valente, E. J.; Knapton, L.; Marques, H. M. *Inorg. Chem.* **1997**, *36*, 3666.
- (6) Gridnev, A. A.; Ittel, S. D.; Fryd, M.; Wayland, B. B. *Organometallics* **1996**, *15*, 222.
- (7) Summers, J. S.; Petersen, J. L.; Stolzenberg, A. M. *J. Am. Chem. Soc.* **1994**, *116*, 7189.
- (8) Kadish, K. M.; Han, B. C.; Endo, A. *Inorg. Chem.* **1991**, *30*, 4502.
- (9) Chopra, M.; Hun, T. S. M.; Leung, W.-H.; Yu, N.-T. *Inorg. Chem.* **1995**, *34*, 5973.
- (10) Brand, H.; Arnold, J. *Organometallics* **1993**, *12*, 3655.
- (11) Brand, H.; Arnold, J. *Coord. Chem. Rev.* **1995**, *140*, 137.
- (12) Leung, W.-H.; Hun, T. S. M.; Wong, K.-Y.; Wong, W.-T. *J. Chem. Soc., Dalton Trans.* **1994**, 2713.
- (13) A *cis* alkyl-hydroxyl complex has been recently proposed as an alternate intermediate in the cytochrome P450 rebound mechanism.¹⁴
- (14) Collman, J. P.; Chien, A. S.; Eberspacher, T. A.; Brauman, J. I. *J. Am. Chem. Soc.* **1998**, *120*, 425.
- (15) Collman, J. P.; Brothers, P. J.; McElwee-White, L.; Rose, E.; Wright, L. J. *J. Am. Chem. Soc.* **1985**, *107*, 4570.
- (16) Bartley, D. W.; Kodadek, T. *J. Am. Chem. Soc.* **1993**, *115*, 1656.

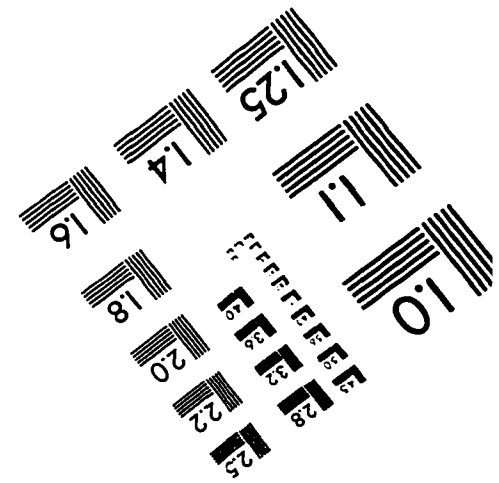
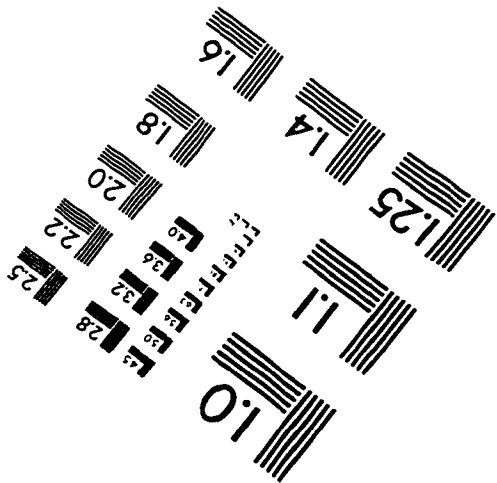
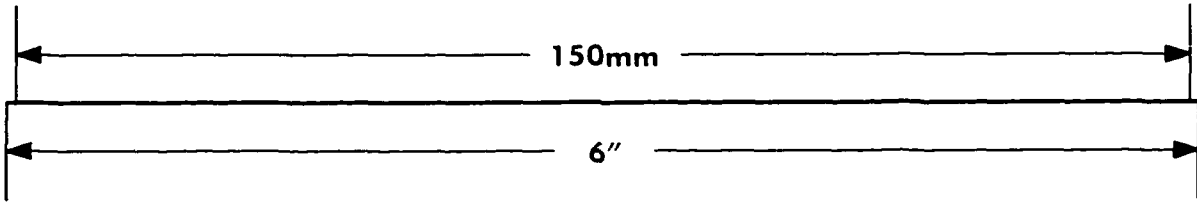
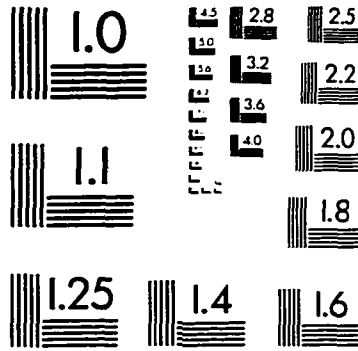
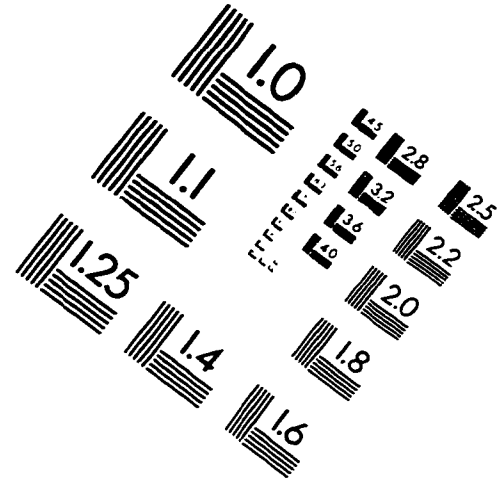
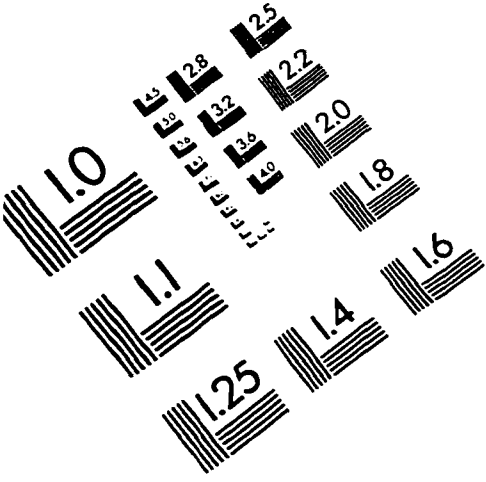
- (17) Collman, J. P.; Brothers, P. J.; McElwee-White, L.; Rose, E. *J. Am. Chem. Soc.* **1985**, *107*, 6110.
- (18) Arnold, J.; Hoffman, C. G.; Dawson, D. Y.; Hollander, F. J. *Organometallics* **1993**, *12*, 3645.
- (19) Setsune, J.-I.; Saito, Y.; Ishimaru, Y.; Ikeda, M.; Kitao, T. *Bull. Chem. Soc. Jpn.* **1992**, *65*, 639.
- (20) Seyler, J. W.; Safford, L. K.; Fanwick, P. E.; Leidner, C. R. *Inorg. Chem.* **1992**, *31*, 1545.
- (21) Guillard, R.; Lecomte, C.; Kadish, K. M. *Struct. Bond.* **1987**, *64*, 205.
- (22) Arafa, I. M.; Shin, K.; Goff, H. M. *J. Am. Chem. Soc.* **1988**, *110*, 5228.
- (23) Li, Z.; Goff, H. M. *Inorg. Chem.* **1992**, *31*, 1547.
- (24) Song, B.; Goff, H. M. *Inorg. Chim. Acta* **1994**, *226*, 231.
- (25) Kadish, K. M.; Tabard, A.; Lee, W.; Liu, Y. H.; Ratti, C.; Guillard, R. *Inorg. Chem.* **1991**, *30*, 1542.
- (26) Seyler, J. W.; Leidner, C. R. *Inorg. Chem.* **1990**, *29*, 3636.
- (27) Seyler, J. W.; Leidner, C. R. *J. Chem. Soc., Chem. Commun.* **1989**, 1794.
- (28) Alexander, C. S.; Rettig, S. J.; James, B. R. *Organometallics* **1994**, *13*, 2542.
- (29) Collman, J. P.; McElwee-White, L.; Brothers, P. J.; Rose, E. *J. Am. Chem. Soc.* **1986**, *108*, 1332.
- (30) Collman, J. P.; Rose, E.; Venburg, G. D. *J. Chem. Soc., Chem. Commun.* **1994**, 11.
- (31) Hodge, S. J.; Wang, L.-S.; Khan, M. A.; Young, V. G.; Richter-Addo, G. B. *Chem. Commun.* **1996**, 2283.
- (32) Ke, M.; Rettig, S. J.; James, B. R.; Dolphin, D. *J. Chem. Soc., Chem. Commun.* **1987**, 1110.
- (33) Sishita, C.; Ke, M.; James, B. R.; Dolphin, D. *J. Chem. Soc., Chem. Commun.* **1986**, 787.

- (34) Ke, M.; Sishita, C.; James, B. R.; Dolphin, D.; Sparapany, J. W.; Ibers, J. A. *Inorg. Chem.* **1991**, *30*, 4766.
- (35) Seyler, J. W.; Fanwick, P. E.; Leidner, C. R. *Inorg. Chem.* **1992**, *31*, 3699.
- (36) Collman, J. P.; Ha, Y.; Wagenknecht, P. S.; Lopez, M.-A.; Guilard, R. J. *Am. Chem. Soc.* **1993**, *115*, 9080.
- (37) The organometallic chemistry of Ru and Os complexes with η^1 -carbon ligands has been reviewed.³⁸
- (38) Hill, A. F. In *Comprehensive Organometallic Chemistry II. A Review of the Literature 1982-1994*; 1st ed.; E. W. Abel; F. G. A. Stone and G. Wilkinson, Ed.; Pergamon: Exeter, U.K., 1995; Vol. 7; pp 299-440.
- (39) Guilard, R.; Lagrange, G.; Tabard, A.; Lançon, D.; Kadish, K. M. *Inorg. Chem.* **1985**, *24*, 3649.
- (40) The (TPP)Fe(NO)(C₅H₅) complex has been claimed,⁴¹ although its ν_{NO} of 1705 cm⁻¹ is very close to that of the known (TPP)Fe(NO).
- (41) Massoudipour, M.; Tewari, S. K.; Pandey, K. K. *Polyhedron* **1989**, *8*, 1447.
- (42) Che, C.-M.; Poon, C.-K.; Chung, W.-C.; Gray, H. B. *Inorg. Chem.* **1985**, *24*, 1277.
- (43) Jolly, W. L.; Maguire, K. D. *Inorg. Synth.* **1967**, *9*, 102.
- (44) Pass, G.; Sutcliffe, H. *Practical Inorganic Chemistry: Preparations, Reactions and Instrumental Methods*; Chapman and Hall: London, U. K., 1968.
- (45) (a) Cheng, L.; Chen, L.; Chung, H.-S.; Young, V. G., Jr.; Khan, M. A.; Richter-Addo, G. B. Submitted to *Organometallics*. (b) Shelly Hodge, Ph.D. dissertation.
- (46) The reaction of RMgX with osmium- and other metallo-porphyrin cations to produce organometallic derivatives has some precedent.^{30,47}
- (47) Ogoshi, H.; Sugimoto, H.; Yoshida, Z.-i.; Kobayashi, H.; Sakai, H.; Maeda, Y. *J. Organomet. Chem.* **1982**, *234*, 185.

- (48) Buchler, J. W.; Kokisch, W.; Smith, P. D. *Struct. Bonding* **1978**, *34*, 79.
- (49) Buchler, J.; Smith, P. D. *Chem. Ber.* **1976**, *109*, 1465.
- (50) Antipas, A.; Buchler, J. W.; Gouterman, M.; Smith, P. D. *J. Am. Chem. Soc.* **1980**, *102*, 198.
- (51) Chen, B.; Hobbs, J. D.; Debrunner, P. G.; Erlebacher, J.; Shelnut, J. A.; Scheidt, W. R. *Inorg. Chem.* **1995**, *34*, 102.
- (52) Swepston, P. N.; Ibers, J. A. *Acta Cryst.* **1985**, *C41*, 671.
- (53) Jiao, X.-D.; Huang, J.-W.; Ji, L.-N.; Luo, B.-S.; Chen, L.-R. *J. Inorg. Biochem.* **1997**, *65*, 229.
- (54) Schaefer, W. P.; Ellis, P. E.; Lyons, J. E.; Shaikh, S. N. *Acta Cryst.* **1995**, *C51*, 2252.
- (55) Gold, A.; Jayaraj, K.; Doppelt, P.; Fischer, J.; Weiss, R. *Inorg. Chim. Acta* **1988**, *150*, 177.
- (56) Lay, K.-L.; Buchler, J. W.; Kenny, J. E.; Scheidt, W. R. *Inorg. Chim. Acta* **1986**, *123*, 91.
- (57) Strauss, S. H.; Pawlik, M. J.; Skowrya, J.; Kennedy, J. R.; Anderson, O. P.; Spertalian, K.; Dye, J. L. *Inorg. Chem.* **1987**, *26*, 724.
- (58) Karlin, K. D.; Nanthakumar, A.; Fox, S.; Murthy, N. N.; Ravi, N.; Huynh, B. H.; Orosz, R. D.; Day, E. P. *J. Am. Chem. Soc.* **1994**, *116*, 4753.
- (59) Landrum, J. T.; Grimmett, D.; Haller, K. J.; Scheidt, W. R.; Reed, C. A. *J. Am. Chem. Soc.* **1981**, *103*, 2640.
- (60) Ivanca, M. A.; Lappin, A. G.; Scheidt, W. R. *Inorg. Chem.* **1991**, *30*, 711.
- (61) Bartczak, T. J.; Latos-Grazynski, L.; Wyslouch, A. *Inorg. Chim. Acta* **1990**, *171*, 205.
- (62) Masuda, H.; Taga, T.; Osaki, K.; Sugimoto, H.; Mori, M.; Ogoshi, H. *J. Am. Chem. Soc.* **1981**, *103*, 2199.

- (63) Masuda, H.; Taga, T.; Osaki, K.; Sugimoto, H.; Mori, M.; Ogoshi, H. *Bull. Chem. Soc. Jpn.* **1982**, *55*, 3887.
- (64) Collman, J. P.; Barnes, C. E.; Brothers, P. J.; Collins, T. J.; Ozawa, T.; Galluci, J. C.; Ibers, J. A. *J. Am. Chem. Soc.* **1984**, *106*, 5151.
- (65) Masuda, H.; Taga, T.; Osaki, K.; Sugimoto, H.; Mori, M. *Bull. Chem. Soc. Jpn.* **1984**, *57*, 2345.
- (66) See Table 6 in reference 51 for an extensive listing of structural parameters for porphyrin μ -oxo dimers.
- (67) Bohle, D. S.; Hung, C.-H.; Powell, A. K.; Smith, B. D.; Wocadlo, S. *Inorg. Chem.* **1997**, *36*, 1992.
- (68) Chivers, T.; Edelmann, F. *Polyhedron* **1986**, *5*, 1661.
- (69) Roesky, H. W.; Pandey, K. K.; Clegg, W.; Noltemeyer, M.; Sheldrick, G. M. *J. Chem. Soc., Dalton Trans.* **1984**, 719.
- (70) Pandey, K. K.; Roesky, H. W.; Noltemeyer, M.; Sheldrick, G. M. *Z. Naturforsch.* **1984**, *39b*, 590.
- (71) Weber, R.; Müller, U.; Dehnicke, K. *Z. Anorg. Allg. Chem.* **1983**, *504*, 13.
- (72) Bats, J. W.; Pandey, K. K.; Roesky, H. W. *J. Chem. Soc., Dalton Trans.* **1984**, 2081.
- (73) Willing, W.; Müller, U.; Demant, U.; Dehnicke, K. *Z. Naturforsch.* **1986**, *41b*, 560.
- (74) Demant, U.; Willing, W.; Müller, U.; Dehnicke, K. *Z. Anorg. Allg. Chem.* **1986**, *532*, 175.

IMAGE EVALUATION TEST TARGET (QA-3)



APPLIED IMAGE, Inc.
1653 East Main Street
Rochester, NY 14609 USA
Phone: 716/482-0300
Fax: 716/288-5989

© 1993, Applied Image, Inc., All Rights Reserved